IN-02
175548
P. 272

NASA Technical Memorandum 4450

Static Internal Performance of a Single Expansion Ramp Nozzle With Multiaxis Thrust Vectoring Capability

Charles J. Capone and Alberto W. Schirmer

July 1993

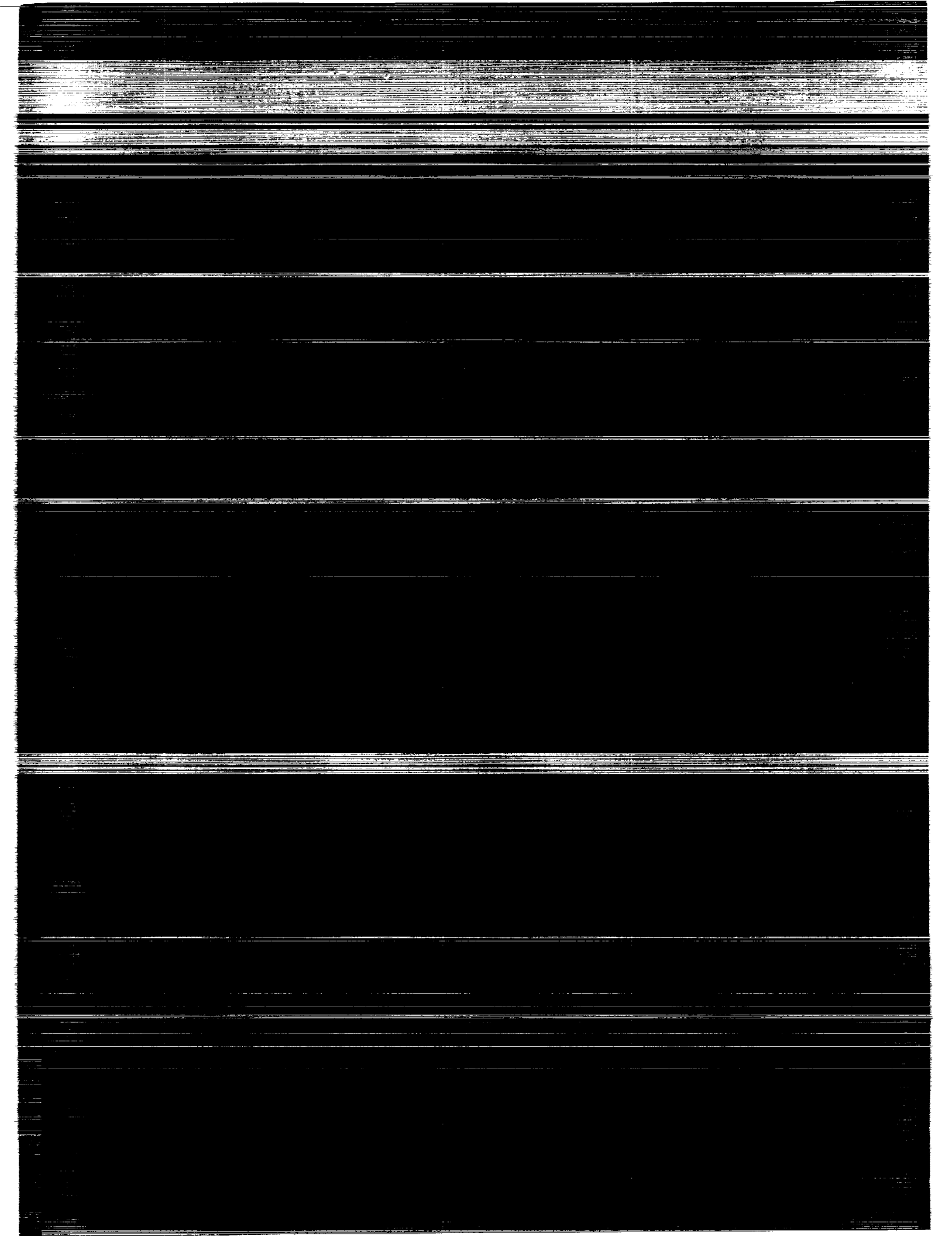

NASA Technical Memorandum 4450

Static Internal Performance of a Single Expansion Ramp Nozzle With Multiaxis Thrust Vectoring Capability

Francis J. Capone
Langley Research Center
Hampton, Virginia

Alberto W. Schirmer
The George Washington University
Joint Institute for Advancement of Flight Sciences
Langley Research Center
Hampton, Virginia

National Aeronautics and
Space Administration
Office of Management
Scientific and Technical
Information Program
1993

Summary

An investigation has been conducted at static conditions in order to determine the internal performance characteristics of a multiaxis thrust vectoring single expansion ramp nozzle. Yaw vectoring was achieved by deflecting yaw flaps in the nozzle sidewall into the nozzle exhaust flow. In order to eliminate any physical interference between the variable angle yaw flap deflected into the exhaust flow and the nozzle upper ramp and lower flap which were deflected for pitch vectoring, the downstream corners of both the nozzle ramp and lower flap were cut off to allow for up to 30° of yaw vectoring. The effects of nozzle upper ramp and lower flap cutout, yaw flap hinge line location and hinge inclination angle, sidewall containment, geometric pitch vector angle, and geometric yaw vector angle were studied. This investigation was conducted in the static-test facility of the Langley 16-Foot Transonic Tunnel at nozzle pressure ratios up to 8.0.

An analysis of the results of this investigation indicates that removal of the downstream corners of both the upper ramp and lower flap for a yaw flap hinge line downstream of the nozzle throat had little or no effect on resultant thrust ratio. However, losses of up to 3.4 percent in resultant thrust ratio occurred with the yaw flap hinge line near the nozzle throat. Pitch vectoring performance was primarily influenced by yaw flap hinge line location rather than ramp cutout. For the nozzle with the yaw flap hinge line near the nozzle throat, there was a 10.3° decrease in resultant pitch vector angle for a negative geometric pitch vector angle of 20° and about a 5° decrease for a positive geometric pitch vector angle of 20°. Yaw thrust vectoring of nozzles with no geometric pitch vectoring caused resultant thrust ratio losses of up to 3.5 percent per 10° of yaw turning and produced resultant yaw vector angles that were typically 33 to 45 percent of the geometric yaw vector angle. Maximum resultant yaw angles occurred for the nozzle with the yaw hinge line near the nozzle throat and with the maximum sidewalls. Yaw thrust vectoring decreased the resultant pitch vector angle for the negative pitched-vectored nozzle and increased resultant pitch angle for the nozzle with no vectoring or with positive pitch vectoring. Most of the yaw turning was produced from the yaw flap deflected into the nozzle exhaust flow.

Introduction

Studies have shown that significant advantages in air combat are gained with the ability to perform transient maneuvers at high angles of attack including brief excursions into poststall conditions (refs. 1 to 3). Expansion of the angle of attack envelope of fighter airplanes to meet the more demanding mission requirements of the future is possible because of recent technological advances such as thrust vectoring in nozzle design. Thrust vectoring, by virtue of being uncoupled from the airplane aerodynamics, has the potential to augment performance characteristics by allowing greater control beyond stall conditions than that provided by the airplane aerodynamic surfaces.

A number of investigations, conducted at both static conditions (wind off) and at forward speeds, have verified the capability of both axisymmetric and nonaxisymmetric multifunction nozzles to provide pitch and yaw thrust vectoring (refs. 4 to 9). Some of these investigations involved adding yaw vectoring capability to nozzles originally designed for pitch vectoring only. This paper presents results from an investigation in which a single expansion ramp nozzle (SERN) has been modified to include multiaxis thrust vectoring capability. The SERN is a nonaxisymmetric, variable-area, internal/external expansion exhaust system (refs. 10 to 14). Basic SERN nozzle components consist of (1) a two-dimensional upper ramp in which a portion of the ramp surface downstream of the throat serves as an external expansion ramp, (2) a relatively short two-dimensional lower flap, and (3) flat, two-dimensional sidewalls. Nozzle power setting (throat area) is changed by varying the geometry of the convergent-divergent upper ramp assembly (refs. 10 to 12), and expansion ratio is varied by rotation of the lower flap. Most SERN designs also provide for pitch thrust vectoring capability through rotation of the entire divergent portion of the ramp surface in conjunction with rotation of the lower flap (refs. 10, 12, and 13).

A single expansion ramp nozzle designed for pitch vectoring (ref. 13) was modified to accommodate yaw vectoring flaps that were located in the nozzle sidewalls. In order to eliminate any physical interference between the yaw flap deflected into the exhaust flow and the nozzle upper ramp and lower flap which were deflected for pitch vectoring, the downstream corners of both the nozzle upper ramp and lower flap were cut off to allow for up to 30° of yaw vectoring. The purpose of this investigation was to study the effects on nozzle internal performance of varying nozzle pitch and yaw vector angle, ramp and flap cutout angle, yaw flap hinge location and inclination angle, and nozzle sidewall containment. This investigation was conducted in the static-test facility of the Langley 16-Foot Transonic Tunnel at static conditions and at nozzle pressure ratios up to 8.0. A summary of some of the results presented herein was previously reported in reference 15.

Symbols

All forces and moments (with the exception of resultant gross thrust) are referred to the model centerline (body axis). The model (balance) moment reference center was located at station 29.39. A discussion of the data reduction procedure and definitions of the force and moment terms and the propulsion relationships used herein can be found in reference 16.

A_e nozzle exit area, in^2

A_t nozzle throat area, in^2

$(A_e/A_t)_i$ internal expansion ratio (A_e measured at end of nozzle lower flap)

F measured thrust along body axis, lbf

F_i ideal isentropic gross thrust, $w_p \left\{ \frac{RT_{t,j}}{g^2} \frac{2\gamma}{\gamma-1} \left[1 - \left(\frac{1}{\text{NPR}} \right)^{(\gamma-1)/\gamma} \right] \right\}^{1/2}$, lbf

F_N measured normal force, lbf

F_r resultant gross thrust, $\sqrt{F^2 + F_N^2 + F_Y^2}$, lbf

F_Y measured side force, lbf

g gravitational constant, 32.174 ft/sec^2

h_t nozzle throat height (fig. 1(b)), in.

l_r axial length of upper ramp measured from nozzle throat to end of ramp, in.

NPR nozzle pressure ratio, $p_{t,j}/p_a$

$(\text{NPR})_{\text{des}}$ design nozzle pressure ratio for ideally expanded flow

p_a ambient pressure, psi

p_f flap local static pressure, psi

p_r ramp local static pressure, psi

$p_{t,j}$ jet total pressure, psi

R gas constant for air, 1716 ft^2/sec^2-°R

$T_{t,j}$ jet total temperature, °R

w_i ideal weight-flow rate, lbf/sec

w_p measured weight-flow rate, lbf/sec

x axial distance measured from nozzle connect station, positive downstream (fig. 1(a)), in.

x_e length from nozzle connect station to ramp or lower flap exit (fig. 1(b)), in.

x_p location of ramp or flap pressure orifices (relative to unvectored nozzle) measured from nozzle throat, positive downstream, in.

x_r longitudinal distance to yaw hinge line measured from nozzle throat along upper ramp (fig. 1(a)), in.

x_t length from nozzle connect station to throat location on ramp or lower flap (fig. 1(b)), in.

y vertical distance measured from model centerline, positive up (fig. 1(a)), in.

y_e vertical distance of nozzle ramp or lower flap trailing edge from model centerline, positive up (fig. 1(b)), in.

y_t vertical distance of nozzle ramp or lower flap throat location from model centerline, positive up (fig. 1(b)), in.

z lateral distance of sidewall measured from inside surface of sidewall (fig. 1(c)), positive for sidewall deflected into flow, in.

γ ratio of specific heats for air, 1.3997

δ_p resultant pitch vector angle, $\tan^{-1} \frac{F_N}{F}$, deg

$\delta_{v,p}$ geometric pitch vector angle measured from nozzle centerline, positive for downward deflection, deg

$\delta_{v,y}$ geometric yaw vector angle measured from nozzle centerline, positive deflection to left looking upstream, deg

δ_y resultant yaw vector angle, $\tan^{-1} \frac{F_Y}{F}$, deg

θ upper ramp cutout angle (fig. 1(d)), deg

ϕ hinge line inclination angle (fig. 1(e)), deg

Subscripts:

l lower flap

r ramp

u upper ramp

Abbreviations:

max maximum

med medium

min	minimum
SERN	single expansion ramp nozzle
sta.	model station, in.

Nozzle Designs

The single expansion ramp nozzle (SERN) is a nonaxisymmetric, variable-area, internal/external expansion exhaust system. Basic SERN nozzle components consist of (1) a two-dimensional upper ramp in which a portion of the ramp surface downstream of the throat serves as an external expansion ramp, (2) a relatively short two-dimensional lower flap, and (3) flat, two-dimensional sidewalls. Nozzle power setting (throat area) is changed by varying the geometry of the convergent-divergent upper ramp assembly (refs. 10 to 12), and expansion ratio is varied by rotation of the lower flap. Most SERN designs also provide for pitch thrust vectoring capability through rotation of the entire divergent portion of the ramp surface in conjunction with rotation of the lower flap (refs. 10, 12, and 13). For the present investigation, the SERN nozzles with geometric pitch vector angles of 0°, −20°, and 20° of reference 13 were chosen as baseline nozzles. All the nozzles had a nominally constant exhaust flow-path width of 4.00 in., throat height of 1.0 in., and a throat area of 4.0 in^2. The throat area of the current SERN test nozzles simulated a typical dry power (cruise) engine setting. Parametric geometry changes were achieved by using interchangeable upper ramps, lower flaps, and sidewalls. All the nozzle configurations tested are presented in table 1. This table includes the ramp, flap, and sidewall that were used for each nozzle and the major geometric parameters for each nozzle, which are the geometric vector angles $\delta_{v,p}$ and $\delta_{v,y}$, location of the yaw hinge line x_r/l_r, ramp or flap cutout angle θ, and hinge line inclination angle ϕ. In addition, table 1 serves as an index to both tabulated performance and pressure data for each nozzle.

A sketch of the baseline unvectored ($\delta_{v,p} = 0°$) nozzle is presented in figure 1(a). The baseline upper ramp contained a moderate amount of axial ramp curvature (concave shape). The ratio of ramp length to the nominal throat height was 3.621 and the ramp chord angle was 5.1°. The exit area that is associated with the nozzle internal expansion ratio is determined at the end of the flap or at $x_{e,l}$ shown in figure 1(b). This exit area is the product of the nozzle width and the distance made up of $y_{e,l}$ plus the vertical distance to the upper ramp from the nozzle centerline. The exit area associated with the nozzle external expansion ratio is determined at the end of the ramp or at $x_{e,u}$, also shown in figure 1(b). This exit area would be the product of the nozzle width and the distance made up of $y_{e,l} + y_{e,u}$.

The two pitch-vectored nozzle configurations that were tested in this investigation are shown in figure 1(b). The locations of both the ramp and lower flap hinge points result from mechanical design considerations since the nozzles were designed to have a pitch vector range of up to 60° (ref. 13). For geometric pitch vector angles of −20° and 0°, the lower flap remains fixed. For a pitch vector angle of 20°, the lower flap is rotated downward. As the geometric pitch vector angle is increased, the nozzle geometric throat (shown for $\delta_{v,p} = 0°$) translates toward the lower flap exit. Of course, this also means that the nozzle internal area ratio varies (approaches unity) with increases in pitch vector angle. Coordinates for the upper ramp and lower flap centerline profiles are found in tables 2 and 3, respectively.

All the nozzles were tested with varying amounts of sidewall containment from minimum to maximum as shown in figure 1(c). Consideration must be given to the size of sidewalls because they can have a direct impact on the weight of the full-scale nozzle, on the amount of surface area that requires cooling, and on the extent of seals required between the nozzle ramp and flap and sidewalls. The minimum and maximum containment sidewalls were those used in reference 13, whereas the medium containment sidewall was designed as an intermediate step between the other two sidewalls. The amount of sidewall area for the maximum containment sidewall was 11.9 percent greater than that for the medium containment sidewall and 36.3 percent greater than that for the minimum containment sidewall. Coordinates for all the sidewalls used in this investigation are given in table 4. Each sidewall in table 4 is also identified by the amount of sidewall containment.

In this investigation, thrust vectoring in the yaw plane was accomplished by deflecting the sidewalls about a vertical hinge line. In order to eliminate any physical interference between the yaw flap deflected into the exhaust stream and the upper ramp or lower flap, which are used for pitch thrust vectoring, the downstream corners of both the ramp and lower flap were cut off to allow for up to 30° of yaw flap deflection. As shown in figure 1(d), this cutout was made on both sides of the ramp and lower flap to allow for both positive and negative yaw vector angles. Nozzles were tested with cutout angles of $\theta = 20°$ and 30°. The cutout started at the edge of the ramp and lower flap, where the yaw flap hinge line was located and ended at the end of the ramp or lower flap. Three separate yaw flap hinge line locations were also investigated as indicated in figure 1(d).

These locations correspond to 42, 20, and 2 percent of the upper ramp length. The most upstream location of $x_r/l_r = 0.02$ was used to examine the effects of placing the hinge line close to the nozzle throat. The inclination angle ϕ of one of the yaw hinge lines was also varied as a parameter. As seen in figure 1(e), the top of the hinge line located at $x_r/l_r = 0.20$ was pivoted to the rear about the nozzle centerline. Inclination angles of 0°, 15°, and 30° were investigated.

As previously mentioned, thrust vectoring in the yaw plane was accomplished by deflecting a yaw flap (portion of sidewall) about a vertical or inclined hinge line. One flap was deflected into the exhaust flow, and the other yaw flap was deflected the same amount away from the exhaust flow. Some typical yaw thrust vector configurations are shown in figure 1(f). The location of the nozzle throat on the ramp is also shown in order to show the proximity of the throat to the yaw hinge line. A photograph of a typical test nozzle is presented in figure 2.

Apparatus and Procedure

Static-Test Facility

This investigation was conducted in the static-test facility of the Langley 16-Foot Transonic Tunnel. The test apparatus was installed in a room with a high ceiling. The simulated jet exhausts to the atmosphere through a ceiling-mounted vent located aft of the nozzle test apparatus. The control room is remotely located from the test area, and a closed-circuit television camera is used to observe the model. This facility utilizes the same clean, dry air supply as that used in the 16-Foot Transonic Tunnel and a similar air control system—including valves, filters, and a heat exchanger (to operate the jet flow at constant stagnation temperature).

Single-Engine Propulsion Simulation System

A sketch of the single-engine propulsion simulation system is presented in figure 3 with a typical nozzle configuration installed, and a photograph is shown in figure 4.

An external high-pressure air system provided a continuous flow of clean, dry air at a controlled temperature of about 540°R at the nozzles. This high-pressure air was brought through the dolly-mounted support strut by six tubes which connect to a high-pressure plenum chamber. As shown in figure 3, the air was then discharged perpendicularly into the model low-pressure plenum through eight multiholed sonic nozzles equally spaced around the high-pressure plenum. This method was designed to minimize any forces imposed by the transfer of axial momentum as the air passed from the nonmetric high-pressure plenum to the metric low-pressure plenum (mounted on the force balance). Two flexible metal bellows were used as seals and served to compensate for axial forces caused by pressurization. The air was then passed from the model low-pressure plenum through a transition section, a choke plate, instrumentation section, and nozzles, as shown in figure 3.

Instrumentation

A six-component strain-gauge balance was used to measure forces and moments on the model (fig. 3). Jet total pressure was measured at a fixed location in the instrumentation section by means of a four-probe rake through the upper surface, a three-probe rake through the side, and a three-probe rake through the corner. (See fig. 3.) A thermocouple, also located in the instrumentation section, was used to measure jet total temperature. Weight flow of the high-pressure air supplied to the exhaust nozzle was measured by a pair of critical flow venturis. Internal static pressure orifices were located along the upper ramp and lower flap as indicated in table 5. All pressures were measured simultaneously with individual pressure transducers.

Data Reduction

All data were recorded simultaneously on magnetic tape. Approximately 50 frames of data, taken at a rate of 10 frames/sec, were used for each data point; average values were used in computations. Data were obtained in an ascending order of $p_{t,j}$.

The basic performance parameters used for the presentation of results were $F/F_i, F_r/F_i, \delta_p, \delta_y$, and w_p/w_i. With the exception of resultant gross thrust F_r, all force data in this report are referenced to the body axis (centerline). Internal thrust ratio F/F_i represents the ratio of actual nozzle thrust (along the body axis) to ideal nozzle thrust, where ideal nozzle thrust is based on measured weight-flow rate and total pressure and total temperature conditions in the instrumentation section, as defined by the equation in the symbol definitions. Significant differences between F_r/F_i and F/F_i can occur when the jet-exhaust flow is directed away from the axial direction. Resultant thrust vector angles in the longitudinal (pitch) plane δ_p and the lateral (yaw) plane δ_y are presented for evaluating the exhaust flow turning capability of the various thrust-vectored configurations. Nozzle discharge coefficient w_p/w_i is the ratio of measured weight flow to ideal weight flow, where

ideal weight flow is based on jet total pressure $p_{t,j}$, jet total temperature $T_{t,j}$, and measured nozzle throat area. Nozzle discharge coefficient reflects the ability of a nozzle to pass weight flow and is reduced by any momentum and vena contracta losses (effective throat area less than measured throat area A_t).

The balance force measurements from which actual thrust is subsequently obtained are initially corrected for model weight tares and balance interactions. Although the bellows arrangement was designed to eliminate pressure and momentum interactions with the balance, small bellows tares on all balance components still exist. These tares result from a small pressure difference between the ends of the bellows when internal velocities are high and also small differences in the forward and aft bellows spring constants when the bellows are pressurized. As discussed in reference 17, these bellows tares were determined by testing calibration nozzles with known performance over a range of expected normal- and side-force and yawing-, pitching-, and rolling-moment loadings. The balance data were then corrected in a manner similar to that discussed in references 16 and 17. The resultant gross thrust F_r used in the resultant thrust ratio F_r/F_i was then determined from these corrected balance data.

Presentation of Results

The results of this investigation are presented in both tabular and plotted forms. Table 1 is an index to the tabular results contained in tables 6 to 190. Static internal nozzle performance characteristics are presented in tables 6 to 190. Nozzle internal performance characteristics are graphically presented as resultant thrust ratio F_r/F_i, internal thrust ratio F/F_i, resultant pitch vector angle δ_p, and resultant yaw vector angle δ_y. Comparison and summary plots for selected nozzle configurations are presented as follows:

Discussion of Results

Baseline Nozzle Performance

Forward thrust nozzles. Static performance characteristics for the baseline forward thrust nozzle are presented in figure 5 for the nozzles with each of the three sidewalls. Resultant thrust ratio F_r/F_i, internal thrust ratio F/F_i, resultant pitch thrust vector angle δ_p, and resultant yaw thrust vector angle δ_y are shown as a function of nozzle pressure ratio NPR. Nozzle discharge coefficients w_p/w_i for these nozzles are presented in table 6.

The internal performance data presented in figure 5 are typical of other single expansion ramp nozzles (refs. 11 to 14). Generally, a tendency exists for two performance peaks to occur for nozzle thrust ratio for these type nozzles. These peaks occur because the exhaust flow expansion process for single expansion ramp nozzles occurs both internally and externally. That is, internal expansion of the flow occurs from the nozzle throat up to the end of the lower flap, where it is contained by the internal surfaces of the nozzle and is controlled by the internal expansion ratio. External expansion, which occurs downstream of the lower flap trailing edge, is bounded by the expansion ramp and the free (ambient/exhaust) boundary and is controlled by the external expansion ratio.

For the forward thrust nozzle with maximum containment, peak nozzle performance of $F_r/F_i = 0.989$ occurred at NPR = 4.0, which is above $(\text{NPR})_{\text{des}} = 3.23$, the nozzle pressure ratio for optimum internal expansion; this indicates an increase in the effective internal area ratio. A second performance peak for this nozzle probably occurs at a nozzle pressure greater than was tested. This peak nozzle performance is essentially the same as that reported in reference 13. Resultant thrust ratio levels remained near peak levels over a much wider range of nozzle pressure ratio than would be expected for a typical convergent-divergent nozzle (ref. 18). This performance characteristic, which results from the two separate flow expansion processes (internal and external), could be a significant advantage for SERN nozzles, as less (or no) expansion-ratio control may be required (particularly for an all subsonic-mission airplane) and reductions in exhaust-system weight and complexity could be achieved.

The effect of sidewall containment on nozzle internal performance for the baseline nozzles is also shown in figure 5. For the forward thrust nozzle and for the other nonvectored nozzles tested, the amount of sidewall containment did not significantly affect either resultant or internal thrust ratio characteristics. The minimum containment sidewall caused about a 0.5-percent loss in resultant thrust at the highest NPR. Some consideration must be given to containment variations because they can have a direct impact on the weight of the nozzle, on the amount of surface area that requires cooling, and on the extent of seals required between the nozzle ramp and flap and sidewalls.

The nonlinear variation of resultant pitch vector angle δ_p with nozzle pressure ratio for the unvectored, forward thrust configurations is characteristic of SERN nozzles and is caused by the changing compression-expansion wave patterns impinging on the ramp (unopposed by an opposite wall) as NPR is varied. An axial-force (body axis) performance penalty would be associated with any value of resultant thrust vector angle which is nonzero because the resultant thrust is being turned away from the axial direction. For example, this performance penalty

would occur at all nozzle pressure ratios except approximately 3.0 and 5.0. Since the ramp has a large, unopposed, normal projected area, values of normal force can change significantly with varying nozzle pressure ratio.

Nozzle discharge coefficient characteristics for these nozzles are presented in table 6. Nozzle discharge coefficient w_p/w_i is a measure of the ability of the nozzle to pass mass flow and is reduced by boundary-layer thickness and nonuniform flow in the nozzle throat. Changes in nozzle geometry that occur downstream of the nozzle throat (supersonic exhaust) usually do not affect nozzle discharge coefficient characteristics. This characteristic is shown by the data in table 6. The three nozzles shown in figure 5 all have levels of w_p/w_i that are typical for this class of nozzles. Values of w_p/w_i greater than 1 are believed to be caused by an inability to determine accurately the nozzle throat areas. An examination of discharge coefficients presented in the tables for other nozzles shows little or no effect on the discharge coefficients due to varying the geometric parameters used to define the nozzles of this investigation.

Pitch-vectored nozzles. The effect of varying geometric pitch vector angle on nozzle internal performance is shown in figures 6 and 7. The results of this investigation show similar variations in nozzle performance parameters and pitch turning capabilities for changes in $\delta_{v,p}$ as reported in references 12 and 13. Axial thrust ratios are quite different in magnitude, depending on the pitch vector angle. These large differences in F/F_i are mostly caused by decreases in the axial component of thrust created by the turning (vectoring) of the flow away from the axial direction by the upper ramp surface. Figure 6 shows that the losses in resultant thrust are only significant for $\delta_{v,p} = -20°$, where losses of 5.7 percent at NPR = 3.0 to losses of 3.0 percent at NPR = 6.0 occurred. It should be noted that decreases in resultant thrust ratio can be interpreted as flow turning losses. Resultant pitch vector angle is also highly dependent on NPR for all $\delta_{v,p}$ settings as previously noted. Pitch turning efficiency is quite high, with δ_p values exceeding their geometric settings. Resultant pitch vector angle from the unvectored nozzle increased 20° to 27° for $\delta_{v,p} = -20°$, and turning increased 16° to 25° for $\delta_{v,p} = 20°$.

Some insight as to the causes of this behavior can be seen by examining the internal pressure distributions. The effect of pitch vector angle on the upper ramp and lower flap pressures is shown in figure 8. The ramp pressure distributions for $\delta_{v,p} = -20°$ indicate a throat location ($p_r/p_{t,j} = 0.528$) which is upstream of the geometric throat ($x_p/l_r = 0$). As a result, some additional supersonic flow turning is present, which generally results in turning losses. In addition, shock-induced internal flow separation appears to occur on the ramp between $x_p/l_r = 0.20$ and 0.40, which can also contribute to the large losses in resultant thrust ratio experienced by the negative pitch-vectored nozzle (fig. 6). The movement of the sonic line toward the exit plane as the nozzle ramp was pitched down (positive $\delta_{v,p}$) permitted the more effective vectoring of subsonic flow upstream of the throat; this increased $\delta_{v,p}$ and F_r/F_i.

As shown in figure 7, flow turning capability improved at both negative and positive geometric pitch vector angles as sidewall containment was increased from minimum to maximum. When the nozzle was vectored negatively in pitch, large differences in internal thrust ratio F/F_i and resultant pitch vector angles occurred with changes in sidewall containment at NPR lower than 5.0 (fig. 7(a)). Increasing containment for the negatively pitched nozzles decreased the internal thrust ratio by almost 5 percent at NPR = 3.0 and increased δ_p about 8.7°. The net effect on resultant thrust ratio was less than 1 percent. Greater containment allows for a confined expansion of the exhaust gas in the nozzle exit region so that all the exhaust flow can follow the internal surfaces (and most importantly the upper ramp) more closely. For configurations with less sidewall containment, some of the exhaust gas expands laterally and exits the nozzle before being turned. These results are indicated by the internal pressures on the ramp presented in figure 9(a) for $\delta_{v,p} = -20°$. Increasing sidewall containment decreases the static pressure on the ramp downstream of the exhaust shock at $x_p/l_r > 0.3$. These data indicate that a smaller (or more negative) normal force would result from the ramp surface as sidewall containment is increased.

For positive $\delta_{v,p}$, increased resultant thrust ratios and resultant pitch vector angles occurred as sidewall containment increased (fig. 7(b)). These effects suggest that the predominant factor causing poor performance at minimum containment is lateral expansion of the exhaust flow before the flow is expanded or turned by the nozzle geometry. The effect of sidewall containment on the ramp pressure distributions (fig. 9(b)) for the $\delta_{v,p} = 20°$ nozzle is much smaller than those previously discussed for the $\delta_{v,p} = -20°$ nozzle. A small increase occurs in the static pressure at the end of the ramp as containment is increased; this increased positive resultant pitch vector angle. These observations on the effect of sidewall containment for the pitch-vectored nozzles are typically true for other nozzles of this investigation that were tested

with varying amounts of flap cutout and/or yaw hinge line locations.

Effects of Flap Cutout and Hinge Line Location

The effect of flap cutout angle on nozzle internal performance for the nozzle with $x_r/l_r = 0.20$ and maximum containment is shown in figure 10. Figure 11 presents the effect of the location of the yaw hinge line for the nozzle with $\theta = 30°$ and maximum sidewall containment. These results are similar to those obtained for the other nozzle configurations tested. Only the relative magnitudes of the various performance parameters are different for these other configurations. Consequently, results for the other configurations are presented in the tables but are not plotted. Figures 12 to 17 summarize the effects of cutout angle and hinge line location at nozzle pressure ratios of 3.0 and 6.0.

Forward thrust nozzles. As shown in figure 10(a), essentially no changes in resultant thrust for the forward thrust nozzle occurred as the cutout angle was varied from 0° to 30° up to a nozzle pressure ratio of about 5.0. Above NPR = 5.0, losses in F_r/F_i were present with a maximum loss of 1.1 percent occurring at NPR = 8.0. For the other nozzle configurations with the hinge line located at $x_r/l_r = 0.20$ and 0.42 with any of the sidewalls, resultant thrust ratio was either constant or increased as cutout angle increased (fig. 12). Greater reductions in resultant thrust ratio were observed at NPR = 6.0 as cutout was increased when the yaw hinge line was located at $x_r/l_r = 0.02$, the location closest to the nozzle throat (fig. 12). This location created a larger cutout area through which exhaust gases could escape laterally without producing useful thrust. The losses produced by this sideways expansion of the gases result from a reduction in nozzle expansion surface for the exhaust gas to act on as well as a nonaxial direction of the exhaust momentum (divergence losses).

Figure 11(a) indicates that there was a loss in F_r/F_i of about 3.5 percent at NPR = 8.0 when the hinge line location at $\theta = 30°$ was moved from $x_r/l_r = 1.00$ to $x_r/l_r = 0.02$. The fact that the differences in F_r/F_i between $x_r/l_r = 1.00$ and $x_r/l_r = 0.20$ were less than one half those produced when the hinge was moved from $x_r/l_r = 0.20$ to $x_r/l_r = 0.02$ (for $\theta = 30°$) indicates that ventilation of the exhaust gases is highly accentuated if the jet is not contained in the immediate vicinity of the throat area. In this respect, effects of cutout angle were smaller relative to those produced by changes in hinge line location (fig. 11). These results are similar to those of reference 8 for a two-dimensional convergent-divergent nozzle and to reference 19 for an axisymmetric nozzle with longitudinal slots in the divergent flaps. Note that these nozzle configurations represent the nozzle geometry during cruise which generally constitutes the majority of the airplane flight profile. As always, performance-weight trades exist, and the adverse effect of a loss in thrust ratio due to flap cutout might be offset by a decrease in the nozzle weight and internal nozzle surface to be cooled. In addition, the benefits realized from thrust vectoring (which requires a flap cut out) must be traded against any cruise thrust losses.

Pitch-vectored nozzles. The effect of flap cutout on internal performance for the vectored nozzles is shown in figures 10, 13, and 14. In general, as the ramp-flap cutout angle was increased for the $\delta_{v,p} = -20°$ nozzle, there was a slight increase in F_r/F_i and a large decrease in the magnitude of negative δ_p values, with the largest decreases in δ_p occurring at low nozzle pressure ratios and $x_r/l_r = 0.02$ (fig. 13). This decrease in negative resultant pitch vector angle was caused by an increase in pressures along the ramp as flap cutout angle was increased as shown in figure 18(b). As shown in figure 14, increasing flap cutout angle when the nozzle was pitched down 20° caused large losses in both resultant thrust ratio and pitch vector angle for the nozzles with $x_r/l_r = 0.20$ and 0.02 at NPR = 6.0. Figure 18(c) indicates essentially no effects to the ramp pressures as cutout was increased at NPR = 3.0.

The effects of yaw hinge line location for the vectored nozzles are presented in figures 11, 16, and 17. There was a 1.1-percent increase in F_r/F_i and a 10.3° decrease in negative δ_p values as the hinge line was moved forward from the nozzle exit to $x_r/l_r = 0.02$ for $\delta_{v,p} = -20°$ and $\theta = 30°$ at NPR = 3.0 (fig. 11(b)). As previously noted, decreases in negative resultant pitch angle for the nozzle with $\delta_{v,p} = -20°$ result from an increase in pressures on the ramp (fig. 19(b)). For the nozzle with $\delta_{v,p} = 20°$ and $\theta = 30°$ at NPR = 3.0 (fig. 11(c)), resultant thrust ratio decreased about 3.2 percent and resultant pitch vector angle decreased about 5° for the same variation in x_r/l_r. Decreases in resultant thrust ratio can be interpreted as turning losses. Because the trends in the variation of either F_r/F_i and δ_p with x_r/l_r were essentially the same for both $\theta = 20°$ and 30° (figs. 16 and 17), these results would indicate that the changes in performance noted previously are primarily caused by changes in the location of the yaw hinge line rather than flap cutout.

Although this discussion was for the nozzles with maximum containment, the effects discussed are similar for the negative vectored nozzle with the medium containment sidewalls (fig. 16(b)) and the positive vectored nozzle with the medium and minimum sidewalls (figs. 17(b) and (c)). For the negative vectored nozzle, decreases in negative δ_p values were much less for the nozzle with the minimum sidewall (fig. 16(c)). At NPR = 3.0, there was a decrease in δ_p of about 3° (compared with 10.3° with the maximum sidewall) as the yaw flap hinge line was moved from $x_r/l_r = 1.00$ (nozzle exit) to $x_r/l_r = 0.02$.

Effects of Yaw Vectoring

Basic yaw vectoring effect. Typical effects of yaw vectoring on nozzle performance are presented in figure 20 for the nozzle with $x_r/l_r = 0.20$, $\theta = 30°$, and maximum containment sidewalls. Figures 21 to 26 summarize the effects of yaw vectoring for the remaining nozzle configurations. Losses of 1.9 to 3.5 percent in F_r/F_i per 10° of turning occurred when vectoring the flow sideways to produce yaw for $\delta_{v,p} = 0°$. For the two vectored nozzles, losses of 3.8 to 6.3 percent in F_r/F_i occurred for $\delta_{v,p} = -20°$, whereas the nozzle with $\delta_{v,p} = 20°$ experienced losses up to 1.5 percent. These losses for $\delta_{v,p} = 0°$ and $\delta_{v,p} = 20°$ are in general small and similar to those observed previously in references 7 and 8 for comparable yaw vectoring schemes. Because the flow being vectored is downstream of the throat and is thus supersonic, these performance losses are related to shock-induced momentum losses resulting from the supersonic flow turning process and from some sidewall spillage. The effect of a turn-generated shock that probably emanates from the corner of the left hinge line (compression turn) in the direction of turning is shown in the pressure distributions on the ramp in figure 27. For $\delta_{v,y} = 0°$, there is a shock that is located on the ramp at $x_p/l_r \approx 0.55$. This shock moves forward to $x_p/l_r \approx 0.40$ for $\delta_{v,y} = -30°$ because of interaction effects of the turn-generated shock. In addition, the pressure distributions indicate that some shock-induced internal flow separation may be present during single-axis yaw vectoring operation. In contrast to the pitch vectoring of 0° and −20° (figs. 27(a) and 27(b)), pressure measurements indicate that for $\delta_{v,p} = 20°$ (fig. 27(c)), the effect of the turn-generated shock is less than for $\delta_{v,p} = 0°$ and −20° and may explain why greater resultant thrust ratios were achieved for $\delta_{v,p} = 20°$ (fig. 20(c)).

Although higher pressure ratios did improve turning effectiveness slightly, resultant yaw turning angles did not amount to more than 33 to 45 percent of the geometric yaw angle for the three nozzle pitch vector angles tested (fig. 20). These results are typical for other nozzle configurations tested with the yaw hinge line located at $x_r/l_r = 0.42$ and 0.02. (For example, see figs. 21 and 23.) Maximum resultant yaw vector angles achieved were about 20° and occurred at high nozzle pressure ratios for the nozzle with $x_r/l_r = 0.02$ and the maximum sidewall (fig. 23(a)). In general, yaw turning performance is lower than that of reference 8, which utilized a similar simultaneous pitch/yaw vectoring scheme but on a two-dimensional convergent-divergent nozzle. Average resultant yaw vector angles of about 53 percent of the yaw geometric angle were measured for this investigation. The maximum values of δ_y were about 75 percent of the geometric angle.

The effects of yaw vectoring on resultant pitch vector angle vary depending on the geometric pitch vector angle ($\delta_{v,p}$). Unlike geometric pitch vector angles of 0° and 20°, where δ_p increases in magnitude as the sidewall flaps are deflected, resultant pitch turning angle decreased (becomes less negative) as geometric yaw vector angle increased for $\delta_{v,p} = -20°$ to result in about one half the geometric pitch angle setting at $\delta_{v,y} = -30°$ (fig. 20(b)). In general, there was a decrease in negative values of δ_p from 7° to 11° for $\delta_{v,p} = -20°$ for each of the three hinge line locations with both maximum and medium sidewall containments (figs. 21 to 23(b)). For the hinge line location at $x_r/l_r = 0.02$ with the minimum sidewall, only a 4° decrease occurred in negative δ_p values (fig. 23(c)). For the nozzles with $\delta_{v,p} = 0°$ and 20°, just the opposite occurred; that is, δ_p increased from 7° to 11° or 4° for the same nozzle conditions as stated for the nozzle with $\delta_{v,p} = -20°$.

Effect of hinge line location. The one advantage provided by moving the yaw flap hinge lines upstream was an increase in the sidewall area to be used for yaw vectoring without increasing the size of the sidewall itself. As shown in figure 24, resultant yaw angles can be increased as much as 15° by moving the hinge lines forward from $x_r/l_r = 0.42$ to $x_r/l_r = 0.02$ for $\delta_{v,p} = 20°$. Resultant yaw turning was 20 to 42 percent of the geometric flap setting at $x_r/l_r = 0.20$ and about 35 to 70 percent at $x_r/l_r = 0.02$ (100 percent occurs when $\delta_y = \delta_{v,y}$). Yaw turning effectiveness was very low for the hinge line at $x_r/l_r = 0.42$. Resultant yaw angles achieved only 15 to 33 percent of the geometric flap setting, compared with 35 to 70 percent for the location at $x_r/l_r = 0.02$.

Effect of sidewall containment. The effects of sidewall containment or yaw flap length on

nozzle performance are summarized in figures 25 and 26. For $\delta_{v,p} = 0°$ and 20°, increasing sidewall length had little or no effect on resultant yaw angle. However, for $\delta_{v,p} = -20°$, lengthening the sidewalls (i.e., increasing containment) for $x_r/l_r = 0.20$ increased magnitude of the resultant yaw turning angle by almost 8° at $\delta_{v,y} = -30°$ and NPR = 3.0 (fig. 25(a)). However, this improvement in yaw vector performance was accompanied by a loss of resultant thrust that reached values of up to 3.4 percent when $\delta_{v,y} = -30°$. For those nozzle configurations with the yaw hinge line at $x_r/l_r = 0.02$ (fig. 26), increasing the length of the yaw flap resulted in increases in resultant yaw vector angle magnitude of 6° to 8° for the three pitch vector angles tested at NPR = 3.0 and 6.0. Generally (at $\delta_{v,y} = -30°$), most of this increase occurred as the sidewall was increased from medium to maximum containment.

Effect of single yaw flap deflection. Some limited tests were conducted by deflecting either the left yaw flap into the exhaust flow or the right yaw flap out of the flow while maintaining the other flap at 0°. These tests were conducted in order to ascertain the performance of a single flap in producing yaw vectoring. Typical effects of single yaw flap vectoring on nozzle performance are presented in figure 28. In general, most of the resultant yaw vector angle is produced by the flap which is deflected into the exhaust flow (left flap for current test). Some turning results from deflection of the opposing (right) flap out of the exhaust flow. The final resultant yaw vector angle is essentially the sum of the values of deflecting the left and right yaw flaps individually. This is in contrast to the results of reference 20 for a two-dimensional convergent-divergent nozzle with sidewall yaw vector flaps, where nearly equal amounts of resultant yaw vector angles were produced with individual single flap deflections. However for the nozzle of reference 20, the yaw vector angles which resulted from deflection of both flaps were greater than the sum of the yaw angles obtained by deflection of the individual flaps; this indicates a favorable interaction between the left and right yaw flaps.

Effect of Hinge Angle Inclination

The effect of inclining the yaw hinge axis on nozzle performance is shown in figure 29. These results for $x_r/l_r = 0.20$, $\theta = 30°$, $\delta_{v,y} = -30°$, and medium sidewall are typical for the other nozzle configurations. For the entire range of geometric pitch vector angles, but particularly for $\delta_{v,p} = -20°$, inclining the hinge axis had the effect of increasing axial and resultant thrust ratios while shifting δ_p toward more negative values (beneficial for configurations with negative $\delta_{v,p}$ and detrimental for those with positive $\delta_{v,p}$). For example, figure 29(a) shows an increase of nearly 1 percent in resultant thrust ratio with an accompanying decrease in δ_p of about 1° for $\delta_{v,p} = 0°$ as hinge inclination angle ϕ is varied from 0° to 30° over the nozzle pressure range. However, for $\delta_{v,p} = -20°$, F_r/F_i increased up to 3 percent with an increase in δ_p magnitude of about 3° (more negative values of δ_p). These increases in F_r/F_i and δ_p were nearly constant over the range of nozzle pressure ratios and occurred primarily as ϕ was changed from 15° to 30° (fig. 29(c)). When the sidewall yaw flaps are deployed, inclining the hinge axis is believed to create a larger cavity between the upper edge of the receding sidewall and the corresponding side of the upper flap. The slanted sidewall surfaces then force the flow to escape through this cavity; this rotates the thrust vector up. The increase in F_r/F_i is most probably caused by a more obtuse vector angle in yaw that would decrease the strength of the sidewall-generated shock.

Although resultant yaw turning angles were still around 30 percent of the geometric setting for $\delta_{v,y} = -30°$, a small increase occurred in yaw turning effectiveness for $\delta_{v,p} = 20°$ (fig. 29(c)), probably because the sidewall hinge line and exhaust flow centerline were more perpendicular for positive pitch-vectored configurations.

Conclusions

An investigation has been conducted at static conditions in order to determine the internal performance characteristics of a multiaxis thrust vectoring single expansion ramp nozzle. Yaw vectoring was achieved by deflecting yaw flaps in the nozzle sidewalls. In order to eliminate any physical interference between the yaw flap deflected into the exhaust flow and the nozzle upper ramp and lower flap deflected for pitch vectoring, the downstream corners of both the nozzle ramp and flap were cut off to allow for up to 30° of yaw vectoring. The effects of nozzle upper ramp and lower flap cutout, yaw hinge line location and inclination angle, sidewall containment, geometric pitch vector angle, and geometric yaw vector angle were studied. This investigation was conducted in the static-test facility of the Langley 16-Foot Transonic Tunnel at nozzle pressure ratios up to 8.0. An analysis of the results indicates the following conclusions:

1. The removal of the downstream corners of both the upper ramp and lower flap for a yaw hinge line downstream of the nozzle throat had little or no effect on resultant thrust ratio. However, losses of up to 3.4 percent in resultant thrust

ratio occurred with the hinge line located near the nozzle throat.

2. Pitch vectoring performance was primarily influenced by hinge line location rather than ramp cutout. For the nozzle with the hinge line near the nozzle throat, there was a 10.3° decrease in resultant pitch vector angle for the nozzle pitched up 20° and about a 5° decrease for the nozzle pitched down 20°.

3. Yaw thrust vectoring of nozzles with no pitch vectoring caused resultant thrust ratio losses of up to 3.5 percent per 10° of yaw turning and produced resultant yaw vector angles that were typically 33 to 45 percent of the geometric yaw vector angle.

4. Maximum resultant yaw vector angles occurred for the nozzle with the yaw hinge line near the nozzle throat and with the maximum sidewalls.

5. Yaw thrust vectoring decreased the resultant pitch vector angle for the negative pitch-vectored nozzle and increased resultant pitch vector angle for the nozzle with no vectoring or with positive pitch vectoring.

6. Most of the yaw turning was produced from the yaw flap deflected into the nozzle exhaust flow.

NASA Langley Research Center
Hampton, VA 23681-0001
March 10, 1993

References

1. Herbst, W. B.: Future Fighter Technologies. *J. Aircr.*, vol. 17, no. 8, Aug. 1980, pp. 561–566.

2. Costes, Philippe: Investigation of Thrust Vectoring and Post-Stall Capability in Air Combat. *A Collection of Technical Papers, Part 2 AIAA Guidance, Navigation and Control Conference,* Aug. 1988, pp. 893–905. (Available as AIAA-88-4160-CP.)

3. Powers, Sidney A.; and Schellenger, Harvey G.: The X-31: High Performance at Low Cost. AIAA-89-2122, July–Aug. 1989.

4. Berrier, Bobby L.; and Mason, Mary L.: *Static Performance of an Axisymmetric Nozzle With Post-Exit Vanes for Multiaxis Thrust Vectoring.* NASA TP-2800, 1988.

5. Carson, George T., Jr.; and Capone, Francis J.: *Static Internal Performance of an Axisymmetric Nozzle With Multiaxis Thrust-Vectoring Capability.* NASA TM-4237, 1991.

6. Capone, Francis J.; and Bare, E. Ann: *Multiaxis Control Power From Thrust Vectoring for a Supersonic Fighter Aircraft Model at Mach* 0.20 *to* 2.47. NASA TP-2712, 1987.

7. Berrier, Bobby L.: Results From NASA Langley Experimental Studies of Multiaxis Thrust Vectoring Nozzles. *SAE* 1988 *Transactions—Journal of Aerospace,* Section 1—Volume 97, c.1989, pp. 1.1289–1.1304. (Available as SAE Paper 881481.)

8. Taylor, John T.: *Static Investigation of a Two-Dimensional Convergent-Divergent Exhaust Nozzle With Multiaxis Thrust-Vectoring Capability.* NASA TP-2973, 1990.

9. Capone, Francis J.; Mason, Mary L.; and Carson, George T., Jr.: *Aeropropulsive Characteristics of Canted Twin Pitch-Vectoring Nozzles at Mach* 0.20 *to* 1.20. NASA TP-3060, 1991.

10. Dusa, D. J.; and Wooten, W. H.: Single Expansion Ramp Nozzle Development Status. AIAA-84-2455, Oct.–Nov. 1984.

11. Capone, Francis J.; and Berrier, Bobby L.: *Investigation of Axisymmetric and Nonaxisymmetric Nozzles Installed on a* 0.10*-Scale F-18 Prototype Model.* NASA TP-1638, 1980.

12. Re, Richard J.; and Berrier, Bobby L.: *Static Internal Performance of Single Expansion-Ramp Nozzles With Thrust Vectoring and Reversing.* NASA TP-1962, 1982.

13. Berrier, Bobby L.; and Leavitt, Laurence D.: *Static Internal Performance of Single-Expansion-Ramp Nozzles With Thrust Vectoring Capability up to* 60°. NASA TP-2364, 1984.

14. Capone, Francis J.; Re, Richard J.; and Bare, E. Ann: *Parametric Investigation of Single-Expansion-Ramp Nozzles at Mach Numbers From* 0.60 *to* 1.20. NASA TP-3240, 1992.

15. Schirmer, Alberto W.; and Capone, Francis J.: Parametric Study of a Simultaneous Pitch/Yaw Thrust Vectoring Single Expansion Ramp Nozzle. AIAA-89-2812, July 1989.

16. Mercer, Charles E.; Berrier, Bobby L.; Capone, Francis J.; and Grayston, Alan M.: *Data Reduction Formula for the* 16*-Foot Transonic Tunnel NASA Langley Research Center,* Revision 2. NASA TM-107646, 1992.

17. Staff of the Propulsion Aerodynamics Branch: *A User's Guide to the Langley* 16*-Foot Transonic Tunnel Complex,* Revision 1. NASA TM-102750, 1990.

18. Stitt, Leonard E.: *Exhaust Nozzles for Propulsion Systems With Emphasis on Supersonic Cruise Aircraft.* NASA RP-1235, 1990.

19. Leavitt, Laurence D.; and Bangert, Linda S.: *Performance Characteristics of Axisymmetric Convergent-Divergent Exhaust Nozzles With Longitudinal Slots in the Divergent Flaps.* NASA TP-2013, 1982.

20. Mason, Mary L.; and Berrier, Bobby L.: *Static Investigation of Several Yaw Vectoring Concepts on Nonaxisymmetric Nozzles.* NASA TP-2432, 1985.

Table 1. Nozzle Configurations Tested and Index to Data Tables

Test nozzle	$\delta_{v,p}$, deg	$\delta_{v,y}$, deg	x_r/l_r	θ, deg	ϕ, deg	Ramp/ flap	Containment/ sidewall number	Table number for—	
								Performance data	Pressure data
1	0	0	1.00	0	0	A/A	Min/21	6	68
2	0	0	1.00	0	0	A/A	Med/12	6	69
3	0	0	1.00	0	0	A/A	Max/1	6	70
4	0	0	0.42	20	0	A/A	Min/21	7	71
5	0	0	0.42	20	0	A/A	Med/12	7	72
6	0	0	0.42	20	0	A/A	Max/1	7	73
7	0	0	0.20	20	0	A/A	Min/21	8	74
8	0	0	0.20	20	0	A/A	Med/12	8	75
9	0	0	0.20	20	0	A/A	Max/1	8	76
10	0	0	0.02	20	0	A/A	Min/21	9	77
11	0	0	0.02	20	0	A/A	Med/12	9	78
12	0	0	0.02	20	0	A/A	Max/1	9	79
13	0	−20	0.42	20	0	A/A	Max/6	10	80
14	0	−20	0.20	20	0	A/A	Med/15	11	81
15	0	−20	0.20	20	0	A/A	Max/4	11	82
16	0	−20	0.02	20	0	A/A	Min/22	12	83
17	0	−20	0.02	20	0	A/A	Med/13	12	84
18	0	−20	0.02	20	0	A/A	Max/2	12	85
19	0	0	0.42	30	0	A/A	Min/21	13	86
20	0	0	0.42	30	0	A/A	Med/12	13	87
21	0	0	0.42	30	0	A/A	Max/1	13	88
22	0	0	0.20	30	0	A/A	Min/21	14	89
23	0	0	0.20	30	0	A/A	Med/12	14	90
24	0	0	0.20	30	0	A/A	Max/1	14	91
25	0	0	0.02	30	0	A/A	Min/21	15	92
26	0	0	0.02	30	0	A/A	Med/12	15	93
27	0	0	0.02	30	0	A/A	Max/1	15	94
28	0	−20	0.20	30	0	A/A	Med/15	16	
29	0	−20	0.20	30	0	A/A	Max/4	16	
30	0	−20	0.02	30	0	A/A	Med/13	17	
31	0	−20	0.02	30	0	A/A	Max/2	17	
32	0	−30	0.42	30	0	A/A	Max/7	18	95
33	0	−30	0.20	30	0	A/A	Med/16	19	96
34	0	−30	0.20	30	0	A/A	Max/5	19	97
35	0	−30	0.02	30	0	A/A	Min/23	20	98
36	0	−30	0.02	30	0	A/A	Med/14	20	99
37	0	−30	0.02	30	0	A/A	Max/3	20	100

Table 1. Continued

Test nozzle	$\delta_{v,p}$, deg	$\delta_{v,y}$, deg	x_r/l_r	θ, deg	ϕ, deg	Ramp/ flap	Containment/ sidewall number	Table number for—	
								Performance data	Pressure data
38	−20	0	1.00	0	0	B/A	Min/21	21	101
39	−20	0	1.00	0	0	B/A	Med/12	21	102
40	−20	0	1.00	0	0	B/A	Max/1	21	103
41	−20	0	0.42	20	0	B/A	Min/21	22	104
42	−20	0	0.42	20	0	B/A	Med/12	22	105
43	−20	0	0.42	20	0	B/A	Max/1	22	106
44	−20	0	0.20	20	0	B/A	Min/21	23	107
45	−20	0	0.20	20	0	B/A	Med/12	23	108
46	−20	0	0.20	20	0	B/A	Max/1	23	109
47	−20	0	0.02	20	0	B/A	Min/21	24	110
48	−20	0	0.02	20	0	B/A	Med/12	24	111
49	−20	0	0.02	20	0	B/A	Max/1	24	112
50	−20	−20	0.42	20	0	B/A	Max/6	25	113
51	−20	−20	0.20	20	0	B/A	Med/15	26	114
52	−20	−20	0.20	20	0	B/A	Max/4	26	115
53	−20	−20	0.02	20	0	B/A	Min/22	27	116
54	−20	−20	0.02	20	0	B/A	Med/13	27	117
55	−20	−20	0.02	20	0	B/A	Max/2	27	118
56	−20	0	0.42	30	0	B/A	Min/21	28	119
57	−20	0	0.42	30	0	B/A	Med/12	28	120
58	−20	0	0.42	30	0	B/A	Max/1	28	121
59	−20	0	0.20	30	0	B/A	Min/21	29	122
60	−20	0	0.20	30	0	B/A	Med/12	29	123
61	−20	0	0.20	30	0	B/A	Max/1	29	124
62	−20	0	0.02	30	0	B/A	Min/21	30	125
63	−20	0	0.02	30	0	B/A	Med/12	30	126
64	−20	0	0.02	30	0	B/A	Max/1	30	127
65	−20	−20	0.20	30	0	B/A	Med/15	31	
66	−20	−20	0.20	30	0	B/A	Max/4	31	
67	−20	−20	0.02	30	0	B/A	Med/13	32	
68	−20	−20	0.02	30	0	B/A	Max/2	32	
69	−20	−30	0.42	30	0	B/A	Max/7	33	128
70	−20	−30	0.20	30	0	B/A	Med/16	34	129
71	−20	−30	0.20	30	0	B/A	Max/5	34	130
72	−20	−30	0.02	30	0	B/A	Min/23	35	131
73	−20	−30	0.02	30	0	B/A	Med/14	35	132
74	−20	−30	0.02	30	0	B/A	Max/4	35	133

Table 1. Continued

Test nozzle	$\delta_{v,p}$, deg	$\delta_{v,y}$, deg	x_r/l_r	θ, deg	ϕ, deg	Ramp/ flap	Containment/ sidewall number	Table number for—	
								Performance data	Pressure data
75	20	0	1.00	0	0	C/B	Min/21	36	134
76	20	0	1.00	0	0	C/B	Med/12	36	135
77	20	0	1.00	0	0	C/B	Max/1	36	136
78	20	0	0.42	20	0	C/B	Min/21	37	137
79	20	0	0.42	20	0	C/B	Med/12	37	138
80	20	0	0.42	20	0	C/B	Max/1	37	139
81	20	0	0.20	20	0	C/B	Min/21	38	140
82	20	0	0.20	20	0	C/B	Med/12	38	141
83	20	0	0.20	20	0	C/B	Max/1	38	142
84	20	0	0.02	20	0	C/B	Min/21	39	143
85	20	0	0.02	20	0	C/B	Med/12	39	144
86	20	0	0.02	20	0	C/B	Max/1	39	145
87	20	−20	0.42	20	0	C/B	Max/6	40	146
88	20	−20	0.20	20	0	C/B	Med/15	41	147
89	20	−20	0.20	20	0	C/B	Max/4	41	148
90	20	−20	0.02	20	0	C/B	Min/22	42	149
91	20	−20	0.02	20	0	C/B	Med/13	42	150
92	20	−20	0.02	20	0	C/B	Max/2	42	151
93	20	0	0.42	30	0	C/B	Min/21	43	152
94	20	0	0.42	30	0	C/B	Med/12	43	153
95	20	0	0.42	30	0	C/B	Max/1	43	154
96	20	0	0.20	30	0	C/B	Min/21	44	155
97	20	0	0.20	30	0	C/B	Med/12	44	156
98	20	0	0.20	30	0	C/B	Max/1	44	157
99	20	0	0.02	30	0	C/B	Min/21	45	158
100	20	0	0.02	30	0	C/B	Med/12	45	159
101	20	0	0.02	30	0	C/B	Max/1	45	160
102	20	−20	0.20	30	0	C/B	Med/15	46	
103	20	−20	0.20	30	0	C/B	Max/4	46	
104	20	−20	0.02	30	0	C/B	Med/13	47	
105	20	−20	0.02	30	0	C/B	Max/2	47	
106	20	−30	0.42	30	0	C/B	Max/7	48	161
107	20	−30	0.20	30	0	C/B	Med/16	49	162
108	20	−30	0.20	30	0	C/B	Max/5	49	163
109	20	−30	0.02	30	0	C/B	Min/23	50	164
110	20	−30	0.02	30	0	C/B	Med/14	50	165
111	20	−30	0.02	30	0	C/B	Max/3	50	166

Table 1. Concluded

Test nozzle	$\delta_{v,p}$, deg	$\delta_{v,y}$, deg	x_r/l_r	θ, deg	ϕ, deg	Ramp/ flap	Containment/ sidewall number	Table number for—	
								Performance data	Pressure data
112	0	−20/0	0.02	20	0	A/A	Max/2	51	
113	0	0/−20	0.02	20	0	A/A	Max/2	51	
114	0	−20/0	0.20	20	0	A/A	Max/4	52	
115	0	0/−20	0.20	20	0	A/A	Max/4	52	
116	0	−30/0	0.20	30	0	A/A	Max/4	53	
117	0	0/−30	0.20	30	0	A/A	Max/4	53	
118	20	−20/0	0.02	20	0	C/B	Max/2	54	
119	20	0/−20	0.02	20	0	C/B	Max/2	54	
120	20	−30/0	0.20	30	0	C/B	Max/4	55	
121	20	0/−30	0.20	30	0	C/B	Max/4	55	
122	0	−15	0.20	30	15	A/A	Med/17	56	167
123	0	−15	0.20	30	15	A/A	Max/8	56	168
124	0	−30	0.20	30	15	A/A	Med/19	57	169
125	0	−30	0.20	30	15	A/A	Max/10	57	170
126	0	−15	0.20	30	30	A/A	Med/18	58	171
127	0	−15	0.20	30	30	A/A	Max/9	58	172
128	0	−30	0.20	30	30	A/A	Med/20	59	173
129	0	−30	0.20	30	30	A/A	Max/11	59	174
130	−20	−15	0.20	30	15	B/A	Med/17	60	175
131	−20	−15	0.20	30	15	B/A	Max/8	60	176
132	−20	−30	0.20	30	15	B/A	Med/19	61	177
133	−20	−30	0.20	30	15	B/A	Max/10	61	178
134	−20	−15	0.20	30	30	B/A	Med/18	62	179
135	−20	−15	0.20	30	30	B/A	Max/9	62	180
136	−20	−30	0.20	30	30	B/A	Med/20	63	181
137	−20	−30	0.20	30	30	B/A	Max/11	63	182
138	20	−15	0.20	30	15	C/B	Med/17	64	183
139	20	−15	0.20	30	15	C/B	Max/8	64	184
140	20	−30	0.20	30	15	C/B	Med/19	65	185
141	20	−30	0.20	30	15	C/B	Max/10	65	186
142	20	−15	0.20	30	30	C/B	Med/18	66	187
143	20	−15	0.20	30	30	C/B	Max/9	66	188
144	20	−30	0.20	30	30	C/B	Med/20	67	189
145	20	−30	0.20	30	30	C/B	Max/11	67	190

Table 2. Coordinates for Upper Ramp

Ramp A		Ramp B		Ramp C	
x, in.	y, in.	x, in.	y, in.	x, in.	y, in.
0.000	1.390	0.000	1.390	0.000	1.390
1.437	1.390	1.437	1.390	1.437	1.390
1.521	1.376	1.521	1.376	1.521	1.376
1.688	1.312	1.688	1.312	1.688	1.312
1.855	1.230	1.855	1.230	1.855	1.230
1.883	1.215	1.883	1.215	1.883	1.215
3.555	0.274	3.555	0.274	3.555	0.274
3.722	0.197	3.722	0.197	3.722	0.197
3.889	0.148	3.889	0.148	3.889	0.148
5.065	0.125	5.065	0.125	5.065	0.125
4.224	0.122	4.224	0.122	4.224	0.122
4.310	0.133	4.310	0.133	4.310	0.133
4.558	0.156	4.558	0.156	4.558	0.156
4.756	0.223	4.753	0.188	4.753	0.154
4.954	0.332	4.948	0.223	4.905	0.123
5.201	0.470	5.227	0.269	5.182	0.070
5.449	0.601	5.505	0.306	5.457	0.010
5.699	0.729	5.784	0.342	5.731	−0.052
5.950	0.856	6.062	0.371	6.004	−0.116
6.202	0.979	6.341	0.404	6.276	−0.184
6.354	1.049	6.508	0.418	6.438	−0.228
6.584	1.150	6.759	0.435	6.679	−0.298
6.839	1.263	7.038	0.453	6.947	−0.376
7.019	1.338	7.232	0.462	7.134	−0.434
7.950	1.714	8.236	0.497	8.088	−0.744

Table 3. Coordinates for Lower Flap

Flap A		Flap B	
x, in.	y, in.	x, in.	y, in.
0.000	−1.391	0.000	−1.391
0.697	−1.391	0.697	−1.391
1.187	−1.397	1.187	−1.397
1.214	−1.397	1.214	−1.397
1.382	−1.383	1.382	−1.383
1.549	−1.354	1.549	−1.354
1.716	−1.329	1.716	−1.329
1.883	−1.321	1.883	−1.321
1.967	−1.321	1.967	−1.321
2.440	−1.303	2.450	−1.302
2.998	−1.237	3.009	−1.282
3.555	−1.130	3.571	−1.119
4.112	−0.986	4.134	−1.082
4.669	−0.825	4.698	−0.946
4.753	−0.811	4.782	−0.936
4.837	−0.801	4.866	−0.929
4.920	−0.794	4.950	−0.926
5.004	−0.791	5.034	−0.927
5.087	−0.793	5.117	−0.932
5.171	−0.798	5.200	−0.941
5.254	−0.806	5.283	−0.954
5.338	−0.819	5.366	−0.970

Table 4. Coordinates for Sidewalls

[Values of z are for left sidewall; values of z for right sidewall are negative of those given]

Maximum containment, sidewall 1

x, in.	y, in.	z, in.
0.000	2.375	0.000
4.969	2.275	0.000
7.950	1.714	0.000
8.146	1.118	0.000
8.236	0.497	0.000
8.216	−0.130	0.000
6.137	−0.964	0.000
5.407	−1.670	0.000
3.213	−2.375	0.000
0.000	−2.375	0.000

Maximum containment, sidewall 2

x, in.	y, in.	z, in.
0.000	2.375	0.000
4.696	2.275	0.000
7.754	1.714	1.113
7.938	1.118	1.180
8.022	0.497	1.211
8.004	−0.130	1.204
6.050	−0.964	0.493
5.364	−1.670	0.244
4.696	−1.890	0.000
3.213	−2.375	0.000
0.000	−2.375	0.000

Maximum containment, sidewall 3

x, in.	y, in.	z, in.
0.000	2.375	0.000
4.696	2.375	0.000
7.514	1.714	1.627
7.684	1.118	1.725
7.762	0.497	1.770
7.745	−0.130	1.760
5.944	−0.964	0.720
5.312	−1.670	0.356
4.696	−1.890	0.000
3.213	−2.375	0.000
0.000	−2.375	0.000

Maximum containment, sidewall 4

x, in.	y, in.	z, in.
0.000	2.375	0.000
4.696	2.375	0.000
5.360	1.714	0.000
7.794	1.118	0.886
7.798	0.497	0.953
8.062	−0.130	0.984
6.090	−0.964	0.977
5.404	−1.670	0.266
5.360	−1.890	0.000
3.213	−2.375	0.000
0.000	−2.375	0.000

Maximum containment, sidewall 5

x, in.	y, in.	z, in.
0.000	2.375	0.000
4.696	2.375	0.000
5.360	2.240	0.000
7.063	1.714	1.295
7.773	1.118	1.393
7.851	0.497	1.438
7.834	−0.130	1.428
6.033	−0.964	0.388
5.401	−1.670	0.024
5.360	−1.690	0.000
3.213	−2.375	0.000
0.000	−2.375	0.000

Maximum containment, sidewall 6

x, in.	y, in.	z, in.
0.000	2.375	0.000
4.696	2.375	0.000
6.137	2.082	0.000
7.841	1.714	0.620
8.025	1.118	0.687
8.109	0.497	0.718
8.091	−0.130	0.711
6.137	−0.964	0.000
3.213	−2.375	0.000
0.000	−2.375	0.000

Table 4. Continued

Maximum containment, sidewall 7

x, in.	y, in.	z, in.
0.000	2.375	0.000
4.696	2.375	0.000
6.137	2.082	0.000
7.003	1.714	0.907
7.877	1.118	1.005
7.954	0.497	1.050
7.938	−0.130	1.040
6.137	−0.965	0.000
3.213	−2.375	0.000
0.000	−2.375	0.000

Maximum containment, sidewall 8

x, in.	y, in.	z, in.
0.000	2.375	0.000
4.696	2.375	0.000
5.929	2.117	0.000
7.882	1.732	0.389
8.067	1.139	0.480
8.149	0.521	0.580
8.124	−0.105	0.623
6.104	−0.956	0.299
5.391	−1.670	0.277
4.866	−1.830	0.000
3.213	−2.375	0.000
0.000	−2.375	0.000

Maximum containment, sidewall 9

x, in.	y, in.	z, in.
0.000	2.375	0.000
4.696	2.375	0.000
5.929	2.117	0.000
7.684	1.786	1.029
7.835	1.202	1.201
7.893	0.589	1.325
7.855	−0.033	1.396
6.007	−0.930	0.500
5.345	−1.650	0.239
4.866	−1.830	0.000
3.213	0.000	0.000
0.000	0.000	0.000

Maximum containment, sidewall 10

x, in.	y, in.	z, in.
0.000	2.375	0.000
4.696	2.375	0.000
6.518	2.117	0.000
7.909	1.732	0.389
8.091	1.139	0.480
8.170	0.521	0.580
8.145	−0.105	0.623
6.103	−0.956	0.299
5.381	−1.670	0.277
4.165	−1.830	0.000
3.213	−2.375	0.000
0.000	−2.375	0.000

Maximum containment, sidewall 11

x, in.	y, in.	z, in.
0.000	2.375	0.000
4.696	2.375	0.000
6.518	2.008	0.000
7.789	1.807	0.693
7.931	1.242	0.927
7.976	0.648	1.121
7.922	0.040	1.269
6.003	−0.887	0.577
5.304	−1.610	0.438
4.165	−2.080	0.000
3.213	−2.375	0.000
0.000	−2.375	0.000

Medium containment, sidewall 12

x, in.	y, in.	z, in.
0.000	2.375	0.000
4.969	2.375	0.000
6.350	2.039	0.000
6.958	0.000	0.000
6.167	−0.967	0.000
5.407	−1.670	0.000
3.213	−2.375	0.000
0.000	−2.375	0.000

Table 4. Continued

Medium containment, sidewall 13

x, in.	y, in.	z, in.
0.000	2.375	0.000
4.696	2.375	0.000
6.250	2.039	0.566
6.822	0.000	0.744
6.078	−0.967	0.503
5.364	−1.670	0.243
4.696	−1.890	0.000
3.213	−2.375	0.000
0.000	−2.375	0.000

Medium containment, sidewall 14

x, in.	y, in.	z, in.
0.000	2.375	0.000
4.696	2.375	0.000
6.129	2.039	0.827
6.655	0.000	1.131
5.970	−0.967	0.735
5.312	−1.670	0.355
4.696	−1.890	0.000
3.213	−2.375	0.000
0.000	−2.375	0.000

Medium containment, sidewall 15

x, in.	y, in.	z, in.
0.000	2.375	0.000
4.696	2.375	0.000
5.360	2.240	0.000
6.291	2.039	0.339
6.862	0.000	0.547
6.118	−0.967	0.276
5.404	−1.670	0.016
5.360	−1.690	0.000
3.213	−2.375	0.000
0.000	−2.375	0.000

Medium containment, sidewall 16

x, in.	y, in.	z, in.
0.000	2.375	0.000
4.696	2.375	0.000
4.360	2.240	0.000
6.218	2.039	0.495
6.744	0.000	0.799
6.507	−0.967	0.403
5.401	−1.670	0.024
5.360	−1.690	0.000
3.213	−2.375	0.000
0.000	−2.375	0.000

Medium containment, sidewall 17

x, in.	y, in.	z, in.
0.000	2.375	0.000
4.696	2.375	0.000
5.929	2.117	0.000
6.336	2.043	0.111
6.908	0.014	0.400
6.133	−0.958	0.266
5.391	−1.650	0.124
4.860	−1.890	0.000
3.213	−2.375	0.000
0.000	−2.375	0.000

Medium containment, sidewall 18

x, in.	y, in.	z, in.
0.000	2.375	0.000
4.696	2.375	0.000
5.929	2.117	0.000
6.295	2.054	0.214
6.759	0.054	0.772
6.034	−0.931	0.515
5.345	−1.660	0.239
4.860	−1.560	0.000
3.213	−2.375	0.000
0.000	−2.375	0.000

Table 4. Concluded

Medium containment, sidewall 19

x, in.	y, in.	z, in.
0.000	2.375	0.000
4.696	2.375	0.000
6.350	2.039	0.000
6.414	2.008	0.000
6.918	0.024	0.358
6.132	−0.947	0.306
5.381	−1.650	0.227
4.165	−1.880	0.000
3.213	−2.375	0.000
0.000	−2.375	0.000

Medium containment, sidewall 20

x, in.	y, in.	z, in.
0.000	2.375	0.000
4.696	2.375	0.000
6.350	2.039	0.000
6.414	2.008	0.000
6.797	0.093	0.692
6.030	−0.888	0.591
5.305	−1.610	0.438
4.165	−1.880	0.000
3.213	−2.375	0.000
0.000	−2.375	0.000

Minimum containment, sidewall 21

x, in.	y, in.	z, in.
0.000	2.375	0.000
4.696	2.375	0.000
5.394	0.825	0.000
5.867	0.017	0.000
5.338	−0.819	0.000
3.213	−2.375	0.000
0.000	−2.375	0.000

Minimum containment, sidewall 22

x, in.	y, in.	z, in.
0.000	2.375	0.000
4.696	2.375	0.000
5.352	0.825	0.239
5.797	0.017	0.401
5.229	−0.819	0.220
3.213	−2.375	0.000
0.000	−2.375	0.000

Minimum containment, sidewall 23

x, in.	y, in.	z, in.
0.000	2.375	0.000
4.696	2.375	0.000
5.300	0.825	0.349
5.711	0.017	0.589
5.252	−0.819	0.321
3.213	−2.375	0.000
0.000	−2.375	0.000

Table 5. Location of Ramp and Flap Pressure Orifices

[All pressure orifices are located on centerline of ramp or flap]

(a) Upper ramp

$\delta_{v,p} = 0°$ and $-20°$		$\delta_{v,p} = 20°$	
x_p, in.	x_p/l_r	x_p, in.	x_p/l_r
−1.115	−0.308		
−0.615	−0.170	−0.615	−0.170
−0.365	−0.101		
−0.115	−0.032	−0.115	−0.032
0.135	0.037		
0.385	0.106	0.385	0.106
0.635	0.175	0.635	0.175
0.885	0.244	0.885	0.244
1.385	0.382	1.385	0.382
1.885	0.520	1.885	0.520
2.385	0.659	2.385	0.659
2.885	0.797	2.885	0.797

(b) All lower flaps

x_p, in.	x_p/l_r
−1.115	−0.308
−0.615	−0.170
−0.115	−0.032
0.135	0.037
0.285	0.079
0.435	0.120
0.585	0.162

Table 6. Static Performance Characteristics for Nozzles With $x_r/l_r = 1.00$, $\theta = 0°$, $\phi = 0°$, $\delta_{v,p} = 0°$, and $\delta_{v,y} = 0°$

NPR	F_r/F_i	F/F_i	δ_p, deg	δ_y, deg	w_p/w_i
(a) Nozzle 1, minimum sidewall					
2.00	0.9779	0.9762	−3.37	−0.49	0.9952
2.50	0.9840	0.9828	−2.79	−0.38	0.9944
3.00	0.9863	0.9862	0.65	−0.39	0.9955
3.50	0.9901	0.9894	−2.16	−0.27	0.9962
4.00	0.9899	0.9888	−2.66	−0.21	0.9974
5.01	0.9883	0.9882	−0.80	−0.16	0.9980
6.00	0.9845	0.9838	2.06	−0.22	0.9996
7.00	0.9828	0.9798	4.48	−0.22	1.0009
8.00	0.9828	0.9765	6.50	−0.27	1.0020
(b) Nozzle 2, medium sidewall					
2.00	0.9815	0.9807	−2.33	−0.47	0.9948
2.50	0.9824	0.9813	−2.70	−0.50	0.9946
3.00	0.9830	0.9830	−0.18	−0.41	0.9946
3.50	0.9867	0.9842	−4.10	−0.28	0.9962
4.00	0.9885	0.9865	−3.61	−0.25	0.9971
5.00	0.9876	0.9876	−0.26	−0.23	0.9976
6.00	0.9854	0.9838	3.27	−0.27	0.9987
7.00	0.9862	0.9805	6.15	−0.34	0.9999
8.00	0.9874	0.9769	8.35	−0.37	1.0011
(c) Nozzle 3, maximum sidewall					
2.00	0.9780	0.9776	−1.66	−0.45	0.9934
2.50	0.9836	0.9834	−1.16	−0.39	0.9924
3.00	0.9846	0.9842	1.43	−0.46	0.9933
3.50	0.9882	0.9844	−5.01	−0.32	0.9943
4.00	0.9893	0.9854	−5.04	−0.16	0.9958
5.00	0.9880	0.9877	−1.34	−0.16	0.9965
6.00	0.9856	0.9844	2.91	−0.22	0.9979
7.00	0.9862	0.9807	6.08	−0.30	0.9996
8.00	0.9887	0.9779	8.47	−0.33	1.0006

Table 7. Static Performance Characteristics for Nozzles With $x_r/l_r = 0.42$, $\theta = 20°$, $\phi = 0°$, $\delta_{v,p} = 0°$, and $\delta_{v,y} = 0°$

NPR	F_r/F_i	F/F_i	δ_p, deg	δ_y, deg	w_p/w_i
(a) Nozzle 4, minimum sidewall					
2.00	0.9798	0.9777	−3.71	−0.57	0.9902
2.50	0.9873	0.9861	−2.81	−0.60	0.9895
3.00	0.9891	0.9891	−0.02	−0.44	0.9903
3.50	0.9920	0.9912	−2.26	−0.34	0.9914
4.00	0.9921	0.9911	−2.57	−0.31	0.9922
5.00	0.9898	0.9898	−0.30	−0.23	0.9928
6.00	0.9867	0.9854	2.93	−0.27	0.9953
7.00	0.9861	0.9820	5.24	−0.29	0.9957
8.01	0.9858	0.9781	7.15	−0.31	0.9967
(b) Nozzle 5, medium sidewall					
2.00	0.9812	0.9798	−2.99	−0.55	0.9915
2.50	0.9838	0.9820	−3.50	−0.55	0.9913
3.00	0.9866	0.9865	−0.76	−0.49	0.9919
3.50	0.9905	0.9892	−2.88	−0.38	0.9927
4.00	0.9914	0.9904	−2.62	−0.33	0.9939
5.00	0.9901	0.9900	0.34	−0.31	0.9946
6.00	0.9876	0.9857	3.57	−0.29	0.9958
7.00	0.9871	0.9815	6.12	−0.33	0.9969
8.00	0.9874	0.9776	8.08	−0.35	0.9979
(c) Nozzle 6, maximum sidewall					
2.00	0.9781	0.9768	−2.84	−0.54	0.9912
2.50	0.9796	0.9779	−3.38	−0.42	0.9904
3.00	0.9855	0.9854	−0.65	−0.31	0.9911
3.50	0.9894	0.9880	−3.03	−0.31	0.9921
4.00	0.9908	0.9897	−2.57	−0.27	0.9929
5.00	0.9889	0.9889	0.37	−0.25	0.9939
6.00	0.9866	0.9846	3.59	−0.23	0.9953
7.00	0.9869	0.9812	6.14	−0.25	0.9963
8.00	0.9867	0.9768	8.12	−0.29	0.9979

Table 8. Static Performance Characteristics for Nozzles With $x_r/l_r = 0.20$, $\theta = 20°$, $\phi = 0°$, $\delta_{v,p} = 0°$, and $\delta_{v,y} = 0°$

NPR	F_r/F_i	F/F_i	δ_p, deg	δ_y, deg	w_p/w_i
(a) Nozzle 7, minimum sidewall					
2.00	0.9815	0.9789	−4.17	−0.58	0.9931
2.50	0.9863	0.9848	−3.16	−0.49	0.9925
3.00	0.9905	0.9903	−0.98	−0.49	0.9928
3.51	0.9922	0.9914	−2.30	−0.37	0.9939
4.00	0.9912	0.9904	−2.26	−0.33	0.9951
5.00	0.9896	0.9895	0.21	−0.30	0.9952
6.00	0.9850	0.9837	2.92	−0.30	0.9965
7.01	0.9827	0.9789	5.03	−0.34	0.9973
8.00	0.9802	0.9734	6.72	−0.35	0.9986
(b) Nozzle 8, medium sidewall					
2.00	0.9783	0.9756	−4.20	−0.49	0.9918
2.50	0.9840	0.9822	−3.43	−0.36	0.9915
3.00	0.9870	0.9867	−1.39	−0.32	0.9923
3.51	0.9886	0.9875	−2.65	−0.30	0.9935
4.00	0.9893	0.9883	−2.50	−0.30	0.9941
5.00	0.9859	0.9859	0.13	−0.27	0.9951
6.00	0.9831	0.9819	2.86	−0.25	0.9961
7.00	0.9803	0.9765	5.08	−0.17	0.9974
8.00	0.9781	0.9711	6.85	−0.16	0.9988
(c) Nozzle 9, maximum sidewall					
2.00	0.9759	0.9732	−4.19	−0.64	0.9910
2.50	0.9815	0.9798	−3.29	−0.47	0.9915
3.00	0.9847	0.9844	−1.23	−0.40	0.9919
3.50	0.9880	0.9869	−2.67	−0.30	0.9929
3.50	0.9883	0.9872	−2.70	−0.34	0.9932
4.00	0.9887	0.9878	−2.42	−0.30	0.9947
5.01	0.9857	0.9857	0.23	−0.23	0.9952
6.00	0.9821	0.9808	2.96	−0.25	0.9966
7.01	0.9795	0.9756	5.14	−0.27	0.9979
8.00	0.9774	0.9704	6.87	−0.28	0.9993

Table 9. Static Performance Characteristics for Nozzles With $x_r/l_r = 0.02$, $\theta = 20°$, $\phi = 0°$, $\delta_{v,p} = 0°$, and $\delta_{v,y} = 0°$

NPR	F_r/F_i	F/F_i	δ_p, deg	δ_y, deg	w_p/w_i
(a) Nozzle 10, minimum sidewall					
2.00	0.9787	0.9764	−3.91	−0.35	0.9828
2.50	0.9813	0.9788	−4.08	−0.27	0.9824
3.00	0.9828	0.9817	−2.77	−0.32	0.9830
3.49	0.9814	0.9796	−3.47	−0.29	0.9843
4.00	0.9801	0.9780	−3.76	−0.19	0.9853
5.00	0.9712	0.9708	−1.66	−0.19	0.9862
6.00	0.9646	0.9645	0.89	−0.28	0.9872
7.99	0.9569	0.9541	4.33	−0.25	0.9894
(b) Nozzle 11, medium sidewall					
2.00	0.9794	0.9769	−4.12	−0.50	0.9860
2.50	0.9804	0.9778	−4.12	−0.45	0.9863
3.00	0.9788	0.9775	−2.97	−0.35	0.9868
3.50	0.9803	0.9785	−3.43	−0.33	0.9881
4.00	0.9786	0.9766	−3.64	−0.19	0.9887
5.00	0.9723	0.9721	−1.25	−0.03	0.9894
5.99	0.9660	0.9658	1.04	0.26	0.9908
8.00	0.9584	0.9552	4.68	−0.34	0.9932
(c) Nozzle 12, maximum sidewall					
2.00	0.9773	0.9749	−4.01	−0.32	0.9842
2.50	0.9782	0.9759	−3.98	−0.33	0.9841
3.00	0.9783	0.9772	−2.72	−0.35	0.9854
3.51	0.9795	0.9780	−3.18	−0.25	0.9862
4.00	0.9774	0.9756	−3.47	−0.24	0.9879
5.00	0.9725	0.9723	−1.09	−0.21	0.9888
6.00	0.9670	0.9667	1.38	−0.09	0.9901
8.00	0.9581	0.9549	4.70	−0.23	0.9930

Table 10. Static Performance Characteristics for Nozzles With $x_r/l_r = 0.42$, $\theta = 20°$, $\phi = 0°$, $\delta_{v,p} = 0°$, and $\delta_{v,y} = -20°$

NPR	F_r/F_i	F/F_i	δ_p, deg	δ_y, deg	w_p/w_i
Nozzle 13, maximum sidewall					
2.01	0.9604	0.9539	1.68	−6.48	0.9917
2.51	0.9631	0.9563	2.59	−6.28	0.9919
3.05	0.9679	0.9600	4.43	−5.83	0.9928
3.00	0.9664	0.9585	4.34	−5.93	0.9923
3.50	0.9683	0.9614	4.05	−5.48	0.9932
4.00	0.9673	0.9616	3.53	−5.19	0.9947
5.00	0.9658	0.9577	4.96	−5.56	0.9952
6.00	0.9687	0.9569	7.25	−5.34	0.9962
7.01	0.9713	0.9539	9.52	−5.34	0.9976
8.01	0.9738	0.9504	11.38	−5.49	0.9986

Table 11. Static Performance Characteristics for Nozzles With $x_r/l_r = 0.20$, $\theta = 20°$, $\phi = 0°$, $\delta_{v,p} = 0°$, and $\delta_{v,y} = -20°$

NPR	F_r/F_i	F/F_i	δ_p, deg	δ_y, deg	w_p/w_i
(a) Nozzle 14, medium sidewall					
2.00	0.9644	0.9599	−0.02	−5.58	0.9907
2.50	0.9641	0.9596	1.01	−5.46	0.9898
3.00	0.9702	0.9651	2.72	−5.19	0.9909
3.50	0.9697	0.9640	2.83	−5.52	0.9917
4.00	0.9701	0.9633	3.51	−5.86	0.9928
5.00	0.9718	0.9612	5.87	−6.17	0.9929
6.00	0.9712	0.9551	8.13	−6.63	0.9944
7.00	0.9721	0.9498	10.17	−7.05	0.9959
8.00	0.9734	0.9456	11.80	−7.22	0.9970
(b) Nozzle 15, maximum sidewall					
2.00	0.9551	0.9457	2.58	−7.65	0.9923
2.50	0.9582	0.9479	3.83	−7.53	0.9923
3.00	0.9658	0.9542	5.28	−7.15	0.9924
3.50	0.9667	0.9565	4.77	−6.87	0.9939
4.00	0.9668	0.9559	5.01	−7.08	0.9950
5.00	0.9680	0.9519	7.23	−7.65	0.9954
5.00	0.9676	0.9516	7.20	−7.63	0.9955
6.00	0.9672	0.9446	9.41	−8.22	0.9969
7.00	0.9691	0.9393	11.41	−8.74	0.9977
8.00	0.9705	0.9341	13.03	−9.14	0.9989

Table 12. Static Performance Characteristics for Nozzles With $x_r/l_r = 0.02$, $\theta = 20°$, $\phi = 0°$, $\delta_{v,p} = 0°$, and $\delta_{v,y} = -20°$

NPR	F_r/F_i	F/F_i	δ_p, deg	δ_y, deg	w_p/w_i
(a) Nozzle 16, minimum sidewall					
2.00	0.9729	0.9677	−1.60	−5.70	0.9795
2.50	0.9743	0.9675	−1.27	−6.64	0.9782
3.01	0.9762	0.9687	−0.36	−7.07	0.9791
3.50	0.9780	0.9700	−1.08	−7.24	0.9801
4.00	0.9773	0.9691	−0.73	−7.37	0.9813
5.00	0.9766	0.9675	1.97	−7.57	0.9820
6.00	0.9753	0.9641	4.29	−7.60	0.9833
8.00	0.9731	0.9563	7.52	−7.66	0.9858
(b) Nozzle 17, medium sidewall					
2.00	0.9705	0.9632	0.07	−7.03	0.9767
2.50	0.9749	0.9666	−0.31	−7.47	0.9764
3.00	0.9778	0.9675	1.18	−8.26	0.9771
3.50	0.9752	0.9632	1.30	−8.90	0.9786
4.00	0.9743	0.9602	2.18	−9.50	0.9793
5.00	0.9732	0.9547	4.65	−10.21	0.9800
6.00	0.9723	0.9475	7.17	−10.92	0.9808
8.01	0.9722	0.9362	10.59	−11.75	0.9827
(c) Nozzle 18, maximum sidewall					
2.00	0.9644	0.9538	1.50	−8.37	0.9780
2.50	0.9695	0.9571	1.70	−8.99	0.9772
3.00	0.9747	0.9635	1.45	−8.61	0.9776
3.50	0.9747	0.9626	1.25	−8.95	0.9785
3.99	0.9731	0.9588	2.29	−9.57	0.9799
5.00	0.9717	0.9512	5.18	−10.66	0.9801
6.00	0.9719	0.9430	7.96	−11.67	0.9812
8.00	0.9725	0.9292	11.55	−13.04	0.9830

Table 13. Static Performance Characteristics for Nozzles With $x_r/l_r = 0.42$, $\theta = 30°$, $\phi = 0°$, $\delta_{v,p} = 0°$, and $\delta_{v,y} = 0°$

NPR	F_r/F_i	F/F_i	δ_p, deg	δ_y, deg	w_p/w_i
(a) Nozzle 19, minimum sidewall					
2.00	0.9804	0.9780	−3.97	−0.67	0.9961
2.50	0.9860	0.9847	−2.97	−0.44	0.9957
3.00	0.9881	0.9880	−1.00	−0.50	0.9968
3.50	0.9912	0.9901	−2.71	−0.39	0.9977
4.00	0.9922	0.9912	−2.52	−0.35	0.9985
5.00	0.9900	0.9900	0.56	−0.31	0.9995
5.99	0.9882	0.9864	3.43	−0.33	1.0002
6.99	0.9871	0.9822	5.69	−0.35	1.0018
7.99	0.9874	0.9790	7.48	−0.39	1.0026
(b) Nozzle 20, medium sidewall					
2.00	0.9778	0.9761	−3.37	−0.42	0.9977
2.50	0.9825	0.9802	−3.97	−0.45	0.9974
3.00	0.9855	0.9849	−1.94	−0.30	0.9977
3.50	0.9902	0.9885	−3.35	−0.29	0.9997
4.00	0.9913	0.9904	−2.35	−0.31	1.0000
5.00	0.9910	0.9908	0.91	−0.27	1.0010
6.00	0.9898	0.9873	4.02	−0.30	1.0022
6.99	0.9891	0.9829	6.41	−0.32	1.0036
8.00	0.9889	0.9787	8.24	−0.38	1.0047
(c) Nozzle 21, maximum sidewall					
1.99	0.9784	0.9769	−3.14	−0.48	0.9982
2.50	0.9821	0.9799	−3.80	−0.44	0.9978
3.00	0.9859	0.9854	−1.88	−0.29	0.9981
3.50	0.9891	0.9874	−3.34	−0.26	0.9998
4.00	0.9905	0.9896	−2.35	−0.22	1.0005
4.99	0.9897	0.9895	0.99	−0.24	1.0014
6.00	0.9885	0.9860	4.07	−0.25	1.0028
7.00	0.9877	0.9814	6.47	−0.29	1.0041
8.00	0.9880	0.9777	8.29	−0.33	1.0051

Table 14. Static Performance Characteristics for Nozzles With $x_r/l_r = 0.20$, $\theta = 30°$, $\phi = 0°$, $\delta_{v,p} = 0°$, and $\delta_{v,y} = 0°$

NPR	F_r/F_i	F/F_i	δ_p, deg	δ_y, deg	w_p/w_i
(a) Nozzle 22, minimum sidewall					
1.99	0.9851	0.9808	−5.31	−0.53	0.9924
2.50	0.9880	0.9855	−4.00	−0.42	0.9928
3.00	0.9903	0.9891	−2.75	−0.41	0.9931
3.50	0.9927	0.9917	−2.67	−0.29	0.9943
4.00	0.9913	0.9909	−1.61	−0.28	0.9959
4.99	0.9900	0.9898	1.15	−0.25	0.9964
6.00	0.9862	0.9844	3.42	−0.27	0.9972
6.99	0.9833	0.9793	5.18	−0.29	0.9988
8.00	0.9805	0.9741	6.56	−0.33	0.9997
(b) Nozzle 23, medium sidewall					
2.00	0.9830	0.9791	−5.06	−0.45	0.9947
2.50	0.9870	0.9846	−3.99	−0.40	0.9945
3.01	0.9890	0.9878	−2.82	−0.36	0.9955
3.50	0.9912	0.9900	−2.79	−0.32	0.9964
4.00	0.9909	0.9905	−1.56	−0.30	0.9977
5.00	0.9886	0.9884	1.18	−0.27	0.9979
6.00	0.9837	0.9819	3.48	−0.26	0.9992
7.00	0.9811	0.9770	5.22	−0.28	1.0002
8.00	0.9775	0.9709	6.66	−0.28	1.0016
(c) Nozzle 24, maximum sidewall					
2.00	0.9780	0.9740	−5.13	−0.44	0.9933
2.50	0.9830	0.9806	−3.99	−0.40	0.9939
3.00	0.9868	0.9856	−2.74	−0.45	0.9945
3.50	0.9891	0.9880	−2.74	−0.28	0.9961
4.00	0.9891	0.9887	−1.55	−0.27	0.9969
4.99	0.9865	0.9862	1.22	−0.24	0.9976
6.00	0.9827	0.9808	3.58	−0.26	0.9987
7.01	0.9802	0.9759	5.34	−0.23	1.0000
8.00	0.9777	0.9709	6.75	−0.29	1.0013

Table 15. Static Performance Characteristics for Nozzles With $x_r/l_r = 0.02$, $\theta = 30°$, $\phi = 0°$, $\delta_{v,p} = 0°$, and $\delta_{v,y} = 0°$

NPR	F_r/F_i	F/F_i	δ_p, deg	δ_y, deg	w_p/w_i
(a) Nozzle 25, minimum sidewall					
2.00	0.9823	0.9777	−5.55	−0.61	0.9973
2.50	0.9852	0.9814	−5.02	−0.53	0.9975
3.00	0.9876	0.9846	−4.42	−0.48	0.9979
3.51	0.9867	0.9846	−3.73	−0.45	0.9991
4.00	0.9831	0.9822	−2.53	−0.44	0.9998
5.00	0.9731	0.9731	−0.34	−0.35	1.0006
6.01	0.9620	0.9617	1.38	−0.43	1.0019
6.00	0.9621	0.9618	1.32	−0.42	1.0017
8.00	0.9477	0.9459	3.57	−0.36	1.0042
(b) Nozzle 26, medium sidewall					
2.01	0.9777	0.9728	−5.75	−0.46	0.9966
2.50	0.9822	0.9781	−5.25	−0.48	0.9964
3.00	0.9826	0.9793	−4.63	−0.53	0.9968
3.51	0.9834	0.9810	−3.96	−0.38	0.9984
4.00	0.9803	0.9792	−2.68	−0.38	0.9994
5.00	0.9730	0.9730	−0.28	−0.28	1.0001
6.00	0.9661	0.9658	1.46	−0.25	1.0012
8.01	0.9544	0.9524	3.76	−0.28	1.0034
(c) Nozzle 27, maximum sidewall					
2.00	0.9804	0.9757	−5.59	−0.37	0.9966
2.50	0.9803	0.9764	−5.13	−0.42	0.9965
3.01	0.9820	0.9791	−4.41	−0.44	0.9973
3.50	0.9821	0.9799	−3.80	−0.38	0.9982
4.01	0.9792	0.9782	−2.45	−0.32	0.9993
5.01	0.9729	0.9729	−0.08	−0.34	1.0004
6.00	0.9658	0.9654	1.62	−0.30	1.0017
8.00	0.9546	0.9526	3.76	−0.28	1.0044

Table 16. Static Performance Characteristics for Nozzles With $x_r/l_r = 0.20$, $\theta = 30°$, $\phi = 0°$, $\delta_{v,p} = 0°$, and $\delta_{v,y} = -20°$

NPR	F_r/F_i	F/F_i	δ_p, deg	δ_y, deg	w_p/w_i
(a) Nozzle 28, medium sidewall					
2.00	0.9453	0.9388	−1.93	−6.44	0.9935
2.51	0.9483	0.9426	−0.92	−6.22	0.9939
3.01	0.9555	0.9511	0.26	−5.50	0.9952
3.50	0.9558	0.9510	0.66	−5.69	0.9967
4.00	0.9564	0.9509	1.82	−5.89	0.9976
5.00	0.9558	0.9465	4.58	−6.57	0.9991
6.00	0.9549	0.9406	6.88	−7.28	1.0004
6.99	0.9538	0.9344	8.67	−7.77	1.0010
8.00	0.9532	0.9294	10.07	−8.13	1.0018
(b) Nozzle 29, maximum sidewall					
2.00	0.9534	0.9482	−2.57	−5.41	0.9929
2.50	0.9563	0.9523	−1.63	−5.04	0.9933
3.00	0.9620	0.9587	−0.09	−4.73	0.9941
3.50	0.9603	0.9562	0.51	−5.28	0.9951
4.01	0.9611	0.9562	1.68	−5.53	0.9960
5.00	0.9598	0.9517	4.35	−6.07	0.9974
6.00	0.9575	0.9450	6.57	−6.61	0.9987
7.00	0.9570	0.9400	8.41	−6.93	0.9993
8.00	0.9592	0.9385	9.89	−6.79	1.0000

Table 17. Static Performance Characteristics for Nozzles With $x_r/l_r = 0.02$, $\theta = 30°$, $\phi = 0°$, $\delta_{v,p} = 0°$, and $\delta_{v,y} = -20°$

NPR	F_r/F_i	F/F_i	δ_p, deg	δ_y, deg	w_p/w_i
(a) Nozzle 30, medium sidewall					
2.00	0.9563	0.9473	−3.21	−7.22	0.9721
2.50	0.9590	0.9487	−3.51	−7.63	0.9728
3.00	0.9607	0.9506	−3.25	−7.68	0.9740
3.50	0.9580	0.9482	−2.08	−7.95	0.9753
4.00	0.9557	0.9455	−0.27	−8.37	0.9762
5.00	0.9528	0.9385	2.65	−9.59	0.9780
6.00	0.9485	0.9298	4.66	−10.46	0.9792
7.00	0.9444	0.9217	6.06	−11.11	0.9801
8.00	0.9413	0.9141	7.10	−11.94	0.9805
(b) Nozzle 31, maximum sidewall					
2.00	0.9609	0.9530	−3.42	−6.50	0.9733
2.50	0.9631	0.9550	−3.22	−6.72	0.9743
3.00	0.9624	0.9533	−2.68	−7.44	0.9755
3.50	0.9592	0.9489	−1.61	−8.27	0.9766
4.00	0.9582	0.9468	−0.14	−8.83	0.9773
5.00	0.9517	0.9369	2.63	−9.79	0.9790
5.99	0.9481	0.9298	4.65	−10.32	0.9800
7.00	0.9468	0.9259	5.96	−10.56	0.9808
8.00	0.9446	0.9213	6.98	−10.77	0.9813

Table 18. Static Performance Characteristics for Nozzles With $x_r/l_r = 0.42$, $\theta = 30°$, $\phi = 0°$, $\delta_{v,p} = 0°$, and $\delta_{v,y} = -30°$

NPR	F_r/F_i	F/F_i	δ_p, deg	δ_y, deg	w_p/w_i
Nozzle 32, maximum sidewall					
2.00	0.9434	0.9260	5.97	−9.33	0.9931
2.50	0.9430	0.9246	6.47	−9.41	0.9941
3.00	0.9495	0.9296	7.75	−8.94	0.9942
3.50	0.9494	0.9295	8.22	−8.53	0.9960
4.00	0.9501	0.9304	8.39	−8.25	0.9968
5.00	0.9523	0.9291	9.88	−8.11	0.9975
5.99	0.9549	0.9258	11.79	−8.09	0.9986
7.00	0.9582	0.9227	13.53	−8.18	0.9999
8.00	0.9613	0.9194	15.00	−8.31	1.0009

Table 19. Static Performance Characteristics for Nozzles With $x_r/l_r = 0.20$, $\theta = 30°$, $\phi = 0°$, $\delta_{r,p} = 0°$, and $\delta_{v,y} = -30°$

NPR	F_r/F_i	F/F_i	δ_p, deg	δ_y, deg	w_p/w_i
(a) Nozzle 33, medium sidewall					
2.00	0.9462	0.9335	3.01	−8.95	0.9963
2.50	0.9487	0.9346	4.76	−8.68	0.9964
3.00	0.9525	0.9370	5.87	−8.60	0.9969
3.50	0.9536	0.9361	6.73	−8.77	0.9979
4.00	0.9525	0.9324	7.70	−9.03	0.9996
5.00	0.9543	0.9270	9.98	−9.64	0.9999
5.99	0.9546	0.9192	12.07	−10.27	1.0010
7.00	0.9567	0.9146	13.73	−10.53	1.0023
8.00	0.9582	0.9105	15.01	−10.69	1.0034
(b) Nozzle 34, maximum sidewall					
2.00	0.9437	0.9221	6.20	−10.68	0.9953
2.50	0.9470	0.9224	7.98	−10.49	0.9959
3.00	0.9502	0.9223	9.20	−10.65	0.9970
3.50	0.9512	0.9218	9.71	−10.66	0.9984
4.01	0.9502	0.9178	10.45	−11.02	0.9997
5.06	0.9503	0.9079	12.71	−11.93	1.0006
6.00	0.9531	0.9023	14.48	−12.48	1.0017
7.00	0.9549	0.8959	16.14	−12.89	1.0026
7.80	0.9560	0.8917	17.10	−13.18	1.0038

Table 20. Static Performance Characteristics for Nozzles With $x_r/l_r = 0.02$, $\theta = 30°$, $\phi = 0°$, $\delta_{v,p} = 0°$, and $\delta_{v,y} = -30°$

NPR	F_r/F_i	F/F_i	δ_p, deg	δ_y, deg	w_p/w_i
(a) Nozzle 35, minimum sidewall					
2.00	0.9722	0.9617	−1.34	−8.33	0.9390
2.50	0.9769	0.9651	−1.03	−8.86	0.9400
3.00	0.9749	0.9608	−0.99	−9.70	0.9404
3.50	0.9761	0.9618	0.10	−9.80	0.9414
4.00	0.9771	0.9625	1.62	−9.80	0.9422
5.00	0.9762	0.9594	3.99	−9.88	0.9431
6.00	0.9741	0.9547	5.69	−9.99	0.9445
7.99	0.9686	0.9449	7.85	−10.12	0.9470
(b) Nozzle 36, medium sidewall					
1.99	0.9615	0.9435	1.50	−11.02	0.9357
2.50	0.9664	0.9454	1.97	−11.81	0.9357
3.00	0.9669	0.9423	2.84	−12.66	0.9363
3.50	0.9659	0.9369	4.15	−13.49	0.9372
4.00	0.9651	0.9317	5.90	−14.02	0.9383
5.01	0.9656	0.9246	8.46	−14.69	0.9393
5.99	0.9647	0.9175	10.20	−15.14	0.9403
7.80	0.9610	0.9051	12.24	−15.81	0.9420
(c) Nozzle 37, maximum sidewall					
2.00	0.9544	0.9276	3.66	−13.15	0.9349
2.50	0.9558	0.9254	4.18	−13.93	0.9360
3.00	0.9574	0.9251	4.15	−14.38	0.9365
3.50	0.9558	0.9190	5.36	−15.11	0.9377
4.00	0.9571	0.9143	7.23	−15.77	0.9386
5.00	0.9591	0.9050	10.03	−16.86	0.9391
6.01	0.9586	0.8947	12.01	−17.77	0.9411
6.69	0.9573	0.8880	12.98	−18.28	0.9416

Table 21. Static Performance Characteristics for Nozzles With $x_r/l_r = 1.00$, $\theta = 0°$, $\phi = 0°$, $\delta_{v,p} = -20°$, and $\delta_{v,y} = 0°$

NPR	F_r/F_i	F/F_i	δ_p, deg	δ_y, deg	w_p/w_i
(a) Nozzle 38, minimum sidewall					
2.00	0.9226	0.8616	−20.95	−0.47	0.9898
2.50	0.9285	0.8819	−18.24	−0.28	0.9904
3.00	0.9349	0.8876	−18.30	−0.13	0.9917
3.50	0.9445	0.8997	−17.70	0.04	0.9925
4.01	0.9500	0.9066	−17.38	0.11	0.9935
5.00	0.9540	0.9023	−18.94	0.27	0.9947
6.00	0.9600	0.9217	−16.25	0.25	0.9958
7.00	0.9633	0.9339	−14.18	0.17	0.9965
8.00	0.9658	0.9429	−12.52	0.15	0.9969
(b) Nozzle 39, medium sidewall					
2.00	0.9148	0.8266	−25.36	0.18	0.9976
2.50	0.9199	0.8264	−26.05	0.34	0.9982
3.00	0.9284	0.8367	−25.68	0.30	0.9990
3.50	0.9373	0.8741	−21.17	0.09	1.0002
4.00	0.9432	0.8782	−21.39	0.30	1.0010
5.00	0.9508	0.8892	−20.73	0.36	1.0023
6.00	0.9565	0.9124	−17.46	0.32	1.0034
7.00	0.9610	0.9297	−14.66	0.24	1.0040
8.01	0.9651	0.9422	−12.49	0.19	1.0043
(c) Nozzle 40, maximum sidewall					
2.00	0.9178	0.8344	−24.61	−0.18	0.9965
2.50	0.9161	0.8323	−24.71	−0.12	0.9971
3.00	0.9269	0.8254	−27.07	0.12	0.9985
3.50	0.9370	0.8309	−27.53	0.40	0.9994
4.00	0.9437	0.8485	−25.96	0.50	1.0002
5.00	0.9503	0.8833	−21.64	0.28	1.0018
6.00	0.9550	0.9057	−18.49	0.38	1.0031
7.00	0.9590	0.9242	−15.48	0.32	1.0037
8.00	0.9627	0.9379	−13.03	0.23	1.0045

Table 22. Static Performance Characteristics for Nozzles With $x_r/l_r = 0.42$, $\theta = 20°$, $\phi = 0°$, $\delta_{v,p} = -20°$, and $\delta_{v,y} = 0°$

NPR	F_r/F_i	F/F_i	δ_p, deg	δ_y, deg	w_p/w_i
(a) Nozzle 41, minimum sidewall					
2.00	0.9247	0.8606	−21.44	−0.94	0.9954
2.50	0.9303	0.8823	−18.47	−0.17	0.9962
3.00	0.9367	0.8896	−18.25	−0.14	0.9971
3.50	0.9453	0.9003	−17.74	−0.09	0.9980
4.00	0.9498	0.9067	−17.34	0.01	0.9991
5.01	0.9537	0.9018	−18.99	0.17	1.0004
6.00	0.9586	0.9204	−16.23	0.14	1.0015
7.00	0.9622	0.9331	−14.12	0.11	1.0021
8.00	0.9649	0.9425	−12.38	0.08	1.0026
(b) Nozzle 42, medium sidewall					
2.00	0.9155	0.8244	−25.77	0.45	0.9959
2.51	0.9203	0.8434	−23.58	0.79	0.9966
3.00	0.9269	0.8417	−24.75	0.79	0.9979
3.50	0.9369	0.8723	−21.40	−0.21	0.9991
4.00	0.9434	0.8770	−21.62	0.05	0.9998
5.01	0.9506	0.8934	−19.96	0.35	1.0013
6.00	0.9580	0.9187	−16.46	0.26	1.0024
7.00	0.9621	0.9334	−14.04	0.16	1.0031
8.00	0.9651	0.9433	−12.18	0.12	1.0036
(c) Nozzle 43, maximum sidewall					
2.00	0.9144	0.8236	−25.74	0.20	0.9956
2.50	0.9199	0.8270	−25.98	0.08	0.9961
3.00	0.9269	0.8341	−25.85	0.45	0.9976
3.50	0.9359	0.8551	−23.98	0.42	0.9985
4.00	0.9414	0.8678	−22.80	0.65	0.9993
5.00	0.9508	0.8948	−19.72	1.17	1.0011
6.01	0.9565	0.9172	−16.48	0.34	1.0023
7.00	0.9609	0.9321	−14.07	0.19	1.0033
8.00	0.9642	0.9426	−12.15	0.12	1.0040

Table 23. Static Performance Characteristics for Nozzles With $x_r/l_r = 0.20$, $\theta = 20°$, $\phi = 0°$, $\delta_{v,p} = -20°$, and $\delta_{v,y} = 0°$

NPR	F_r/F_i	F/F_i	δ_p, deg	δ_y, deg	w_p/w_i
(a) Nozzle 44, minimum sidewall					
2.01	0.9258	0.8688	−20.21	0.50	0.9872
2.50	0.9288	0.8825	−18.15	−0.39	0.9880
3.00	0.9361	0.8891	−18.25	−0.24	0.9890
3.50	0.9457	0.9017	−17.54	−0.09	0.9901
4.00	0.9516	0.9089	−17.22	0.00	0.9908
5.00	0.9558	0.9086	−18.08	0.12	0.9923
6.00	0.9611	0.9260	−15.52	0.10	0.9934
7.00	0.9641	0.9372	−13.56	0.07	0.9941
(b) Nozzle 45, medium sidewall					
2.00	0.9184	0.8643	−19.76	−0.41	0.9874
2.50	0.9226	0.8604	−21.17	0.30	0.9874
3.00	0.9312	0.8719	−20.56	0.47	0.9889
3.51	0.9418	0.8899	−19.10	0.44	0.9896
4.00	0.9484	0.9004	−18.30	0.44	0.9905
5.00	0.9560	0.9136	−17.14	0.19	0.9918
6.00	0.9610	0.9276	−15.14	0.18	0.9932
8.00	0.9652	0.9444	−11.93	0.13	0.9941
(c) Nozzle 46, maximum sidewall					
2.00	0.9129	0.8493	−21.51	0.22	0.9873
2.50	0.9182	0.8616	−20.21	0.56	0.9876
3.00	0.9271	0.8678	−20.61	0.12	0.9890
3.50	0.9371	0.8842	−19.34	0.32	0.9903
4.00	0.9448	0.8945	−18.79	0.25	0.9912
5.00	0.9529	0.9097	−17.32	0.21	0.9927
6.00	0.9584	0.9248	−15.22	0.22	0.9941
7.99	0.9637	0.9428	−11.96	0.13	0.9957

Table 24. Static Performance Characteristics for Nozzles With $x_r/l_r = 0.02$, $\theta = 20°$, $\phi = 0°$, $\delta_{v,p} = -20°$, and $\delta_{v,y} = 0°$

NPR	F_r/F_i	F/F_i	δ_p, deg	δ_y, deg	w_p/w_i
(a) Nozzle 47, minimum sidewall					
2.00	0.9323	0.8950	−16.27	−0.48	1.0013
2.50	0.9365	0.9013	−15.76	−0.33	1.0014
3.00	0.9436	0.9089	−15.57	−0.21	1.0026
3.50	0.9515	0.9174	−15.37	−0.13	1.0034
4.00	0.9554	0.9218	−15.24	−0.05	1.0043
5.00	0.9571	0.9218	−15.61	0.09	1.0059
6.00	0.9588	0.9284	−14.49	0.09	1.0069
8.00	0.9620	0.9415	−11.85	0.04	1.0079
(b) Nozzle 48, medium sidewall					
2.00	0.9311	0.8916	−16.73	−0.33	1.0076
2.50	0.9356	0.8993	−16.02	−0.21	1.0084
3.00	0.9428	0.9064	−15.97	−0.08	1.0095
3.50	0.9475	0.9113	−15.89	−0.03	1.0108
4.00	0.9518	0.9157	−15.83	0.09	1.0117
5.00	0.9553	0.9189	−15.87	0.14	1.0130
6.01	0.9583	0.9282	−14.39	0.15	1.0137
8.00	0.9597	0.9391	−11.89	0.11	1.0150
(c) Nozzle 49, maximum sidewall					
2.00	0.9238	0.8826	−17.19	−0.32	1.0067
2.50	0.9304	0.8928	−16.33	−0.03	1.0074
3.00	0.9385	0.9020	−16.04	−0.06	1.0083
3.50	0.9450	0.9083	−16.02	0.06	1.0095
4.00	0.9500	0.9136	−15.90	0.10	1.0104
5.00	0.9539	0.9169	−16.01	0.30	1.0122
6.00	0.9560	0.9250	−14.62	0.15	1.0132
8.00	0.9586	0.9382	−11.84	0.18	1.0148

Table 25. Static Performance Characteristics for Nozzles With $x_r/l_r = 0.42$, $\theta = 20°$, $\phi = 0°$, $\delta_{v,p} = -20°$, and $\delta_{v,y} = -20°$

NPR	F_r/F_i	F/F_i	δ_p, deg	δ_y, deg	w_p/w_i
Nozzle 50, maximum sidewall					
2.00	0.8982	0.8355	−20.54	−7.08	0.9882
2.50	0.8987	0.8392	−19.78	−7.57	0.9888
3.01	0.9059	0.8613	−17.23	−5.75	0.9902
3.50	0.9089	0.8608	−17.69	−6.51	0.9911
4.00	0.9238	0.8799	−17.28	−4.28	0.9919
5.00	0.9384	0.8867	−19.00	−2.18	0.9933
6.00	0.9439	0.9093	−15.38	−2.55	0.9945
8.00	0.9514	0.9343	−10.37	−3.36	0.9956

Table 26. Static Performance Characteristics for Nozzles With $x_r/l_r = 0.20$, $\theta = 20°$, $\phi = 0°$, $\delta_{v,p} = -20°$, and $\delta_{v,y} = -20°$

NPR	F_r/F_i	F/F_i	δ_p, deg	δ_y, deg	w_p/w_i
(a) Nozzle 51, medium sidewall					
2.00	0.9127	0.8738	−16.53	−3.08	0.9904
2.50	0.9182	0.8821	−15.93	−2.63	0.9911
3.00	0.9335	0.8946	−16.57	−1.05	0.9920
3.50	0.9409	0.9075	−15.22	−1.69	0.9931
4.00	0.9448	0.9149	−14.27	−2.27	0.9938
5.00	0.9435	0.9104	−14.91	−3.29	0.9951
6.00	0.9458	0.9212	−12.42	−4.34	0.9963
8.00	0.9530	0.9381	−8.82	−5.09	0.9976
(b) Nozzle 52, maximum sidewall					
2.01	0.8979	0.8595	−15.41	−7.09	0.9907
2.50	0.9084	0.8780	−13.40	−6.63	0.9913
3.00	0.9174	0.8879	−13.29	−6.13	0.9923
3.50	0.9281	0.8998	−13.02	−5.82	0.9933
4.01	0.9386	0.9100	−13.60	−4.14	0.9943
5.00	0.9433	0.9108	−14.70	−3.51	0.9955
6.00	0.9431	0.9185	−11.99	−5.48	0.9967
8.00	0.9469	0.9304	−8.21	−7.01	0.9978

Table 27. Static Performance Characteristics for Nozzles With $x_r/l_r = 0.02$, $\theta = 20°$, $\phi = 0°$, $\delta_{v,p} = -20°$, and $\delta_{v,y} = -20°$

NPR	F_r/F_i	F/F_i	δ_p, deg	δ_y, deg	w_p/w_i
(a) Nozzle 53, minimum sidewall					
2.00	0.9310	0.8971	−15.27	−2.77	0.9904
2.50	0.9382	0.9085	−13.90	−4.13	0.9906
3.01	0.9460	0.9181	−13.13	−4.85	0.9918
3.50	0.9533	0.9270	−12.53	−5.20	0.9926
4.00	0.9574	0.9323	−12.05	−5.40	0.9932
5.00	0.9567	0.9285	−12.80	−5.74	0.9945
6.00	0.9601	0.9355	−11.70	−5.80	0.9958
8.00	0.9637	0.9461	−9.35	−5.84	0.9972
8.39	1.0185	1.0073	−6.29	−5.75	1.3966
(b) Nozzle 54, medium sidewall					
2.01	0.9304	0.8968	−14.97	−3.90	0.9900
2.50	0.9401	0.9067	−14.98	−3.34	0.9904
3.00	0.9500	0.9173	−14.75	−3.28	0.9915
3.50	0.9549	0.9267	−13.21	−4.61	0.9923
4.00	0.9570	0.9314	−12.13	−5.61	0.9930
5.00	0.9558	0.9288	−11.89	−6.87	0.9943
6.00	0.9579	0.9343	−10.28	−7.67	0.9953
8.00	0.9586	0.9386	−7.74	−8.92	0.9965
(c) Nozzle 55, maximum sidewall					
2.00	0.9212	0.8910	−13.11	−6.93	0.9897
2.50	0.9287	0.8989	−12.53	−7.62	0.9900
3.05	0.9376	0.9085	−12.27	−7.61	0.9919
3.50	0.9455	0.9165	−12.42	−7.16	0.9920
4.01	0.9586	0.9294	−13.53	−4.31	0.9925
5.00	0.9579	0.9319	−12.04	−6.01	0.9939
6.00	0.9590	0.9368	−9.96	−7.47	0.9950
8.00	0.9582	0.9375	−7.14	−9.65	0.9960

Table 28. Static Performance Characteristics for Nozzles With $x_r/l_r = 0.42$, $\theta = 30°$, $\phi = 0°$, $\delta_{v,p} = -20°$, and $\delta_{v,y} = 0°$

NPR	F_r/F_i	F/F_i	δ_p, deg	δ_y, deg	w_p/w_i
(a) Nozzle 56, minimum sidewall					
2.01	0.9248	0.8657	−20.60	−0.47	0.9973
2.50	0.9285	0.8804	−18.52	−0.09	0.9976
3.01	0.9359	0.8888	−18.25	−0.07	0.9989
3.50	0.9453	0.8993	−17.96	−0.02	0.9998
4.00	0.9506	0.9060	−17.62	0.07	1.0006
5.01	0.9547	0.9038	−18.78	0.21	1.0023
6.00	0.9603	0.9233	−15.95	0.19	1.0033
7.00	0.9645	0.9367	−13.77	0.15	1.0041
8.00	0.9674	0.9461	−12.05	0.11	1.0045
(b) Nozzle 57, medium sidewall					
2.01	0.9160	0.8321	−24.71	0.10	0.9990
2.50	0.9210	0.8442	−23.54	−1.32	0.9992
3.00	0.9291	0.8551	−23.00	−1.02	1.0006
3.50	0.9386	0.8746	−21.27	−0.06	1.0016
3.99	0.9435	0.8789	−21.33	0.08	1.0023
5.00	0.9536	0.9021	−18.92	0.22	1.0036
6.00	0.9596	0.9228	−15.91	0.16	1.0048
7.00	0.9639	0.9364	−13.71	0.08	1.0053
8.00	0.9668	0.9460	−11.88	0.05	1.0059
(c) Nozzle 58, maximum sidewall					
2.01	0.9112	0.8197	−25.90	−0.12	0.9972
2.50	0.9187	0.8289	−25.54	−0.20	0.9979
3.00	0.9275	0.8384	−25.33	0.01	0.9988
3.50	0.9344	0.8604	−22.96	0.08	0.9998
4.00	0.9418	0.8729	−22.05	0.14	1.0006
5.00	0.9517	0.9000	−18.97	0.37	1.0023
6.00	0.9583	0.9219	−15.85	0.16	1.0037
7.00	0.9631	0.9357	−13.70	0.16	1.0045
8.00	0.9666	0.9459	−11.88	0.11	1.0053

Table 29. Static Performance Characteristics for Nozzles With $x_r/l_r = 0.20$, $\theta = 30°$, $\phi = 0°$, $\delta_{v,p} = -20°$, and $\delta_{v,y} = 0°$

NPR	F_r/F_i	F/F_i	δ_p, deg	δ_y, deg	w_p/w_i
(a) Nozzle 59, minimum sidewall					
2.00	0.9549	0.9313	−12.75	−0.60	0.9922
2.50	0.9281	0.8784	−18.82	−0.31	0.9926
3.00	0.9332	0.8799	−19.46	−0.18	0.9941
3.50	0.9432	0.8943	−18.53	−0.08	0.9948
4.00	0.9501	0.9059	−17.53	−0.04	0.9956
5.00	0.9583	0.9198	−16.28	0.12	0.9970
6.00	0.9635	0.9333	−14.39	0.08	0.9982
7.00	0.9670	0.9431	−12.77	0.06	0.9987
8.01	0.9687	0.9496	−11.40	0.05	0.9992
(b) Nozzle 60, medium sidewall					
2.00	0.9584	0.9400	−11.23	−0.39	0.9936
2.50	0.9211	0.8585	−21.22	1.03	0.9940
3.00	0.9316	0.8726	−20.49	0.48	0.9946
3.50	0.9411	0.8897	−19.02	0.53	0.9956
4.00	0.9490	0.9030	−17.92	0.29	0.9963
5.00	0.9578	0.9197	−16.23	0.20	0.9976
6.00	0.9627	0.9327	−14.35	0.16	0.9987
7.00	0.9653	0.9416	−12.72	0.11	0.9993
8.01	0.9679	0.9489	−11.37	0.07	0.9997
(c) Nozzle 61, maximum sidewall					
2.00	0.9497	0.9288	−12.03	−0.48	0.9922
2.51	0.9180	0.8530	−21.68	−0.10	0.9926
3.00	0.9281	0.8688	−20.58	0.16	0.9935
3.50	0.9390	0.8871	−19.13	0.16	0.9945
4.00	0.9469	0.9005	−18.02	0.09	0.9955
5.00	0.9557	0.9176	−16.24	0.19	0.9971
6.00	0.9616	0.9316	−14.33	0.20	0.9983
7.00	0.9648	0.9410	−12.75	0.17	0.9990
8.00	0.9662	0.9472	−11.40	0.14	0.9997

Table 30. Static Performance Characteristics for Nozzles With $x_r/l_r = 0.02$, $\theta = 30°$, $\phi = 0°$, $\delta_{v,p} = -20°$, and $\delta_{v,y} = 0°$

NPR	F_r/F_i	F/F_i	δ_p, deg	δ_y, deg	w_p/w_i
(a) Nozzle 62, minimum sidewall					
2.00	0.9365	0.8989	−16.28	−0.51	0.9898
2.50	0.9391	0.9022	−16.11	−0.49	0.9904
3.00	0.9453	0.9084	−16.06	−0.37	0.9916
3.50	0.9525	0.9177	−15.53	−0.18	0.9924
4.00	0.9567	0.9235	−15.15	−0.15	0.9934
5.00	0.9608	0.9311	−14.29	0.00	0.9946
6.00	0.9642	0.9394	−13.02	0.04	0.9956
8.00	0.9649	0.9474	−10.92	−0.01	0.9965
(b) Nozzle 63, medium sidewall					
2.00	0.9317	0.8912	−16.94	−0.23	0.9902
2.50	0.9375	0.8982	−16.64	−0.28	0.9908
3.00	0.9429	0.9043	−16.44	−0.12	0.9920
3.50	0.9503	0.9143	−15.84	−0.02	0.9929
4.00	0.9545	0.9202	−15.39	0.01	0.9937
5.00	0.9608	0.9312	−14.26	0.03	0.9954
6.00	0.9630	0.9384	−12.97	0.02	0.9964
8.00	0.9626	0.9453	−10.89	0.02	0.9974
(c) Nozzle 64, maximum sidewall					
2.00	0.9253	0.8858	−16.79	−0.40	0.9868
2.50	0.9315	0.8913	−16.89	−0.08	0.9877
3.00	0.9387	0.8988	−16.77	−0.06	0.9893
3.51	0.9468	0.9096	−16.10	0.06	0.9904
4.00	0.9521	0.9169	−15.61	0.08	0.9914
5.00	0.9579	0.9274	−14.51	0.13	0.9932
6.01	0.9605	0.9353	−13.16	0.18	0.9945
8.00	0.9598	0.9419	−11.07	0.16	0.9961

Table 31. Static Performance Characteristics for Nozzles With $x_r/l_r = 0.20$, $\theta = 30°$, $\phi = 0°$, $\delta_{v,p} = -20°$, and $\delta_{v,y} = -20°$

NPR	F_r/F_i	F/F_i	δ_p, deg	δ_y, deg	w_p/w_i
(a) Nozzle 65, medium sidewall					
2.01	0.8876	0.8349	−19.20	−5.41	0.9947
2.51	0.8972	0.8522	−17.67	−4.72	0.9953
3.01	0.9102	0.8673	−17.23	−4.10	0.9964
3.51	0.9176	0.8763	−16.70	−4.56	0.9974
4.00	0.9297	0.8905	−16.37	−3.47	0.9981
5.00	0.9359	0.9009	−15.34	−3.52	0.9999
6.01	0.9362	0.9091	−13.02	−4.81	1.0009
7.01	0.9388	0.9171	−11.10	−5.54	1.0016
8.00	0.9388	0.9202	−9.64	−6.26	1.0021
(b) Nozzle 66, maximum sidewall					
2.01	0.9235	0.8906	−14.88	−3.89	0.9931
2.51	0.9106	0.8638	−18.34	−2.23	0.9932
3.00	0.9265	0.8804	−18.13	−1.05	0.9951
3.50	0.9340	0.8921	−17.17	−1.37	0.9960
4.00	0.9396	0.9026	−16.02	−2.07	0.9966
5.00	0.9386	0.9044	−15.12	−3.62	0.9985
6.00	0.9404	0.9135	−12.98	−4.65	0.9998
8.01	0.9447	0.9278	−9.50	−5.35	1.0012
7.01	0.9434	0.9221	−11.10	−5.24	1.0020

Table 32. Static Performance Characteristics for Nozzles With $x_r/l_r = 0.02$, $\theta = 30°$, $\phi = 0°$, $\delta_{v,p} = -20°$, and $\delta_{v,y} = -20°$

NPR	F_r/F_i	F/F_i	δ_p, deg	δ_y, deg	w_p/w_i
(a) Nozzle 67, medium sidewall					
2.00	0.9151	0.8764	−15.75	−5.90	0.9833
2.50	0.9203	0.8810	−15.59	−6.54	0.9846
3.00	0.9285	0.8923	−14.80	−6.45	0.9859
3.51	0.9318	0.8954	−14.73	−6.73	0.9870
4.01	0.9437	0.9115	−14.20	−5.08	0.9879
5.00	0.9458	0.9179	−12.91	−5.48	0.9894
6.00	0.9429	0.9179	−11.41	−6.84	0.9909
7.00	0.9429	0.9200	−10.10	−7.76	0.9917
8.01	0.9413	0.9191	−9.02	−8.74	0.9923
(b) Nozzle 68, maximum sidewall					
2.01	0.9281	0.8913	−15.79	−3.77	0.9857
2.50	0.9337	0.8979	−15.47	−3.88	0.9864
3.00	0.9447	0.9114	−14.90	−3.32	0.9879
3.50	0.9477	0.9161	−14.25	−4.37	0.9890
4.00	0.9466	0.9161	−13.71	−5.20	0.9899
5.00	0.9428	0.9133	−12.84	−6.70	0.9918
6.00	0.9435	0.9170	−11.49	−7.53	0.9931
7.01	0.9429	0.9187	−10.18	−8.26	0.9939
8.00	0.9427	0.9204	−9.05	−8.75	0.9947

Table 33. Static Performance Characteristics for Nozzles With $x_r/l_r = 0.42$, $\theta = 30°$, $\phi = 0°$, $\delta_{v,p} = -20°$, and $\delta_{v,y} = -30°$

NPR	F_r/F_i	F/F_i	δ_p, deg	δ_y, deg	w_p/w_i
Nozzle 69, maximum sidewall					
2.00	0.8725	0.8225	−16.99	−10.13	1.0081
2.50	0.8764	0.8276	−16.38	−10.59	1.0082
3.00	0.8793	0.8347	−15.57	−10.14	1.0097
3.50	0.8851	0.8430	−14.62	−10.48	1.0107
4.00	0.8903	0.8520	−13.70	−10.24	1.0115
5.00	0.9107	0.8808	−12.82	−7.50	1.0130
6.00	0.9159	0.8901	−11.61	−7.33	1.0140
7.00	0.9218	0.9020	−9.42	−7.41	1.0148
8.00	0.9251	0.9093	−7.57	−7.54	1.0153

Table 34. Static Performance Characteristics for Nozzles With $x_r/l_r = 0.20$, $\theta = 30°$, $\phi = 0°$, $\delta_{v,p} = -20°$, and $\delta_{v,y} = -30°$

NPR	F_r/F_i	F/F_i	δ_p, deg	δ_y, deg	w_p/w_i
(a) Nozzle 70, medium sidewall					
2.00	0.8965	0.8632	−14.16	−6.98	0.9944
2.50	0.8982	0.8673	−13.65	−6.66	0.9947
3.00	0.9080	0.8789	−13.33	−6.00	0.9960
3.50	0.9149	0.8889	−12.23	−6.38	0.9967
4.00	0.9195	0.8962	−11.15	−6.72	0.9977
5.00	0.9213	0.8973	−10.93	−7.41	0.9993
6.01	0.9255	0.9051	−9.21	−7.92	1.0004
7.00	0.9290	0.9119	−7.40	−8.26	1.0010
8.00	0.9326	0.9174	−5.91	−8.55	1.0015
(b) Nozzle 71, maximum sidewall					
2.00	0.8723	0.8343	−11.99	−12.36	1.0011
2.50	0.8702	0.8312	−11.30	−13.34	1.0016
3.00	0.8790	0.8453	−9.50	−13.02	1.0027
3.50	0.8913	0.8623	−8.58	−12.06	1.0037
4.00	0.9034	0.8782	−8.29	−10.91	1.0045
5.00	0.9105	0.8864	−8.71	−10.08	1.0059
6.00	0.9133	0.8899	−7.38	−10.80	1.0071
7.00	0.9175	0.8952	−5.46	−11.49	1.0077
8.00	0.9199	0.8972	−3.93	−12.19	1.0081

Table 35. Static Performance Characteristics for Nozzles With $x_r/l_r = 0.02$, $\theta = 30°$, $\phi = 0°$, $\delta_{v,p} = -20°$, and $\delta_{v,y} = -30°$

NPR	F_r/F_i	F/F_i	δ_p, deg	δ_y, deg	w_p/w_i
(a) Nozzle 72, minimum sidewall					
2.01	0.9402	0.9113	−13.04	−5.90	0.9685
2.50	0.9432	0.9151	−12.29	−6.95	0.9687
3.00	0.9491	0.9207	−11.87	−7.70	0.9709
3.50	0.9532	0.9259	−11.33	−8.00	0.9718
4.00	0.9560	0.9290	−11.07	−8.17	0.9728
5.00	0.9576	0.9308	−10.91	−8.29	0.9744
6.00	0.9601	0.9371	−9.54	−8.34	0.9757
8.00	0.9624	0.9443	−7.44	−8.36	0.9773
(b) Nozzle 73, medium sidewall					
2.00	0.9298	0.9024	−11.53	−8.05	0.9739
2.50	0.9399	0.9120	−11.82	−7.71	0.9741
3.00	0.9449	0.9171	−11.27	−8.40	0.9753
3.50	0.9465	0.9190	−10.01	−9.76	0.9762
4.00	0.9472	0.9188	−9.30	−10.72	0.9771
5.00	0.9443	0.9144	−8.41	−11.92	0.9787
6.00	0.9473	0.9187	−6.81	−12.48	0.9796
8.00	0.9486	0.9204	−4.53	−13.30	0.9810
(c) Nozzle 74, maximum sidewall					
2.00	0.9112	0.8773	−9.02	−13.03	0.9744
2.50	0.9148	0.8785	−8.66	−13.90	0.9748
3.00	0.9199	0.8821	−8.57	−14.27	0.9761
3.50	0.9277	0.8903	−8.32	−14.24	0.9770
4.01	0.9367	0.9042	−8.70	−12.59	0.9780
5.01	0.9383	0.9042	−7.68	−13.62	0.9793
6.00	0.9397	0.9039	−5.80	−14.85	0.9808
7.27	0.9415	0.9027	−3.98	−16.05	0.9815

Table 36. Static Performance Characteristics for Nozzles With $x_r/l_r = 1.00$, $\theta = 0°$, $\phi = 0°$, $\delta_{v,p} = 20°$, and $\delta_{v,y} = 0°$

NPR	F_r/F_i	F/F_i	δ_p, deg	δ_y, deg	w_p/w_i
(a) Nozzle 75, minimum sidewall					
2.00	0.9848	0.9437	16.58	−0.95	0.9817
2.50	0.9881	0.9389	18.14	−0.88	0.9843
3.00	0.9893	0.9521	15.74	−0.82	0.9855
3.50	0.9887	0.9536	15.29	−0.74	0.9868
4.00	0.9854	0.9438	16.69	−0.69	0.9881
5.01	0.9816	0.9177	20.77	−0.79	0.9899
6.00	0.9800	0.8951	24.02	−0.88	0.9913
7.00	0.9808	0.8785	26.39	−0.95	0.9924
7.99	0.9817	0.8660	28.08	−1.07	0.9936
(b) Nozzle 76, medium sidewall					
2.00	0.9864	0.9413	17.38	−0.82	0.9826
2.50	0.9913	0.9395	18.59	−0.79	0.9850
3.00	0.9927	0.9477	17.31	−0.70	0.9863
3.50	0.9924	0.9426	18.23	−0.73	0.9876
4.01	0.9916	0.9303	20.23	−0.76	0.9885
5.00	0.9907	0.9035	24.20	−0.84	0.9906
6.00	0.9937	0.8805	27.60	−0.94	0.9921
7.00	0.9970	0.8633	30.00	−1.08	0.9935
7.21	0.9982	0.8609	30.39	−1.09	0.9938
(c) Nozzle 77, maximum sidewall					
2.00	0.9866	0.9404	17.59	−0.68	0.9785
2.50	0.9921	0.9401	18.62	−0.74	0.9809
3.00	0.9937	0.9503	16.97	−0.66	0.9823
3.50	0.9918	0.9438	17.90	−0.66	0.9834
3.90	0.9911	0.9336	19.59	−0.68	0.9843
4.00	0.9906	0.9306	20.03	−0.67	0.9844
5.00	0.9910	0.9024	24.41	−0.81	0.9869
6.01	0.9942	0.8775	28.02	−0.92	0.9888
7.00	0.9991	0.8603	30.56	−1.05	0.9904

Table 37. Static Performance Characteristics for Nozzles With $x_r/l_r = 0.42$, $\theta = 20°$, $\phi = 0°$, $\delta_{v,p} = 20°$, and $\delta_{v,y} = 0°$

NPR	F_r/F_i	F/F_i	δ_p, deg	δ_y, deg	w_p/w_i
(a) Nozzle 78, minimum sidewall					
2.00	0.9873	0.9468	16.45	−0.86	0.9745
2.50	0.9921	0.9459	17.53	−0.82	0.9765
3.00	0.9915	0.9547	15.65	−0.69	0.9784
3.50	0.9919	0.9543	15.83	−0.66	0.9796
4.00	0.9876	0.9407	17.71	−0.65	0.9808
5.00	0.9844	0.9122	22.06	−0.76	0.9826
6.00	0.9828	0.8912	24.92	−0.81	0.9841
7.00	0.9821	0.8744	27.08	−0.90	0.9855
7.89	0.9825	0.8634	28.50	−1.03	0.9863
(b) Nozzle 79, medium sidewall					
2.00	0.9879	0.9452	16.89	−0.84	0.9770
2.50	0.9930	0.9447	17.93	−0.80	0.9797
3.00	0.9949	0.9502	17.22	−0.71	0.9811
3.50	0.9929	0.9426	18.29	−0.69	0.9821
4.00	0.9911	0.9296	20.28	−0.70	0.9832
5.00	0.9884	0.9016	24.17	−0.79	0.9854
6.00	0.9891	0.8784	27.36	−0.89	0.9870
7.01	0.9918	0.8623	29.60	−0.90	0.9882
7.41	0.9924	0.8565	30.32	−0.94	0.9886
(c) Nozzle 80, maximum sidewall					
2.01	0.9877	0.9447	16.95	−0.84	0.9736
2.50	0.9942	0.9450	18.09	−0.85	0.9760
3.00	0.9923	0.9475	17.27	−0.74	0.9778
3.50	0.9917	0.9415	18.30	−0.69	0.9789
4.00	0.9898	0.9277	20.38	−0.69	0.9800
5.00	0.9887	0.9012	24.29	−0.77	0.9823
6.01	0.9903	0.8787	27.45	−0.88	0.9844
7.00	0.9918	0.8613	29.72	−1.01	0.9860
7.40	0.9925	0.8556	30.44	−1.01	0.9865

Table 38. Static Performance Characteristics for Nozzles With $x_r/l_r = 0.20$, $\theta = 20°$, $\phi = 0°$, $\delta_{v,p} = 20°$, and $\delta_{v,y} = 0°$

NPR	F_r/F_i	F/F_i	δ_p, deg	δ_y, deg	w_p/w_i
(a) Nozzle 81, minimum sidewall					
2.00	0.9870	0.9526	15.14	−0.94	0.9722
2.50	0.9881	0.9500	15.95	−0.94	0.9750
3.00	0.9870	0.9530	15.05	−0.82	0.9767
3.50	0.9841	0.9471	15.75	−0.73	0.9779
4.03	0.9796	0.9330	17.73	−0.77	0.9798
5.00	0.9749	0.9084	21.27	−0.82	0.9813
6.00	0.9721	0.8881	23.98	−0.84	0.9828
7.00	0.9705	0.8726	25.94	−0.81	0.9841
8.00	0.9691	0.8610	27.31	−0.90	0.9851
(b) Nozzle 82, medium sidewall					
2.00	0.9833	0.9478	15.42	−0.77	0.9728
2.50	0.9856	0.9459	16.30	−0.76	0.9748
3.00	0.9857	0.9500	15.43	−0.77	0.9765
3.50	0.9805	0.9413	16.26	−0.73	0.9778
4.00	0.9763	0.9274	18.20	−0.57	0.9789
5.00	0.9715	0.9007	22.01	−0.62	0.9808
5.99	0.9690	0.8795	24.81	−0.80	0.9821
7.00	0.9670	0.8626	26.87	−0.79	0.9833
8.00	0.9663	0.8503	28.35	−0.74	0.9842
(c) Nozzle 83, maximum sidewall					
2.00	0.9841	0.9481	15.53	−0.70	0.9694
2.50	0.9864	0.9465	16.35	−0.64	0.9720
3.00	0.9849	0.9486	15.59	−0.59	0.9742
3.50	0.9811	0.9414	16.35	−0.47	0.9755
4.00	0.9764	0.9274	18.23	−0.38	0.9767
5.00	0.9729	0.9011	22.14	−0.64	0.9793
6.00	0.9696	0.8791	24.94	−0.74	0.9812
7.00	0.9684	0.8634	26.93	−0.77	0.9829
8.00	0.9686	0.8524	28.35	−0.91	0.9840

Table 39. Static Performance Characteristics for Nozzles With $x_r/l_r = 0.02$, $\theta = 20°$, $\phi = 0°$, $\delta_{v,p} = 20°$, and $\delta_{v,y} = 0°$

NPR	F_r/F_i	F/F_i	δ_p, deg	δ_y, deg	w_p/w_i
(a) Nozzle 84, minimum sidewall					
2.00	0.9679	0.9451	12.43	−0.81	1.0115
2.50	0.9583	0.9343	12.82	−0.71	1.0169
3.00	0.9548	0.9319	12.57	−0.56	1.0204
3.50	0.9504	0.9261	12.98	−0.58	1.0222
4.00	0.9440	0.9137	14.56	−0.54	1.0234
5.00	0.9332	0.8885	17.80	−0.60	1.0257
5.99	0.9275	0.8701	20.25	−0.71	1.0273
8.00	0.9217	0.8414	24.08	−0.74	1.0294
(b) Nozzle 85, medium sidewall					
2.01	0.9692	0.9446	12.90	−0.84	1.0172
2.50	0.9622	0.9363	13.30	−0.60	1.0246
3.00	0.9576	0.9330	13.02	0.04	1.0281
3.50	0.9503	0.9247	13.33	0.68	1.0304
4.01	0.9397	0.9074	15.04	0.91	1.0319
5.00	0.9323	0.8833	18.65	−0.59	1.0344
6.00	0.9233	0.8614	21.10	−0.13	1.0359
8.00	0.9203	0.8398	24.15	−0.44	1.0378
(c) Nozzle 86, maximum sidewall					
2.00	0.9659	0.9413	12.95	−0.58	1.0127
2.50	0.9643	0.9382	13.35	−0.59	1.0189
3.00	0.9496	0.9260	12.81	−0.42	1.0225
3.50	0.9465	0.9212	13.26	0.16	1.0244
4.01	0.9431	0.9093	15.40	−0.42	1.0259
5.00	0.9378	0.8878	18.79	−0.50	1.0281
6.00	0.9327	0.8708	20.98	−0.59	1.0299
8.00	0.9259	0.8460	23.96	−0.80	1.0322

Table 40. Static Performance Characteristics for Nozzles With $x_r/l_r = 0.42$, $\theta = 20°$, $\phi = 0°$, $\delta_{v,p} = 20°$, and $\delta_{v,y} = -20°$

NPR	F_r/F_i	F/F_i	δ_p, deg	δ_y, deg	w_p/w_i
Nozzle 87, maximum sidewall					
2.00	0.9827	0.9222	19 86	−4.09	0.9727
2.50	0.9858	0.9183	21.04	−3.77	0.9762
3.00	0.9870	0.9175	21.39	−3.55	0.9777
3.50	0.9849	0.9115	22.05	−3.28	0.9791
4.00	0.9834	0.9000	23.59	−3.24	0.9803
5.00	0.9860	0.8775	26.97	−3.45	0.9822
6.00	0.9898	0.8569	29.88	−3.68	0.9837
7.00	0.9934	0.8410	32.01	−3.92	0.9849

Table 41. Static Performance Characteristics for Nozzles With $x_r/l_r = 0.20$, $\theta = 20°$, $\phi = 0°$, $\delta_{v,p} = 20°$, and $\delta_{v,y} = -20°$

NPR	F_r/F_i	F/F_i	δ_p, deg	δ_y, deg	w_p/w_i
(a) Nozzle 88, medium sidewall					
2.00	0.9802	0.9230	18.56	−7.02	0.9577
2.50	0.9825	0.9186	19.68	−7.21	0.9637
3.00	0.9814	0.9175	19.64	−7.39	0.9657
3.50	0.9785	0.9077	20.81	−7.57	0.9673
4.00	0.9782	0.8966	22.51	−7.77	0.9684
5.00	0.9782	0.8738	25.77	−8.05	0.9705
6.00	0.9793	0.8552	28.31	−8.24	0.9721
7.00	0.9811	0.8416	30.14	−8.42	0.9734
7.60	0.9824	0.8355	30.97	−8.51	0.9740
(b) Nozzle 89, maximum sidewall					
2.00	0.9802	0.9193	19.05	−7.59	0.9557
2.50	0.9833	0.9168	20.01	−7.60	0.9619
3.00	0.9808	0.9122	20.35	−7.72	0.9642
3.50	0.9788	0.9027	21.57	−7.98	0.9657
4.01	0.9791	0.8909	23.38	−8.17	0.9664
5.00	0.9782	0.8661	26.67	−8.64	0.9685
6.00	0.9811	0.8480	29.24	−9.02	0.9698
7.00	0.9822	0.8323	31.17	−9.32	0.9710
7.40	0.9843	0.8293	31.70	−9.35	0.9712

Table 42. Static Performance Characteristics for Nozzles With $x_r/l_r = 0.02$, $\theta = 20°$, $\phi = 0°$, $\delta_{v,p} = 20°$, and $\delta_{v,y} = -20°$

NPR	F_r/F_i	F/F_i	δ_p, deg	δ_y, deg	w_p/w_i
(a) Nozzle 90, minimum sidewall					
2.00	0.9720	0.9327	13.47	−9.62	0.9458
2.50	0.9768	0.9356	13.93	−9.59	0.9499
3.00	0.9776	0.9386	13.48	−9.42	0.9513
3.50	0.9771	0.9383	13.53	−9.25	0.9530
4.00	0.9730	0.9281	15.10	−9.23	0.9540
5.00	0.9662	0.9060	18.44	−9.21	0.9564
6.00	0.9624	0.8905	20.65	−9.18	0.9584
7.98	0.9575	0.8678	23.60	−9.24	0.9616
8.00	0.9574	0.8677	23.62	−9.24	0.9617
(b) Nozzle 91, medium sidewall					
2.00	0.9721	0.9183	15.21	−12.18	0.9358
2.50	0.9765	0.9158	16.30	−12.77	0.9409
3.00	0.9767	0.9161	16.21	−12.85	0.9423
3.50	0.9745	0.9076	17.40	−13.16	0.9434
4.00	0.9717	0.8960	18.99	−13.48	0.9447
5.00	0.9674	0.8749	21.95	−13.77	0.9463
6.07	0.9657	0.8577	24.42	−13.96	0.9478
6.00	0.9659	0.8582	24.35	−13.99	0.9477
8.00	0.9635	0.8358	27.23	−14.22	0.9494
(c) Nozzle 92, maximum sidewall					
2.00	0.9749	0.9180	15.76	−12.37	0.9346
2.50	0.9786	0.9170	16.60	−12.61	0.9399
3.00	0.9782	0.9143	16.90	−12.88	0.9416
3.50	0.9749	0.9045	18.08	−13.24	0.9428
4.00	0.9729	0.8922	19.85	−13.64	0.9438
5.00	0.9681	0.8682	22.91	−14.26	0.9456
6.00	0.9674	0.8518	25.26	−14.55	0.9465
7.99	0.9651	0.8288	28.13	−14.84	0.9485

Table 43. Static Performance Characteristics for Nozzles With $x_r/l_r = 0.42$, $\theta = 30°$, $\phi = 0°$, $\delta_{v,p} = 20°$, and $\delta_{v,y} = 0°$

NPR	F_r/F_i	F/F_i	δ_p, deg	δ_y, deg	w_p/w_i
(a) Nozzle 93, minimum sidewall					
2.00	0.9901	0.9514	16.04	−0.79	0.9866
2.50	0.9934	0.9501	16.96	−0.88	0.9886
3.00	0.9940	0.9579	15.46	−0.74	0.9900
3.50	0.9921	0.9512	16.49	−0.65	0.9913
4.00	0.9898	0.9361	18.94	−0.72	0.9925
5.00	0.9859	0.9096	22.67	−0.78	0.9944
6.00	0.9849	0.8892	25.45	−0.86	0.9962
7.00	0.9842	0.8730	27.49	−0.90	0.9973
7.90	0.9840	0.8619	28.83	−1.03	0.9982
(b) Nozzle 94, medium sidewall					
2.00	0.9864	0.9413	17.39	−0.68	0.9876
2.50	0.9920	0.9430	18.07	−0.64	0.9899
3.00	0.9934	0.9458	17.80	−0.61	0.9910
3.50	0.9920	0.9371	19.16	−0.62	0.9927
4.00	0.9914	0.9242	21.22	−0.67	0.9936
5.00	0.9902	0.8976	24.97	−0.77	0.9956
6.00	0.9906	0.8763	27.78	−0.83	0.9973
7.00	0.9926	0.8611	29.82	−0.95	0.9982
7.40	0.9925	0.8550	30.50	−1.00	0.9989
(c) Nozzle 95, maximum sidewall					
2.00	0.9887	0.9472	16.65	−0.60	0.9836
2.50	0.9920	0.9460	17.51	−0.64	0.9869
3.00	0.9940	0.9486	17.37	−0.58	0.9884
3.50	0.9917	0.9388	18.79	−0.59	0.9898
4.00	0.9910	0.9254	20.95	−0.63	0.9911
5.00	0.9902	0.8988	24.81	−0.73	0.9935
6.00	0.9896	0.8758	27.73	−0.81	0.9955
7.00	0.9920	0.8609	29.79	−0.98	0.9969
7.39	0.9926	0.8557	30.44	−0.97	0.9975

Table 44. Static Performance Characteristics for Nozzles With $x_r/l_r = 0.20$, $\theta = 30°$, $\phi = 0°$, $\delta_{v,p} = 20°$, and $\delta_{v,y} = 0°$

NPR	F_r/F_i	F/F_i	δ_p, deg	δ_y, deg	w_p/w_i
(a) Nozzle 96, minimum sidewall					
2.00	0.9872	0.9582	13.90	−0.88	0.9882
2.50	0.9908	0.9586	14.63	−0.80	0.9903
3.00	0.9889	0.9551	14.99	−0.78	0.9916
3.50	0.9829	0.9423	16.52	−0.76	0.9931
4.00	0.9794	0.9288	18.48	−0.70	0.9939
5.00	0.9733	0.9052	21.55	−0.80	0.9961
6.00	0.9678	0.8862	23.69	−0.82	0.9976
7.00	0.9638	0.8718	25.23	−0.88	0.9986
8.00	0.9605	0.8605	26.37	−0.97	0.9995
(b) Nozzle 97, medium sidewall					
2.00	0.9870	0.9569	14.16	−0.71	0.9882
2.50	0.9874	0.9545	14.83	−0.62	0.9904
3.00	0.9870	0.9527	15.12	−0.65	0.9919
3.50	0.9831	0.9416	16.69	−0.65	0.9931
4.00	0.9780	0.9266	18.66	−0.67	0.9942
5.00	0.9715	0.9020	21.80	−0.70	0.9962
6.00	0.9662	0.8818	24.12	−0.75	0.9978
6.99	0.9632	0.8675	25.75	−0.84	0.9989
8.00	0.9603	0.8560	26.94	−0.91	0.9997
(c) Nozzle 98, maximum sidewall					
2.00	0.9852	0.9549	14.22	−0.70	0.9856
2.50	0.9868	0.9537	14.88	−0.66	0.9878
3.00	0.9871	0.9522	15.27	−0.59	0.9890
3.51	0.9827	0.9404	16.86	−0.64	0.9906
4.01	0.9786	0.9261	18.85	−0.63	0.9921
5.01	0.9718	0.9013	21.94	−0.67	0.9944
6.00	0.9679	0.8826	24.22	−0.78	0.9963
7.00	0.9646	0.8685	25.78	−0.86	0.9978
8.00	0.9629	0.8586	26.91	−0.87	0.9989

Table 45. Static Performance Characteristics for Nozzles With $x_r/l_r = 0.02$, $\theta = 30°$, $\phi = 0°$, $\delta_{v,p} = 20°$, and $\delta_{v,y} = 0°$

NPR	F_r/F_i	F/F_i	δ_p, deg	δ_y, deg	w_p/w_i
(a) Nozzle 99, minimum sidewall					
2.00	0.9687	0.9530	10.31	−0.77	1.0190
2.50	0.9580	0.9414	10.66	−0.69	1.0255
3.00	0.9446	0.9254	11.54	−0.72	1.0290
3.50	0.9300	0.9054	13.18	−0.69	1.0306
4.00	0.9198	0.8901	14.59	−0.70	1.0320
5.00	0.9120	0.8721	16.91	−1.92	1.0340
6.00	0.9028	0.8556	18.52	−2.02	1.0353
8.00	0.8949	0.8360	20.88	−0.85	1.0374
(b) Nozzle 100, medium sidewall					
2.01	0.9703	0.9544	10.39	−0.60	1.0199
2.50	0.9676	0.9507	10.72	−0.67	1.0266
3.01	0.9594	0.9397	11.61	−0.65	1.0303
3.50	0.9510	0.9262	13.10	−0.57	1.0318
4.00	0.9418	0.9109	14.69	−0.65	1.0333
5.00	0.9206	0.8800	17.03	−1.32	1.0356
6.00	0.9157	0.8670	18.75	−0.78	1.0371
8.00	0.9069	0.8492	20.55	−0.41	1.0386
(c) Nozzle 101, maximum sidewall					
2.00	0.9711	0.9547	10.51	−0.68	0.9946
2.50	0.9676	0.9499	10.96	−0.61	1.0010
3.00	0.9612	0.9409	11.79	−0.57	1.0046
3.50	0.9535	0.9279	13.29	−0.52	1.0064
4.00	0.9453	0.9135	14.88	−0.48	1.0079
5.00	0.9329	0.8911	17.22	−0.47	1.0103
6.00	0.9223	0.8732	18.79	−0.47	1.0122
8.00	0.9106	0.8519	20.69	−0.63	1.0143

Table 46. Static Performance Characteristics for Nozzles With $x_r/l_r = 0.20$, $\theta = 30°$, $\phi = 0°$, $\delta_{v,p} = 20°$, and $\delta_{v,y} = -20°$

NPR	F_r/F_i	F/F_i	δ_p, deg	δ_y, deg	w_p/w_i
(a) Nozzle 102, medium sidewall					
2.00	0.9659	0.9216	16.16	−6.85	0.9533
2.50	0.9698	0.9216	16.94	−6.86	0.9582
3.00	0.9684	0.9154	17.81	−7.20	0.9596
3.50	0.9649	0.9020	19.59	−7.59	0.9609
4.00	0.9661	0.8909	21.66	−7.70	0.9620
5.00	0.9628	0.8674	24.68	−8.23	0.9636
6.00	0.9611	0.8494	26.91	−8.57	0.9651
7.00	0.9597	0.8353	28.53	−8.88	0.9663
8.01	0.9574	0.8235	29.73	−9.06	0.9671
8.00	0.9584	0.8246	29.71	−9.03	0.9671
(b) Nozzle 103, maximum sidewall					
2.00	0.9684	0.9251	15.98	−6.70	0.9539
2.50	0.9717	0.9244	16.77	−6.78	0.9587
3.00	0.9717	0.9200	17.59	−7.01	0.9604
3.50	0.9702	0.9091	19.32	−7.26	0.9616
4.00	0.9687	0.8961	21.22	−7.63	0.9628
5.00	0.9651	0.8725	24.29	−8.01	0.9648
6.00	0.9640	0.8555	26.50	−8.28	0.9662
7.00	0.9631	0.8427	28.05	−8.50	0.9671
8.00	0.9606	0.8315	29.16	−8.68	0.9682

Table 47. Static Performance Characteristics for Nozzles With $x_r/l_r = 0.02$, $\theta = 30°$, $\phi = 0°$, $\delta_{v,p} = 20°$, and $\delta_{v,y} = -20°$

NPR	F_r/F_i	F/F_i	δ_p, deg	δ_y, deg	w_p/w_i
(a) Nozzle 104, medium sidewall					
2.00	0.9477	0.9119	11.35	−11.28	0.9381
2.50	0.9491	0.9097	11.89	−11.88	0.9421
3.00	0.9509	0.9066	13.53	−11.62	0.9440
3.50	0.9461	0.8929	15.43	−12.16	0.9458
4.00	0.9414	0.8797	17.11	−12.65	0.9469
5.00	0.9332	0.8585	19.49	−13.35	0.9488
6.00	0.9264	0.8418	21.24	−13.79	0.9501
7.00	0.9231	0.8318	22.34	−14.05	0.9512
8.00	0.9199	0.8244	23.07	−14.16	0.9522
(b) Nozzle 105, maximum sidewall					
2.00	0.9541	0.9167	11.63	−11.42	0.9398
2.50	0.9500	0.9084	12.32	−12.09	0.9440
3.00	0.9520	0.9059	13.32	−12.40	0.9457
3.50	0.9471	0.8936	14.94	−12.86	0.9472
4.00	0.9441	0.8829	16.51	−13.27	0.9480
5.00	0.9356	0.8620	18.93	−13.84	0.9499
6.00	0.9298	0.8467	20.65	−14.18	0.9515
7.00	0.9260	0.8375	22.00	−13.66	0.9524
8.00	0.9199	0.8265	22.87	−13.85	0.9532

Table 48. Static Performance Characteristics for Nozzles With $x_r/l_r = 0.42$, $\theta = 30°$, $\phi = 0°$, $\delta_{v,p} = 20°$, and $\delta_{v,y} = -30°$

NPR	F_r/F_i	F/F_i	δ_p, deg	δ_y, deg	w_p/w_i
Nozzle 106, maximum sidewall					
2.00	0.9803	0.9091	21.53	−4.86	0.9707
2.50	0.9846	0.9055	22.73	−4.70	0.9757
3.00	0.9822	0.8976	23.62	−4.53	0.9776
3.40	0.9822	0.8915	24.50	−4.46	0.9788
3.50	0.9815	0.8890	24.77	−4.47	0.9788
4.00	0.9828	0.8801	26.16	−4.31	0.9802
5.00	0.9841	0.8585	29.03	−4.35	0.9821
6.00	0.9872	0.8395	31.53	−4.58	0.9840
6.90	0.9911	0.8266	33.27	−4.80	0.9849

Table 49. Static Performance Characteristics for Nozzles With $x_r/l_r = 0.20$, $\theta = 30°$, $\phi = 0°$, $\delta_{v,p} = 20°$, and $\delta_{v,y} = -30°$

NPR	F_r/F_i	F/F_i	δ_p, deg	δ_y, deg	w_p/w_i
(a) Nozzle 107, medium sidewall					
2.01	0.9676	0.8917	20.66	−10.63	0.9177
2.50	0.9686	0.8847	21.92	−10.84	0.9269
3.00	0.9669	0.8765	22.93	−11.02	0.9302
3.50	0.9661	0.8651	24.48	−11.29	0.9318
4.00	0.9660	0.8534	26.09	−11.50	0.9328
5.01	0.9661	0.8331	28.75	−11.83	0.9350
6.00	0.9680	0.8169	30.84	−12.33	0.9364
7.00	0.9679	0.8034	32.34	−12.69	0.9376
7.50	0.9677	0.7982	32.89	−12.81	0.9380
(b) Nozzle 108, maximum sidewall					
2.00	0.9711	0.8961	20.52	−10.47	0.9309
2.50	0.9711	0.8875	21.99	−10.50	0.9399
3.00	0.9707	0.8791	23.16	−10.79	0.9428
3.50	0.9693	0.8657	24.89	−11.07	0.9445
4.00	0.9698	0.8539	26.57	−11.28	0.9458
5.00	0.9717	0.8334	29.35	−11.73	0.9479
6.00	0.9729	0.8166	31.40	−12.19	0.9493
7.00	0.9732	0.8032	32.89	−12.55	0.9502
7.40	0.9731	0.7992	33.32	−12.65	0.9508

Table 50. Static Performance Characteristics for Nozzles With $x_r/l_r = 0.02$, $\theta = 30°$, $\phi = 0°$, $\delta_{v,p} = 20°$, and $\delta_{v,y} = -30°$

NPR	F_r/F_i	F/F_i	δ_p, deg	δ_y, deg	w_p/w_i
(a) Nozzle 109, minimum sidewall					
2.01	0.9772	0.9348	12.46	−11.84	0.8917
2.50	0.9790	0.9367	12.62	−11.61	0.8967
3.00	0.9800	0.9348	13.37	−11.66	0.8980
3.50	0.9761	0.9261	14.71	−11.59	0.8999
4.00	0.9717	0.9160	16.08	−11.61	0.9012
5.00	0.9649	0.8996	18.23	−11.58	0.9031
6.00	0.9587	0.8859	19.75	−11.59	0.9049
8.00	0.9512	0.8682	21.69	−11.60	0.9075
(b) Nozzle 110, medium sidewall					
2.00	0.9686	0.9004	15.37	−15.95	0.8612
2.50	0.9695	0.8949	16.40	−16.44	0.8683
3.00	0.9715	0.8900	17.66	−16.71	0.8701
3.50	0.9676	0.8768	19.32	−17.12	0.8722
4.00	0.9655	0.8665	20.74	−17.39	0.8732
5.00	0.9605	0.8471	22.98	−18.01	0.8751
6.00	0.9568	0.8327	24.57	−18.45	0.8767
7.60	0.9520	0.8170	26.23	−18.74	0.8783
(c) Nozzle 111, maximum sidewall					
2.00	0.9691	0.8947	16.12	−16.69	0.8627
2.50	0.9696	0.8883	17.31	−17.06	0.8699
3.00	0.9684	0.8772	18.95	−17.63	0.8718
3.50	0.9662	0.8644	20.68	−18.10	0.8735
4.00	0.9637	0.8526	22.18	−18.47	0.8746
5.00	0.9603	0.8336	24.47	−19.10	0.8762
6.00	0.9568	0.8175	26.14	−19.75	0.8775
7.21	0.9527	0.8033	27.47	−20.26	0.8789

Table 51. Static Performance Characteristics for Nozzles With $x_r/l_r = 0.02$, $\theta = 20°$, $\phi = 0°$, $\delta_{v,p} = 0°$, and Maximum Sidewall

NPR	F_r/F_i	F/F_i	δ_p, deg	δ_y, deg	w_p/w_i
(a) Nozzle 112, $\delta_{v,y,l} = -20°$, $\delta_{v,y,r} = 0°$					
2.00	0.9717	0.9629	2.04	−7.44	0.9700
2.50	0.9743	0.9644	2.39	−7.83	0.9705
3.00	0.9764	0.9679	2.49	−7.15	0.9717
3.50	0.9721	0.9635	2.21	−7.31	0.9728
4.00	0.9697	0.9592	3.44	−7.70	0.9737
5.01	0.9636	0.9474	6.53	−8.30	0.9754
6.00	0.9612	0.9378	9.24	−8.83	0.9764
7.00	0.9620	0.9316	11.28	−9.26	0.9775
7.99	0.9615	0.9257	12.75	−9.45	0.9781
(b) Nozzle 113, $\delta_{v,y,l} = 0°$, $\delta_{v,y,r} = -20°$					
2.00	0.9730	0.9706	−3.98	−0.96	0.9923
2.50	0.9740	0.9713	−4.08	−1.32	0.9926
3.00	0.9741	0.9721	−3.30	−1.42	0.9938
3.50	0.9767	0.9743	−3.76	−1.58	0.9951
4.00	0.9763	0.9733	−4.18	−1.68	0.9959
5.00	0.9739	0.9727	−1.70	−2.16	0.9975
5.99	0.9691	0.9681	0.44	−2.50	0.9987
6.99	0.9665	0.9647	2.16	−2.76	0.9995
8.00	0.9635	0.9602	3.54	−3.16	1.0003

Table 52. Static Performance Characteristics for Nozzles With $x_r/l_r = 0.20$, $\theta = 20°$, $\phi = 0°$, $\delta_{v,p} = 0°$, and Maximum Sidewall

NPR	F_r/F_i	F/F_i	δ_p, deg	δ_y, deg	w_p/w_i
(a) Nozzle 114, $\delta_{v,y,l} = -20°$, $\delta_{v,y,r} = 0°$					
2.00	0.9584	0.9510	2.68	−6.62	0.9825
2.50	0.9645	0.9559	3.85	−6.64	0.9835
3.00	0.9687	0.9585	5.34	−6.42	0.9846
3.50	0.9692	0.9605	4.75	−6.07	0.9857
4.00	0.9688	0.9592	5.12	−6.25	0.9865
5.00	0.9672	0.9528	7.43	−6.66	0.9881
6.00	0.9665	0.9457	9.70	−7.03	0.9892
7.00	0.9667	0.9392	11.72	−7.30	0.9900
7.99	0.9676	0.9341	13.34	−7.40	0.9907
(b) Nozzle 115, $\delta_{v,y,l} = 0°$, $\delta_{v,y,r} = -20°$					
2.01	0.9745	0.9719	−4.01	−1.29	0.9820
2.50	0.9802	0.9787	−3.09	−0.55	0.9822
3.00	0.9800	0.9797	−1.22	−0.69	0.9835
3.50	0.9808	0.9797	−2.61	−0.76	0.9848
4.00	0.9817	0.9807	−2.52	−0.83	0.9856
5.00	0.9800	0.9798	0.16	−0.99	0.9872
6.00	0.9767	0.9753	2.80	−1.29	0.9883
7.00	0.9758	0.9718	4.89	−1.58	0.9892
8.00	0.9756	0.9688	6.52	−1.90	0.9899

Table 53. Static Performance Characteristics for Nozzles With $x_r/l_r = 0.20$, $\theta = 30°$, $\phi = 0°$, $\delta_{v,p} = 0°$, and Maximum Sidewall

NPR	F_r/F_i	F/F_i	δ_p, deg	δ_y, deg	w_p/w_i
(a) Nozzle 116, $\delta_{v,y,l} = -30°$, $\delta_{v,y,r} = 0°$					
2.00	0.9438	0.9232	6.33	−10.29	0.9930
2.50	0.9454	0.9211	7.79	−10.55	0.9942
3.00	0.9483	0.9210	9.08	−10.55	0.9960
3.50	0.9483	0.9203	9.61	−10.32	0.9970
4.00	0.9483	0.9172	10.54	−10.49	0.9978
5.00	0.9486	0.9094	12.67	−10.94	0.9994
6.00	0.9495	0.9023	14.58	−11.27	1.0006
7.03	0.9501	0.8958	16.19	−11.41	1.0014
8.00	0.9500	0.8898	17.41	−11.53	1.0020
(b) Nozzle 117, $\delta_{v,y,l} = 0°$, $\delta_{v,y,r} = -30°$					
2.00	0.9764	0.9726	−4.97	−0.88	0.9938
2.50	0.9789	0.9768	−3.77	−0.44	0.9943
3.00	0.9832	0.9822	−2.62	−0.35	0.9953
3.50	0.9857	0.9847	−2.53	−0.35	0.9965
4.00	0.9866	0.9862	−1.48	−0.45	0.9973
5.00	0.9812	0.9809	1.24	−0.93	0.9991
6.00	0.9786	0.9766	3.49	−1.16	1.0004
7.01	0.9771	0.9728	5.24	−1.38	1.0014
8.00	0.9758	0.9688	6.66	−1.67	1.0019

Table 54. Static Performance Characteristics for Nozzles With $x_r/l_r = 0.02$, $\theta = 20°$, $\phi = 0°$, $\delta_{v,p} = 20°$, and Maximum Sidewall

NPR	F_r/F_i	F/F_i	δ_p, deg	δ_y, deg	w_p/w_i
(a) Nozzle 118, $\delta_{v,y,l} = -20°$, $\delta_{v,y,r} = 0°$					
2.00	0.9792	0.9178	19.64	−5.97	0.9477
2.50	0.9808	0.9130	20.72	−5.97	0.9552
3.00	0.9768	0.9057	21.31	−6.02	0.9571
3.50	0.9746	0.8949	22.71	−5.95	0.9583
4.00	0.9717	0.8803	24.52	−5.87	0.9595
5.00	0.9737	0.8575	27.80	−6.13	0.9613
6.00	0.9764	0.8386	30.38	−6.22	0.9629
7.00	0.9779	0.8236	32.23	−6.26	0.9640
7.30	0.9791	0.8208	32.65	−6.32	0.9643
(b) Nozzle 119, $\delta_{v,y,l} = 0°$, $\delta_{v,y,r} = -20°$					
2.00	0.9781	0.9452	14.75	−2.19	0.9792
2.50	0.9824	0.9454	15.65	−2.11	0.9809
3.00	0.9829	0.9492	14.88	−2.32	0.9821
3.50	0.9801	0.9434	15.56	−2.47	0.9837
4.00	0.9772	0.9313	17.44	−2.74	0.9847
5.00	0.9727	0.9064	21.09	−3.13	0.9867
6.00	0.9700	0.8860	23.81	−3.55	0.9885
7.00	0.9696	0.8714	25.79	−3.86	0.9898
8.00	0.9689	0.8594	27.29	−4.04	0.9910

Table 55. Static Performance Characteristics for Nozzles With $x_r/l_r = 0.20$, $\theta = 30°$, $\phi = 0°$, $\delta_{v,p} = 20°$, and Maximum Sidewall

NPR	F_r/F_i	F/F_i	δ_p, deg	δ_y, deg	w_p/w_i
(a) Nozzle 120, $\delta_{v,y,l} = -30°$, $\delta_{v,y,r} = 0°$					
2.00	0.9721	0.8971	21.18	−8.86	0.9195
2.50	0.9736	0.8899	22.59	−8.80	0.9292
3.01	0.9719	0.8799	23.85	−8.89	0.9326
3.50	0.9709	0.8668	25.63	−8.87	0.9343
4.00	0.9699	0.8538	27.29	−8.85	0.9355
5.00	0.9688	0.8319	29.96	−8.79	0.9375
6.00	0.9692	0.8150	32.00	−8.77	0.9386
7.00	0.9689	0.8017	33.45	−8.80	0.9401
7.30	0.9697	0.7995	33.76	−8.82	0.9403
(b) Nozzle 121, $\delta_{v,y,l} = 0°$, $\delta_{v,y,r} = -30°$					
2.00	0.9811	0.9515	13.96	−2.09	0.9754
2.50	0.9807	0.9493	14.40	−2.16	0.9768
3.00	0.9822	0.9490	14.78	−2.36	0.9780
3.50	0.9786	0.9385	16.28	−2.58	0.9793
4.00	0.9756	0.9256	18.23	−2.84	0.9806
5.00	0.9711	0.9034	21.31	−3.27	0.9827
6.00	0.9672	0.8855	23.48	−3.71	0.9845
7.00	0.9645	0.8719	25.06	−4.06	0.9858
8.00	0.9625	0.8621	26.14	−4.34	0.9869

Table 56. Static Performance Characteristics for Nozzles With $x_r/l_r = 0.20$, $\theta = 30°$, $\phi = 15°$, $\delta_{v,p} = 0°$, and $\delta_{v,y} = -15°$

NPR	F_r/F_i	F/F_i	δ_p, deg	δ_y, deg	w_p/w_i
(a) Nozzle 122, medium sidewall					
2.00	0.9704	0.9678	−0.78	−4.17	0.9945
2.51	0.9737	0.9718	−0.35	−3.58	0.9948
3.00	0.9775	0.9750	1.87	−3.67	0.9961
3.50	0.9784	0.9758	1.15	−4.03	0.9972
4.00	0.9777	0.9746	1.50	−4.37	0.9981
5.00	0.9766	0.9709	3.70	−4.96	0.9994
6.00	0.9754	0.9653	6.26	−5.43	1.0006
7.00	0.9776	0.9621	8.56	−5.70	1.0013
8.01	0.9798	0.9589	10.35	−5.89	1.0018
(b) Nozzle 123, maximum sidewall					
2.00	0.9660	0.9614	0.61	−5.55	0.9953
2.50	0.9697	0.9655	1.46	−5.15	0.9959
3.00	0.9743	0.9694	3.05	−4.87	0.9968
3.50	0.9770	0.9736	1.68	−4.53	0.9980
4.00	0.9766	0.9727	1.99	−4.76	0.9989
5.00	0.9750	0.9679	4.28	−5.47	1.0007
6.00	0.9745	0.9622	6.80	−6.11	1.0019
7.00	0.9761	0.9573	9.15	−6.71	1.0025
8.00	0.9777	0.9526	10.97	−7.17	1.0031

Table 57. Static Performance Characteristics for Nozzles With $x_r/l_r = 0.20$, $\theta = 30°$, $\phi = 15°$, $\delta_{v,p} = 0°$, and $\delta_{v,y} = -30°$

NPR	F_r/F_i	F/F_i	δ_p, deg	δ_y, deg	w_p/w_i
(a) Nozzle 124, medium sidewall					
2.00	0.9594	0.9477	2.54	−8.59	0.9916
2.50	0.9613	0.9487	4.13	−8.33	0.9934
3.00	0.9640	0.9492	5.50	−8.44	0.9949
3.50	0.9638	0.9475	6.10	−8.66	0.9960
4.00	0.9622	0.9432	7.07	−9.04	0.9968
5.00	0.9602	0.9334	9.51	−9.86	0.9982
6.00	0.9622	0.9277	11.71	−10.27	0.9994
7.00	0.9641	0.9225	13.49	−10.56	1.0002
8.00	0.9656	0.9180	14.82	−10.78	1.0007
(b) Nozzle 125, maximum sidewall					
2.00	0.9478	0.9252	6.06	−11.04	0.9886
2.50	0.9529	0.9280	7.63	−10.78	0.9907
3.00	0.9551	0.9277	8.66	−10.87	0.9923
3.50	0.9554	0.9268	9.07	−10.92	0.9934
4.00	0.9542	0.9216	9.85	−11.57	0.9945
5.00	0.9536	0.9117	12.05	−12.44	0.9962
6.00	0.9562	0.9050	14.09	−13.01	0.9971
7.00	0.9585	0.8988	15.78	−13.47	0.9980
8.00	0.9604	0.8932	17.10	−13.91	0.9986

Table 58. Static Performance Characteristics for Nozzles With $x_r/l_r = 0.20$, $\theta = 30°$, $\phi = 30°$, $\delta_{v,p} = 0°$, and $\delta_{v,y} = -15°$

NPR	F_r/F_i	F/F_i	δ_p, deg	δ_y, deg	w_p/w_i
(a) Nozzle 126, medium sidewall					
2.00	0.9732	0.9709	−1.14	−3.72	0.9915
2.51	0.9775	0.9757	−1.14	−3.28	0.9924
3.00	0.9818	0.9797	1.39	−3.48	0.9935
3.50	0.9805	0.9782	0.54	−3.92	0.9948
4.00	0.9805	0.9777	0.91	−4.29	0.9954
5.00	0.9786	0.9735	3.21	−4.92	0.9969
6.00	0.9788	0.9695	5.85	−5.39	0.9979
6.99	0.9795	0.9648	8.20	−5.68	0.9989
8.00	0.9820	0.9621	10.03	−5.87	0.9995
(b) Nozzle 127, maximum sidewall					
2.00	0.9724	0.9692	0.05	−4.62	0.9908
2.50	0.9769	0.9739	0.57	−4.47	0.9915
3.00	0.9810	0.9779	2.19	−3.99	0.9929
3.50	0.9810	0.9785	0.89	−4.00	0.9941
4.00	0.9813	0.9781	1.14	−4.44	0.9949
5.00	0.9785	0.9727	3.51	−5.19	0.9966
6.00	0.9775	0.9666	6.25	−5.90	0.9981
7.00	0.9788	0.9616	8.65	−6.47	0.9989
7.99	0.9802	0.9570	10.50	−6.94	0.9996

Table 59. Static Performance Characteristics for Nozzles With $x_r/l_r = 0.20$, $\theta = 30°$, $\phi = 30°$, $\delta_{v,p} = 0°$, and $\delta_{v,y} = -30°$

NPR	F_r/F_i	F/F_i	δ_p, deg	δ_y, deg	w_p/w_i
(a) Nozzle 128, medium sidewall					
2.00	0.9630	0.9547	1.73	−7.34	0.9862
2.50	0.9609	0.9507	2.57	−7.96	0.9887
3.00	0.9589	0.9457	4.02	−8.68	0.9897
3.50	0.9604	0.9455	4.61	−9.02	0.9910
4.00	0.9620	0.9446	5.77	−9.30	0.9917
5.01	0.9643	0.9405	8.31	−9.81	0.9934
6.00	0.9666	0.9352	10.68	−10.26	0.9947
7.00	0.9696	0.9308	12.64	−10.57	0.9955
8.00	0.9717	0.9265	14.13	−10.84	0.9962
(b) Nozzle 129, maximum sidewall					
2.00	0.9538	0.9373	4.54	−9.69	0.9857
2.50	0.9538	0.9342	5.22	−10.48	0.9881
3.00	0.9563	0.9345	6.45	−10.51	0.9893
3.50	0.9528	0.9289	6.68	−11.06	0.9905
4.00	0.9572	0.9301	7.83	−11.32	0.9913
5.00	0.9591	0.9242	10.27	−11.88	0.9930
6.00	0.9621	0.9176	12.57	−12.56	0.9942
7.00	0.9654	0.9119	14.48	−13.10	0.9949
7.00	0.9655	0.9120	14.48	−13.10	0.9949
8.01	0.9672	0.9063	15.91	−13.52	0.9955

Table 60. Static Performance Characteristics for Nozzles With $x_r/l_r = 0.20$, $\theta = 30°$, $\phi = 15°$, $\delta_{v,p} = -20°$, and $\delta_{v,y} = -15°$

NPR	F_r/F_i	F/F_i	δ_p, deg	δ_y, deg	w_p/w_i
(a) Nozzle 130, medium sidewall					
2.00	0.9154	0.8611	−19.80	−1.55	0.9944
2.50	0.9224	0.8736	−18.72	−0.66	0.9946
3.00	0.9351	0.8808	−19.60	0.88	0.9962
3.50	0.9403	0.8899	−18.84	−0.35	0.9969
4.00	0.9419	0.8930	−18.49	−1.52	0.9979
5.00	0.9466	0.9015	−17.62	−2.35	0.9994
6.00	0.9519	0.9198	−14.63	−3.02	1.0005
7.00	0.9560	0.9319	−12.41	−3.52	1.0013
8.00	0.9591	0.9404	−10.69	−3.84	1.0017
(b) Nozzle 131, maximum sidewall					
2.00	0.8991	0.8382	−20.69	−5.04	0.9943
2.50	0.9184	0.8750	−17.48	−2.94	0.9950
3.00	0.9274	0.8831	−17.68	−1.97	0.9963
3.50	0.9338	0.8896	−17.52	−2.74	0.9972
4.00	0.9435	0.8893	−19.50	−0.43	0.9981
5.00	0.9460	0.8984	−18.21	−1.30	0.9998
6.00	0.9526	0.9212	−14.58	−2.33	1.0008
7.00	0.9551	0.9317	−12.24	−3.46	1.0014
8.00	0.9572	0.9389	−10.41	−4.31	1.0019

Table 61. Static Performance Characteristics for Nozzles With $x_r/l_r = 0.20$, $\theta = 30°$, $\phi = 15°$, $\delta_{v,p} = -20°$, and $\delta_{v,y} = -30°$

NPR	F_r/F_i	F/F_i	δ_p, deg	δ_y, deg	w_p/w_i
(a) Nozzle 132, medium sidewall					
2.00	0.9061	0.8752	−14.16	−5.17	0.9948
2.50	0.9117	0.8821	−13.81	−5.03	0.9956
3.00	0.9247	0.8939	−14.27	−4.21	0.9968
3.50	0.9296	0.9027	−12.94	−5.00	0.9979
4.00	0.9338	0.9094	−11.93	−5.63	0.9989
5.00	0.9313	0.9036	−12.38	−6.72	1.0005
6.00	0.9324	0.9077	−10.83	−7.75	1.0016
7.00	0.9354	0.9150	−8.90	−8.16	1.0024
8.00	0.9386	0.9211	−7.31	−8.41	1.0030
(b) Nozzle 133, maximum sidewall					
2.00	0.8827	0.8467	−12.74	−10.69	0.9931
2.50	0.8900	0.8571	−11.45	−10.91	0.9942
3.00	0.8989	0.8687	−10.35	−10.94	0.9957
3.50	0.9077	0.8796	−9.81	−10.59	0.9964
4.00	0.9179	0.8927	−9.93	−9.25	0.9972
4.99	0.9215	0.8952	−10.51	−9.05	0.9988
6.00	0.9178	0.8887	−9.73	−10.91	0.9998
7.00	0.9205	0.8934	−7.74	−11.71	1.0006
8.00	0.9256	0.9001	−6.03	−12.12	1.0011

Table 62. Static Performance Characteristics for Nozzles With $x_r/l_r = 0.20$, $\theta = 30°$, $\phi = 30°$, $\delta_{v,p} = -20°$, and $\delta_{v,y} = -15°$

NPR	F_r/F_i	F/F_i	δ_p, deg	δ_y, deg	w_p/w_i
(a) Nozzle 134, medium sidewall					
2.01	0.9202	0.8560	−21.51	−0.96	0.9946
2.50	0.9175	0.8372	−24.14	−0.67	0.9954
3.00	0.9276	0.8435	−24.58	−0.72	0.9962
3.50	0.9372	0.8751	−20.96	−0.65	0.9972
4.00	0.9441	0.8885	−19.72	−1.14	0.9981
5.01	0.9494	0.8973	−19.01	−1.84	0.9997
6.00	0.9541	0.9189	−15.36	−2.92	1.0009
7.00	0.9580	0.9319	−13.06	−3.14	1.0016
7.99	0.9605	0.9403	−11.26	−3.55	1.0021
(b) Nozzle 135, maximum sidewall					
2.00	0.9058	0.8339	−22.63	−4.39	0.9948
2.50	0.9070	0.8365	−22.43	−4.19	0.9955
3.00	0.9160	0.8389	−23.52	−3.02	0.9961
3.50	0.9281	0.8519	−23.29	−2.33	0.9975
4.00	0.9411	0.8623	−23.62	−0.07	0.9981
5.00	0.9479	0.8921	−19.72	−1.28	0.9999
6.00	0.9526	0.9169	−15.54	−2.60	1.0012
7.00	0.9562	0.9298	−13.06	−3.53	1.0020
8.00	0.9597	0.9393	−11.11	−4.24	1.0026

Table 63. Static Performance Characteristics for Nozzles With $x_r/l_r = 0.20$, $\theta = 30°$, $\phi = 30°$, $\delta_{v,p} = -20°$, and $\delta_{v,y} = -30°$

NPR	F_r/F_i	F/F_i	δ_p, deg	δ_y, deg	w_p/w_i
(a) Nozzle 136, medium sidewall					
2.00	0.9205	0.8739	−18.02	−3.53	0.9936
2.51	0.9251	0.8830	−17.13	−3.02	0.9947
3.00	0.9345	0.8911	−17.35	−2.60	0.9959
3.50	0.9392	0.9046	−15.15	−3.89	0.9969
4.00	0.9419	0.9103	−14.23	−4.58	0.9977
5.00	0.9380	0.8988	−15.57	−6.15	0.9991
6.00	0.9423	0.9121	−12.97	−6.78	1.0003
7.00	0.9477	0.9249	−10.70	−6.84	1.0011
8.00	0.9508	0.9322	−8.99	−7.03	1.0016
(b) Nozzle 137, maximum sidewall					
2.00	0.9050	0.8620	−16.19	−7.63	0.9948
2.50	0.9056	0.8657	−14.93	−8.68	0.9953
3.00	0.9152	0.8787	−14.09	−8.40	0.9965
3.50	0.9214	0.8831	−14.64	−8.15	0.9972
4.00	0.9314	0.8913	−15.82	−6.17	0.9984
5.00	0.9301	0.8889	−15.35	−7.94	0.9999
6.00	0.9284	0.8933	−13.01	−9.27	1.0009
7.00	0.9357	0.9080	−10.37	−9.60	1.0016
7.99	0.9394	0.9147	−8.57	−10.15	1.0021

Table 64. Static Performance Characteristics for Nozzles With $x_r/l_r = 0.20$, $\theta = 30°$, $\phi = 15°$, $\delta_{v,p} = 20°$, and $\delta_{v,y} = -15°$

NPR	F_r/F_i	F/F_i	δ_p, deg	δ_y, deg	w_p/w_i
(a) Nozzle 138, medium sidewall					
2.00	0.9777	0.9237	17.95	−7.05	0.9613
2.50	0.9800	0.9205	18.93	−7.19	0.9662
3.00	0.9803	0.9230	18.48	−7.27	0.9679
3.50	0.9788	0.9179	19.12	−7.38	0.9691
4.01	0.9784	0.9078	20.79	−7.54	0.9701
5.00	0.9776	0.8836	24.40	−7.72	0.9719
6.01	0.9798	0.8649	27.23	−7.79	0.9734
7.00	0.9817	0.8501	29.26	−7.93	0.9745
7.76	0.9828	0.8416	30.40	−7.98	0.9754
(b) Nozzle 139, maximum sidewall					
2.00	0.9798	0.9246	18.20	−6.98	0.9614
2.50	0.9834	0.9237	18.98	−7.04	0.9669
3.00	0.9847	0.9254	18.80	−7.30	0.9687
3.50	0.9825	0.9185	19.60	−7.53	0.9698
4.00	0.9803	0.9056	21.37	−7.81	0.9708
5.01	0.9790	0.8790	25.11	−8.23	0.9726
6.01	0.9814	0.8592	27.98	−8.49	0.9740
7.01	0.9830	0.8437	30.03	−8.67	0.9751
7.62	0.9840	0.8363	30.98	−8.77	0.9758

Table 65. Static Performance Characteristics for Nozzles With $x_r/l_r = 0.20$, $\theta = 30°$, $\phi = 15°$, $\delta_{v,p} = 20°$, and $\delta_{v,y} = -30°$

NPR	F_r/F_i	F/F_i	δ_p, deg	δ_y, deg	w_p/w_i
(a) Nozzle 140, medium sidewall					
2.00	0.9695	0.8993	19.31	−11.24	0.9150
2.50	0.9724	0.8954	20.42	−11.42	0.9230
3.01	0.9717	0.8886	21.38	−11.62	0.9257
3.51	0.9722	0.8782	23.09	−11.81	0.9275
4.00	0.9712	0.8661	24.74	−12.02	0.9288
5.00	0.9707	0.8455	27.45	−12.39	0.9307
6.00	0.9722	0.8306	29.49	−12.64	0.9321
7.01	0.9717	0.8175	30.98	−12.91	0.9332
7.90	0.9704	0.8084	31.90	−13.02	0.9339
(b) Nozzle 141, maximum sidewall					
2.00	0.9690	0.8916	20.32	−11.84	0.9139
2.50	0.9699	0.8851	21.46	−12.14	0.9228
3.00	0.9689	0.8747	22.86	−12.49	0.9263
3.50	0.9678	0.8608	24.73	−12.87	0.9280
4.01	0.9693	0.8496	26.44	−13.12	0.9295
5.00	0.9692	0.8286	29.10	−13.59	0.9314
6.00	0.9717	0.8133	31.14	−14.02	0.9327
7.01	0.9714	0.8000	32.59	−14.36	0.9340
7.63	0.9711	0.7938	33.24	−14.51	0.9346

Table 66. Static Performance Characteristics for Nozzles With $x_r/l_r = 0.20$, $\theta = 30°$, $\phi = 30°$, $\delta_{v,p} = -20°$, and $\delta_{v,y} = -15°$

NPR	F_r/F_i	F/F_i	δ_p, deg	δ_y, deg	w_p/w_i
(a) Nozzle 142, medium sidewall					
2.00	0.9814	0.9281	17.71	−7.24	0.9598
2.50	0.9843	0.9251	18.67	−7.63	0.9641
3.00	0.9841	0.9264	18.28	−7.89	0.9655
3.50	0.9824	0.9213	18.87	−8.09	0.9669
4.00	0.9803	0.9100	20.48	−8.24	0.9679
5.01	0.9795	0.8860	24.11	−8.38	0.9698
6.00	0.9801	0.8657	27.00	−8.49	0.9712
7.00	0.9820	0.8507	29.09	−8.61	0.9724
7.79	0.9830	0.8415	30.29	−8.66	0.9731
(b) Nozzle 143, maximum sidewall					
2.00	0.9821	0.9275	17.88	−7.43	0.9591
2.50	0.9847	0.9243	18.82	−7.81	0.9639
3.00	0.9861	0.9265	18.56	−8.03	0.9652
3.51	0.9830	0.9192	19.23	−8.41	0.9665
4.00	0.9807	0.9068	20.92	−8.71	0.9675
5.00	0.9790	0.8810	24.62	−8.95	0.9694
6.00	0.9807	0.8613	27.51	−9.09	0.9708
7.00	0.9826	0.8456	29.64	−9.24	0.9719
7.70	0.9835	0.8374	30.71	−9.25	0.9727

Table 67. Static Performance Characteristics for Nozzles With $x_r/l_r = 0.20$, $\theta = 30°$, $\phi = 30°$, $\delta_{v,p} = 20°$, and $\delta_{v,y} = -30°$

NPR	F_r/F_i	F/F_i	δ_p, deg	δ_y, deg	w_p/w_i
(a) Nozzle 144, medium sidewall					
2.00	0.9687	0.8986	18.72	−12.26	0.8741
2.50	0.9707	0.8938	19.79	−12.62	0.8815
3.00	0.9725	0.8904	20.56	−12.89	0.8837
3.50	0.9722	0.8799	22.22	−13.05	0.8855
4.00	0.9712	0.8673	24.00	−13.28	0.8870
5.00	0.9713	0.8467	26.86	−13.70	0.8887
6.00	0.9723	0.8306	29.04	−13.97	0.8902
7.00	0.9734	0.8188	30.59	−14.19	0.8915
7.99	0.9734	0.8094	31.68	−14.32	0.8925
(b) Nozzle 145, maximum sidewall					
2.00	0.9695	0.8932	19.45	−13.02	0.8753
2.50	0.9729	0.8897	20.58	−13.18	0.8829
3.00	0.9732	0.8820	21.79	−13.51	0.8853
3.50	0.9725	0.8688	23.63	−13.94	0.8871
4.00	0.9729	0.8561	25.49	−14.21	0.8885
5.01	0.9724	0.8339	28.33	−14.71	0.8904
6.00	0.9734	0.8173	30.44	−15.13	0.8918
7.00	0.9740	0.8043	31.97	−15.49	0.8928
7.85	0.9736	0.7959	32.88	−15.62	0.8936

Table 68. Static Pressure Ratios for Nozzle 1, $x_r/l_r = 1.0$, $\theta = 0°$, $\phi = 0°$, Minimum Sidewall, $\delta_{v,p} = 0°$, and $\delta_{v,y} = 0°$

(a) Upper ramp

NPR	Static pressure ratios at x_r/l_r of—											
	−0.308	−0.170	−0.101	−0.032	0.037	0.106	0.175	0.244	0.382	0.520	0.659	0.797
2.00	0.852	0.636	0.562	0.523	0.493	0.463	0.427	0.500	0.555	0.542	0.536	0.500
2.50	0.851	0.635	0.560	0.522	0.492	0.462	0.424	0.376	0.273	0.500	0.498	0.383
3.00	0.850	0.634	0.557	0.521	0.489	0.461	0.421	0.374	0.272	0.207	0.408	0.492
3.50	0.850	0.632	0.556	0.521	0.488	0.461	0.419	0.373	0.272	0.207	0.240	0.267
4.00	0.850	0.632	0.556	0.520	0.488	0.461	0.417	0.380	0.272	0.206	0.166	0.195
5.01	0.849	0.631	0.554	0.519	0.486	0.461	0.415	0.381	0.272	0.205	0.165	0.127
6.00	0.849	0.630	0.553	0.520	0.486	0.461	0.413	0.381	0.271	0.204	0.164	0.127
7.00	0.848	0.629	0.552	0.519	0.485	0.461	0.412	0.382	0.272	0.204	0.164	0.127
8.00	0.848	0.628	0.551	0.518	0.485	0.461	0.411	0.382	0.272	0.204	0.164	0.127

(b) Lower flap

NPR	Static pressure ratios at x_r/l_r of—						
	−0.308	−0.170	−0.032	0.037	0.079	0.120	0.162
2.00	0.892	0.836	0.627	0.473	0.399	0.408	0.458
2.50	0.892	0.835	0.627	0.472	0.399	0.296	0.305
3.00	0.892	0.835	0.626	0.471	0.399	0.292	0.264
3.50	0.892	0.835	0.626	0.470	0.396	0.289	0.262
4.00	0.892	0.835	0.626	0.470	0.394	0.287	0.261
5.01	0.893	0.835	0.626	0.469	0.393	0.286	0.260
6.00	0.893	0.834	0.626	0.468	0.393	0.285	0.258
7.00	0.893	0.834	0.626	0.468	0.391	0.286	0.259
8.00	0.893	0.833	0.626	0.467	0.391	0.286	0.260

Table 69. Static Pressure Ratios for Nozzle 2, $x_r/l_r = 1.0$, $\theta = 0°$, $\phi = 0°$, Medium Sidewall, $\delta_{v,p} = 0°$, and $\delta_{v,y} = 0°$

(a) Upper ramp

NPR	Static pressure ratios at x_r/l_r of—											
	−0.308	−0.170	−0.101	−0.032	0.037	0.106	0.175	0.244	0.382	0.520	0.659	0.797
2.00	0.852	0.635	0.562	0.523	0.492	0.463	0.426	0.505	0.557	0.546	0.534	0.498
2.50	0.851	0.635	0.559	0.522	0.490	0.462	0.422	0.377	0.275	0.493	0.515	0.395
3.00	0.851	0.634	0.558	0.522	0.489	0.462	0.420	0.376	0.274	0.208	0.350	0.486
3.50	0.850	0.633	0.557	0.521	0.487	0.462	0.418	0.376	0.274	0.207	0.240	0.262
4.00	0.850	0.632	0.556	0.521	0.488	0.462	0.416	0.376	0.274	0.207	0.167	0.196
5.00	0.849	0.631	0.555	0.520	0.487	0.462	0.415	0.375	0.273	0.206	0.166	0.128
6.00	0.849	0.630	0.553	0.520	0.486	0.462	0.413	0.375	0.273	0.205	0.165	0.127
7.00	0.848	0.629	0.552	0.519	0.486	0.462	0.413	0.376	0.272	0.204	0.165	0.127
8.00	0.848	0.628	0.551	0.519	0.486	0.463	0.412	0.376	0.272	0.204	0.164	0.127

(b) Lower flap

NPR	Static pressure ratios at x_r/l_r of—						
	−0.308	−0.170	−0.032	0.037	0.079	0.120	0.162
2.00	0.892	0.836	0.626	0.470	0.394	0.380	0.465
2.50	0.891	0.836	0.626	0.470	0.393	0.301	0.303
3.00	0.891	0.836	0.626	0.470	0.392	0.297	0.266
3.50	0.892	0.836	0.626	0.469	0.392	0.293	0.264
4.00	0.892	0.835	0.626	0.469	0.391	0.291	0.263
5.00	0.893	0.835	0.626	0.469	0.391	0.288	0.263
6.00	0.893	0.834	0.626	0.469	0.391	0.286	0.263
7.00	0.893	0.834	0.626	0.469	0.391	0.286	0.263
8.00	0.893	0.833	0.626	0.468	0.392	0.285	0.263

Table 70. Static Pressure Ratios for Nozzle 3, $x_r/l_r = 1.0$, $\theta = 0°$, $\phi = 0°$, Maximum Sidewall, $\delta_{v,p} = 0°$, and $\delta_{v,y} = 0°$

(a) Upper ramp

NPR	Static pressure ratios at x_r/l_r of —											
	−0.308	−0.170	−0.101	−0.032	0.037	0.106	0.175	0.244	0.382	0.520	0.659	0.797
2.00	0.852	0.636	0.561	0.524	0.491	0.462	0.426	0.500	0.557	0.546	0.536	0.499
2.50	0.851	0.636	0.559	0.523	0.491	0.462	0.422	0.378	0.274	0.494	0.514	0.396
3.00	0.851	0.635	0.557	0.522	0.488	0.462	0.419	0.376	0.274	0.207	0.350	0.492
3.50	0.850	0.634	0.557	0.522	0.488	0.462	0.417	0.376	0.274	0.207	0.241	0.263
4.00	0.850	0.633	0.556	0.522	0.488	0.462	0.416	0.376	0.273	0.206	0.166	0.196
5.00	0.850	0.632	0.555	0.521	0.487	0.462	0.415	0.374	0.273	0.206	0.165	0.128
6.00	0.849	0.630	0.554	0.520	0.487	0.463	0.414	0.375	0.272	0.205	0.165	0.127
7.00	0.848	0.629	0.553	0.520	0.486	0.463	0.413	0.376	0.272	0.205	0.165	0.127
8.00	0.848	0.628	0.552	0.519	0.486	0.463	0.412	0.376	0.272	0.204	0.164	0.127

(b) Lower flap

NPR	Static pressure ratios at x_r/l_r of—						
	−0.308	−0.170	−0.032	0.037	0.079	0.120	0.162
2.00	0.892	0.836	0.626	0.471	0.394	0.384	0.463
2.50	0.892	0.836	0.626	0.470	0.393	0.303	0.304
3.00	0.891	0.835	0.626	0.470	0.393	0.298	0.266
3.50	0.892	0.835	0.626	0.469	0.392	0.293	0.264
4.00	0.892	0.835	0.626	0.469	0.392	0.290	0.263
5.00	0.893	0.835	0.626	0.469	0.391	0.287	0.263
6.00	0.893	0.834	0.626	0.469	0.391	0.285	0.263
7.00	0.893	0.834	0.626	0.469	0.391	0.284	0.263
8.00	0.893	0.833	0.626	0.469	0.391	0.284	0.263

Table 71. Static Pressure Ratios for Nozzle 4, $x_r/l_r = 0.42$, $\theta = 20°$, $\phi = 0°$, Minimum Sidewall, $\delta_{v,p} = 0°$, and $\delta_{v,y} = 0°$

(a) Upper ramp

NPR	Static pressure ratios at x_r/l_r of–											
	−0.308	−0.170	−0.101	−0.032	0.037	0.106	0.175	0.244	0.382	0.520	0.659	0.797
2.00	0.858	0.650	0.577	0.528	0.492	0.459	0.428	0.490	0.557	0.551	0.532	0.525
2.50	0.858	0.650	0.575	0.527	0.490	0.457	0.424	0.379	0.275	0.501	0.498	0.402
3.00	0.858	0.649	0.575	0.527	0.490	0.457	0.422	0.378	0.275	0.213	0.397	0.501
3.50	0.858	0.649	0.575	0.527	0.490	0.457	0.420	0.378	0.275	0.213	0.245	0.285
4.00	0.858	0.649	0.574	0.527	0.489	0.458	0.420	0.377	0.275	0.213	0.165	0.212
5.00	0.858	0.648	0.574	0.526	0.488	0.457	0.419	0.377	0.274	0.212	0.165	0.131
6.00	0.858	0.648	0.573	0.525	0.488	0.457	0.418	0.378	0.274	0.212	0.164	0.131
7.00	0.857	0.647	0.573	0.525	0.488	0.457	0.417	0.378	0.274	0.211	0.164	0.131
8.01	0.857	0.646	0.573	0.525	0.488	0.457	0.417	0.378	0.274	0.211	0.163	0.130

(b) Lower flap

NPR	Static pressure ratios at x_r/l_r of–						
	−0.308	−0.170	−0.032	0.037	0.079	0.120	0.162
2.00	0.893	0.841	0.626	0.477	0.400	0.318	0.477
2.50	0.893	0.841	0.626	0.476	0.400	0.307	0.279
3.00	0.893	0.841	0.625	0.476	0.399	0.307	0.253
3.50	0.893	0.841	0.625	0.475	0.399	0.306	0.252
4.00	0.894	0.841	0.625	0.475	0.399	0.306	0.252
5.00	0.894	0.841	0.625	0.474	0.398	0.306	0.251
6.00	0.894	0.840	0.625	0.474	0.398	0.305	0.250
7.00	0.894	0.840	0.625	0.473	0.398	0.305	0.249
8.01	0.894	0.839	0.625	0.472	0.398	0.305	0.249

Table 72. Static Pressure Ratios for Nozzle 5, $x_r/l_r = 0.42$, $\theta = 20°$, $\phi = 0°$, Medium Sidewall, $\delta_{v,p} = 0°$, and $\delta_{v,y} = 0°$

(a) Upper ramp

NPR	Static pressure ratios at x_r/l_r of –											
	−0.308	−0.170	−0.101	−0.032	0.037	0.106	0.175	0.244	0.382	0.520	0.659	0.797
2.00	0.858	0.649	0.577	0.528	0.492	0.459	0.428	0.491	0.559	0.551	0.531	0.523
2.50	0.858	0.650	0.575	0.527	0.491	0.458	0.425	0.380	0.276	0.495	0.515	0.417
3.00	0.858	0.649	0.573	0.527	0.488	0.457	0.422	0.379	0.275	0.213	0.359	0.505
3.50	0.858	0.649	0.573	0.526	0.488	0.457	0.421	0.378	0.275	0.213	0.242	0.281
4.00	0.858	0.648	0.573	0.526	0.488	0.457	0.420	0.378	0.275	0.213	0.165	0.212
5.00	0.858	0.648	0.573	0.525	0.487	0.456	0.418	0.377	0.274	0.212	0.165	0.131
6.00	0.858	0.647	0.573	0.525	0.488	0.456	0.417	0.377	0.274	0.211	0.164	0.131
7.00	0.857	0.647	0.572	0.525	0.488	0.457	0.417	0.378	0.274	0.211	0.163	0.131
8.00	0.857	0.646	0.572	0.524	0.488	0.457	0.416	0.378	0.274	0.211	0.163	0.130

(b) Lower flap

NPR	Static pressure ratios at x_r/l_r of –						
	−0.308	−0.170	−0.032	0.037	0.079	0.120	0.162
2.00	0.893	0.841	0.626	0.477	0.400	0.317	0.475
2.50	0.893	0.841	0.625	0.476	0.399	0.307	0.281
3.00	0.893	0.841	0.625	0.476	0.399	0.307	0.255
3.50	0.893	0.841	0.625	0.475	0.398	0.306	0.254
4.00	0.893	0.841	0.625	0.474	0.398	0.306	0.253
5.00	0.894	0.840	0.625	0.474	0.398	0.305	0.252
6.00	0.894	0.840	0.625	0.474	0.398	0.305	0.252
7.00	0.894	0.839	0.625	0.473	0.398	0.305	0.252
8.00	0.894	0.839	0.624	0.472	0.398	0.305	0.251

Table 73. Static Pressure Ratios for Nozzle 6, $x_r/l_r = 0.42$, $\theta = 20°$, $\phi = 0°$, Maximum Sidewall, $\delta_{v,p} = 0°$, and $\delta_{v,y} = 0°$

(a) Upper ramp

NPR	Static pressure ratios at x_r/l_r of—											
	−0.308	−0.170	−0.101	−0.032	0.037	0.106	0.175	0.244	0.382	0.520	0.659	0.797
2.00	0.858	0.649	0.576	0.527	0.492	0.458	0.428	0.489	0.559	0.551	0.532	0.524
2.50	0.858	0.650	0.574	0.527	0.490	0.457	0.425	0.380	0.276	0.492	0.517	0.419
3.00	0.858	0.649	0.574	0.527	0.490	0.457	0.423	0.378	0.275	0.214	0.357	0.503
3.50	0.858	0.649	0.574	0.527	0.489	0.457	0.421	0.378	0.275	0.213	0.245	0.281
4.00	0.858	0.649	0.574	0.526	0.489	0.457	0.420	0.378	0.275	0.213	0.165	0.211
5.00	0.858	0.648	0.573	0.526	0.488	0.457	0.418	0.377	0.275	0.212	0.164	0.131
6.00	0.858	0.647	0.573	0.525	0.488	0.457	0.417	0.377	0.274	0.212	0.164	0.131
7.00	0.857	0.647	0.572	0.525	0.488	0.457	0.417	0.378	0.274	0.212	0.164	0.131
8.00	0.857	0.646	0.572	0.524	0.488	0.457	0.416	0.378	0.274	0.212	0.163	0.131

(b) Lower flap

NPR	Static pressure ratios at x_r/l_r of—						
	−0.308	−0.170	−0.032	0.037	0.079	0.120	0.162
2.00	0.893	0.841	0.625	0.476	0.400	0.317	0.475
2.50	0.893	0.841	0.625	0.476	0.399	0.307	0.276
3.00	0.892	0.841	0.625	0.475	0.399	0.307	0.252
3.50	0.893	0.841	0.625	0.475	0.398	0.306	0.251
4.00	0.893	0.841	0.625	0.474	0.398	0.306	0.250
5.00	0.894	0.840	0.625	0.474	0.398	0.305	0.250
6.00	0.894	0.840	0.625	0.473	0.398	0.305	0.249
7.00	0.894	0.839	0.624	0.473	0.398	0.305	0.249
8.00	0.894	0.839	0.624	0.472	0.398	0.305	0.248

Table 74. Static Pressure Ratios for Nozzle 7, $x_r/l_r = 0.20$, $\theta = 20°$, $\phi = 0°$, Minimum Sidewall, $\delta_{v,p} = 0°$, and $\delta_{v,y} = 0°$

(a) Upper ramp

NPR	Static pressure ratios at x_r/l_r of—											
	−0.308	−0.170	−0.101	−0.032	0.037	0.106	0.175	0.244	0.382	0.520	0.659	0.797
2.00	0.852	0.652	0.561	0.537	0.485	0.451	0.426	0.490	0.552	0.548	0.530	0.521
2.50	0.852	0.652	0.560	0.536	0.484	0.450	0.423	0.379	0.274	0.496	0.496	0.393
3.00	0.852	0.652	0.558	0.536	0.482	0.450	0.421	0.377	0.273	0.213	0.394	0.492
3.51	0.852	0.652	0.559	0.535	0.482	0.450	0.419	0.377	0.273	0.212	0.243	0.289
4.00	0.852	0.652	0.558	0.535	0.481	0.450	0.418	0.377	0.272	0.212	0.165	0.211
5.00	0.852	0.651	0.558	0.535	0.481	0.450	0.416	0.376	0.272	0.211	0.165	0.130
6.00	0.851	0.651	0.558	0.534	0.480	0.449	0.415	0.376	0.272	0.210	0.164	0.130
7.01	0.851	0.650	0.558	0.534	0.481	0.449	0.415	0.376	0.271	0.210	0.164	0.130
8.00	0.851	0.650	0.558	0.534	0.481	0.449	0.414	0.377	0.272	0.210	0.164	0.130

(b) Lower flap

NPR	Static pressure ratios at x_r/l_r of—						
	−0.308	−0.170	−0.032	0.037	0.079	0.120	0.162
2.00	0.893	0.841	0.626	0.478	0.402	0.320	0.476
2.50	0.893	0.842	0.626	0.477	0.401	0.309	0.251
3.00	0.893	0.843	0.626	0.477	0.401	0.308	0.244
3.51	0.893	0.843	0.626	0.476	0.400	0.308	0.245
4.00	0.894	0.843	0.626	0.476	0.400	0.307	0.245
5.00	0.894	0.842	0.626	0.475	0.400	0.307	0.245
6.00	0.894	0.842	0.626	0.474	0.400	0.307	0.245
7.01	0.894	0.841	0.626	0.474	0.400	0.307	0.245
8.00	0.894	0.841	0.625	0.474	0.400	0.306	0.244

Table 75. Static Pressure Ratios for Nozzle 8, $x_r/l_r = 0.20$, $\theta = 20°$, $\phi = 0°$, Medium Sidewall, $\delta_{v,p} = 0°$, and $\delta_{v,y} = 0°$

(a) Upper ramp

NPR	Static pressure ratios at x_r/l_r of—											
	−0.308	−0.170	−0.101	−0.032	0.037	0.106	0.175	0.244	0.382	0.520	0.659	0.797
2.00	0.853	0.653	0.561	0.537	0.485	0.451	0.426	0.485	0.552	0.547	0.529	0.520
2.50	0.853	0.653	0.560	0.536	0.484	0.450	0.423	0.378	0.273	0.496	0.496	0.388
3.00	0.852	0.652	0.559	0.536	0.482	0.450	0.420	0.377	0.273	0.212	0.379	0.500
3.51	0.852	0.652	0.558	0.535	0.481	0.450	0.419	0.376	0.273	0.212	0.243	0.277
4.00	0.852	0.652	0.559	0.535	0.481	0.450	0.418	0.376	0.273	0.212	0.165	0.211
5.00	0.852	0.651	0.558	0.535	0.480	0.449	0.416	0.375	0.272	0.211	0.165	0.130
6.00	0.851	0.651	0.558	0.534	0.481	0.449	0.415	0.376	0.272	0.210	0.164	0.130
7.00	0.851	0.650	0.558	0.534	0.481	0.449	0.415	0.376	0.271	0.210	0.164	0.130
8.00	0.851	0.650	0.557	0.534	0.481	0.449	0.414	0.377	0.271	0.210	0.163	0.130

(b) Lower flap

NPR	Static pressure ratios at x_r/l_r of—						
	−0.308	−0.170	−0.032	0.037	0.079	0.120	0.162
2.00	0.893	0.842	0.627	0.478	0.402	0.318	0.474
2.50	0.893	0.843	0.626	0.477	0.401	0.309	0.251
3.00	0.893	0.843	0.626	0.477	0.401	0.308	0.245
3.51	0.893	0.843	0.626	0.476	0.400	0.308	0.245
4.00	0.894	0.843	0.626	0.476	0.400	0.308	0.245
5.00	0.894	0.842	0.626	0.475	0.400	0.307	0.245
6.00	0.894	0.842	0.626	0.475	0.400	0.307	0.245
7.00	0.894	0.841	0.626	0.474	0.400	0.307	0.245
8.00	0.894	0.841	0.625	0.474	0.400	0.306	0.244

Table 76. Static Pressure Ratios for Nozzle 9, $x_r/l_r = 0.20$, $\theta = 20°$, $\phi = 0°$, Maximum Sidewall, $\delta_{v,p} = 0°$, and $\delta_{v,y} = 0°$

(a) Upper ramp

NPR	Static pressure ratios at x_r/l_r of—											
	−0.308	−0.170	−0.101	−0.032	0.037	0.106	0.175	0.244	0.382	0.520	0.659	0.797
2.00	0.852	0.653	0.563	0.537	0.485	0.452	0.426	0.491	0.553	0.548	0.530	0.521
2.50	0.853	0.653	0.560	0.537	0.483	0.451	0.423	0.378	0.274	0.496	0.495	0.387
3.00	0.852	0.652	0.561	0.536	0.484	0.451	0.421	0.377	0.273	0.212	0.381	0.500
3.50	0.852	0.652	0.560	0.536	0.482	0.450	0.419	0.376	0.273	0.212	0.243	0.279
3.50	0.852	0.652	0.559	0.536	0.482	0.450	0.419	0.376	0.273	0.212	0.245	0.280
4.00	0.852	0.652	0.559	0.535	0.482	0.450	0.418	0.376	0.273	0.211	0.165	0.211
5.01	0.852	0.651	0.559	0.535	0.481	0.450	0.416	0.375	0.272	0.210	0.164	0.130
6.00	0.851	0.651	0.558	0.534	0.481	0.450	0.416	0.376	0.272	0.210	0.164	0.130
7.01	0.851	0.650	0.557	0.534	0.481	0.449	0.415	0.376	0.272	0.210	0.164	0.130
8.00	0.850	0.650	0.557	0.534	0.481	0.449	0.415	0.377	0.272	0.210	0.163	0.130

(b) Lower flap

NPR	Static pressure ratios at x_r/l_r of						
	−0.308	−0.170	−0.032	0.037	0.079	0.120	0.162
2.00	0.893	0.841	0.627	0.478	0.402	0.319	0.475
2.50	0.893	0.842	0.627	0.477	0.401	0.309	0.251
3.00	0.893	0.843	0.626	0.477	0.401	0.309	0.244
3.50	0.893	0.843	0.626	0.476	0.400	0.308	0.244
3.50	0.893	0.843	0.626	0.476	0.400	0.308	0.244
4.00	0.894	0.843	0.626	0.476	0.400	0.308	0.244
5.01	0.894	0.842	0.626	0.475	0.400	0.307	0.243
6.00	0.894	0.842	0.626	0.475	0.400	0.307	0.243
7.01	0.894	0.841	0.626	0.474	0.400	0.307	0.243
8.00	0.894	0.840	0.625	0.474	0.400	0.306	0.242

Table 77. Static Pressure Ratios for Nozzle 10, $x_r/l_r = 0.02$, $\theta = 20°$, $\phi = 0°$, Minimum Sidewall, $\delta_{v,p} = 0°$, and $\delta_{v,y} = 0°$

(a) Upper ramp

NPR	Static pressure ratios at x_r/l_r of – –											
	−0.308	−0.170	−0.101	−0.032	0.037	0.106	0.175	0.244	0.382	0.520	0.659	0.797
2.00	0.851	0.628	0.574	0.530	0.486	0.455	0.424	0.518	0.547	0.547	0.525	0.513
2.50	0.850	0.626	0.571	0.529	0.484	0.454	0.420	0.362	0.269	0.493	0.475	0.390
3.00	0.851	0.625	0.571	0.529	0.485	0.454	0.418	0.360	0.268	0.210	0.410	0.471
3.49	0.850	0.624	0.570	0.529	0.484	0.454	0.416	0.359	0.267	0.209	0.208	0.336
4.00	0.850	0.623	0.569	0.528	0.483	0.454	0.414	0.358	0.267	0.209	0.155	0.179
5.00	0.849	0.621	0.569	0.528	0.482	0.453	0.413	0.356	0.266	0.208	0.155	0.117
6.00	0.848	0.619	0.568	0.528	0.483	0.453	0.411	0.356	0.265	0.208	0.154	0.117
7.99	0.847	0.617	0.566	0.527	0.483	0.452	0.410	0.355	0.265	0.208	0.154	0.117

(b) Lower flap

NPR	Static pressure ratios at x_r/l_r of –						
	−0.308	−0.170	−0.032	0.037	0.079	0.120	0.162
2.00	0.894	0.832	0.614	0.475	0.397	0.319	0.481
2.50	0.893	0.832	0.614	0.475	0.396	0.318	0.253
3.00	0.893	0.832	0.614	0.475	0.396	0.317	0.252
3.49	0.893	0.832	0.613	0.474	0.395	0.316	0.251
4.00	0.893	0.832	0.613	0.474	0.395	0.316	0.251
5.00	0.894	0.832	0.613	0.474	0.395	0.315	0.250
6.00	0.894	0.832	0.613	0.474	0.394	0.315	0.249
7.99	0.894	0.831	0.613	0.473	0.394	0.315	0.249

Table 78. Static Pressure Ratios for Nozzle 11, $x_r/l_r = 0.02$, $\theta = 20°$, $\phi = 0°$, Medium Sidewall, $\delta_{v,p} = 0°$, and $\delta_{v,y} = 0°$

(a) Upper ramp

NPR	Static pressure ratios at x_r/l_r of											
	−0.308	−0.170	−0.101	−0.032	0.037	0.106	0.175	0.244	0.382	0.520	0.659	0.797
2.00	0.851	0.628	0.574	0.530	0.487	0.456	0.424	0.527	0.547	0.548	0.527	0.515
2.50	0.851	0.626	0.572	0.529	0.486	0.455	0.420	0.363	0.270	0.496	0.470	0.379
3.00	0.850	0.625	0.571	0.529	0.486	0.455	0.417	0.361	0.268	0.210	0.413	0.475
3.50	0.850	0.624	0.569	0.529	0.483	0.454	0.415	0.359	0.268	0.209	0.200	0.321
4.00	0.849	0.623	0.569	0.528	0.483	0.454	0.414	0.358	0.267	0.209	0.155	0.179
5.00	0.849	0.621	0.567	0.528	0.482	0.453	0.412	0.357	0.266	0.208	0.155	0.117
5.99	0.849	0.619	0.568	0.528	0.483	0.453	0.411	0.356	0.266	0.208	0.155	0.117
8.00	0.847	0.617	0.566	0.527	0.483	0.452	0.410	0.355	0.265	0.208	0.154	0.117

(b) Lower flap

NPR	Static pressure ratios at x_r/l_r of						
	−0.308	−0.170	−0.032	0.037	0.079	0.120	0.162
2.00	0.894	0.832	0.614	0.475	0.397	0.319	0.483
2.50	0.893	0.832	0.614	0.475	0.396	0.318	0.253
3.00	0.893	0.832	0.613	0.475	0.396	0.317	0.251
3.50	0.893	0.832	0.613	0.474	0.395	0.316	0.251
4.00	0.893	0.832	0.613	0.474	0.395	0.316	0.250
5.00	0.893	0.832	0.613	0.474	0.395	0.315	0.249
5.99	0.894	0.832	0.613	0.474	0.395	0.315	0.249
8.00	0.894	0.831	0.613	0.474	0.394	0.315	0.248

Table 79. Static Pressure Ratios for Nozzle 12, $x_r/l_r = 0.02$, $\theta = 20°$, $\phi = 0°$, Maximum Sidewall, $\delta_{v,p} = 0°$, and $\delta_{v,y} = 0°$

(a) Upper ramp

NPR	Static pressure ratios at x_r/l_r of—											
	−0.308	−0.170	−0.101	−0.032	0.037	0.106	0.175	0.244	0.382	0.520	0.659	0.797
2.00	0.851	0.629	0.575	0.531	0.488	0.456	0.424	0.516	0.547	0.546	0.525	0.513
2.50	0.851	0.627	0.573	0.530	0.486	0.456	0.421	0.363	0.270	0.495	0.471	0.376
3.00	0.850	0.625	0.571	0.530	0.485	0.455	0.418	0.361	0.268	0.210	0.414	0.475
3.51	0.850	0.624	0.569	0.529	0.483	0.454	0.416	0.359	0.268	0.209	0.200	0.322
4.00	0.850	0.623	0.570	0.529	0.484	0.454	0.415	0.358	0.267	0.209	0.156	0.179
5.00	0.849	0.621	0.569	0.528	0.483	0.454	0.413	0.357	0.267	0.209	0.155	0.117
6.00	0.848	0.619	0.568	0.528	0.483	0.453	0.412	0.356	0.266	0.209	0.155	0.117
8.00	0.847	0.617	0.566	0.527	0.483	0.453	0.410	0.355	0.265	0.209	0.154	0.117

(b) Lower flap

NPR	Static pressure ratios at x_r/l_r of—						
	−0.308	−0.170	−0.032	0.037	0.079	0.120	0.162
2.00	0.894	0.832	0.614	0.475	0.397	0.319	0.482
2.50	0.893	0.832	0.614	0.475	0.396	0.318	0.253
3.00	0.892	0.832	0.613	0.474	0.396	0.317	0.251
3.51	0.893	0.832	0.613	0.474	0.395	0.316	0.251
4.00	0.893	0.832	0.613	0.474	0.395	0.316	0.250
5.00	0.894	0.832	0.613	0.474	0.395	0.315	0.250
6.00	0.894	0.832	0.613	0.474	0.394	0.315	0.249
8.00	0.894	0.831	0.613	0.473	0.394	0.314	0.248

Table 80. Static Pressure Ratios for Nozzle 13, $x_r/l_r = 0.42$, $\theta = 20°$, $\phi = 0°$, Maximum Sidewall, $\delta_{v,p} = 0°$, and $\delta_{v,y} = -20°$

(a) Upper ramp

NPR	Static pressure ratios at x_r/l_r of—											
	−0.308	−0.170	−0.101	−0.032	0.037	0.106	0.175	0.244	0.382	0.520	0.659	0.797
2.01	0.858	0.649	0.574	0.527	0.490	0.457	0.427	0.515	0.567	0.564	0.550	0.539
2.51	0.858	0.649	0.573	0.526	0.488	0.456	0.424	0.378	0.328	0.509	0.499	0.458
3.05	0.857	0.648	0.573	0.526	0.488	0.456	0.421	0.377	0.273	0.355	0.422	0.462
3.00	0.858	0.649	0.573	0.526	0.488	0.456	0.422	0.377	0.273	0.378	0.433	0.464
3.50	0.858	0.648	0.573	0.526	0.487	0.456	0.420	0.376	0.274	0.212	0.333	0.384
4.00	0.858	0.648	0.574	0.525	0.488	0.456	0.419	0.377	0.274	0.211	0.169	0.295
5.00	0.858	0.648	0.573	0.525	0.487	0.456	0.418	0.377	0.274	0.211	0.164	0.194
6.00	0.857	0.647	0.573	0.525	0.488	0.456	0.417	0.377	0.273	0.210	0.164	0.130
7.01	0.857	0.646	0.573	0.524	0.487	0.456	0.416	0.378	0.273	0.210	0.163	0.130
8.01	0.857	0.646	0.572	0.524	0.488	0.456	0.416	0.378	0.273	0.210	0.163	0.130

(b) Lower flap

NPR	Static pressure ratios at x_r/l_r of—						
	−0.308	−0.170	−0.032	0.037	0.079	0.120	0.162
2.01	0.893	0.841	0.625	0.476	0.399	0.319	0.474
2.51	0.893	0.841	0.625	0.475	0.399	0.307	0.254
3.05	0.892	0.841	0.625	0.474	0.398	0.306	0.243
3.00	0.893	0.841	0.625	0.475	0.398	0.306	0.243
3.50	0.893	0.841	0.625	0.474	0.398	0.306	0.243
4.00	0.893	0.841	0.625	0.474	0.398	0.305	0.243
5.00	0.894	0.840	0.625	0.473	0.398	0.305	0.242
6.00	0.894	0.840	0.625	0.473	0.398	0.305	0.242
7.01	0.894	0.839	0.624	0.473	0.398	0.305	0.242
8.01	0.894	0.839	0.624	0.472	0.398	0.304	0.241

Table 81. Static Pressure Ratios for Nozzle 14, $x_r/l_r = 0.20$, $\theta = 20°$, $\phi = 0°$, Medium Sidewall, $\delta_{v,p} = 0°$, and $\delta_{v,y} = -20°$

(a) Upper ramp

NPR	Static pressure ratios at x_r/l_r of—											
	−0.308	−0.170	−0.101	−0.032	0.037	0.106	0.175	0.244	0.382	0.520	0.659	0.797
2.00	0.852	0.653	0.562	0.537	0.485	0.451	0.426	0.562	0.562	0.558	0.537	0.526
2.50	0.852	0.653	0.561	0.536	0.484	0.450	0.423	0.377	0.437	0.535	0.456	0.394
3.00	0.852	0.652	0.559	0.536	0.482	0.450	0.421	0.376	0.272	0.398	0.425	0.430
3.50	0.852	0.652	0.558	0.535	0.481	0.450	0.419	0.376	0.272	0.236	0.361	0.332
4.00	0.852	0.652	0.559	0.535	0.481	0.450	0.418	0.376	0.272	0.233	0.299	0.295
5.00	0.851	0.652	0.559	0.535	0.481	0.450	0.416	0.376	0.272	0.232	0.219	0.236
6.00	0.851	0.651	0.559	0.535	0.481	0.449	0.415	0.376	0.272	0.232	0.218	0.192
7.00	0.851	0.651	0.558	0.534	0.481	0.449	0.415	0.376	0.271	0.232	0.217	0.190
8.00	0.851	0.650	0.558	0.534	0.481	0.449	0.414	0.376	0.271	0.231	0.217	0.190

(b) Lower flap

NPR	Static pressure ratios at x_r/l_r of—						
	−0.308	−0.170	−0.032	0.037	0.079	0.120	0.162
2.00	0.893	0.842	0.627	0.478	0.402	0.316	0.475
2.50	0.893	0.844	0.627	0.477	0.401	0.309	0.255
3.00	0.893	0.844	0.626	0.477	0.401	0.308	0.244
3.50	0.893	0.845	0.626	0.476	0.400	0.308	0.243
4.00	0.893	0.845	0.626	0.476	0.400	0.307	0.243
5.00	0.894	0.844	0.626	0.475	0.400	0.307	0.242
6.00	0.894	0.844	0.626	0.475	0.400	0.307	0.242
7.00	0.894	0.843	0.626	0.474	0.400	0.306	0.241
8.00	0.894	0.843	0.626	0.474	0.400	0.308	0.241

Table 82. Static Pressure Ratios for Nozzle 15, $x_r/l_r = 0.20$, $\theta = 20°$, $\phi = 0°$, Maximum Sidewall, $\delta_{v,p} = 0°$, and $\delta_{v,y} = -20°$

(a) Upper ramp

NPR	Static pressure ratios at x_r/l_r of—											
	−0.308	−0.170	−0.101	−0.032	0.037	0.106	0.175	0.244	0.382	0.520	0.659	0.797
2.00	0.852	0.653	0.563	0.537	0.486	0.452	0.427	0.565	0.566	0.568	0.555	0.544
2.50	0.852	0.653	0.561	0.536	0.483	0.451	0.423	0.377	0.440	0.538	0.474	0.446
3.00	0.852	0.653	0.560	0.536	0.483	0.450	0.421	0.377	0.273	0.400	0.429	0.487
3.50	0.852	0.653	0.560	0.536	0.482	0.450	0.419	0.376	0.273	0.237	0.361	0.349
4.00	0.852	0.652	0.559	0.535	0.481	0.449	0.418	0.376	0.272	0.235	0.299	0.302
5.00	0.852	0.652	0.559	0.535	0.481	0.450	0.417	0.376	0.272	0.234	0.220	0.240
5.00	0.852	0.652	0.559	0.535	0.481	0.450	0.416	0.375	0.272	0.234	0.220	0.240
6.00	0.851	0.651	0.558	0.535	0.481	0.450	0.416	0.376	0.272	0.233	0.218	0.194
7.00	0.851	0.651	0.558	0.534	0.481	0.450	0.415	0.376	0.271	0.233	0.218	0.191
8.00	0.851	0.650	0.558	0.534	0.481	0.449	0.415	0.376	0.271	0.233	0.217	0.191

(b) Lower flap

NPR	Static pressure ratios at x_r/l_r of—						
	−0.308	−0.170	−0.032	0.037	0.079	0.120	0.162
2.00	0.893	0.842	0.627	0.478	0.402	0.323	0.474
2.50	0.893	0.844	0.627	0.477	0.401	0.312	0.255
3.00	0.893	0.844	0.626	0.477	0.401	0.310	0.243
3.50	0.893	0.845	0.626	0.476	0.400	0.309	0.243
4.00	0.893	0.845	0.626	0.476	0.400	0.307	0.243
5.00	0.894	0.844	0.626	0.475	0.400	0.307	0.242
5.00	0.894	0.844	0.626	0.475	0.400	0.307	0.242
6.00	0.894	0.844	0.626	0.474	0.400	0.307	0.242
7.00	0.894	0.843	0.626	0.474	0.400	0.306	0.241
8.00	0.894	0.843	0.626	0.473	0.400	0.306	0.241

Table 83. Static Pressure Ratios for Nozzle 16, $x_r/l_r = 0.02$, $\theta = 20°$, $\phi = 0°$, Minimum Sidewall, $\delta_{v,p} = 0°$, and $\delta_{v,y} = -20°$

(a) Upper ramp

NPR	Static pressure ratios at x_r/l_r of—											
	−0.308	−0.170	−0.101	−0.032	0.037	0.106	0.175	0.244	0.382	0.520	0.659	0.797
2.00	0.857	0.646	0.592	0.552	0.515	0.494	0.470	0.517	0.550	0.554	0.533	0.517
2.50	0.856	0.644	0.590	0.551	0.513	0.493	0.467	0.411	0.323	0.508	0.503	0.414
3.01	0.856	0.643	0.589	0.551	0.512	0.493	0.464	0.409	0.323	0.265	0.286	0.447
3.50	0.856	0.642	0.589	0.551	0.512	0.492	0.462	0.408	0.322	0.265	0.211	0.249
4.00	0.855	0.641	0.588	0.551	0.511	0.492	0.461	0.408	0.321	0.265	0.184	0.143
5.00	0.855	0.641	0.587	0.550	0.511	0.491	0.459	0.407	0.321	0.265	0.183	0.122
6.00	0.854	0.640	0.587	0.549	0.510	0.491	0.458	0.407	0.320	0.265	0.183	0.121
8.00	0.853	0.638	0.585	0.548	0.510	0.490	0.457	0.406	0.320	0.265	0.183	0.121

(b) Lower flap

NPR	Static pressure ratios at x_r/l_r of—						
	−0.308	−0.170	−0.032	0.037	0.079	0.120	0.162
2.00	0.899	0.840	0.630	0.495	0.422	0.344	0.464
2.50	0.898	0.839	0.630	0.495	0.421	0.344	0.280
3.01	0.898	0.839	0.629	0.494	0.421	0.342	0.279
3.50	0.899	0.840	0.629	0.494	0.420	0.342	0.279
4.00	0.899	0.840	0.629	0.494	0.420	0.342	0.278
5.00	0.899	0.840	0.629	0.493	0.420	0.341	0.278
6.00	0.899	0.839	0.629	0.493	0.420	0.341	0.277
8.00	0.899	0.838	0.628	0.493	0.420	0.340	0.277

Table 84. Static Pressure Ratios for Nozzle 17, $x_r/l_r = 0.02$, $\theta = 20°$, $\phi = 0°$, Medium Sidewall, $\delta_{v,p} = 0°$, and $\delta_{v,y} = -20°$

(a) Upper ramp

NPR	Static pressure ratios at x_r/l_r of—											
	−0.308	−0.170	−0.101	−0.032	0.037	0.106	0.175	0.244	0.382	0.520	0.659	0.797
2.00	0.857	0.646	0.594	0.553	0.517	0.495	0.471	0.542	0.560	0.560	0.536	0.519
2.50	0.857	0.645	0.591	0.552	0.514	0.493	0.467	0.412	0.326	0.513	0.495	0.411
3.00	0.856	0.644	0.590	0.552	0.513	0.492	0.464	0.410	0.324	0.282	0.353	0.424
3.50	0.856	0.643	0.589	0.551	0.512	0.492	0.462	0.409	0.323	0.281	0.263	0.260
4.00	0.856	0.642	0.589	0.551	0.511	0.492	0.461	0.408	0.324	0.281	0.221	0.215
5.00	0.855	0.641	0.588	0.550	0.511	0.491	0.459	0.407	0.322	0.280	0.220	0.169
6.00	0.854	0.640	0.587	0.550	0.511	0.490	0.458	0.406	0.321	0.280	0.220	0.169
8.01	0.853	0.639	0.586	0.549	0.511	0.490	0.456	0.405	0.320	0.281	0.219	0.168

(b) Lower flap

NPR	Static pressure ratios at x_r/l_r of −						
	−0.308	−0.170	−0.032	0.037	0.079	0.120	0.162
2.00	0.899	0.840	0.630	0.495	0.422	0.344	0.463
2.50	0.899	0.840	0.630	0.495	0.421	0.343	0.280
3.00	0.899	0.840	0.629	0.494	0.421	0.342	0.279
3.50	0.899	0.840	0.629	0.494	0.420	0.342	0.279
4.00	0.899	0.840	0.629	0.494	0.420	0.342	0.278
5.00	0.899	0.840	0.628	0.493	0.420	0.341	0.278
6.00	0.900	0.839	0.628	0.493	0.420	0.341	0.277
8.01	0.899	0.838	0.628	0.493	0.420	0.340	0.276

C.2

Table 85. Static Pressure Ratios for Nozzle 18, $x_r/l_r = 0.02$, $\theta = 20°$, $\phi = 0°$, Maximum Sidewall, $\delta_{v,p} = 0°$, and $\delta_{v,y} = -20°$

(a) Upper ramp

NPR	Static pressure ratios at x_r/l_r of—											
	−0.308	−0.170	−0.101	−0.032	0.037	0.106	0.175	0.244	0.382	0.520	0.659	0.797
2.00	0.856	0.647	0.594	0.553	0.515	0.494	0.469	0.544	0.563	0.572	0.553	0.534
2.50	0.856	0.645	0.591	0.552	0.513	0.493	0.464	0.411	0.324	0.523	0.518	0.445
3.00	0.856	0.644	0.590	0.552	0.512	0.492	0.462	0.410	0.323	0.282	0.348	0.431
3.50	0.856	0.643	0.590	0.551	0.512	0.492	0.461	0.408	0.322	0.280	0.261	0.267
3.99	0.856	0.642	0.589	0.551	0.511	0.491	0.460	0.407	0.321	0.279	0.219	0.226
5.00	0.855	0.641	0.588	0.550	0.510	0.490	0.458	0.406	0.321	0.280	0.219	0.175
6.00	0.854	0.640	0.587	0.550	0.510	0.490	0.457	0.405	0.320	0.279	0.218	0.174
8.00	0.854	0.639	0.586	0.549	0.510	0.489	0.456	0.405	0.319	0.280	0.218	0.174

(b) Lower flap

NPR	Static pressure ratios at x_r/l_r of—						
	−0.308	−0.170	−0.032	0.037	0.079	0.120	0.162
2.00	0.899	0.839	0.629	0.495	0.422	0.343	0.464
2.50	0.899	0.839	0.629	0.494	0.421	0.342	0.279
3.00	0.898	0.839	0.628	0.494	0.421	0.341	0.279
3.50	0.899	0.839	0.628	0.494	0.420	0.341	0.278
3.99	0.899	0.839	0.628	0.493	0.420	0.341	0.278
5.00	0.899	0.839	0.628	0.493	0.420	0.340	0.277
6.00	0.899	0.839	0.628	0.493	0.420	0.340	0.277
8.00	0.899	0.838	0.627	0.493	0.419	0.339	0.276

Table 86. Static Pressure Ratios for Nozzle 19, $x_r/l_r = 0.42$, $\theta = 30°$, $\phi = 0°$, Minimum Sidewall, $\delta_{v,p} = 0°$, and $\delta_{v,y} = 0°$

(a) Upper ramp

NPR	Static pressure ratios at x_r/l_r of –											
	−0.308	−0.170	−0.101	−0.032	0.037	0.106	0.175	0.244	0.382	0.520	0.659	0.797
2.00	0.860	0.653	0.579	0.531	0.493	0.457	0.427	0.490	0.557	0.552	0.534	0.524
2.50	0.859	0.653	0.577	0.530	0.491	0.456	0.424	0.381	0.276	0.500	0.499	0.401
3.00	0.859	0.653	0.575	0.530	0.489	0.454	0.422	0.379	0.276	0.216	0.392	0.499
3.50	0.859	0.652	0.576	0.529	0.488	0.455	0.420	0.378	0.276	0.215	0.246	0.283
4.00	0.859	0.652	0.575	0.529	0.488	0.454	0.419	0.378	0.276	0.215	0.163	0.212
5.00	0.859	0.652	0.575	0.529	0.488	0.455	0.417	0.377	0.276	0.214	0.163	0.130
5.99	0.859	0.651	0.575	0.528	0.488	0.454	0.417	0.377	0.275	0.213	0.162	0.130
6.99	0.858	0.650	0.574	0.528	0.488	0.454	0.416	0.377	0.275	0.213	0.162	0.130
7.99	0.858	0.650	0.574	0.527	0.489	0.454	0.416	0.378	0.275	0.212	0.162	0.129

(b) Lower flap

NPR	Static pressure ratios at x_r/l_r of—						
	−0.308	−0.170	−0.032	0.037	0.079	0.120	0.162
2.00	0.893	0.838	0.626	0.479	0.413	0.314	0.480
2.50	0.893	0.838	0.626	0.479	0.412	0.304	0.292
3.00	0.893	0.838	0.625	0.478	0.411	0.303	0.238
3.50	0.893	0.838	0.625	0.477	0.410	0.303	0.234
4.00	0.893	0.838	0.625	0.477	0.410	0.303	0.234
5.00	0.894	0.838	0.625	0.476	0.409	0.303	0.235
5.99	0.894	0.837	0.625	0.476	0.408	0.302	0.234
6.99	0.894	0.837	0.625	0.476	0.408	0.302	0.231
7.99	0.894	0.836	0.625	0.475	0.408	0.301	0.230

Table 87. Static Pressure Ratios for Nozzle 20, $x_r/l_r = 0.42$, $\theta = 30°$, $\phi = 0°$, Medium Sidewall, $\delta_{v,p} = 0°$, and $\delta_{v,y} = 0°$

(a) Upper ramp

NPR	Static pressure ratios at x_r/l_r of –											
	−0.308	−0.170	−0.101	−0.032	0.037	0.106	0.175	0.244	0.382	0.520	0.659	0.797
2.00	0.859	0.653	0.575	0.530	0.490	0.455	0.426	0.490	0.558	0.551	0.531	0.521
2.50	0.859	0.653	0.575	0.530	0.490	0.455	0.423	0.380	0.276	0.491	0.513	0.416
3.00	0.859	0.652	0.574	0.529	0.490	0.455	0.421	0.379	0.276	0.216	0.355	0.499
3.50	0.859	0.652	0.573	0.529	0.489	0.455	0.419	0.378	0.275	0.215	0.245	0.279
4.00	0.859	0.652	0.574	0.527	0.488	0.454	0.418	0.378	0.275	0.214	0.163	0.211
5.00	0.859	0.651	0.573	0.528	0.488	0.454	0.417	0.378	0.275	0.213	0.163	0.130
6.00	0.858	0.651	0.573	0.527	0.488	0.454	0.416	0.378	0.275	0.212	0.163	0.130
6.99	0.858	0.650	0.572	0.527	0.487	0.454	0.415	0.378	0.275	0.212	0.162	0.130
8.00	0.858	0.649	0.572	0.527	0.487	0.454	0.415	0.378	0.275	0.212	0.162	0.129

(b) Lower flap

NPR	Static pressure ratios at x_r/l_r of—						
	−0.308	−0.170	−0.032	0.037	0.079	0.120	0.162
2.00	0.893	0.838	0.626	0.479	0.408	0.321	0.474
2.50	0.893	0.838	0.626	0.478	0.407	0.296	0.301
3.00	0.892	0.838	0.625	0.478	0.406	0.296	0.236
3.50	0.893	0.838	0.625	0.478	0.405	0.295	0.235
4.00	0.893	0.838	0.625	0.477	0.405	0.295	0.234
5.00	0.893	0.838	0.625	0.477	0.405	0.294	0.235
6.00	0.894	0.837	0.625	0.476	0.404	0.294	0.234
6.99	0.894	0.837	0.625	0.476	0.404	0.294	0.234
8.00	0.894	0.836	0.625	0.475	0.404	0.293	0.234

Table 88. Static Pressure Ratios for Nozzle 21, $x_r/l_r = 0.42$, $\theta = 30°$, $\phi = 0°$, Maximum Sidewall, $\delta_{v,p} = 0°$, and $\delta_{v,y} = 0°$

(a) Upper ramp

NPR	Static pressure ratios at x_r/l_r of—											
	−0.308	−0.170	−0.101	−0.032	0.037	0.106	0.175	0.244	0.382	0.520	0.659	0.797
1.99	0.859	0.653	0.582	0.530	0.495	0.456	0.426	0.513	0.559	0.555	0.534	0.524
2.50	0.859	0.653	0.577	0.529	0.491	0.455	0.422	0.380	0.275	0.493	0.513	0.416
3.00	0.859	0.652	0.578	0.529	0.491	0.455	0.420	0.380	0.275	0.216	0.353	0.499
3.50	0.859	0.652	0.576	0.528	0.490	0.453	0.419	0.378	0.275	0.215	0.248	0.278
4.00	0.859	0.651	0.576	0.528	0.489	0.453	0.418	0.378	0.275	0.214	0.163	0.212
4.99	0.859	0.651	0.575	0.527	0.488	0.453	0.417	0.377	0.275	0.213	0.163	0.131
6.00	0.858	0.650	0.575	0.529	0.488	0.452	0.416	0.377	0.275	0.212	0.162	0.130
7.00	0.858	0.650	0.575	0.529	0.489	0.452	0.415	0.378	0.275	0.212	0.162	0.130
8.00	0.857	0.649	0.575	0.529	0.488	0.452	0.415	0.378	0.275	0.211	0.161	0.130

(b) Lower flap

NPR	Static pressure ratios at x_r/l_r of—						
	−0.308	−0.170	−0.032	0.037	0.079	0.120	0.162
1.99	0.893	0.838	0.626	0.478	0.410	0.326	0.472
2.50	0.893	0.838	0.625	0.477	0.410	0.303	0.319
3.00	0.892	0.838	0.625	0.476	0.412	0.304	0.241
3.50	0.893	0.838	0.625	0.475	0.411	0.304	0.234
4.00	0.893	0.838	0.625	0.475	0.411	0.305	0.234
4.99	0.893	0.837	0.625	0.474	0.410	0.306	0.233
6.00	0.894	0.837	0.625	0.474	0.410	0.306	0.233
7.00	0.894	0.836	0.625	0.473	0.409	0.306	0.232
8.00	0.894	0.836	0.625	0.473	0.408	0.307	0.231

Table 89. Static Pressure Ratios for Nozzle 22, $x_r/l_r = 0.20$, $\theta = 30°$, $\phi = 0°$, Minimum Sidewall, $\delta_{v,p} = 0°$, and $\delta_{v,y} = 0°$

(a) Upper ramp

NPR	Static pressure ratios at x_r/l_r of—											
	−0.308	−0.170	−0.101	−0.032	0.037	0.106	0.175	0.244	0.382	0.520	0.659	0.797
1.99	0.863	0.643	0.583	0.526	0.493	0.454	0.429	0.516	0.555	0.551	0.531	0.519
2.50	0.863	0.644	0.580	0.525	0.490	0.452	0.427	0.382	0.275	0.499	0.489	0.380
3.00	0.863	0.643	0.580	0.525	0.489	0.451	0.425	0.380	0.275	0.216	0.396	0.479
3.50	0.863	0.643	0.579	0.524	0.488	0.450	0.423	0.380	0.275	0.215	0.248	0.319
4.00	0.863	0.643	0.579	0.524	0.488	0.450	0.422	0.379	0.275	0.214	0.164	0.212
4.99	0.863	0.642	0.579	0.524	0.487	0.449	0.421	0.379	0.274	0.213	0.163	0.129
6.00	0.863	0.642	0.578	0.523	0.487	0.448	0.420	0.379	0.274	0.212	0.162	0.129
6.99	0.863	0.641	0.578	0.523	0.487	0.448	0.420	0.379	0.274	0.212	0.162	0.129
8.00	0.862	0.641	0.578	0.522	0.487	0.448	0.419	0.379	0.274	0.212	0.162	0.129

(b) Lower flap

NPR	Static pressure ratios at x_r/l_r of—						
	−0.308	−0.170	−0.032	0.037	0.079	0.120	0.162
1.99	0.893	0.839	0.626	0.477	0.400	0.316	0.481
2.50	0.893	0.839	0.626	0.476	0.400	0.307	0.285
3.00	0.893	0.839	0.626	0.476	0.399	0.306	0.226
3.50	0.893	0.839	0.626	0.475	0.399	0.305	0.225
4.00	0.894	0.839	0.626	0.475	0.398	0.305	0.225
4.99	0.894	0.838	0.626	0.474	0.398	0.305	0.225
6.00	0.894	0.838	0.625	0.474	0.398	0.305	0.225
6.99	0.894	0.837	0.625	0.473	0.398	0.304	0.225
8.00	0.894	0.837	0.625	0.473	0.398	0.304	0.224

Table 90. Static Pressure Ratios for Nozzle 23, $x_r/l_r = 0.20$, $\theta = 30°$, $\phi = 0°$. Medium Sidewall, $\delta_{v,p} = 0°$, and $\delta_{v,y} = 0°$

(a) Upper ramp

NPR	Static pressure ratios at x_r/l_r of											
	−0.308	−0.170	−0.101	−0.032	0.037	0.106	0.175	0.244	0.382	0.520	0.659	0.797
2.00	0.863	0.643	0.582	0.525	0.491	0.452	0.428	0.509	0.554	0.550	0.529	0.517
2.50	0.863	0.643	0.579	0.525	0.489	0.451	0.426	0.382	0.276	0.502	0.485	0.375
3.01	0.863	0.643	0.578	0.524	0.488	0.450	0.424	0.380	0.275	0.216	0.384	0.489
3.50	0.863	0.642	0.579	0.524	0.487	0.449	0.422	0.380	0.275	0.215	0.246	0.307
4.00	0.863	0.642	0.579	0.523	0.486	0.449	0.421	0.379	0.275	0.214	0.164	0.212
5.00	0.863	0.642	0.578	0.523	0.486	0.449	0.420	0.379	0.275	0.213	0.163	0.130
6.00	0.863	0.641	0.578	0.523	0.486	0.448	0.419	0.379	0.274	0.212	0.162	0.129
7.00	0.862	0.641	0.578	0.522	0.486	0.448	0.419	0.379	0.274	0.212	0.162	0.129
8.00	0.862	0.640	0.578	0.522	0.486	0.447	0.418	0.379	0.274	0.212	0.162	0.129

(b) Lower flap

NPR	Static pressure ratios at x_r/l_r of						
	−0.308	−0.170	−0.032	0.037	0.079	0.120	0.162
2.00	0.893	0.839	0.626	0.477	0.400	0.314	0.481
2.50	0.893	0.839	0.626	0.476	0.400	0.306	0.289
3.01	0.893	0.839	0.625	0.476	0.399	0.306	0.225
3.50	0.893	0.839	0.625	0.475	0.398	0.305	0.225
4.00	0.894	0.839	0.625	0.475	0.398	0.305	0.225
5.00	0.894	0.838	0.625	0.474	0.398	0.304	0.224
6.00	0.894	0.838	0.625	0.473	0.398	0.304	0.224
7.00	0.894	0.837	0.625	0.473	0.398	0.304	0.224
8.00	0.894	0.837	0.625	0.473	0.398	0.304	0.224

Table 91. Static Pressure Ratios for Nozzle 24, $x_r/l_r = 0.20$, $\theta = 30°$, $\phi = 0°$, Maximum Sidewall, $\delta_{v,p} = 0°$, and $\delta_{v,y} = 0°$

(a) Upper ramp

NPR	Static pressure ratios at x_r/l_r of—											
	−0.308	−0.170	−0.101	−0.032	0.037	0.106	0.175	0.244	0.382	0.520	0.659	0.797
2.00	0.862	0.643	0.581	0.525	0.490	0.453	0.429	0.503	0.554	0.548	0.526	0.516
2.50	0.863	0.643	0.581	0.524	0.490	0.452	0.426	0.382	0.276	0.501	0.486	0.374
3.00	0.863	0.643	0.580	0.524	0.488	0.451	0.424	0.381	0.276	0.216	0.381	0.488
3.50	0.863	0.643	0.580	0.524	0.488	0.451	0.423	0.380	0.275	0.215	0.247	0.305
4.00	0.863	0.643	0.579	0.523	0.488	0.450	0.422	0.379	0.275	0.214	0.164	0.210
4.99	0.863	0.642	0.579	0.523	0.487	0.450	0.421	0.379	0.275	0.213	0.163	0.130
6.00	0.863	0.641	0.579	0.522	0.487	0.449	0.420	0.379	0.274	0.212	0.163	0.130
7.01	0.862	0.641	0.579	0.522	0.487	0.449	0.419	0.379	0.274	0.212	0.163	0.130
8.00	0.862	0.641	0.578	0.521	0.487	0.448	0.419	0.379	0.274	0.212	0.162	0.129

(b) Lower flap

NPR	Static pressure ratios at x_r/l_r of						
	−0.308	−0.170	−0.032	0.037	0.079	0.120	0.162
2.00	0.893	0.838	0.625	0.476	0.400	0.315	0.481
2.50	0.893	0.839	0.626	0.476	0.399	0.307	0.297
3.00	0.893	0.839	0.625	0.475	0.399	0.306	0.225
3.50	0.893	0.839	0.625	0.474	0.398	0.305	0.224
4.00	0.893	0.839	0.625	0.474	0.398	0.305	0.224
4.99	0.894	0.838	0.625	0.473	0.398	0.305	0.224
6.00	0.894	0.838	0.625	0.473	0.398	0.304	0.224
7.01	0.894	0.837	0.625	0.472	0.398	0.304	0.224
8.00	0.894	0.837	0.625	0.472	0.398	0.304	0.224

Table 92. Static Pressure Ratios for Nozzle 25, $x_r/l_r = 0.02$, $\theta = 30°$, $\phi = 0°$, Minimum Sidewall, $\delta_{v,p} = 0°$, and $\delta_{v,y} = 0°$

(a) Upper ramp

NPR	Static pressure ratios at x_r/l_r of −											
	−0.308	−0.170	−0.101	−0.032	0.037	0.106	0.175	0.244	0.382	0.520	0.659	0.797
2.00	0.858	0.650	0.575	0.533	0.495	0.461	0.423	0.531	0.545	0.540	0.518	0.508
2.50	0.858	0.650	0.573	0.533	0.494	0.459	0.419	0.375	0.270	0.495	0.451	0.376
3.00	0.858	0.650	0.572	0.533	0.493	0.459	0.416	0.375	0.269	0.209	0.408	0.429
3.51	0.858	0.649	0.572	0.532	0.492	0.459	0.414	0.374	0.268	0.209	0.235	0.342
4.00	0.858	0.649	0.572	0.532	0.493	0.459	0.413	0.373	0.268	0.208	0.156	0.279
5.00	0.858	0.649	0.572	0.532	0.492	0.459	0.411	0.372	0.267	0.207	0.155	0.117
6.01	0.858	0.648	0.571	0.531	0.492	0.459	0.410	0.372	0.267	0.207	0.155	0.117
6.00	0.858	0.648	0.571	0.531	0.492	0.459	0.410	0.372	0.267	0.207	0.154	0.117
8.00	0.857	0.647	0.571	0.531	0.492	0.459	0.408	0.373	0.266	0.207	0.153	0.117

(b) Lower flap

NPR	Static pressure ratios at x_r/l_r of						
	−0.308	−0.170	−0.032	0.037	0.079	0.120	0.162
2.00	0.893	0.830	0.621	0.483	0.392	0.313	0.482
2.50	0.893	0.830	0.621	0.483	0.391	0.310	0.248
3.00	0.893	0.830	0.620	0.483	0.391	0.310	0.244
3.51	0.893	0.830	0.620	0.482	0.390	0.309	0.244
4.00	0.894	0.830	0.620	0.483	0.390	0.309	0.243
5.00	0.894	0.830	0.620	0.483	0.390	0.309	0.242
6.01	0.894	0.830	0.620	0.483	0.390	0.308	0.241
6.00	0.894	0.830	0.620	0.483	0.390	0.308	0.241
8.00	0.895	0.829	0.620	0.483	0.390	0.308	0.240

Table 93. Static Pressure Ratios for Nozzle 26, $x_r/l_r = 0.02$, $\theta = 30°$, $\phi = 0°$, Medium Sidewall, $\delta_{v,p} = 0°$, and $\delta_{v,y} = 0°$

(a) Upper ramp

NPR	Static pressure ratios at x_r/l_r of—											
	−0.308	−0.170	−0.101	−0.032	0.037	0.106	0.175	0.244	0.382	0.520	0.659	0.797
2.01	0.858	0.650	0.575	0.533	0.495	0.460	0.422	0.526	0.543	0.540	0.516	0.506
2.50	0.858	0.650	0.573	0.532	0.494	0.459	0.418	0.375	0.270	0.497	0.451	0.363
3.00	0.858	0.649	0.573	0.532	0.493	0.459	0.416	0.374	0.268	0.209	0.405	0.440
3.51	0.858	0.649	0.572	0.532	0.492	0.459	0.414	0.373	0.268	0.208	0.214	0.334
4.00	0.858	0.649	0.572	0.531	0.492	0.459	0.412	0.373	0.268	0.208	0.156	0.274
5.00	0.858	0.648	0.571	0.531	0.491	0.458	0.410	0.372	0.267	0.207	0.155	0.117
6.00	0.857	0.648	0.571	0.531	0.491	0.458	0.409	0.371	0.267	0.206	0.154	0.117
8.01	0.857	0.647	0.571	0.530	0.492	0.459	0.408	0.372	0.266	0.206	0.153	0.117

(b) Lower flap

NPR	Static pressure ratios at x_r/l_r of—						
	−0.308	−0.170	−0.032	0.037	0.079	0.120	0.162
2.01	0.893	0.830	0.621	0.483	0.392	0.315	0.480
2.50	0.893	0.830	0.621	0.483	0.392	0.311	0.247
3.00	0.893	0.830	0.620	0.483	0.392	0.311	0.243
3.51	0.894	0.830	0.620	0.482	0.391	0.310	0.243
4.00	0.894	0.830	0.620	0.482	0.391	0.310	0.242
5.00	0.894	0.830	0.620	0.482	0.391	0.309	0.241
6.00	0.894	0.830	0.620	0.483	0.391	0.309	0.240
8.01	0.895	0.829	0.620	0.483	0.391	0.309	0.239

Table 94. Static Pressure Ratios for Nozzle 27, $x_r/l_r = 0.02$, $\theta = 30°$, $\phi = 0°$, Maximum Sidewall, $\delta_{v,p} = 0°$, and $\delta_{v,y} = 0°$

(a) Upper ramp

NPR	Static pressure ratios at x_r/l_r of											
	−0.308	−0.170	−0.101	−0.032	0.037	0.106	0.175	0.244	0.382	0.520	0.659	0.797
2.00	0.858	0.650	0.576	0.533	0.495	0.460	0.423	0.535	0.544	0.542	0.518	0.508
2.50	0.858	0.650	0.573	0.532	0.493	0.459	0.419	0.374	0.270	0.494	0.451	0.360
3.01	0.858	0.650	0.573	0.532	0.493	0.459	0.416	0.374	0.269	0.209	0.403	0.439
3.50	0.858	0.649	0.572	0.532	0.491	0.459	0.414	0.373	0.268	0.209	0.218	0.334
4.01	0.858	0.649	0.572	0.532	0.492	0.459	0.413	0.373	0.268	0.208	0.156	0.275
5.01	0.858	0.648	0.572	0.531	0.491	0.459	0.411	0.372	0.268	0.207	0.155	0.117
6.00	0.858	0.648	0.571	0.531	0.491	0.459	0.410	0.372	0.267	0.206	0.154	0.117
8.00	0.857	0.647	0.571	0.530	0.492	0.459	0.408	0.373	0.267	0.207	0.154	0.117

(b) Lower flap

NPR	Static pressure ratios at x_r/l_r of						
	−0.308	−0.170	−0.032	0.037	0.079	0.120	0.162
2.00	0.893	0.830	0.621	0.483	0.392	0.317	0.483
2.50	0.893	0.830	0.620	0.483	0.392	0.311	0.247
3.01	0.893	0.830	0.620	0.483	0.392	0.311	0.244
3.50	0.893	0.830	0.620	0.482	0.391	0.310	0.243
4.01	0.894	0.830	0.620	0.482	0.391	0.310	0.242
5.01	0.894	0.830	0.620	0.482	0.391	0.309	0.241
6.00	0.894	0.830	0.620	0.483	0.391	0.309	0.241
8.00	0.895	0.829	0.620	0.483	0.391	0.309	0.239

Table 95. Static Pressure Ratios for Nozzle 32, $x_r/l_r = 0.42$, $\theta = 30°$, $\phi = 0°$, Maximum Sidewall, $\delta_{v,p} = 0°$, and $\delta_{v,y} = -30°$

(a) Upper ramp

NPR	Static pressure ratios at x_r/l_r of—											
	−0.308	−0.170	−0.101	−0.032	0.037	0.106	0.175	0.244	0.382	0.520	0.659	0.797
2.00	0.859	0.652	0.579	0.530	0.492	0.456	0.427	0.550	0.583	0.591	0.583	0.566
2.50	0.859	0.652	0.576	0.530	0.490	0.454	0.424	0.379	0.453	0.528	0.524	0.485
3.00	0.859	0.652	0.576	0.529	0.490	0.454	0.422	0.378	0.276	0.409	0.460	0.470
3.50	0.859	0.651	0.575	0.529	0.489	0.454	0.420	0.377	0.275	0.350	0.374	0.405
4.00	0.859	0.651	0.575	0.529	0.488	0.454	0.419	0.377	0.276	0.214	0.325	0.333
5.00	0.859	0.651	0.575	0.528	0.488	0.454	0.418	0.377	0.275	0.212	0.282	0.266
5.99	0.858	0.650	0.575	0.527	0.488	0.453	0.417	0.377	0.275	0.211	0.248	0.249
7.00	0.858	0.650	0.575	0.527	0.488	0.454	0.416	0.377	0.274	0.211	0.215	0.238
8.00	0.857	0.649	0.574	0.527	0.488	0.453	0.416	0.377	0.274	0.211	0.191	0.233

(b) Lower flap

NPR	Static pressure ratios at x_r/l_r of—						
	−0.308	−0.170	−0.032	0.037	0.079	0.120	0.162
2.00	0.893	0.838	0.625	0.476	0.400	0.313	0.480
2.50	0.893	0.838	0.625	0.475	0.399	0.306	0.285
3.00	0.893	0.838	0.624	0.475	0.398	0.306	0.223
3.50	0.893	0.838	0.624	0.474	0.398	0.305	0.223
4.00	0.893	0.838	0.624	0.474	0.397	0.305	0.223
5.00	0.893	0.837	0.624	0.473	0.397	0.304	0.222
5.99	0.894	0.837	0.624	0.473	0.397	0.304	0.222
7.00	0.894	0.836	0.624	0.473	0.397	0.304	0.222
8.00	0.894	0.836	0.623	0.472	0.397	0.304	0.222

Table 96. Static Pressure Ratios for Nozzle 33, $x_r/l_r = 0.20$, $\theta = 30°$, $\phi = 0°$, Medium Sidewall, $\delta_{v,p} = 0°$, and $\delta_{v,y} = -30°$

(a) Upper ramp

NPR	Static pressure ratios at x_r/l_r of											
	−0.308	−0.170	−0.101	−0.032	0.037	0.106	0.175	0.244	0.382	0.520	0.659	0.797
2.00	0.863	0.643	0.581	0.526	0.491	0.454	0.496	0.585	0.588	0.577	0.546	0.525
2.50	0.863	0.643	0.578	0.525	0.489	0.451	0.426	0.386	0.526	0.534	0.441	0.406
3.00	0.863	0.643	0.579	0.525	0.489	0.451	0.424	0.381	0.328	0.475	0.426	0.374
3.50	0.863	0.643	0.579	0.524	0.488	0.450	0.423	0.380	0.315	0.407	0.372	0.300
4.00	0.863	0.643	0.578	0.524	0.487	0.449	0.422	0.380	0.313	0.355	0.343	0.264
5.00	0.863	0.642	0.579	0.523	0.486	0.448	0.421	0.379	0.312	0.329	0.294	0.226
5.99	0.863	0.642	0.579	0.523	0.486	0.448	0.420	0.379	0.311	0.326	0.279	0.204
7.00	0.863	0.641	0.578	0.523	0.486	0.448	0.419	0.380	0.311	0.326	0.276	0.196
8.00	0.862	0.641	0.578	0.522	0.487	0.448	0.419	0.380	0.312	0.326	0.277	0.194

(b) Lower flap

NPR	Static pressure ratios at x_r/l_r of						
	−0.308	−0.170	−0.032	0.037	0.079	0.120	0.162
2.00	0.893	0.838	0.626	0.477	0.401	0.314	0.478
2.50	0.893	0.839	0.626	0.476	0.400	0.306	0.289
3.00	0.893	0.839	0.626	0.476	0.399	0.306	0.226
3.50	0.893	0.839	0.626	0.475	0.399	0.305	0.226
4.00	0.894	0.839	0.625	0.475	0.398	0.305	0.226
5.00	0.894	0.838	0.625	0.474	0.398	0.305	0.225
5.99	0.894	0.838	0.625	0.474	0.398	0.304	0.225
7.00	0.894	0.837	0.625	0.473	0.398	0.304	0.225
8.00	0.894	0.837	0.625	0.473	0.398	0.304	0.224

Table 97. Static Pressure Ratios for Nozzle 34, $x_r/l_r = 0.20$, $\theta = 30°$, $\phi = 0°$, Maximum Sidewall, $\delta_{v,p} = 0°$, and $\delta_{v,y} = -30°$

(a) Upper ramp

NPR	Static pressure ratios at x_r/l_r of --											
	−0.308	−0.170	−0.101	−0.032	0.037	0.106	0.175	0.244	0.382	0.520	0.659	0.797
2.00	0.863	0.644	0.584	0.527	0.492	0.456	0.500	0.588	0.599	0.604	0.584	0.547
2.50	0.863	0.644	0.579	0.526	0.489	0.451	0.426	0.386	0.532	0.552	0.513	0.467
3.00	0.863	0.643	0.580	0.525	0.489	0.451	0.424	0.381	0.325	0.489	0.495	0.461
3.50	0.863	0.643	0.580	0.524	0.487	0.451	0.423	0.380	0.314	0.410	0.424	0.413
4.01	0.863	0.643	0.579	0.524	0.487	0.450	0.422	0.380	0.312	0.354	0.379	0.367
5.06	0.863	0.642	0.579	0.523	0.487	0.449	0.421	0.380	0.311	0.327	0.318	0.315
6.00	0.863	0.642	0.579	0.523	0.487	0.449	0.420	0.380	0.311	0.325	0.298	0.288
7.00	0.863	0.641	0.578	0.523	0.486	0.448	0.420	0.380	0.311	0.324	0.292	0.270
7.80	0.862	0.641	0.578	0.523	0.487	0.448	0.419	0.380	0.311	0.324	0.292	0.265

(b) Lower flap

NPR	Static pressure ratios at x_r/l_r of						
	−0.308	−0.170	−0.032	0.037	0.079	0.120	0.162
2.00	0.893	0.838	0.627	0.477	0.401	0.314	0.479
2.50	0.893	0.839	0.626	0.477	0.400	0.307	0.286
3.00	0.893	0.839	0.625	0.476	0.399	0.306	0.226
3.50	0.893	0.839	0.625	0.475	0.398	0.305	0.226
4.01	0.894	0.838	0.625	0.475	0.398	0.305	0.226
5.06	0.894	0.838	0.625	0.474	0.398	0.304	0.225
6.00	0.894	0.838	0.625	0.474	0.398	0.304	0.225
7.00	0.894	0.837	0.625	0.473	0.398	0.304	0.225
7.80	0.894	0.837	0.625	0.473	0.398	0.304	0.225

Table 98. Static Pressure Ratios for Nozzle 35, $x_r/l_r = 0.02$, $\theta = 30°$, $\phi = 0°$, Minimum Sidewall, $\delta_{v,p} = 0°$, and $\delta_{v,y} = -30°$

(a) Upper ramp

NPR	Static pressure ratios at x_r/l_r of—											
	−0.308	−0.170	−0.101	−0.032	0.037	0.106	0.175	0.244	0.382	0.520	0.659	0.797
2.00	0.873	0.686	0.620	0.589	0.562	0.543	0.512	0.518	0.551	0.552	0.524	0.510
2.50	0.873	0.686	0.617	0.588	0.557	0.542	0.506	0.462	0.351	0.486	0.481	0.414
3.00	0.873	0.685	0.617	0.587	0.558	0.542	0.504	0.461	0.348	0.267	0.335	0.421
3.50	0.873	0.685	0.617	0.587	0.558	0.542	0.502	0.461	0.347	0.259	0.200	0.290
4.00	0.873	0.685	0.616	0.587	0.557	0.542	0.501	0.461	0.346	0.258	0.172	0.204
5.00	0.872	0.684	0.616	0.587	0.557	0.541	0.500	0.461	0.345	0.258	0.166	0.122
6.00	0.872	0.683	0.618	0.586	0.557	0.542	0.499	0.461	0.345	0.257	0.166	0.111
7.99	0.871	0.682	0.617	0.586	0.557	0.542	0.497	0.462	0.344	0.258	0.165	0.111

(b) Lower flap

NPR	Static pressure ratios at x_r/l_r of—						
	−0.308	−0.170	−0.032	0.037	0.079	0.120	0.162
2.00	0.905	0.848	0.657	0.530	0.452	0.372	0.403
2.50	0.905	0.847	0.658	0.529	0.451	0.371	0.310
3.00	0.904	0.848	0.657	0.529	0.450	0.370	0.309
3.50	0.905	0.848	0.657	0.529	0.450	0.370	0.308
4.00	0.905	0.848	0.657	0.529	0.450	0.370	0.308
5.00	0.906	0.848	0.657	0.529	0.450	0.369	0.307
6.00	0.906	0.847	0.657	0.529	0.450	0.369	0.306
7.99	0.906	0.846	0.657	0.529	0.450	0.368	0.305

Table 99. Static Pressure Ratios for Nozzle 36, $x_r/l_r = 0.02$, $\theta = 30°$, $\phi = 0°$, Medium Sidewall, $\delta_{v.p} = 0°$, and $\delta_{v.y} = -30°$

(a) Upper ramp

NPR	Static pressure ratios at x_r/l_r of—											
	−0.308	−0.170	−0.101	−0.032	0.037	0.106	0.175	0.244	0.382	0.520	0.659	0.797
1.99	0.874	0.689	0.625	0.594	0.569	0.554	0.533	0.570	0.576	0.565	0.533	0.514
2.50	0.874	0.688	0.621	0.592	0.564	0.549	0.515	0.478	0.410	0.504	0.469	0.407
3.00	0.874	0.688	0.620	0.591	0.562	0.548	0.512	0.475	0.391	0.396	0.318	0.387
3.50	0.874	0.687	0.620	0.591	0.561	0.549	0.511	0.475	0.389	0.354	0.281	0.284
4.00	0.874	0.687	0.621	0.591	0.562	0.548	0.510	0.475	0.388	0.350	0.253	0.234
5.01	0.873	0.687	0.621	0.591	0.562	0.548	0.508	0.475	0.387	0.348	0.247	0.155
5.99	0.873	0.686	0.621	0.590	0.562	0.549	0.507	0.475	0.386	0.348	0.247	0.138
7.80	0.873	0.685	0.620	0.590	0.563	0.549	0.506	0.476	0.386	0.349	0.247	0.134

(b) Lower flap

NPR	Static pressure ratios at x_r/l_r of—						
	−0.308	−0.170	−0.032	0.037	0.079	0.120	0.162
1.99	0.906	0.849	0.661	0.534	0.457	0.378	0.354
2.50	0.905	0.849	0.659	0.532	0.455	0.375	0.316
3.00	0.905	0.849	0.659	0.532	0.454	0.374	0.315
3.50	0.906	0.849	0.659	0.532	0.454	0.374	0.314
4.00	0.906	0.849	0.659	0.532	0.454	0.373	0.313
5.01	0.906	0.848	0.659	0.532	0.454	0.373	0.312
5.99	0.907	0.848	0.659	0.532	0.454	0.373	0.311
7.80	0.907	0.848	0.659	0.532	0.454	0.372	0.310

Table 100. Static Pressure Ratios for Nozzle 37, $x_r/l_r = 0.02$, $\theta = 30°$, $\phi = 0°$, Maximum Sidewall, $\delta_{r,p} = 0°$, and $\delta_{r,y} = -30°$

(a) Upper ramp

NPR	Static pressure ratios at x_r/l_r of -											
	−0.308	−0.170	−0.101	−0.032	0.037	0.106	0.175	0.244	0.382	0.520	0.659	0.797
2.00	0.874	0.689	0.623	0.594	0.566	0.553	0.534	0.572	0.593	0.598	0.576	0.537
2.50	0.874	0.688	0.623	0.592	0.564	0.549	0.516	0.477	0.412	0.550	0.525	0.464
3.00	0.874	0.688	0.620	0.591	0.562	0.548	0.512	0.475	0.394	0.398	0.399	0.438
3.50	0.874	0.687	0.621	0.591	0.562	0.548	0.511	0.475	0.391	0.355	0.350	0.339
4.00	0.874	0.687	0.621	0.591	0.561	0.549	0.510	0.475	0.391	0.350	0.310	0.311
5.00	0.873	0.687	0.621	0.591	0.562	0.549	0.508	0.476	0.390	0.349	0.298	0.269
6.01	0.873	0.686	0.621	0.590	0.562	0.549	0.507	0.476	0.390	0.349	0.297	0.264
6.69	0.873	0.686	0.621	0.590	0.562	0.549	0.507	0.476	0.390	0.349	0.297	0.264

(b) Lower flap

NPR	Static pressure ratios at x_r/l_r of						
	−0.308	−0.170	−0.032	0.037	0.079	0.120	0.162
2.00	0.906	0.849	0.661	0.534	0.457	0.378	0.343
2.50	0.905	0.849	0.660	0.532	0.455	0.375	0.316
3.00	0.905	0.848	0.659	0.532	0.454	0.374	0.315
3.50	0.906	0.849	0.659	0.532	0.454	0.373	0.314
4.00	0.906	0.849	0.659	0.532	0.454	0.373	0.313
5.00	0.906	0.849	0.659	0.532	0.454	0.373	0.312
6.01	0.907	0.848	0.659	0.532	0.454	0.372	0.311
6.69	0.907	0.848	0.659	0.532	0.454	0.372	0.311

Table 101. Static Pressure Ratios for Nozzle 38, $x_r/l_r = 1.00$, $\theta = 0°$, $\phi = 0°$, Minimum Sidewall, $\delta_{v,p} = -20°$, and $\delta_{v,y} = 0°$

(a) Upper ramp

NPR	Static pressure ratios at x_r/l_r of –											
	−0.308	−0.170	−0.101	−0.032	0.037	0.106	0.175	0.244	0.382	0.520	0.659	0.797
2.00	0.848	0.647	0.571	0.468	0.285	0.393	0.396	0.401	0.433	0.469	0.503	0.518
2.50	0.848	0.647	0.569	0.468	0.235	0.190	0.321	0.326	0.356	0.380	0.420	0.444
3.00	0.848	0.647	0.567	0.467	0.233	0.190	0.186	0.173	0.285	0.307	0.340	0.375
3.50	0.848	0.646	0.567	0.467	0.233	0.190	0.185	0.172	0.169	0.246	0.281	0.363
4.01	0.847	0.646	0.567	0.467	0.232	0.189	0.183	0.172	0.141	0.218	0.230	0.282
5.00	0.847	0.645	0.567	0.468	0.230	0.189	0.181	0.171	0.140	0.117	0.095	0.162
6.00	0.846	0.645	0.566	0.468	0.230	0.188	0.180	0.171	0.140	0.117	0.094	0.077
7.00	0.846	0.644	0.566	0.468	0.229	0.187	0.179	0.170	0.140	0.117	0.094	0.077
8.00	0.846	0.644	0.566	0.467	0.229	0.187	0.178	0.170	0.140	0.116	0.094	0.077

(b) Lower flap

NPR	Static pressure ratios at x_r/l_r of—						
	−0.308	−0.170	−0.032	0.037	0.079	0.120	0.162
2.00	0.891	0.836	0.626	0.467	0.385	0.389	0.472
2.50	0.891	0.836	0.626	0.467	0.384	0.291	0.325
3.00	0.891	0.835	0.626	0.466	0.384	0.289	0.235
3.50	0.892	0.836	0.626	0.466	0.383	0.288	0.231
4.01	0.893	0.835	0.626	0.465	0.384	0.287	0.230
5.00	0.893	0.835	0.626	0.465	0.384	0.286	0.231
6.00	0.893	0.835	0.626	0.465	0.384	0.280	0.230
7.00	0.893	0.834	0.626	0.466	0.385	0.280	0.230
8.00	0.893	0.833	0.626	0.466	0.385	0.279	0.230

Table 102. Static Pressure Ratios for Nozzle 39, $x_r/l_r = 1.00$, $\theta = 0°$, $\phi = 0°$, Medium Sidewall, $\delta_{v,p} = -20°$, and $\delta_{v,y} = 0°$

(a) Upper ramp

NPR	Static pressure ratios at x_r/l_r of—											
	−0.308	−0.170	−0.101	−0.032	0.037	0.106	0.175	0.244	0.382	0.520	0.659	0.797
2.00	0.848	0.647	0.571	0.469	0.241	0.344	0.362	0.373	0.418	0.477	0.529	0.537
2.50	0.848	0.647	0.569	0.468	0.237	0.191	0.189	0.312	0.322	0.339	0.390	0.432
3.00	0.848	0.646	0.568	0.468	0.236	0.190	0.186	0.173	0.274	0.294	0.303	0.323
3.50	0.847	0.646	0.568	0.468	0.235	0.190	0.185	0.172	0.142	0.243	0.260	0.299
4.00	0.847	0.646	0.568	0.468	0.235	0.189	0.184	0.172	0.141	0.118	0.212	0.237
5.00	0.847	0.645	0.567	0.467	0.233	0.188	0.182	0.171	0.141	0.117	0.095	0.172
6.00	0.846	0.644	0.566	0.467	0.232	0.187	0.180	0.171	0.140	0.117	0.094	0.077
7.00	0.846	0.644	0.566	0.467	0.231	0.187	0.179	0.171	0.140	0.116	0.094	0.077
8.01	0.845	0.643	0.566	0.467	0.231	0.186	0.178	0.170	0.140	0.116	0.094	0.077

(b) Lower flap

NPR	Static pressure ratios at x_r/l_r of—						
	−0.308	−0.170	−0.032	0.037	0.079	0.120	0.162
2.00	0.891	0.836	0.626	0.467	0.386	0.399	0.466
2.50	0.891	0.836	0.626	0.466	0.385	0.297	0.319
3.00	0.891	0.836	0.626	0.466	0.385	0.293	0.243
3.50	0.892	0.836	0.626	0.465	0.384	0.288	0.237
4.00	0.892	0.835	0.626	0.465	0.384	0.285	0.237
5.00	0.893	0.835	0.625	0.464	0.383	0.283	0.236
6.00	0.893	0.835	0.626	0.464	0.383	0.281	0.236
7.00	0.893	0.834	0.626	0.464	0.384	0.281	0.236
8.01	0.893	0.833	0.626	0.464	0.384	0.280	0.236

Table 103. Static Pressure Ratios for Nozzle 40. $x_r/l_r = 1.00$. $\theta = 0°$. $\phi = 0°$. Maximum Sidewall, $\delta_{v,p} = -20°$, and $\delta_{v,y} = 0°$

(a) Upper ramp

NPR	Static pressure ratios at x_r/l_r of –											
	−0.308	−0.170	−0.101	−0.032	0.037	0.106	0.175	0.244	0.382	0.520	0.659	0.797
2.00	0.849	0.647	0.571	0.469	0.239	0.340	0.362	0.375	0.422	0.479	0.529	0.536
2.50	0.848	0.647	0.568	0.468	0.237	0.190	0.189	0.309	0.319	0.338	0.403	0.448
3.00	0.848	0.646	0.568	0.468	0.235	0.189	0.186	0.173	0.263	0.282	0.294	0.327
3.50	0.848	0.646	0.568	0.468	0.234	0.189	0.185	0.173	0.141	0.225	0.240	0.259
4.00	0.847	0.646	0.567	0.468	0.234	0.189	0.183	0.172	0.141	0.117	0.209	0.218
5.00	0.847	0.645	0.567	0.467	0.233	0.188	0.182	0.171	0.141	0.117	0.095	0.176
6.00	0.847	0.644	0.567	0.467	0.232	0.187	0.180	0.171	0.140	0.116	0.094	0.077
7.00	0.846	0.644	0.566	0.467	0.231	0.187	0.179	0.170	0.140	0.116	0.094	0.077
8.00	0.845	0.644	0.566	0.466	0.231	0.187	0.178	0.170	0.140	0.116	0.094	0.077

(b) Lower flap

NPR	Static pressure ratios at x_r/l_r of–						
	−0.308	−0.170	−0.032	0.037	0.079	0.120	0.162
2.00	0.892	0.836	0.626	0.467	0.386	0.397	0.467
2.50	0.892	0.836	0.626	0.466	0.385	0.296	0.317
3.00	0.892	0.836	0.625	0.465	0.384	0.293	0.243
3.50	0.892	0.836	0.626	0.465	0.384	0.288	0.237
4.00	0.892	0.835	0.626	0.464	0.383	0.285	0.237
5.00	0.893	0.835	0.626	0.464	0.383	0.283	0.236
6.00	0.893	0.834	0.626	0.464	0.383	0.282	0.236
7.00	0.893	0.834	0.625	0.464	0.383	0.281	0.236
8.00	0.893	0.833	0.625	0.464	0.383	0.281	0.236

Table 104. Static Pressure Ratios for Nozzle 41, $x_r/l_r = 0.42$, $\theta = 20°$, $\phi = 0°$, Minimum Sidewall, $\delta_{v.p} = -20°$, and $\delta_{v.y} = 0°$

(a) Upper ramp

NPR	Static pressure ratios at x_r/l_r of—											
	−0.308	−0.170	−0.101	−0.032	0.037	0.106	0.175	0.244	0.382	0.520	0.659	0.797
2.00	0.858	0.643	0.574	0.467	0.259	0.383	0.394	0.401	0.437	0.474	0.498	0.511
2.50	0.858	0.643	0.570	0.466	0.253	0.184	0.279	0.317	0.348	0.375	0.413	0.441
3.00	0.857	0.642	0.569	0.465	0.253	0.185	0.183	0.160	0.290	0.314	0.337	0.374
3.50	0.857	0.642	0.568	0.465	0.251	0.184	0.181	0.159	0.149	0.245	0.279	0.366
4.00	0.857	0.642	0.568	0.464	0.251	0.183	0.179	0.158	0.134	0.221	0.232	0.280
5.01	0.857	0.641	0.568	0.464	0.249	0.183	0.177	0.157	0.133	0.117	0.085	0.158
6.00	0.856	0.640	0.568	0.463	0.249	0.182	0.176	0.156	0.133	0.117	0.085	0.078
7.00	0.856	0.640	0.567	0.463	0.249	0.181	0.174	0.156	0.133	0.116	0.084	0.079
8.00	0.855	0.639	0.567	0.462	0.249	0.181	0.173	0.155	0.133	0.116	0.084	0.078

(b) Lower flap

NPR	Static pressure ratios at x_r/l_r of—						
	−0.308	−0.170	−0.032	0.037	0.079	0.120	0.162
2.00	0.893	0.842	0.624	0.472	0.392	0.361	0.473
2.50	0.893	0.843	0.624	0.471	0.392	0.297	0.282
3.00	0.893	0.844	0.624	0.471	0.391	0.296	0.239
3.50	0.893	0.844	0.624	0.470	0.391	0.296	0.239
4.00	0.893	0.844	0.624	0.470	0.391	0.295	0.240
5.01	0.894	0.844	0.624	0.469	0.391	0.295	0.239
6.00	0.894	0.843	0.624	0.469	0.391	0.295	0.239
7.00	0.894	0.842	0.623	0.468	0.391	0.295	0.238
8.00	0.894	0.842	0.623	0.468	0.391	0.294	0.238

Table 105. Static Pressure Ratios for Nozzle 42, $x_r/l_r = 0.42$, $\theta = 20°$, $\phi = 0°$, Medium Sidewall, $\delta_{v,p} = -20°$, and $\delta_{v,y} = 0°$

(a) Upper ramp

NPR	Static pressure ratios at x_r/l_r of—											
	−0.308	−0.170	−0.101	−0.032	0.037	0.106	0.175	0.244	0.382	0.520	0.659	0.797
2.00	0.857	0.643	0.573	0.467	0.257	0.318	0.352	0.370	0.430	0.493	0.531	0.536
2.51	0.857	0.643	0.569	0.466	0.254	0.184	0.185	0.296	0.317	0.343	0.423	0.461
3.00	0.857	0.642	0.570	0.465	0.253	0.184	0.183	0.161	0.263	0.279	0.301	0.357
3.50	0.857	0.642	0.569	0.465	0.252	0.184	0.181	0.159	0.135	0.243	0.260	0.294
4.00	0.856	0.642	0.569	0.465	0.252	0.184	0.179	0.158	0.133	0.118	0.209	0.238
5.01	0.856	0.641	0.568	0.464	0.250	0.183	0.177	0.157	0.133	0.117	0.085	0.172
6.00	0.856	0.640	0.568	0.463	0.250	0.182	0.176	0.157	0.133	0.116	0.084	0.079
7.00	0.855	0.640	0.567	0.463	0.250	0.182	0.174	0.156	0.133	0.116	0.084	0.078
8.00	0.855	0.639	0.567	0.463	0.249	0.181	0.174	0.155	0.133	0.116	0.084	0.078

(b) Lower flap

NPR	Static pressure ratios at x_r/l_r of—						
	−0.308	−0.170	−0.032	0.037	0.079	0.120	0.162
2.00	0.893	0.842	0.624	0.472	0.392	0.363	0.473
2.51	0.892	0.843	0.624	0.471	0.392	0.297	0.312
3.00	0.892	0.843	0.624	0.471	0.391	0.296	0.236
3.50	0.893	0.844	0.624	0.470	0.391	0.296	0.238
4.00	0.893	0.844	0.624	0.470	0.391	0.295	0.239
5.01	0.894	0.843	0.624	0.469	0.391	0.295	0.240
6.00	0.894	0.843	0.623	0.469	0.391	0.295	0.241
7.00	0.894	0.842	0.623	0.468	0.391	0.295	0.241
8.00	0.894	0.842	0.623	0.468	0.391	0.294	0.240

Table 106. Static Pressure Ratios for Nozzle 43, $x_r/l_r = 0.42$, $\theta = 20°$, $\phi = 0°$, Maximum Sidewall, $\delta_{v,p} = -20°$, and $\delta_{v,y} = 0°$

(a) Upper ramp

NPR	Static pressure ratios at x_r/l_r of—											
	−0.308	−0.170	−0.101	−0.032	0.037	0.106	0.175	0.244	0.382	0.520	0.659	0.797
2.00	0.857	0.643	0.571	0.466	0.252	0.315	0.353	0.369	0.425	0.491	0.532	0.537
2.50	0.857	0.643	0.571	0.465	0.253	0.183	0.186	0.306	0.322	0.339	0.403	0.450
3.00	0.857	0.642	0.570	0.464	0.252	0.184	0.183	0.161	0.265	0.281	0.295	0.348
3.50	0.857	0.642	0.569	0.464	0.251	0.183	0.182	0.159	0.134	0.230	0.248	0.282
4.00	0.856	0.642	0.569	0.463	0.250	0.183	0.180	0.159	0.134	0.122	0.215	0.236
5.00	0.856	0.641	0.568	0.463	0.249	0.182	0.178	0.158	0.133	0.117	0.085	0.179
6.01	0.856	0.640	0.568	0.463	0.248	0.181	0.177	0.157	0.133	0.117	0.085	0.079
7.00	0.855	0.640	0.567	0.462	0.248	0.181	0.175	0.156	0.133	0.116	0.084	0.078
8.00	0.855	0.639	0.567	0.463	0.248	0.180	0.174	0.156	0.133	0.116	0.084	0.078

(b) Lower flap

NPR	Static pressure ratios at x_r/l_r of—						
	−0.308	−0.170	−0.032	0.037	0.079	0.120	0.162
2.00	0.892	0.842	0.623	0.471	0.392	0.364	0.472
2.50	0.892	0.843	0.623	0.471	0.391	0.296	0.327
3.00	0.892	0.843	0.623	0.470	0.391	0.296	0.232
3.50	0.893	0.843	0.623	0.470	0.390	0.295	0.233
4.00	0.893	0.843	0.623	0.469	0.390	0.295	0.234
5.00	0.893	0.843	0.623	0.469	0.390	0.294	0.235
6.01	0.894	0.843	0.623	0.468	0.390	0.294	0.235
7.00	0.894	0.842	0.623	0.468	0.390	0.294	0.235
8.00	0.894	0.841	0.623	0.467	0.390	0.294	0.234

Table 107. Static Pressure Ratios for Nozzle 44, $x_r/l_r = 0.20$, $\theta = 20°$, $\phi = 0°$, Minimum Sidewall, $\delta_{v,p} = -20°$, and $\delta_{v,y} = 0°$

(a) Upper ramp

NPR	Static pressure ratios at x_r/l_r of											
	−0.308	−0.170	−0.101	−0.032	0.037	0.106	0.175	0.244	0.382	0.520	0.659	0.797
2.01	0.860	0.645	0.575	0.485	0.262	0.389	0.401	0.409	0.441	0.474	0.496	0.504
2.50	0.860	0.646	0.574	0.485	0.242	0.183	0.306	0.331	0.359	0.391	0.426	0.436
3.00	0.860	0.645	0.572	0.485	0.240	0.182	0.183	0.173	0.274	0.302	0.363	0.385
3.50	0.860	0.645	0.572	0.485	0.239	0.182	0.182	0.173	0.211	0.252	0.292	0.348
4.00	0.860	0.645	0.573	0.484	0.239	0.182	0.181	0.172	0.137	0.227	0.240	0.289
5.00	0.859	0.644	0.573	0.484	0.237	0.181	0.179	0.171	0.137	0.119	0.094	0.172
6.00	0.859	0.644	0.573	0.484	0.237	0.181	0.178	0.171	0.137	0.119	0.094	0.077
7.00	0.859	0.643	0.572	0.484	0.237	0.181	0.177	0.171	0.137	0.119	0.094	0.077

(b) Lower flap

NPR	Static pressure ratios at x_r/l_r of—						
	−0.308	−0.170	−0.032	0.037	0.079	0.120	0.162
2.01	0.893	0.841	0.625	0.474	0.394	0.337	0.474
2.50	0.893	0.844	0.625	0.473	0.394	0.299	0.276
3.00	0.893	0.845	0.625	0.473	0.394	0.298	0.244
3.50	0.893	0.847	0.625	0.472	0.393	0.298	0.244
4.00	0.893	0.847	0.625	0.472	0.393	0.297	0.244
5.00	0.894	0.847	0.625	0.471	0.393	0.297	0.243
6.00	0.894	0.847	0.625	0.471	0.393	0.297	0.242
7.00	0.894	0.846	0.624	0.470	0.393	0.297	0.242

Table 108. Static Pressure Ratios for Nozzle 45, $x_r/l_r = 0.20$, $\theta = 20°$, $\phi = 0°$, Medium Sidewall, $\delta_{v,p} = -20°$, and $\delta_{v,y} = 0°$

(a) Upper ramp

NPR	Static pressure ratios at x_r/l_r of											
	−0.308	−0.170	−0.101	−0.032	0.037	0.106	0.175	0.244	0.382	0.520	0.659	0.797
2.00	0.860	0.645	0.574	0.486	0.247	0.358	0.377	0.402	0.466	0.500	0.514	0.515
2.50	0.860	0.646	0.572	0.485	0.240	0.183	0.283	0.328	0.348	0.371	0.398	0.417
3.00	0.860	0.645	0.573	0.485	0.240	0.184	0.182	0.173	0.287	0.305	0.334	0.353
3.51	0.860	0.645	0.572	0.485	0.239	0.183	0.180	0.172	0.233	0.261	0.285	0.305
4.00	0.860	0.645	0.573	0.485	0.239	0.183	0.178	0.172	0.137	0.229	0.246	0.273
5.00	0.859	0.644	0.572	0.484	0.238	0.183	0.176	0.171	0.137	0.120	0.105	0.207
6.00	0.859	0.644	0.572	0.484	0.237	0.182	0.175	0.171	0.137	0.119	0.094	0.109
8.00	0.858	0.643	0.572	0.484	0.236	0.182	0.173	0.170	0.136	0.119	0.094	0.078

(b) Lower flap

NPR	Static pressure ratios at x_r/l_r of						
	−0.308	−0.170	−0.032	0.037	0.079	0.120	0.162
2.00	0.892	0.841	0.625	0.473	0.394	0.344	0.474
2.50	0.892	0.844	0.625	0.473	0.394	0.299	0.278
3.00	0.892	0.846	0.625	0.472	0.393	0.298	0.240
3.51	0.893	0.847	0.625	0.472	0.393	0.297	0.241
4.00	0.893	0.847	0.625	0.471	0.393	0.297	0.240
5.00	0.894	0.847	0.625	0.471	0.393	0.297	0.239
6.00	0.894	0.847	0.624	0.470	0.393	0.297	0.238
8.00	0.894	0.845	0.624	0.469	0.393	0.296	0.237

Table 109. Static Pressure Ratios for Nozzle 46, $x_r/l_r = 0.20$, $\theta = 20°$, $\phi = 0°$, Maximum Sidewall, $\delta_{v,p} = -20°$, and $\delta_{v,y} = 0°$

(a) Upper ramp

NPR	Static pressure ratios at x_r/l_r of											
	−0.308	−0.170	−0.101	−0.032	0.037	0.106	0.175	0.244	0.382	0.520	0.659	0.797
2.00	0.860	0.645	0.576	0.486	0.261	0.389	0.401	0.408	0.437	0.470	0.493	0.503
2.50	0.860	0.645	0.573	0.485	0.240	0.183	0.223	0.313	0.339	0.382	0.424	0.429
3.00	0.860	0.645	0.573	0.485	0.238	0.183	0.185	0.173	0.287	0.313	0.334	0.346
3.50	0.860	0.645	0.573	0.484	0.239	0.184	0.183	0.173	0.220	0.263	0.292	0.308
4.00	0.860	0.645	0.573	0.484	0.239	0.184	0.182	0.172	0.137	0.224	0.244	0.272
5.00	0.859	0.644	0.572	0.484	0.238	0.183	0.180	0.172	0.137	0.119	0.099	0.206
6.00	0.859	0.643	0.572	0.484	0.237	0.182	0.178	0.171	0.136	0.119	0.094	0.114
7.99	0.858	0.642	0.571	0.484	0.236	0.182	0.176	0.170	0.136	0.119	0.094	0.077

(b) Lower flap

NPR	Static pressure ratios at x_r/l_r of						
	−0.308	−0.170	−0.032	0.037	0.079	0.120	0.162
2.00	0.893	0.841	0.625	0.473	0.394	0.348	0.474
2.50	0.892	0.844	0.624	0.473	0.393	0.298	0.280
3.00	0.893	0.845	0.624	0.472	0.393	0.298	0.239
3.50	0.893	0.846	0.624	0.471	0.392	0.297	0.239
4.00	0.893	0.847	0.624	0.471	0.392	0.297	0.239
5.00	0.894	0.847	0.624	0.470	0.392	0.297	0.239
6.00	0.894	0.846	0.624	0.470	0.392	0.296	0.238
7.99	0.894	0.845	0.624	0.469	0.392	0.296	0.236

Table 110. Static Pressure Ratios for Nozzle 47, $x_r/l_r = 0.02$, $\theta = 20°$, $\phi = 0°$, Minimum Sidewall, $\delta_{v,p} = -20°$, and $\delta_{v,y} = 0°$

(a) Upper ramp

NPR	Static pressure ratios at x_r/l_r of—											
	−0.308	−0.170	−0.101	−0.032	0.037	0.106	0.175	0.244	0.382	0.520	0.659	0.797
2.00	0.856	0.647	0.581	0.488	0.273	0.383	0.402	0.429	0.485	0.512	0.529	0.530
2.50	0.857	0.647	0.580	0.488	0.237	0.185	0.300	0.327	0.378	0.428	0.444	0.435
3.00	0.855	0.647	0.577	0.487	0.235	0.184	0.185	0.174	0.283	0.344	0.384	0.373
3.50	0.856	0.647	0.577	0.487	0.235	0.185	0.183	0.173	0.255	0.272	0.330	0.337
4.00	0.856	0.646	0.577	0.487	0.235	0.184	0.182	0.172	0.137	0.239	0.275	0.307
5.00	0.856	0.646	0.577	0.487	0.234	0.184	0.180	0.171	0.137	0.118	0.160	0.226
6.00	0.855	0.645	0.577	0.486	0.233	0.183	0.179	0.171	0.137	0.118	0.095	0.138
8.00	0.854	0.644	0.576	0.486	0.232	0.182	0.177	0.170	0.136	0.118	0.095	0.077

(b) Lower flap

NPR	Static pressure ratios at x_r/l_r of—						
	−0.308	−0.170	−0.032	0.037	0.079	0.120	0.162
2.00	0.894	0.831	0.613	0.472	0.390	0.319	0.486
2.50	0.894	0.832	0.613	0.471	0.390	0.308	0.292
3.00	0.894	0.832	0.612	0.471	0.390	0.307	0.237
3.50	0.894	0.832	0.612	0.470	0.389	0.307	0.237
4.00	0.894	0.832	0.612	0.470	0.389	0.306	0.236
5.00	0.894	0.832	0.612	0.470	0.389	0.306	0.236
6.00	0.894	0.832	0.612	0.470	0.388	0.305	0.235
8.00	0.894	0.831	0.611	0.470	0.388	0.305	0.235

Table 111. Static Pressure Ratios for Nozzle 48. $x_r/l_r = 0.02$, $\theta = 20°$, $\phi = 0°$, Medium Sidewall, $\delta_{r,p} = -20°$, and $\delta_{r,y} = 0°$

(a) Upper ramp

NPR	Static pressure ratios at x_r/l_r of—											
	−0.308	−0.170	−0.101	−0.032	0.037	0.106	0.175	0.244	0.382	0.520	0.659	0.797
2.00	0.856	0.647	0.581	0.488	0.266	0.381	0.400	0.428	0.483	0.508	0.523	0.526
2.50	0.856	0.647	0.578	0.487	0.238	0.185	0.280	0.323	0.370	0.425	0.442	0.433
3.00	0.856	0.647	0.578	0.487	0.237	0.185	0.187	0.174	0.281	0.341	0.383	0.376
3.50	0.855	0.646	0.577	0.487	0.235	0.185	0.185	0.174	0.250	0.267	0.323	0.333
4.00	0.855	0.646	0.577	0.487	0.235	0.184	0.184	0.173	0.137	0.231	0.258	0.303
5.00	0.855	0.646	0.577	0.487	0.234	0.184	0.182	0.172	0.137	0.118	0.127	0.215
6.01	0.855	0.645	0.577	0.486	0.233	0.183	0.180	0.172	0.137	0.118	0.096	0.151
8.00	0.854	0.644	0.577	0.486	0.232	0.182	0.179	0.171	0.136	0.118	0.095	0.077

(b) Lower flap

NPR	Static pressure ratios at x_r/l_r of—						
	−0.308	−0.170	−0.032	0.037	0.079	0.120	0.162
2.00	0.894	0.831	0.613	0.472	0.390	0.318	0.486
2.50	0.894	0.831	0.613	0.471	0.390	0.308	0.296
3.00	0.893	0.831	0.612	0.471	0.390	0.307	0.237
3.50	0.893	0.832	0.612	0.470	0.389	0.307	0.237
4.00	0.894	0.832	0.612	0.470	0.389	0.306	0.237
5.00	0.894	0.832	0.612	0.470	0.389	0.306	0.236
6.01	0.894	0.831	0.611	0.470	0.388	0.305	0.236
8.00	0.894	0.831	0.611	0.470	0.388	0.305	0.235

Table 112. Static Pressure Ratios for Nozzle 49. $x_r/l_r = 0.02$, $\theta = 20°$, $\phi = 0°$. Maximum Sidewall, $\delta_{v,p} = -20°$, and $\delta_{v,y} = 0°$

(a) Upper ramp

NPR	Static pressure ratios at x_r/l_r of—											
	−0.308	−0.170	−0.101	−0.032	0.037	0.106	0.175	0.244	0.382	0.520	0.659	0.797
2.00	0.856	0.647	0.580	0.489	0.260	0.379	0.399	0.428	0.482	0.507	0.519	0.521
2.50	0.855	0.647	0.578	0.488	0.237	0.184	0.243	0.317	0.370	0.426	0.438	0.427
3.00	0.855	0.647	0.578	0.487	0.236	0.184	0.187	0.175	0.279	0.340	0.383	0.371
3.50	0.855	0.647	0.578	0.487	0.235	0.185	0.186	0.174	0.246	0.262	0.321	0.339
4.00	0.855	0.646	0.578	0.487	0.235	0.185	0.184	0.173	0.137	0.230	0.252	0.304
5.00	0.855	0.646	0.577	0.487	0.234	0.184	0.182	0.173	0.137	0.119	0.101	0.210
6.00	0.855	0.645	0.577	0.486	0.233	0.183	0.181	0.172	0.137	0.118	0.095	0.111
8.00	0.854	0.644	0.576	0.486	0.232	0.182	0.179	0.171	0.136	0.118	0.095	0.077

(b) Lower flap

NPR	Static pressure ratios at x_r/l_r of—						
	−0.308	−0.170	−0.032	0.037	0.079	0.120	0.162
2.00	0.894	0.831	0.613	0.471	0.390	0.319	0.486
2.50	0.894	0.831	0.612	0.471	0.390	0.307	0.299
3.00	0.893	0.831	0.612	0.471	0.390	0.307	0.237
3.50	0.893	0.832	0.612	0.470	0.389	0.306	0.237
4.00	0.894	0.832	0.611	0.470	0.388	0.306	0.236
5.00	0.894	0.832	0.611	0.470	0.388	0.305	0.236
6.00	0.894	0.831	0.611	0.470	0.388	0.305	0.235
8.00	0.894	0.830	0.611	0.469	0.388	0.305	0.235

Table 113. Static Pressure Ratios for Nozzle 50, $x_r/l_r = 0.42$, $\theta = 20°$, $\phi = 0°$, Maximum Sidewall, $\delta_{v,p} = -20°$, and $\delta_{v,y} = -20°$

(a) Upper ramp

NPR	Static pressure ratios at x_r/l_r of—											
	−0.308	−0.170	−0.101	−0.032	0.037	0.106	0.175	0.244	0.382	0.520	0.659	0.797
2.00	0.857	0.642	0.572	0.466	0.255	0.363	0.379	0.391	0.445	0.488	0.513	0.519
2.50	0.857	0.643	0.570	0.465	0.253	0.184	0.187	0.314	0.331	0.376	0.436	0.459
3.01	0.857	0.642	0.569	0.465	0.252	0.183	0.183	0.160	0.294	0.305	0.339	0.379
3.50	0.857	0.642	0.569	0.464	0.252	0.183	0.182	0.159	0.134	0.258	0.252	0.382
4.00	0.856	0.641	0.569	0.464	0.251	0.183	0.180	0.159	0.134	0.181	0.234	0.269
5.00	0.856	0.641	0.569	0.463	0.250	0.182	0.178	0.157	0.133	0.117	0.084	0.163
6.00	0.856	0.640	0.568	0.463	0.249	0.181	0.177	0.156	0.133	0.117	0.084	0.102
8.00	0.855	0.639	0.567	0.462	0.249	0.181	0.174	0.155	0.133	0.116	0.083	0.098

(b) Lower flap

NPR	Static pressure ratios at x_r/l_r of—						
	−0.308	−0.170	−0.032	0.037	0.079	0.120	0.162
2.00	0.893	0.842	0.624	0.471	0.392	0.352	0.472
2.50	0.893	0.844	0.624	0.471	0.392	0.296	0.276
3.01	0.893	0.845	0.624	0.470	0.391	0.296	0.231
3.50	0.893	0.845	0.624	0.470	0.391	0.295	0.230
4.00	0.893	0.845	0.624	0.470	0.391	0.295	0.230
5.00	0.894	0.845	0.624	0.469	0.391	0.295	0.230
6.00	0.894	0.845	0.623	0.469	0.391	0.294	0.229
8.00	0.894	0.843	0.623	0.468	0.391	0.294	0.230

Table 114. Static Pressure Ratios for Nozzle 51, $x_r/l_r = 0.20$, $\theta = 20°$, $\phi = 0°$, Medium Sidewall, $\delta_{v,p} = -20°$, and $\delta_{v,y} = -20°$

(a) Upper ramp

NPR	Static pressure ratios at x_r/l_r of- -											
	−0.308	−0.170	−0.101	−0.032	0.037	0.106	0.175	0.244	0.382	0.520	0.659	0.797
2.00	0.860	0.645	0.573	0.486	0.255	0.383	0.398	0.420	0.472	0.505	0.524	0.524
2.50	0.860	0.645	0.573	0.485	0.239	0.184	0.317	0.324	0.356	0.388	0.435	0.436
3.00	0.860	0.645	0.572	0.485	0.238	0.184	0.186	0.173	0.297	0.322	0.357	0.381
3.50	0.860	0.645	0.573	0.485	0.238	0.184	0.185	0.173	0.262	0.275	0.318	0.355
4.00	0.860	0.645	0.573	0.485	0.237	0.184	0.184	0.173	0.137	0.248	0.260	0.323
5.00	0.860	0.645	0.573	0.485	0.237	0.184	0.182	0.172	0.137	0.121	0.148	0.181
6.00	0.859	0.644	0.573	0.484	0.236	0.183	0.180	0.172	0.137	0.122	0.147	0.119
8.00	0.858	0.643	0.572	0.484	0.235	0.182	0.178	0.171	0.137	0.127	0.147	0.118

(b) Lower flap

NPR	Static pressure ratios at x_r/l_r of						
	−0.308	−0.170	−0.032	0.037	0.079	0.120	0.162
2.00	0.893	0.842	0.625	0.473	0.394	0.341	0.474
2.50	0.893	0.844	0.625	0.473	0.394	0.299	0.277
3.00	0.893	0.845	0.625	0.472	0.393	0.298	0.246
3.50	0.893	0.846	0.625	0.472	0.393	0.298	0.247
4.00	0.893	0.847	0.625	0.472	0.393	0.297	0.247
5.00	0.894	0.847	0.625	0.471	0.393	0.297	0.246
6.00	0.894	0.847	0.625	0.471	0.393	0.297	0.245
8.00	0.894	0.846	0.624	0.470	0.393	0.296	0.243

Table 115. Static Pressure Ratios for Nozzle 52, $x_r/l_r = 0.20$, $\theta = 20°$, $\phi = 0°$, Maximum Sidewall, $\delta_{v,p} = -20°$, and $\delta_{v,y} = -20°$

(a) Upper ramp

NPR	Static pressure ratios at x_r/l_r of—											
	−0.308	−0.170	−0.101	−0.032	0.037	0.106	0.175	0.244	0.382	0.520	0.659	0.797
2.01	0.860	0.645	0.576	0.486	0.291	0.400	0.413	0.428	0.459	0.478	0.502	0.511
2.50	0.860	0.646	0.573	0.485	0.238	0.183	0.320	0.334	0.357	0.393	0.459	0.466
3.00	0.860	0.645	0.573	0.485	0.239	0.185	0.187	0.174	0.278	0.300	0.509	0.449
3.50	0.860	0.645	0.573	0.485	0.238	0.184	0.185	0.173	0.241	0.257	0.350	0.424
4.01	0.860	0.645	0.573	0.485	0.238	0.184	0.184	0.172	0.137	0.244	0.259	0.329
5.00	0.859	0.645	0.573	0.485	0.237	0.184	0.182	0.171	0.137	0.126	0.149	0.175
6.00	0.859	0.644	0.573	0.484	0.236	0.183	0.180	0.171	0.137	0.125	0.148	0.122
8.00	0.858	0.643	0.572	0.484	0.236	0.182	0.178	0.170	0.137	0.123	0.148	0.122

(b) Lower flap

NPR	Static pressure ratios at x_r/l_r of—						
	−0.308	−0.170	−0.032	0.037	0.079	0.120	0.162
2.01	0.893	0.841	0.625	0.474	0.394	0.335	0.474
2.50	0.893	0.844	0.625	0.473	0.394	0.299	0.273
3.00	0.893	0.846	0.625	0.473	0.394	0.299	0.245
3.50	0.893	0.847	0.625	0.472	0.393	0.298	0.245
4.01	0.894	0.847	0.625	0.472	0.393	0.298	0.245
5.00	0.894	0.847	0.625	0.471	0.393	0.297	0.245
6.00	0.894	0.847	0.625	0.471	0.393	0.297	0.245
8.00	0.894	0.846	0.624	0.470	0.393	0.296	0.244

Table 116. Static Pressure Ratios for Nozzle 53. $x_r/l_r = 0.02$. $\theta = 20°$. $o = 0°$. Minimum Sidewall. $\delta_{v.p} = -20°$. and $\delta_{v.y} = -20°$

(a) Upper ramp

NPR	Static pressure ratios at x_r/l_r of—											
	−0.308	−0.170	−0.101	−0.032	0.037	0.106	0.175	0.244	0.382	0.520	0.659	0.797
2.00	0.840	0.653	0.588	0.494	0.249	0.367	0.382	0.407	0.495	0.528	0.538	0.531
2.50	0.836	0.653	0.583	0.493	0.238	0.187	0.333	0.344	0.384	0.440	0.460	0.437
3.01	0.838	0.652	0.582	0.492	0.237	0.187	0.193	0.187	0.306	0.377	0.433	0.367
3.50	0.843	0.652	0.583	0.492	0.238	0.189	0.191	0.180	0.281	0.312	0.365	0.359
4.00	0.849	0.652	0.583	0.492	0.238	0.189	0.190	0.179	0.191	0.255	0.290	0.380
5.00	0.852	0.651	0.583	0.492	0.237	0.188	0.188	0.179	0.190	0.180	0.134	0.209
6.00	0.856	0.651	0.582	0.492	0.236	0.187	0.187	0.178	0.191	0.181	0.134	0.092
8.00	0.853	0.649	0.582	0.491	0.235	0.187	0.185	0.178	0.191	0.181	0.134	0.092
8.39	1.002	0.906	0.814	0.687	0.328	0.260	0.256	0.249	0.267	0.256	0.188	0.129

(b) Lower flap

NPR	Static pressure ratios at x_r/l_r of—						
	−0.308	−0.170	−0.032	0.037	0.079	0.120	0.162
2.00	0.896	0.836	0.618	0.478	0.397	0.317	0.483
2.50	0.895	0.836	0.618	0.478	0.396	0.314	0.253
3.01	0.895	0.836	0.617	0.477	0.396	0.313	0.243
3.50	0.895	0.836	0.617	0.477	0.395	0.313	0.243
4.00	0.896	0.836	0.617	0.477	0.395	0.313	0.242
5.00	0.896	0.836	0.617	0.476	0.395	0.312	0.242
6.00	0.896	0.835	0.617	0.476	0.395	0.312	0.241
8.00	0.896	0.834	0.617	0.476	0.395	0.311	0.241
8.39	1.252	1.161	0.863	0.666	0.552	0.436	0.337

Table 117. Static Pressure Ratios for Nozzle 54, $x_r/l_r = 0.02$, $\theta = 20°$, $\phi = 0°$, Medium Sidewall, $\delta_{v,p} = -20°$, and $\delta_{v,y} = -20°$

(a) Upper ramp

NPR	Static pressure ratios at x_r/l_r of—											
	−0.308	−0.170	−0.101	−0.032	0.037	0.106	0.175	0.244	0.382	0.520	0.659	0.797
2.01	0.832	0.652	0.585	0.493	0.260	0.382	0.401	0.427	0.489	0.525	0.538	0.533
2.50	0.840	0.653	0.583	0.493	0.240	0.189	0.316	0.334	0.377	0.430	0.453	0.438
3.00	0.853	0.652	0.583	0.492	0.240	0.190	0.193	0.193	0.327	0.358	0.378	0.356
3.50	0.846	0.652	0.583	0.492	0.239	0.189	0.191	0.181	0.285	0.298	0.342	0.366
4.00	0.852	0.652	0.583	0.492	0.238	0.189	0.190	0.181	0.191	0.256	0.287	0.370
5.00	0.851	0.651	0.583	0.492	0.237	0.189	0.188	0.180	0.190	0.187	0.170	0.181
6.00	0.859	0.651	0.583	0.492	0.236	0.188	0.186	0.179	0.189	0.187	0.170	0.137
8.00	0.854	0.649	0.582	0.491	0.235	0.187	0.184	0.178	0.189	0.187	0.170	0.137

(b) Lower flap

NPR	Static pressure ratios at x_r/l_r of—						
	−0.308	−0.170	−0.032	0.037	0.079	0.120	0.162
2.01	0.896	0.834	0.617	0.477	0.396	0.316	0.483
2.50	0.896	0.835	0.617	0.477	0.396	0.313	0.254
3.00	0.895	0.834	0.617	0.476	0.395	0.313	0.242
3.50	0.896	0.835	0.617	0.476	0.395	0.312	0.242
4.00	0.896	0.835	0.617	0.476	0.395	0.312	0.242
5.00	0.896	0.835	0.617	0.476	0.395	0.311	0.241
6.00	0.896	0.834	0.616	0.476	0.394	0.311	0.241
8.00	0.896	0.833	0.616	0.476	0.394	0.311	0.240

Table 118. Static Pressure Ratios for Nozzle 55, $x_r/l_r = 0.02$, $\theta = 20°$, $\phi = 0°$, Maximum Sidewall, $\delta_{v,p} = -20°$, and $\delta_{v,y} = -20°$

(a) Upper ramp

NPR	Static pressure ratios at x_r/l_r of—											
	−0.308	−0.170	−0.101	−0.032	0.037	0.106	0.175	0.244	0.382	0.520	0.659	0.797
2.00	0.858	0.653	0.588	0.494	0.285	0.395	0.410	0.432	0.493	0.532	0.549	0.541
2.50	0.859	0.653	0.585	0.493	0.241	0.189	0.337	0.349	0.387	0.441	0.478	0.468
3.05	0.851	0.653	0.584	0.492	0.238	0.189	0.193	0.266	0.328	0.353	0.389	0.414
3.50	0.859	0.653	0.584	0.493	0.238	0.189	0.191	0.181	0.285	0.303	0.337	0.392
4.01	0.858	0.652	0.584	0.493	0.238	0.189	0.190	0.181	0.190	0.241	0.279	0.305
5.00	0.858	0.652	0.584	0.492	0.237	0.188	0.188	0.180	0.190	0.187	0.169	0.183
6.00	0.858	0.651	0.584	0.492	0.237	0.187	0.187	0.179	0.189	0.187	0.169	0.147
8.00	0.857	0.650	0.583	0.492	0.235	0.187	0.185	0.179	0.189	0.187	0.169	0.147

(b) Lower flap

NPR	Static pressure ratios at x_r/l_r of—						
	−0.308	−0.170	−0.032	0.037	0.079	0.120	0.162
2.00	0.896	0.835	0.618	0.478	0.397	0.316	0.484
2.50	0.896	0.835	0.618	0.477	0.396	0.314	0.254
3.05	0.895	0.835	0.617	0.476	0.395	0.312	0.242
3.50	0.896	0.835	0.617	0.477	0.395	0.312	0.242
4.01	0.896	0.835	0.617	0.476	0.395	0.312	0.242
5.00	0.896	0.835	0.617	0.476	0.395	0.312	0.242
6.00	0.896	0.835	0.617	0.476	0.395	0.311	0.241
8.00	0.896	0.834	0.617	0.476	0.395	0.311	0.241

Table 119. Static Pressure Ratios for Nozzle 56. $x_r/l_r = 0.42$, $\theta = 30°$, $o = 0°$. Minimum Sidewall, $\delta_{v,p} = -20°$, and $\delta_{v,y} = 0°$

(a) Upper ramp

NPR	Static pressure ratios at x_r/l_r of—											
	−0.308	−0.170	−0.101	−0.032	0.037	0.106	0.175	0.244	0.382	0.520	0.659	0.797
2.01	0.860	0.649	0.581	0.485	0.245	0.376	0.391	0.407	0.451	0.484	0.505	0.508
2.50	0.860	0.649	0.575	0.484	0.237	0.185	0.292	0.323	0.350	0.376	0.419	0.438
3.01	0.860	0.649	0.575	0.484	0.235	0.185	0.186	0.170	0.288	0.310	0.339	0.365
3.50	0.860	0.649	0.576	0.483	0.234	0.185	0.184	0.170	0.157	0.246	0.285	0.356
4.00	0.860	0.649	0.576	0.483	0.235	0.185	0.183	0.169	0.138	0.221	0.231	0.278
5.01	0.860	0.648	0.575	0.483	0.234	0.184	0.182	0.169	0.138	0.119	0.094	0.157
6.00	0.860	0.648	0.575	0.482	0.233	0.183	0.180	0.169	0.138	0.119	0.094	0.076
7.00	0.859	0.647	0.575	0.482	0.233	0.183	0.179	0.168	0.138	0.119	0.094	0.076
8.00	0.859	0.647	0.575	0.482	0.232	0.182	0.178	0.168	0.138	0.119	0.094	0.076

(b) Lower flap

NPR	Static pressure ratios at x_r/l_r of—						
	−0.308	−0.170	−0.032	0.037	0.079	0.120	0.162
2.01	0.892	0.838	0.624	0.472	0.393	0.339	0.477
2.50	0.892	0.839	0.624	0.472	0.393	0.298	0.319
3.01	0.892	0.839	0.623	0.471	0.393	0.297	0.215
3.50	0.892	0.839	0.623	0.470	0.392	0.297	0.214
4.00	0.893	0.839	0.623	0.470	0.392	0.296	0.214
5.01	0.893	0.838	0.623	0.469	0.392	0.296	0.213
6.00	0.893	0.838	0.623	0.469	0.392	0.296	0.213
7.00	0.894	0.837	0.623	0.469	0.392	0.296	0.213
8.00	0.894	0.837	0.623	0.468	0.392	0.296	0.213

Table 120. Static Pressure Ratios for Nozzle 57. $x_r/l_r = 0.42$, $\theta = 30°$, $\phi = 0°$, Medium Sidewall, $\delta_{c,p} = -20°$, and $\delta_{c,y} = 0°$

(a) Upper ramp

NPR	Static pressure ratios at x_r/l_r of—											
	−0.308	−0.170	−0.101	−0.032	0.037	0.106	0.175	0.244	0.382	0.520	0.659	0.797
2.01	0.859	0.649	0.577	0.485	0.236	0.323	0.355	0.374	0.437	0.489	0.521	0.521
2.50	0.860	0.649	0.576	0.484	0.236	0.185	0.188	0.308	0.319	0.348	0.432	0.437
3.00	0.860	0.649	0.575	0.483	0.235	0.184	0.186	0.170	0.267	0.280	0.315	0.354
3.50	0.860	0.648	0.576	0.483	0.235	0.185	0.185	0.169	0.141	0.245	0.262	0.298
3.99	0.860	0.648	0.576	0.483	0.234	0.184	0.183	0.169	0.138	0.199	0.225	0.248
5.00	0.859	0.648	0.576	0.482	0.234	0.184	0.182	0.168	0.138	0.119	0.094	0.192
6.00	0.859	0.647	0.575	0.482	0.232	0.183	0.180	0.168	0.138	0.119	0.094	0.079
7.00	0.859	0.647	0.575	0.482	0.232	0.182	0.179	0.168	0.138	0.119	0.094	0.076
8.00	0.859	0.646	0.574	0.482	0.232	0.182	0.178	0.167	0.138	0.118	0.094	0.076

(b) Lower flap

NPR	Static pressure ratios at x_r/l_r of—						
	−0.308	−0.170	−0.032	0.037	0.079	0.120	0.162
2.01	0.892	0.838	0.623	0.472	0.393	0.334	0.476
2.50	0.892	0.839	0.624	0.471	0.393	0.297	0.318
3.00	0.892	0.839	0.623	0.471	0.392	0.296	0.215
3.50	0.892	0.839	0.623	0.470	0.392	0.296	0.214
3.99	0.893	0.839	0.623	0.470	0.391	0.295	0.214
5.00	0.893	0.838	0.623	0.469	0.392	0.295	0.214
6.00	0.893	0.838	0.623	0.469	0.392	0.295	0.213
7.00	0.893	0.837	0.623	0.468	0.392	0.295	0.213
8.00	0.894	0.837	0.623	0.468	0.392	0.295	0.213

Table 121. Static Pressure Ratios for Nozzle 58, $x_r/l_r = 0.42$, $\theta = 30°$, $\phi = 0°$, Maximum Sidewall, $\delta_{v,p} = -20°$, and $\delta_{v,y} = 0°$

(a) Upper ramp

NPR	Static pressure ratios at x_r/l_r of											
	−0.308	−0.170	−0.101	−0.032	0.037	0.106	0.175	0.244	0.382	0.520	0.659	0.797
2.01	0.860	0.649	0.578	0.485	0.238	0.308	0.348	0.368	0.437	0.502	0.535	0.526
2.50	0.860	0.649	0.577	0.484	0.239	0.184	0.188	0.310	0.326	0.341	0.395	0.438
3.00	0.860	0.649	0.577	0.484	0.237	0.184	0.186	0.170	0.273	0.290	0.301	0.331
3.50	0.860	0.649	0.576	0.483	0.237	0.184	0.185	0.169	0.139	0.238	0.258	0.287
4.00	0.860	0.649	0.576	0.483	0.236	0.184	0.184	0.168	0.139	0.150	0.229	0.257
5.00	0.860	0.648	0.576	0.483	0.236	0.183	0.182	0.168	0.138	0.119	0.095	0.192
6.00	0.859	0.647	0.575	0.482	0.235	0.182	0.180	0.167	0.138	0.119	0.094	0.083
7.00	0.859	0.647	0.575	0.482	0.235	0.182	0.179	0.167	0.138	0.119	0.094	0.076
8.00	0.859	0.646	0.575	0.482	0.234	0.182	0.179	0.167	0.138	0.119	0.094	0.076

(b) Lower flap

NPR	Static pressure ratios at x_r/l_r of						
	−0.308	−0.170	−0.032	0.037	0.079	0.120	0.162
2.01	0.892	0.838	0.623	0.471	0.393	0.337	0.477
2.50	0.892	0.839	0.624	0.471	0.392	0.296	0.317
3.00	0.892	0.839	0.623	0.471	0.392	0.296	0.215
3.50	0.892	0.839	0.623	0.470	0.391	0.295	0.214
4.00	0.892	0.839	0.623	0.470	0.391	0.295	0.214
5.00	0.893	0.838	0.623	0.469	0.391	0.295	0.213
6.00	0.893	0.838	0.623	0.468	0.391	0.295	0.213
7.00	0.894	0.837	0.623	0.468	0.391	0.295	0.213
8.00	0.894	0.837	0.623	0.468	0.391	0.294	0.213

Table 122. Static Pressure Ratios for Nozzle 59, $x_r/l_r = 0.20$, $\theta = 30°$, $\phi = 0°$, Minimum Sidewall, $\delta_{v,p} = -20°$, and $\delta_{v,y} = 0°$

(a) Upper ramp

NPR	Static pressure ratios at x_r/l_r of—											
	−0.308	−0.170	−0.101	−0.032	0.037	0.106	0.175	0.244	0.382	0.520	0.659	0.797
2.00	0.857	0.648	0.570	0.463	0.442	0.474	0.474	0.476	0.481	0.487	0.492	0.495
2.50	0.857	0.647	0.568	0.461	0.242	0.178	0.312	0.328	0.364	0.387	0.430	0.443
3.00	0.857	0.646	0.566	0.460	0.240	0.177	0.175	0.169	0.271	0.302	0.369	0.372
3.50	0.857	0.645	0.567	0.460	0.241	0.178	0.173	0.169	0.245	0.276	0.310	0.316
4.00	0.856	0.645	0.566	0.459	0.238	0.177	0.172	0.168	0.130	0.231	0.268	0.287
5.00	0.856	0.644	0.565	0.457	0.238	0.176	0.170	0.168	0.129	0.112	0.161	0.222
6.00	0.856	0.642	0.565	0.457	0.238	0.175	0.168	0.167	0.129	0.112	0.095	0.164
7.00	0.855	0.642	0.564	0.456	0.237	0.175	0.167	0.166	0.128	0.111	0.095	0.077
8.01	0.855	0.641	0.563	0.455	0.235	0.174	0.166	0.166	0.128	0.111	0.095	0.077

(b) Lower flap

NPR	Static pressure ratios at x_r/l_r of—						
	−0.308	−0.170	−0.032	0.037	0.079	0.120	0.162
2.00	0.893	0.841	0.624	0.472	0.392	0.347	0.477
2.50	0.893	0.842	0.624	0.472	0.392	0.297	0.338
3.00	0.893	0.842	0.623	0.471	0.392	0.296	0.216
3.50	0.893	0.842	0.624	0.471	0.391	0.296	0.214
4.00	0.893	0.842	0.623	0.470	0.391	0.295	0.214
5.00	0.894	0.841	0.623	0.469	0.391	0.295	0.213
6.00	0.894	0.841	0.623	0.469	0.391	0.295	0.213
7.00	0.894	0.840	0.623	0.469	0.391	0.295	0.213
8.01	0.894	0.839	0.623	0.468	0.391	0.295	0.213

Table 123. Static Pressure Ratios for Nozzle 60, $x_r/l_r = 0.20$, $\theta = 30°$, $\phi = 0°$, Medium Sidewall, $\delta_{v,p} = -20°$, and $\delta_{v,y} = 0°$

(a) Upper ramp

NPR	Static pressure ratios at x_r/l_r of—											
	−0.308	−0.170	−0.101	−0.032	0.037	0.106	0.175	0.244	0.382	0.520	0.659	0.797
2.00	0.857	0.648	0.568	0.462	0.455	0.480	0.482	0.483	0.486	0.490	0.493	0.496
2.50	0.857	0.647	0.568	0.461	0.237	0.176	0.306	0.324	0.345	0.361	0.391	0.414
3.00	0.857	0.646	0.567	0.460	0.238	0.176	0.174	0.170	0.297	0.316	0.326	0.334
3.50	0.857	0.645	0.567	0.459	0.238	0.176	0.172	0.169	0.226	0.263	0.286	0.297
4.00	0.856	0.645	0.567	0.458	0.238	0.176	0.171	0.169	0.130	0.233	0.258	0.271
5.00	0.856	0.644	0.566	0.457	0.237	0.175	0.169	0.168	0.129	0.112	0.170	0.217
6.00	0.856	0.643	0.565	0.456	0.236	0.174	0.167	0.168	0.129	0.111	0.095	0.169
7.00	0.855	0.642	0.564	0.455	0.235	0.173	0.166	0.167	0.128	0.111	0.095	0.077
8.01	0.855	0.641	0.563	0.454	0.234	0.173	0.165	0.167	0.128	0.111	0.094	0.077

(b) Lower flap

NPR	Static pressure ratios at x_r/l_r of—						
	−0.308	−0.170	−0.032	0.037	0.079	0.120	0.162
2.00	0.893	0.840	0.624	0.472	0.392	0.349	0.478
2.50	0.893	0.841	0.623	0.471	0.392	0.297	0.326
3.00	0.893	0.841	0.623	0.471	0.391	0.296	0.215
3.50	0.893	0.842	0.623	0.470	0.391	0.296	0.214
4.00	0.893	0.841	0.623	0.470	0.391	0.295	0.213
5.00	0.894	0.841	0.623	0.469	0.391	0.295	0.213
6.00	0.894	0.840	0.623	0.469	0.391	0.295	0.213
7.00	0.894	0.840	0.623	0.469	0.391	0.295	0.212
8.01	0.894	0.839	0.623	0.468	0.391	0.295	0.213

Table 124. Static Pressure Ratios for Nozzle 61, $x_r/l_r = 0.20$, $\theta = 30°$, $\phi = 0°$, Maximum Sidewall, $\delta_{v,p} = -20°$, and $\delta_{v,y} = 0°$

(a) Upper ramp

NPR	Static pressure ratios at x_r/l_r of—											
	−0.308	−0.170	−0.101	−0.032	0.037	0.106	0.175	0.244	0.382	0.520	0.659	0.797
2.00	0.857	0.648	0.570	0.462	0.442	0.473	0.477	0.478	0.482	0.486	0.490	0.493
2.51	0.857	0.647	0.567	0.461	0.237	0.175	0.298	0.334	0.353	0.371	0.393	0.407
3.00	0.857	0.646	0.567	0.460	0.237	0.176	0.174	0.170	0.295	0.313	0.324	0.335
3.50	0.856	0.645	0.566	0.459	0.237	0.176	0.172	0.169	0.226	0.270	0.294	0.299
4.00	0.856	0.645	0.566	0.458	0.237	0.176	0.171	0.169	0.130	0.229	0.259	0.271
5.00	0.856	0.643	0.565	0.456	0.235	0.175	0.168	0.168	0.129	0.112	0.169	0.216
6.00	0.856	0.642	0.564	0.455	0.235	0.174	0.167	0.167	0.129	0.111	0.095	0.169
7.00	0.855	0.641	0.563	0.454	0.234	0.173	0.166	0.167	0.128	0.111	0.094	0.077
8.00	0.854	0.640	0.562	0.454	0.233	0.173	0.165	0.166	0.128	0.111	0.095	0.077

(b) Lower flap

NPR	Static pressure ratios at x_r/l_r of—						
	−0.308	−0.170	−0.032	0.037	0.079	0.120	0.162
2.00	0.893	0.841	0.624	0.472	0.392	0.346	0.478
2.51	0.892	0.841	0.624	0.472	0.392	0.297	0.328
3.00	0.893	0.842	0.624	0.471	0.392	0.296	0.216
3.50	0.893	0.842	0.624	0.470	0.391	0.296	0.214
4.00	0.893	0.842	0.624	0.470	0.391	0.295	0.214
5.00	0.894	0.841	0.624	0.470	0.391	0.295	0.214
6.00	0.894	0.841	0.624	0.469	0.391	0.295	0.214
7.00	0.894	0.840	0.623	0.469	0.391	0.295	0.213
8.00	0.894	0.839	0.623	0.468	0.391	0.295	0.213

Table 125. Static Pressure Ratios for Nozzle 62, $x_r/l_r = 0.02$, $\theta = 30°$, $\phi = 0°$, Minimum Sidewall, $\delta_{v,p} = -20°$, and $\delta_{v,y} = 0°$

(a) Upper ramp

NPR	Static pressure ratios at x_r/l_r of—											
	−0.308	−0.170	−0.101	−0.032	0.037	0.106	0.175	0.244	0.382	0.520	0.659	0.797
2.00	0.845	0.642	0.577	0.449	0.263	0.392	0.407	0.428	0.475	0.507	0.521	0.521
2.50	0.845	0.642	0.576	0.446	0.234	0.183	0.296	0.320	0.379	0.425	0.427	0.416
3.00	0.844	0.642	0.576	0.445	0.234	0.183	0.172	0.168	0.294	0.357	0.363	0.341
3.50	0.843	0.643	0.576	0.443	0.231	0.182	0.170	0.166	0.248	0.304	0.329	0.301
4.00	0.843	0.643	0.576	0.443	0.231	0.182	0.169	0.165	0.130	0.243	0.286	0.282
5.00	0.842	0.642	0.576	0.441	0.229	0.181	0.166	0.164	0.129	0.112	0.214	0.222
6.00	0.842	0.642	0.576	0.439	0.227	0.180	0.165	0.163	0.128	0.111	0.089	0.187
8.00	0.840	0.641	0.576	0.438	0.226	0.179	0.163	0.162	0.128	0.111	0.089	0.076

(b) Lower flap

NPR	Static pressure ratios at x_r/l_r of—						
	−0.308	−0.170	−0.032	0.037	0.079	0.120	0.162
2.00	0.893	0.828	0.618	0.478	0.383	0.362	0.480
2.50	0.893	0.828	0.618	0.477	0.383	0.298	0.330
3.00	0.892	0.828	0.618	0.477	0.383	0.297	0.227
3.50	0.893	0.829	0.617	0.477	0.382	0.297	0.226
4.00	0.894	0.829	0.617	0.477	0.382	0.297	0.226
5.00	0.894	0.828	0.617	0.477	0.382	0.296	0.225
6.00	0.894	0.828	0.617	0.477	0.382	0.296	0.224
8.00	0.894	0.828	0.618	0.478	0.382	0.296	0.223

Table 126. Static Pressure Ratios for Nozzle 63, $x_r/l_r = 0.02$, $\theta = 30°$, $\phi = 0°$, Medium Sidewall, $\delta_{v,p} = -20°$, and $\delta_{v,y} = 0°$

(a) Upper ramp

NPR	Static pressure ratios at x_r/l_r of—											
	−0.308	−0.170	−0.101	−0.032	0.037	0.106	0.175	0.244	0.382	0.520	0.659	0.797
2.00	0.845	0.643	0.577	0.449	0.264	0.395	0.411	0.432	0.477	0.508	0.519	0.519
2.50	0.844	0.643	0.577	0.446	0.234	0.182	0.313	0.330	0.392	0.425	0.426	0.416
3.00	0.844	0.643	0.576	0.444	0.234	0.183	0.173	0.169	0.297	0.354	0.356	0.343
3.50	0.843	0.643	0.576	0.443	0.232	0.183	0.171	0.166	0.246	0.304	0.321	0.297
4.00	0.843	0.642	0.576	0.442	0.230	0.182	0.169	0.166	0.130	0.251	0.280	0.278
5.00	0.842	0.642	0.576	0.441	0.228	0.181	0.167	0.164	0.129	0.112	0.218	0.216
6.00	0.841	0.641	0.575	0.440	0.227	0.180	0.165	0.163	0.128	0.112	0.090	0.187
8.00	0.840	0.640	0.575	0.437	0.226	0.179	0.163	0.162	0.128	0.111	0.089	0.076

(b) Lower flap

NPR	Static pressure ratios at x_r/l_r of—						
	−0.308	−0.170	−0.032	0.037	0.079	0.120	0.162
2.00	0.893	0.828	0.617	0.477	0.383	0.368	0.480
2.50	0.892	0.828	0.617	0.477	0.383	0.298	0.329
3.00	0.892	0.828	0.617	0.477	0.383	0.297	0.227
3.50	0.893	0.828	0.617	0.477	0.382	0.297	0.226
4.00	0.893	0.829	0.617	0.477	0.382	0.297	0.226
5.00	0.893	0.828	0.617	0.477	0.382	0.296	0.225
6.00	0.894	0.828	0.617	0.477	0.382	0.296	0.224
8.00	0.894	0.828	0.617	0.477	0.382	0.296	0.223

Table 127. Static Pressure Ratios for Nozzle 64, $x_r/l_r = 0.02$, $\theta = 30°$, $\phi = 0°$, Maximum Sidewall, $\delta_{v,p} = -20°$, and $\delta_{v,y} = 0°$

(a) Upper ramp

NPR	Static pressure ratios at x_r/l_r of—											
	−0.308	−0.170	−0.101	−0.032	0.037	0.106	0.175	0.244	0.382	0.520	0.659	0.797
2.00	0.846	0.645	0.580	0.450	0.254	0.390	0.411	0.434	0.483	0.509	0.518	0.517
2.50	0.845	0.645	0.578	0.447	0.237	0.185	0.297	0.321	0.372	0.420	0.421	0.413
3.00	0.845	0.645	0.576	0.446	0.234	0.184	0.174	0.169	0.298	0.355	0.358	0.342
3.51	0.844	0.644	0.576	0.444	0.232	0.183	0.172	0.167	0.245	0.300	0.321	0.295
4.00	0.844	0.644	0.577	0.444	0.231	0.182	0.170	0.166	0.129	0.255	0.277	0.274
5.00	0.843	0.644	0.577	0.442	0.229	0.182	0.168	0.165	0.129	0.110	0.215	0.215
6.01	0.842	0.643	0.576	0.441	0.228	0.180	0.166	0.164	0.128	0.110	0.086	0.185
8.00	0.841	0.642	0.576	0.440	0.226	0.180	0.164	0.163	0.128	0.109	0.086	0.075

(b) Lower flap

NPR	Static pressure ratios at x_r/l_r of—						
	−0.308	−0.170	−0.032	0.037	0.079	0.120	0.162
2.00	0.893	0.829	0.618	0.478	0.384	0.361	0.481
2.50	0.893	0.829	0.618	0.477	0.383	0.298	0.336
3.00	0.893	0.829	0.617	0.477	0.383	0.297	0.228
3.51	0.893	0.829	0.617	0.477	0.382	0.297	0.227
4.00	0.894	0.830	0.617	0.477	0.382	0.296	0.226
5.00	0.894	0.829	0.617	0.477	0.382	0.296	0.225
6.01	0.894	0.829	0.617	0.477	0.382	0.296	0.225
8.00	0.894	0.828	0.618	0.478	0.382	0.296	0.224

Table 128. Static Pressure Ratios for Nozzle 69, $x_r/l_r = 0.42$, $\theta = 30°$, $\phi = 0°$, Maximum Sidewall, $\delta_{r,p} = -20°$, and $\delta_{r,y} = -30°$

(a) Upper ramp

NPR	Static pressure ratios at x_r/l_r of—											
	−0.308	−0.170	−0.101	−0.032	0.037	0.106	0.175	0.244	0.382	0.520	0.659	0.797
2.00	0.860	0.649	0.582	0.485	0.255	0.387	0.403	0.425	0.452	0.481	0.508	0.510
2.50	0.860	0.649	0.577	0.484	0.237	0.184	0.309	0.332	0.345	0.389	0.452	0.457
3.00	0.860	0.649	0.576	0.484	0.236	0.185	0.186	0.212	0.304	0.313	0.351	0.400
3.50	0.860	0.649	0.576	0.483	0.235	0.184	0.184	0.171	0.263	0.274	0.311	0.416
4.00	0.860	0.649	0.575	0.483	0.234	0.184	0.183	0.170	0.139	0.252	0.263	0.425
5.00	0.860	0.648	0.575	0.482	0.234	0.183	0.182	0.169	0.138	0.126	0.191	0.239
6.00	0.859	0.647	0.575	0.482	0.233	0.183	0.180	0.169	0.138	0.119	0.183	0.120
7.00	0.859	0.647	0.574	0.482	0.232	0.182	0.179	0.168	0.138	0.119	0.179	0.118
8.00	0.859	0.646	0.574	0.482	0.231	0.182	0.178	0.168	0.138	0.118	0.178	0.116

(b) Lower flap

NPR	Static pressure ratios at x_r/l_r of—						
	−0.308	−0.170	−0.032	0.037	0.079	0.120	0.162
2.00	0.893	0.838	0.624	0.472	0.393	0.340	0.479
2.50	0.892	0.839	0.624	0.471	0.393	0.298	0.319
3.00	0.892	0.839	0.623	0.471	0.392	0.297	0.214
3.50	0.892	0.839	0.623	0.470	0.391	0.297	0.213
4.00	0.893	0.838	0.623	0.470	0.391	0.296	0.213
5.00	0.893	0.838	0.623	0.469	0.391	0.296	0.212
6.00	0.893	0.838	0.623	0.469	0.391	0.296	0.212
7.00	0.893	0.837	0.623	0.468	0.391	0.296	0.212
8.00	0.893	0.837	0.623	0.468	0.391	0.296	0.212

Table 129. Static Pressure Ratios for Nozzle 70, $x_r/l_r = 0.20$, $\theta = 30°$, $\phi = 0°$, Medium Sidewall, $\delta_{v,p} = -20°$, and $\delta_{v,y} = -30°$

(a) Upper ramp

NPR	Static pressure ratios at x_r/l_r of −											
	−0.308	−0.170	−0.101	−0.032	0.037	0.106	0.175	0.244	0.382	0.520	0.659	0.797
2.00	0.858	0.648	0.573	0.464	0.262	0.396	0.416	0.435	0.438	0.453	0.542	0.537
2.50	0.857	0.647	0.568	0.462	0.243	0.178	0.266	0.331	0.373	0.424	0.485	0.435
3.00	0.857	0.646	0.568	0.461	0.242	0.178	0.175	0.170	0.323	0.347	0.406	0.396
3.50	0.857	0.645	0.567	0.460	0.241	0.177	0.173	0.169	0.247	0.291	0.372	0.401
4.00	0.857	0.645	0.567	0.459	0.241	0.177	0.172	0.168	0.230	0.184	0.316	0.420
5.00	0.856	0.644	0.567	0.458	0.240	0.176	0.169	0.168	0.225	0.176	0.144	0.172
6.01	0.856	0.643	0.565	0.457	0.238	0.175	0.168	0.167	0.223	0.174	0.139	0.140
7.00	0.855	0.642	0.564	0.456	0.238	0.174	0.166	0.166	0.223	0.174	0.137	0.137
8.00	0.855	0.641	0.563	0.455	0.237	0.174	0.165	0.166	0.222	0.173	0.137	0.136

(b) Lower flap

NPR	Static pressure ratios at x_r/l_r of −						
	−0.308	−0.170	−0.032	0.037	0.079	0.120	0.162
2.00	0.893	0.841	0.624	0.472	0.392	0.343	0.476
2.50	0.893	0.842	0.624	0.471	0.392	0.297	0.331
3.00	0.893	0.842	0.624	0.471	0.392	0.296	0.215
3.50	0.893	0.842	0.623	0.471	0.391	0.296	0.214
4.00	0.894	0.842	0.624	0.470	0.391	0.295	0.214
5.00	0.894	0.841	0.624	0.470	0.391	0.295	0.214
6.01	0.894	0.841	0.623	0.469	0.391	0.295	0.213
7.00	0.894	0.840	0.623	0.469	0.391	0.295	0.213
8.00	0.894	0.839	0.623	0.468	0.391	0.295	0.213

Table 130. Static Pressure Ratios for Nozzle 71, $x_r/l_r = 0.20$, $\theta = 30°$, $\phi = 0°$, Maximum Sidewall, $\delta_{v,p} = -20°$, and $\delta_{v,y} = -30°$

(a) Upper ramp

NPR	Static pressure ratios at x_r/l_r of—											
	−0.308	−0.170	−0.101	−0.032	0.037	0.106	0.175	0.244	0.382	0.520	0.659	0.797
2.00	0.858	0.649	0.572	0.464	0.255	0.389	0.410	0.427	0.442	0.491	0.626	0.555
2.50	0.857	0.647	0.569	0.462	0.242	0.178	0.306	0.336	0.378	0.452	0.568	0.469
3.00	0.857	0.646	0.568	0.461	0.242	0.178	0.175	0.204	0.337	0.373	0.556	0.456
3.50	0.857	0.645	0.567	0.460	0.240	0.177	0.173	0.170	0.284	0.337	0.488	0.457
4.00	0.857	0.645	0.566	0.459	0.240	0.177	0.172	0.169	0.230	0.256	0.395	0.466
5.00	0.856	0.644	0.566	0.458	0.239	0.176	0.169	0.168	0.225	0.179	0.174	0.265
6.00	0.856	0.643	0.565	0.457	0.238	0.175	0.168	0.167	0.224	0.177	0.164	0.234
7.00	0.855	0.642	0.565	0.456	0.237	0.175	0.167	0.166	0.223	0.176	0.160	0.226
8.00	0.855	0.641	0.564	0.455	0.237	0.174	0.166	0.166	0.223	0.175	0.159	0.222

(b) Lower flap

NPR	Static pressure ratios at x_r/l_r of—						
	−0.308	−0.170	−0.032	0.037	0.079	0.120	0.162
2.00	0.893	0.841	0.624	0.472	0.392	0.347	0.477
2.50	0.893	0.842	0.624	0.472	0.392	0.297	0.331
3.00	0.893	0.842	0.624	0.471	0.392	0.296	0.216
3.50	0.893	0.842	0.623	0.470	0.391	0.296	0.214
4.00	0.893	0.841	0.623	0.470	0.391	0.296	0.214
5.00	0.894	0.841	0.623	0.469	0.391	0.295	0.214
6.00	0.894	0.840	0.623	0.469	0.391	0.295	0.214
7.00	0.894	0.840	0.623	0.469	0.391	0.295	0.214
8.00	0.894	0.839	0.623	0.468	0.391	0.295	0.213

Table 131. Static Pressure Ratios for Nozzle 72. $x_r/l_r = 0.02$, $\theta = 30°$, $o = 0°$, Minimum Sidewall, $\delta_{r,p} = -20°$, and $\delta_{r,y} = -30°$

(a) Upper ramp

NPR	Static pressure ratios at x_r/l_r of −											
	−0.308	−0.170	−0.101	−0.032	0.037	0.106	0.175	0.241	0.382	0.520	0.659	0.797
2.01	0.853	0.658	0.591	0.458	0.255	0.393	0.416	0.445	0.501	0.518	0.515	0.507
2.50	0.852	0.659	0.593	0.456	0.246	0.195	0.344	0.363	0.414	0.428	0.443	0.396
3.00	0.851	0.658	0.592	0.454	0.243	0.194	0.190	0.278	0.305	0.438	0.341	0.328
3.50	0.851	0.658	0.592	0.453	0.242	0.194	0.188	0.261	0.224	0.336	0.457	0.304
4.00	0.850	0.658	0.592	0.451	0.240	0.193	0.186	0.261	0.224	0.166	0.324	0.420
5.00	0.849	0.657	0.592	0.450	0.239	0.192	0.184	0.260	0.225	0.164	0.131	0.181
6.00	0.849	0.657	0.592	0.449	0.237	0.191	0.182	0.260	0.225	0.164	0.108	0.142
8.00	0.847	0.655	0.592	0.447	0.235	0.190	0.180	0.259	0.226	0.163	0.108	0.078

(b) Lower flap

NPR	Static pressure ratios at x_r/l_r of −						
	−0.308	−0.170	−0.032	0.037	0.079	0.120	0.162
2.01	0.898	0.836	0.631	0.491	0.400	0.318	0.477
2.50	0.898	0.836	0.631	0.491	0.400	0.313	0.247
3.00	0.898	0.836	0.631	0.490	0.399	0.312	0.242
3.50	0.898	0.836	0.631	0.491	0.399	0.312	0.242
4.00	0.898	0.836	0.631	0.491	0.399	0.312	0.241
5.00	0.899	0.836	0.631	0.491	0.399	0.311	0.240
6.00	0.899	0.835	0.631	0.491	0.399	0.311	0.239
8.00	0.899	0.835	0.631	0.491	0.399	0.311	0.238

Table 132. Static Pressure Ratios for Nozzle 73, $x_r/l_r = 0.02$, $\theta = 30°$, $\phi = 0°$, Medium Sidewall, $\delta_{v,p} = -20°$, and $\delta_{v,y} = -30°$

(a) Upper ramp

NPR	Static pressure ratios at x_r/l_r of—											
	−0.308	−0.170	−0.101	−0.032	0.037	0.106	0.175	0.244	0.382	0.520	0.659	0.797
2.00	0.853	0.658	0.592	0.459	0.253	0.388	0.415	0.449	0.524	0.530	0.523	0.508
2.50	0.852	0.659	0.591	0.456	0.245	0.195	0.343	0.358	0.427	0.427	0.453	0.396
3.00	0.851	0.658	0.592	0.454	0.244	0.194	0.189	0.280	0.321	0.454	0.348	0.323
3.50	0.851	0.658	0.592	0.453	0.243	0.195	0.188	0.263	0.259	0.291	0.444	0.294
4.00	0.850	0.658	0.592	0.452	0.241	0.193	0.186	0.262	0.259	0.251	0.218	0.411
5.00	0.849	0.658	0.592	0.450	0.238	0.192	0.184	0.261	0.259	0.250	0.167	0.181
6.00	0.849	0.657	0.592	0.449	0.237	0.192	0.182	0.261	0.259	0.250	0.163	0.144
8.00	0.848	0.656	0.592	0.447	0.236	0.191	0.180	0.260	0.260	0.249	0.162	0.095

(b) Lower flap

NPR	Static pressure ratios at x_r/l_r of—						
	−0.308	−0.170	−0.032	0.037	0.079	0.120	0.162
2.00	0.898	0.836	0.631	0.491	0.400	0.319	0.479
2.50	0.898	0.836	0.631	0.491	0.400	0.313	0.247
3.00	0.898	0.836	0.631	0.491	0.400	0.312	0.242
3.50	0.898	0.836	0.631	0.491	0.400	0.312	0.241
4.00	0.898	0.836	0.631	0.491	0.400	0.312	0.241
5.00	0.899	0.836	0.631	0.491	0.400	0.312	0.240
6.00	0.899	0.836	0.631	0.491	0.400	0.311	0.239
8.00	0.899	0.835	0.631	0.492	0.400	0.311	0.238

Table 133. Static Pressure Ratios for Nozzle 74, $x_r/l_r = 0.02$, $\theta = 30°$, $\phi = 0°$, Maximum Sidewall, $\delta_{v,p} = -20°$, and $\delta_{v,y} = -30°$

(a) Upper ramp

NPR	Static pressure ratios at x_r/l_r of—											
	−0.308	−0.170	−0.101	−0.032	0.037	0.106	0.175	0.244	0.382	0.520	0.659	0.797
2.00	0.853	0.658	0.593	0.458	0.259	0.401	0.425	0.455	0.539	0.580	0.570	0.515
2.50	0.852	0.658	0.593	0.456	0.247	0.196	0.270	0.350	0.516	0.542	0.514	0.449
3.00	0.851	0.658	0.592	0.454	0.244	0.195	0.189	0.314	0.336	0.492	0.488	0.427
3.50	0.851	0.658	0.592	0.453	0.242	0.194	0.187	0.262	0.258	0.425	0.507	0.431
4.01	0.850	0.658	0.591	0.452	0.240	0.193	0.186	0.262	0.258	0.251	0.339	0.438
5.01	0.849	0.657	0.591	0.450	0.239	0.192	0.184	0.260	0.258	0.250	0.230	0.220
6.00	0.849	0.657	0.592	0.449	0.238	0.192	0.182	0.260	0.258	0.250	0.230	0.219
7.27	0.848	0.656	0.592	0.448	0.236	0.191	0.181	0.259	0.258	0.249	0.229	0.218

(b) Lower flap

NPR	Static pressure ratios at x_r/l_r of—						
	−0.308	−0.170	−0.032	0.037	0.079	0.120	0.162
2.00	0.898	0.835	0.630	0.491	0.400	0.319	0.478
2.50	0.898	0.836	0.630	0.491	0.400	0.313	0.247
3.00	0.898	0.836	0.630	0.491	0.400	0.312	0.242
3.50	0.898	0.836	0.630	0.491	0.399	0.312	0.241
4.01	0.898	0.836	0.630	0.491	0.399	0.311	0.240
5.01	0.899	0.836	0.630	0.491	0.399	0.311	0.239
6.00	0.899	0.835	0.630	0.491	0.399	0.311	0.239
7.27	0.899	0.835	0.630	0.491	0.399	0.311	0.238

Table 134. Static Pressure Ratios for Nozzle 75, $x_r/l_r = 1.00$, $\theta = 0°$, $\phi = 0°$, Minimum Sidewall, $\delta_{v,p} = 20°$, and $\delta_{v,y} = 0°$

(a) Upper ramp

NPR	Static pressure ratios at x_r/l_r of—								
	−0.170	−0.032	0.106	0.175	0.244	0.382	0.520	0.659	0.797
2.00	0.729	0.796	0.750	0.688	0.637	0.548	0.550	0.533	0.515
2.50	0.728	0.795	0.749	0.685	0.632	0.471	0.417	0.379	0.511
3.00	0.727	0.795	0.750	0.684	0.631	0.471	0.336	0.298	0.276
3.50	0.726	0.795	0.749	0.684	0.629	0.470	0.331	0.238	0.222
4.00	0.726	0.795	0.750	0.683	0.630	0.470	0.329	0.211	0.179
5.01	0.725	0.794	0.750	0.683	0.630	0.470	0.328	0.210	0.143
6.00	0.724	0.794	0.750	0.682	0.630	0.470	0.328	0.209	0.143
7.00	0.723	0.793	0.750	0.682	0.631	0.470	0.327	0.209	0.143
7.99	0.723	0.793	0.750	0.682	0.631	0.470	0.327	0.209	0.143

(b) Lower flap

NPR	Static pressure ratios at x_r/l_r of—						
	−0.308	−0.170	−0.032	0.037	0.079	0.120	0.162
2.00	0.907	0.859	0.708	0.657	0.591	0.545	0.489
2.50	0.907	0.858	0.705	0.656	0.588	0.542	0.486
3.00	0.907	0.858	0.704	0.655	0.587	0.542	0.485
3.50	0.907	0.858	0.703	0.655	0.587	0.541	0.485
4.00	0.908	0.857	0.702	0.655	0.587	0.541	0.485
5.01	0.908	0.857	0.701	0.655	0.586	0.540	0.484
6.00	0.908	0.856	0.700	0.654	0.585	0.540	0.484
7.00	0.908	0.856	0.700	0.653	0.585	0.540	0.483
7.99	0.908	0.855	0.699	0.653	0.584	0.539	0.483

Table 135. Static Pressure Ratios for Nozzle 76, $x_r/l_r = 1.00$, $\theta = 0°$, $\phi = 0°$, Medium Sidewall, $\delta_{v,p} = 20°$, and $\delta_{v,y} = 0°$

(a) Upper ramp

NPR	Static pressure ratios at x_r/l_r of—								
	−0.170	−0.032	0.106	0.175	0.244	0.382	0.520	0.659	0.797
2.00	0.729	0.796	0.751	0.689	0.643	0.552	0.550	0.531	0.514
2.50	0.727	0.795	0.747	0.685	0.633	0.471	0.421	0.404	0.460
3.00	0.726	0.795	0.750	0.685	0.636	0.471	0.338	0.302	0.302
3.50	0.726	0.795	0.749	0.685	0.634	0.471	0.332	0.243	0.231
4.01	0.726	0.795	0.749	0.684	0.635	0.471	0.331	0.214	0.188
5.00	0.725	0.794	0.750	0.684	0.635	0.470	0.330	0.213	0.147
6.00	0.724	0.794	0.750	0.684	0.635	0.470	0.329	0.212	0.147
7.00	0.723	0.793	0.750	0.683	0.635	0.470	0.329	0.212	0.147
7.21	0.723	0.793	0.750	0.683	0.635	0.470	0.329	0.212	0.147

(b) Lower flap

NPR	Static pressure ratios at x_r/l_r of—						
	−0.308	−0.170	−0.032	0.037	0.079	0.120	0.162
2.00	0.906	0.859	0.710	0.656	0.591	0.543	0.482
2.50	0.905	0.858	0.707	0.654	0.587	0.540	0.478
3.00	0.905	0.857	0.706	0.653	0.587	0.540	0.478
3.50	0.905	0.857	0.704	0.653	0.587	0.539	0.477
4.01	0.906	0.857	0.704	0.653	0.586	0.539	0.477
5.00	0.906	0.856	0.702	0.652	0.585	0.538	0.476
6.00	0.906	0.856	0.702	0.651	0.585	0.538	0.476
7.00	0.906	0.855	0.701	0.651	0.584	0.537	0.475
7.21	0.906	0.855	0.701	0.651	0.584	0.537	0.474

Table 136. Static Pressure Ratios for Nozzle 77, $x_r/l_r = 1.00$, $\theta = 0°$, $\phi = 0°$, Maximum Sidewall, $\delta_{v,p} = 20°$, and $\delta_{v,y} = 0°$

(a) Upper ramp

NPR	Static pressure ratios at x_r/l_r of—								
	−0.170	−0.032	0.106	0.175	0.244	0.382	0.520	0.659	0.797
2.00	0.731	0.797	0.751	0.690	0.643	0.552	0.551	0.533	0.514
2.50	0.730	0.796	0.749	0.686	0.635	0.471	0.420	0.404	0.460
3.00	0.729	0.796	0.749	0.686	0.636	0.471	0.337	0.302	0.301
3.50	0.729	0.796	0.750	0.686	0.635	0.471	0.331	0.242	0.231
3.90	0.728	0.796	0.750	0.686	0.635	0.470	0.330	0.214	0.196
4.00	0.728	0.796	0.751	0.686	0.636	0.471	0.330	0.213	0.188
5.00	0.727	0.795	0.751	0.685	0.636	0.471	0.329	0.212	0.147
6.01	0.726	0.795	0.751	0.685	0.636	0.471	0.328	0.211	0.147
7.00	0.725	0.794	0.750	0.684	0.636	0.471	0.328	0.211	0.147

(b) Lower flap

NPR	Static pressure ratios at x_r/l_r of—						
	−0.308	−0.170	−0.032	0.037	0.079	0.120	0.162
2.00	0.906	0.859	0.711	0.657	0.592	0.544	0.482
2.50	0.905	0.858	0.707	0.655	0.589	0.541	0.479
3.00	0.905	0.858	0.706	0.655	0.588	0.541	0.479
3.50	0.906	0.858	0.705	0.654	0.588	0.540	0.478
3.90	0.906	0.858	0.705	0.654	0.588	0.540	0.478
4.00	0.906	0.858	0.705	0.654	0.588	0.540	0.478
5.00	0.906	0.857	0.704	0.653	0.587	0.539	0.477
6.01	0.907	0.856	0.703	0.653	0.586	0.539	0.476
7.00	0.907	0.856	0.702	0.652	0.586	0.538	0.475

Table 137. Static Pressure Ratios for Nozzle 78, $x_r/l_r = 0.42$, $\theta = 20°$, $\phi = 0°$, Minimum Sidewall, $\delta_{v,p} = 20°$, and $\delta_{v,y} = 0°$

(a) Upper ramp

NPR	Static pressure ratios at x_r/l_r of—								
	−0.170	−0.032	0.106	0.175	0.244	0.382	0.520	0.659	0.797
2.00	0.864	0.732	0.738	0.795	0.824	0.757	0.691	0.631	0.553
2.50	0.863	0.731	0.735	0.794	0.821	0.756	0.686	0.623	0.480
3.00	0.862	0.731	0.735	0.794	0.820	0.756	0.684	0.623	0.480
3.50	0.862	0.730	0.735	0.794	0.820	0.756	0.682	0.623	0.480
4.00	0.861	0.730	0.735	0.794	0.821	0.756	0.682	0.623	0.480
5.00	0.860	0.729	0.735	0.793	0.821	0.756	0.680	0.624	0.481
6.00	0.860	0.729	0.734	0.793	0.822	0.757	0.680	0.624	0.481
7.00	0.859	0.728	0.734	0.792	0.823	0.757	0.679	0.625	0.482
7.89	0.859	0.728	0.734	0.792	0.823	0.756	0.679	0.625	0.482

(b) Lower flap

NPR	Static pressure ratios at x_r/l_r of—						
	−0.308	−0.170	−0.032	0.037	0.079	0.120	0.162
2.00	0.906	0.861	0.710	0.655	0.589	0.542	0.478
2.50	0.905	0.861	0.707	0.653	0.587	0.539	0.475
3.00	0.906	0.860	0.706	0.652	0.586	0.538	0.474
3.50	0.906	0.860	0.705	0.652	0.586	0.538	0.474
4.00	0.906	0.860	0.704	0.652	0.585	0.538	0.473
5.00	0.906	0.860	0.703	0.651	0.585	0.537	0.472
6.00	0.907	0.859	0.702	0.651	0.584	0.537	0.472
7.00	0.907	0.858	0.702	0.650	0.583	0.536	0.472
7.89	0.907	0.858	0.701	0.649	0.584	0.536	0.471

Table 138. Static Pressure Ratios for Nozzle 79, $x_r/l_r = 0.42$, $\theta = 20°$, $\phi = 0°$, Medium Sidewall, $\delta_{v,p} = 20°$, and $\delta_{v,y} = 0°$

(a) Upper ramp

NPR	Static pressure ratios at x_r/l_r of—								
	−0.170	−0.032	0.106	0.175	0.244	0.382	0.520	0.659	0.797
2.00	0.864	0.732	0.737	0.795	0.822	0.758	0.692	0.632	0.557
2.50	0.862	0.730	0.734	0.794	0.819	0.755	0.685	0.623	0.480
3.00	0.862	0.730	0.734	0.794	0.820	0.756	0.684	0.622	0.480
3.50	0.861	0.730	0.734	0.793	0.820	0.756	0.682	0.623	0.480
4.00	0.861	0.729	0.735	0.793	0.820	0.756	0.682	0.623	0.480
5.00	0.860	0.729	0.734	0.793	0.820	0.756	0.681	0.624	0.481
6.00	0.859	0.728	0.734	0.792	0.821	0.756	0.680	0.624	0.482
7.01	0.859	0.727	0.734	0.792	0.822	0.757	0.679	0.625	0.483
7.41	0.859	0.727	0.733	0.792	0.823	0.757	0.679	0.625	0.483

(b) Lower flap

NPR	Static pressure ratios at x_r/l_r of—						
	−0.308	−0.170	−0.032	0.037	0.079	0.120	0.162
2.00	0.906	0.861	0.710	0.655	0.591	0.542	0.479
2.50	0.905	0.860	0.706	0.652	0.587	0.539	0.475
3.00	0.905	0.860	0.705	0.652	0.587	0.538	0.474
3.50	0.905	0.860	0.704	0.652	0.587	0.538	0.474
4.00	0.906	0.860	0.704	0.651	0.586	0.538	0.474
5.00	0.906	0.859	0.702	0.651	0.586	0.537	0.473
6.00	0.906	0.859	0.702	0.650	0.585	0.537	0.472
7.01	0.906	0.858	0.701	0.650	0.584	0.536	0.472
7.41	0.906	0.858	0.701	0.649	0.584	0.536	0.472

Table 139. Static Pressure Ratios for Nozzle 80, $x_r/l_r = 0.42$, $\theta = 20°$, $\phi = 0°$, Maximum Sidewall, $\delta_{v,p} = 20°$, and $\delta_{v,y} = 0°$

(a) Upper ramp

NPR	Static pressure ratios at x_r/l_r of—								
	−0.170	−0.032	0.106	0.175	0.244	0.382	0.520	0.659	0.797
2.01	0.864	0.733	0.736	0.796	0.820	0.756	0.691	0.631	0.555
2.50	0.863	0.732	0.736	0.794	0.820	0.756	0.686	0.623	0.480
3.00	0.862	0.731	0.736	0.794	0.820	0.757	0.684	0.623	0.481
3.50	0.862	0.731	0.736	0.794	0.820	0.757	0.683	0.623	0.480
4.00	0.861	0.731	0.736	0.794	0.820	0.757	0.682	0.623	0.480
5.00	0.861	0.730	0.735	0.793	0.821	0.757	0.681	0.624	0.481
6.01	0.860	0.729	0.735	0.793	0.821	0.757	0.680	0.625	0.482
7.00	0.859	0.728	0.734	0.792	0.822	0.757	0.680	0.625	0.483
7.40	0.859	0.728	0.734	0.792	0.822	0.757	0.679	0.625	0.483

(b) Lower flap

NPR	Static pressure ratios at x_r/l_r of—						
	−0.308	−0.170	−0.032	0.037	0.079	0.120	0.162
2.01	0.906	0.861	0.710	0.655	0.591	0.543	0.479
2.50	0.905	0.861	0.707	0.654	0.588	0.540	0.476
3.00	0.905	0.861	0.706	0.653	0.588	0.539	0.475
3.50	0.906	0.860	0.705	0.653	0.588	0.539	0.475
4.00	0.906	0.860	0.705	0.652	0.587	0.538	0.474
5.00	0.906	0.860	0.703	0.652	0.587	0.538	0.473
6.01	0.906	0.859	0.702	0.651	0.586	0.537	0.473
7.00	0.907	0.858	0.702	0.650	0.585	0.537	0.472
7.40	0.906	0.858	0.701	0.650	0.585	0.537	0.472

Table 140. Static Pressure Ratios for Nozzle 81, $x_r/l_r = 0.20$, $\theta = 20°$, $\phi = 0°$, Minimum Sidewall, $\delta_{v,p} = 20°$, and $\delta_{v,y} = 0°$

(a) Upper ramp

NPR	Static pressure ratios at x_r/l_r of—								
	−0.170	−0.032	0.106	0.175	0.244	0.382	0.520	0.659	0.797
2.00	0.733	0.791	0.747	0.692	0.625	0.546	0.548	0.542	0.510
2.50	0.731	0.790	0.748	0.690	0.619	0.474	0.421	0.393	0.494
3.00	0.731	0.789	0.747	0.689	0.618	0.473	0.344	0.304	0.274
3.50	0.730	0.789	0.748	0.689	0.617	0.473	0.339	0.248	0.213
4.03	0.729	0.789	0.748	0.689	0.616	0.472	0.338	0.219	0.173
5.00	0.728	0.788	0.748	0.689	0.617	0.473	0.337	0.219	0.137
6.00	0.727	0.788	0.749	0.688	0.617	0.474	0.337	0.219	0.137
7.00	0.726	0.787	0.748	0.688	0.617	0.474	0.337	0.220	0.137
8.00	0.725	0.786	0.748	0.688	0.618	0.474	0.337	0.220	0.138

(b) Lower flap

NPR	Static pressure ratios at x_r/l_r of—						
	−0.308	−0.170	−0.032	0.037	0.079	0.120	0.162
2.00	0.905	0.859	0.709	0.653	0.584	0.539	0.479
2.50	0.905	0.858	0.707	0.652	0.582	0.537	0.477
3.00	0.905	0.858	0.705	0.651	0.581	0.536	0.476
3.50	0.906	0.857	0.704	0.651	0.580	0.535	0.476
4.03	0.906	0.857	0.703	0.650	0.579	0.535	0.475
5.00	0.906	0.856	0.702	0.650	0.579	0.534	0.475
6.00	0.906	0.856	0.702	0.649	0.579	0.534	0.474
7.00	0.906	0.855	0.701	0.648	0.578	0.533	0.474
8.00	0.906	0.855	0.700	0.647	0.578	0.533	0.473

Table 141. Static Pressure Ratios for Nozzle 82, $x_r/l_r = 0.20$, $\theta = 20°$, $\phi = 0°$, Medium Sidewall, $\delta_{v,p} = 20°$, and $\delta_{v,y} = 0°$

(a) Upper ramp

NPR	Static pressure ratios at x_r/l_r of—								
	−0.170	−0.032	0.106	0.175	0.244	0.382	0.520	0.659	0.797
2.00	0.733	0.791	0.749	0.693	0.627	0.548	0.549	0.544	0.510
2.50	0.731	0.790	0.747	0.690	0.619	0.472	0.423	0.405	0.478
3.00	0.731	0.790	0.747	0.690	0.618	0.472	0.345	0.306	0.284
3.50	0.730	0.790	0.748	0.690	0.618	0.472	0.340	0.249	0.217
4.00	0.730	0.789	0.748	0.689	0.617	0.472	0.339	0.221	0.177
5.00	0.729	0.789	0.748	0.689	0.618	0.472	0.338	0.221	0.139
5.99	0.728	0.788	0.749	0.689	0.618	0.473	0.338	0.220	0.139
7.00	0.727	0.787	0.748	0.688	0.618	0.473	0.337	0.221	0.139
8.00	0.726	0.787	0.749	0.688	0.619	0.473	0.338	0.221	0.139

(b) Lower flap

NPR	Static pressure ratios at x_r/l_r of—						
	−0.308	−0.170	−0.032	0.037	0.079	0.120	0.162
2.00	0.906	0.859	0.709	0.654	0.585	0.541	0.480
2.50	0.905	0.858	0.707	0.652	0.582	0.538	0.477
3.00	0.905	0.858	0.705	0.652	0.582	0.537	0.476
3.50	0.906	0.858	0.704	0.651	0.581	0.537	0.476
4.00	0.906	0.857	0.704	0.651	0.581	0.537	0.476
5.00	0.906	0.857	0.702	0.651	0.581	0.536	0.475
5.99	0.906	0.856	0.702	0.650	0.580	0.535	0.474
7.00	0.907	0.856	0.701	0.650	0.579	0.535	0.474
8.00	0.907	0.855	0.701	0.649	0.579	0.534	0.474

Table 142. Static Pressure Ratios for Nozzle 83, $x_r/l_r = 0.20$, $\theta = 20°$, $\phi = 0°$, Maximum Sidewall, $\delta_{v,p} = 20°$, and $\delta_{v,y} = 0°$

(a) Upper ramp

NPR	Static pressure ratios at x_r/l_r of—								
	−0.170	−0.032	0.106	0.175	0.244	0.382	0.520	0.659	0.797
2.00	0.734	0.792	0.750	0.694	0.628	0.549	0.549	0.543	0.509
2.50	0.733	0.791	0.748	0.691	0.620	0.473	0.423	0.410	0.478
3.00	0.732	0.790	0.748	0.691	0.619	0.473	0.345	0.307	0.283
3.50	0.731	0.790	0.747	0.690	0.617	0.473	0.340	0.249	0.216
4.00	0.730	0.790	0.748	0.690	0.618	0.473	0.339	0.221	0.176
5.00	0.729	0.789	0.749	0.690	0.618	0.474	0.338	0.221	0.139
6.00	0.728	0.788	0.749	0.689	0.618	0.474	0.338	0.221	0.139
7.00	0.727	0.788	0.749	0.689	0.618	0.474	0.338	0.221	0.139
8.00	0.726	0.787	0.749	0.689	0.618	0.475	0.338	0.222	0.139

(b) Lower flap

NPR	Static pressure ratios at x_r/l_r of—						
	−0.308	−0.170	−0.032	0.037	0.079	0.120	0.162
2.00	0.907	0.860	0.711	0.655	0.587	0.542	0.481
2.50	0.906	0.859	0.708	0.654	0.584	0.539	0.478
3.00	0.906	0.858	0.706	0.653	0.583	0.538	0.477
3.50	0.906	0.858	0.705	0.652	0.583	0.538	0.477
4.00	0.906	0.858	0.705	0.652	0.582	0.537	0.476
5.00	0.906	0.857	0.703	0.651	0.582	0.537	0.475
6.00	0.907	0.856	0.702	0.651	0.581	0.536	0.475
7.00	0.907	0.856	0.702	0.650	0.579	0.535	0.474
8.00	0.907	0.855	0.701	0.649	0.579	0.535	0.474

Table 143. Static Pressure Ratios for Nozzle 84, $x_r/l_r = 0.02$, $\theta = 20°$, $\phi = 0°$, Minimum Sidewall, $\delta_{v,p} = 20°$, and $\delta_{v,y} = 0°$

(a) Upper ramp

NPR	Static pressure ratios at x_r/l_r of—								
	−0.170	−0.032	0.106	0.175	0.244	0.382	0.520	0.659	0.797
2.00	0.717	0.784	0.733	0.677	0.604	0.541	0.544	0.540	0.514
2.50	0.714	0.781	0.730	0.673	0.597	0.454	0.400	0.402	0.483
3.00	0.712	0.780	0.730	0.671	0.595	0.452	0.321	0.285	0.290
3.50	0.711	0.780	0.730	0.671	0.594	0.451	0.319	0.226	0.208
4.00	0.710	0.780	0.730	0.670	0.593	0.451	0.317	0.198	0.165
5.00	0.709	0.779	0.730	0.670	0.594	0.451	0.316	0.198	0.128
5.99	0.708	0.779	0.730	0.670	0.594	0.451	0.315	0.198	0.128
8.00	0.706	0.778	0.730	0.670	0.594	0.452	0.314	0.198	0.128

(b) Lower flap

NPR	Static pressure ratios at x_r/l_r of—						
	−0.308	−0.170	−0.032	0.037	0.079	0.120	0.162
2.00	0.902	0.859	0.716	0.635	0.572	0.501	0.472
2.50	0.901	0.857	0.712	0.631	0.566	0.493	0.468
3.00	0.900	0.857	0.711	0.629	0.564	0.489	0.466
3.50	0.901	0.857	0.711	0.628	0.564	0.488	0.466
4.00	0.901	0.857	0.710	0.628	0.563	0.486	0.466
5.00	0.901	0.856	0.710	0.628	0.563	0.485	0.466
5.99	0.902	0.856	0.710	0.627	0.562	0.484	0.466
8.00	0.902	0.855	0.709	0.626	0.561	0.482	0.467

Table 144. Static Pressure Ratios for Nozzle 85, $x_r/l_r = 0.02$, $\theta = 20°$, $\phi = 0°$, Medium Sidewall, $\delta_{v,p} = 20°$, and $\delta_{v,y} = 0°$

(a) Upper ramp

NPR	Static pressure ratios at x_r/l_r of—								
	−0.170	−0.032	0.106	0.175	0.244	0.382	0.520	0.659	0.797
2.01	0.717	0.784	0.733	0.677	0.602	0.541	0.542	0.538	0.511
2.50	0.712	0.780	0.731	0.672	0.598	0.455	0.401	0.414	0.477
3.00	0.710	0.779	0.729	0.670	0.595	0.452	0.322	0.286	0.293
3.50	0.709	0.779	0.728	0.670	0.594	0.451	0.319	0.227	0.208
4.01	0.708	0.778	0.729	0.669	0.593	0.450	0.317	0.199	0.165
5.00	0.707	0.778	0.729	0.669	0.593	0.450	0.316	0.198	0.127
6.00	0.706	0.777	0.729	0.669	0.593	0.450	0.315	0.198	0.128
8.00	0.704	0.777	0.729	0.668	0.594	0.451	0.314	0.198	0.128

(b) Lower flap

NPR	Static pressure ratios at x_r/l_r of—						
	−0.308	−0.170	−0.032	0.037	0.079	0.120	0.162
2.01	0.901	0.859	0.715	0.635	0.572	0.503	0.471
2.50	0.900	0.857	0.711	0.629	0.565	0.492	0.465
3.00	0.900	0.856	0.710	0.627	0.563	0.489	0.464
3.50	0.900	0.856	0.709	0.627	0.562	0.487	0.464
4.01	0.900	0.856	0.709	0.626	0.561	0.485	0.464
5.00	0.900	0.856	0.708	0.626	0.561	0.484	0.464
6.00	0.901	0.855	0.708	0.625	0.560	0.483	0.464
8.00	0.901	0.854	0.707	0.625	0.559	0.481	0.464

Table 145. Static Pressure Ratios for Nozzle 86, $x_r/l_r = 0.02$, $\theta = 20°$, $\phi = 0°$, Maximum Sidewall, $\delta_{v,p} = 20°$, and $\delta_{v,y} = 0°$

(a) Upper ramp

NPR	Static pressure ratios at x_r/l_r of—								
	−0.170	−0.032	0.106	0.175	0.244	0.382	0.520	0.659	0.797
2.00	0.717	0.784	0.735	0.677	0.605	0.543	0.545	0.541	0.513
2.50	0.713	0.780	0.730	0.672	0.597	0.454	0.400	0.415	0.478
3.00	0.711	0.779	0.729	0.670	0.595	0.452	0.321	0.284	0.292
3.50	0.710	0.779	0.729	0.670	0.593	0.451	0.319	0.226	0.208
4.01	0.709	0.779	0.728	0.669	0.593	0.450	0.317	0.199	0.164
5.00	0.708	0.778	0.729	0.669	0.593	0.450	0.316	0.199	0.128
6.00	0.707	0.778	0.729	0.669	0.593	0.451	0.315	0.198	0.128
8.00	0.705	0.777	0.729	0.669	0.594	0.451	0.315	0.198	0.128

(b) Lower flap

NPR	Static pressure ratios at x_r/l_r of—						
	−0.308	−0.170	−0.032	0.037	0.079	0.120	0.162
2.00	0.902	0.859	0.716	0.635	0.571	0.502	0.471
2.50	0.901	0.857	0.712	0.630	0.565	0.492	0.465
3.00	0.900	0.856	0.710	0.628	0.563	0.489	0.464
3.50	0.900	0.856	0.709	0.627	0.562	0.487	0.464
4.01	0.901	0.856	0.709	0.627	0.562	0.486	0.464
5.00	0.901	0.856	0.709	0.626	0.561	0.485	0.465
6.00	0.901	0.856	0.708	0.626	0.561	0.484	0.465
8.00	0.901	0.854	0.708	0.625	0.560	0.482	0.464

Table 146. Static Pressure Ratios for Nozzle 87, $x_r/l_r = 0.42$, $\theta = 20°$, $\phi = 0°$, Maximum Sidewall, $\delta_{v,p} = 20°$, and $\delta_{v,y} = -20°$

(a) Upper ramp

NPR	Static pressure ratios at x_r/l_r of—								
	−0.170	−0.032	0.106	0.175	0.244	0.382	0.520	0.659	0.797
2.00	0.864	0.732	0.738	0.796	0.823	0.758	0.692	0.634	0.566
2.50	0.862	0.730	0.735	0.794	0.820	0.756	0.685	0.623	0.480
3.00	0.861	0.730	0.735	0.793	0.819	0.756	0.683	0.623	0.480
3.50	0.861	0.730	0.734	0.793	0.819	0.756	0.682	0.623	0.480
4.00	0.860	0.729	0.734	0.793	0.820	0.756	0.681	0.623	0.480
5.00	0.860	0.729	0.734	0.793	0.821	0.756	0.680	0.623	0.481
6.00	0.859	0.728	0.734	0.792	0.822	0.756	0.679	0.624	0.481
7.00	0.859	0.727	0.734	0.792	0.822	0.756	0.679	0.624	0.482

(b) Lower flap

NPR	Static pressure ratios at x_r/l_r of—						
	−0.308	−0.170	−0.032	0.037	0.079	0.120	0.162
2.00	0.906	0.861	0.710	0.655	0.590	0.543	0.479
2.50	0.905	0.860	0.706	0.652	0.586	0.538	0.475
3.00	0.905	0.860	0.705	0.652	0.585	0.538	0.475
3.50	0.906	0.860	0.704	0.651	0.585	0.537	0.474
4.00	0.906	0.860	0.703	0.651	0.585	0.537	0.474
5.00	0.906	0.859	0.702	0.651	0.584	0.537	0.474
6.00	0.906	0.859	0.701	0.650	0.584	0.536	0.473
7.00	0.906	0.858	0.701	0.649	0.583	0.536	0.472

Table 147. Static Pressure Ratios for Nozzle 88, $x_r/l_r = 0.20$, $\theta = 20°$, $\phi = 0°$, Medium Sidewall, $\delta_{v,p} = 20°$, and $\delta_{v,y} = -20°$

(a) Upper ramp

NPR	Static pressure ratios at x_r/l_r of—								
	−0.170	−0.032	0.106	0.175	0.244	0.382	0.520	0.659	0.797
2.00	0.750	0.804	0.764	0.712	0.650	0.567	0.554	0.545	0.512
2.50	0.746	0.801	0.760	0.705	0.635	0.490	0.459	0.416	0.444
3.00	0.745	0.800	0.760	0.704	0.635	0.489	0.365	0.354	0.290
3.50	0.744	0.800	0.760	0.704	0.634	0.489	0.356	0.286	0.256
4.00	0.744	0.800	0.761	0.704	0.634	0.489	0.355	0.244	0.228
5.00	0.743	0.799	0.761	0.703	0.634	0.489	0.354	0.243	0.168
6.00	0.742	0.799	0.761	0.703	0.635	0.490	0.354	0.243	0.168
7.00	0.741	0.798	0.761	0.703	0.635	0.490	0.354	0.243	0.168
7.60	0.740	0.798	0.761	0.702	0.635	0.491	0.354	0.243	0.168

(b) Lower flap

NPR	Static pressure ratios at x_r/l_r of—						
	−0.308	−0.170	−0.032	0.037	0.079	0.120	0.162
2.00	0.911	0.867	0.726	0.674	0.611	0.566	0.504
2.50	0.910	0.865	0.721	0.669	0.605	0.559	0.496
3.00	0.909	0.865	0.719	0.668	0.604	0.557	0.495
3.50	0.910	0.865	0.718	0.667	0.604	0.557	0.494
4.00	0.910	0.865	0.717	0.667	0.604	0.557	0.494
5.00	0.911	0.864	0.716	0.666	0.603	0.556	0.493
6.00	0.911	0.863	0.716	0.666	0.602	0.556	0.493
7.00	0.911	0.863	0.716	0.665	0.602	0.555	0.492
7.60	0.911	0.862	0.715	0.664	0.602	0.555	0.492

Table 148. Static Pressure Ratios for Nozzle 89, $x_r/l_r = 0.20$, $\theta = 20°$, $\phi = 0°$, Maximum Sidewall, $\delta_{v,p} = 20°$, and $\delta_{v,y} = -20°$

(a) Upper ramp

NPR	Static pressure ratios at x_r/l_r of—								
	−0.170	−0.032	0.106	0.175	0.244	0.382	0.520	0.659	0.797
2.00	0.751	0.805	0.764	0.713	0.651	0.570	0.558	0.545	0.512
2.50	0.747	0.802	0.760	0.705	0.637	0.492	0.460	0.422	0.446
3.00	0.745	0.801	0.759	0.704	0.634	0.489	0.366	0.353	0.309
3.50	0.745	0.801	0.761	0.704	0.635	0.490	0.356	0.286	0.269
4.01	0.744	0.801	0.761	0.704	0.634	0.489	0.355	0.243	0.234
5.00	0.743	0.800	0.761	0.704	0.635	0.490	0.354	0.242	0.169
6.00	0.743	0.799	0.761	0.704	0.636	0.490	0.354	0.242	0.169
7.00	0.742	0.799	0.761	0.703	0.636	0.491	0.354	0.243	0.169
7.40	0.741	0.799	0.761	0.703	0.636	0.491	0.354	0.243	0.169

(b) Lower flap

NPR	Static pressure ratios at x_r/l_r of—						
	−0.308	−0.170	−0.032	0.037	0.079	0.120	0.162
2.00	0.911	0.868	0.727	0.674	0.610	0.566	0.505
2.50	0.910	0.866	0.722	0.669	0.603	0.559	0.497
3.00	0.910	0.865	0.720	0.668	0.602	0.558	0.495
3.50	0.910	0.865	0.719	0.668	0.601	0.557	0.495
4.01	0.911	0.865	0.718	0.668	0.601	0.557	0.495
5.00	0.911	0.864	0.717	0.667	0.600	0.556	0.494
6.00	0.911	0.864	0.717	0.666	0.599	0.556	0.494
7.00	0.911	0.863	0.716	0.666	0.598	0.556	0.493
7.40	0.911	0.863	0.716	0.666	0.599	0.555	0.493

Table 149. Static Pressure Ratios for Nozzle 90, $x_r/l_r = 0.02$, $\theta = 20°$, $\phi = 0°$, Minimum Sidewall, $\delta_{v,p} = 20°$, and $\delta_{v,y} = -20°$

(a) Upper ramp

NPR	Static pressure ratios at x_r/l_r of—								
	−0.170	−0.032	0.106	0.175	0.244	0.382	0.520	0.659	0.797
2.00	0.753	0.806	0.755	0.702	0.632	0.547	0.542	0.539	0.513
2.50	0.751	0.804	0.754	0.698	0.623	0.471	0.392	0.446	0.473
3.00	0.750	0.804	0.755	0.697	0.624	0.471	0.323	0.266	0.311
3.50	0.749	0.804	0.755	0.697	0.622	0.471	0.321	0.215	0.184
4.00	0.749	0.803	0.755	0.697	0.622	0.471	0.320	0.197	0.147
5.00	0.748	0.803	0.755	0.697	0.622	0.471	0.319	0.196	0.122
6.00	0.747	0.803	0.754	0.697	0.622	0.471	0.318	0.196	0.122
7.98	0.745	0.802	0.755	0.697	0.622	0.472	0.317	0.196	0.123
8.00	0.745	0.802	0.755	0.697	0.622	0.472	0.317	0.196	0.123

(b) Lower flap

NPR	Static pressure ratios at x_r/l_r of—						
	−0.308	−0.170	−0.032	0.037	0.079	0.120	0.162
2.00	0.914	0.876	0.747	0.670	0.610	0.545	0.500
2.50	0.914	0.875	0.744	0.667	0.605	0.539	0.494
3.00	0.914	0.875	0.744	0.666	0.605	0.538	0.493
3.50	0.914	0.875	0.744	0.666	0.605	0.537	0.492
4.00	0.914	0.875	0.743	0.666	0.604	0.537	0.492
5.00	0.914	0.874	0.743	0.666	0.604	0.535	0.491
6.00	0.915	0.874	0.743	0.665	0.604	0.536	0.491
7.98	0.915	0.873	0.742	0.664	0.602	0.534	0.490
8.00	0.915	0.873	0.742	0.664	0.602	0.534	0.490

Table 150. Static Pressure Ratios for Nozzle 91, $x_r/l_r = 0.02$, $\theta = 20°$, $\phi = 0°$, Medium Sidewall, $\delta_{v,p} = 20°$, and $\delta_{v,y} = -20°$

(a) Upper ramp

NPR	Static pressure ratios at x_r/l_r of—								
	−0.170	−0.032	0.106	0.175	0.244	0.382	0.520	0.659	0.797
2.00	0.760	0.811	0.764	0.712	0.647	0.564	0.544	0.538	0.513
2.50	0.756	0.808	0.758	0.705	0.631	0.485	0.433	0.401	0.461
3.00	0.755	0.808	0.759	0.704	0.630	0.482	0.348	0.324	0.267
3.50	0.755	0.808	0.760	0.704	0.630	0.482	0.340	0.278	0.221
4.00	0.755	0.808	0.760.	0.704	0.630	0.482	0.339	0.229	0.198
5.00	0.754	0.808	0.760	0.704	0.629	0.483	0.337	0.227	0.157
6.07	0.753	0.807	0.761	0.704	0.631	0.483	0.337	0.227	0.156
6.00	0.753	0.808	0.760	0.704	0.631	0.483	0.337	0.227	0.156
8.00	0.752	0.807	0.761	0.704	0.632	0.484	0.336	0.227	0.157

(b) Lower flap

NPR	Static pressure ratios at x_r/l_r of—						
	−0.308	−0.170	−0.032	0.037	0.079	0.120	0.162
2.00	0.916	0.878	0.753	0.678	0.620	0.559	0.511
2.50	0.915	0.877	0.750	0.674	0.613	0.551	0.503
3.00	0.915	0.877	0.749	0.673	0.613	0.549	0.501
3.50	0.915	0.877	0.749	0.673	0.613	0.549	0.501
4.00	0.916	0.877	0.749	0.673	0.613	0.548	0.501
5.00	0.916	0.877	0.749	0.673	0.612	0.547	0.500
6.07	0.916	0.877	0.749	0.672	0.612	0.547	0.500
6.00	0.916	0.877	0.749	0.672	0.612	0.547	0.500
8.00	0.917	0.876	0.749	0.671	0.611	0.545	0.499

Table 151. Static Pressure Ratios for Nozzle 92, $x_r/l_r = 0.02$, $\theta = 20°$, $\phi = 0°$, Maximum Sidewall, $\delta_{v,p} = 20°$, and $\delta_{v,y} = -20°$

(a) Upper ramp

NPR	Static pressure ratios at x_r/l_r of—								
	−0.170	−0.032	0.106	0.175	0.244	0.382	0.520	0.659	0.797
2.00	0.760	0.811	0.764	0.712	0.646	0.565	0.546	0.538	0.512
2.50	0.757	0.808	0.759	0.705	0.631	0.485	0.433	0.421	0.453
3.00	0.756	0.808	0.760	0.705	0.631	0.482	0.347	0.326	0.289
3.50	0.756	0.808	0.760	0.705	0.631	0.482	0.340	0.278	0.248
4.00	0.755	0.808	0.760	0.705	0.630	0.482	0.338	0.228	0.220
5.00	0.755	0.808	0.761	0.705	0.631	0.483	0.337	0.227	0.166
6.00	0.754	0.808	0.761	0.704	0.631	0.483	0.336	0.227	0.165
7.99	0.753	0.808	0.761	0.704	0.632	0.484	0.336	0.227	0.165

(b) Lower flap

NPR	Static pressure ratios at x_r/l_r of—						
	−0.308	−0.170	−0.032	0.037	0.079	0.120	0.162
2.00	0.916	0.879	0.753	0.679	0.620	0.559	0.512
2.50	0.916	0.877	0.750	0.674	0.614	0.551	0.503
3.00	0.915	0.878	0.749	0.673	0.613	0.550	0.502
3.50	0.916	0.878	0.750	0.673	0.613	0.549	0.501
4.00	0.916	0.878	0.749	0.673	0.613	0.549	0.501
5.00	0.916	0.877	0.749	0.673	0.613	0.548	0.500
6.00	0.917	0.877	0.749	0.673	0.613	0.547	0.500
7.99	0.917	0.876	0.749	0.672	0.612	0.546	0.500

Table 152. Static Pressure Ratios for Nozzle 93, $x_r/l_r = 0.42$, $\theta = 30°$, $\phi = 0°$, Minimum Sidewall, $\delta_{v,p} = 20°$, and $\delta_{v,y} = 0°$

(a) Upper ramp

NPR	Static pressure ratios at x_r/l_r of—								
	−0.170	−0.032	0.106	0.175	0.244	0.382	0.520	0.659	0.797
2.00	0.738	0.803	0.745	0.696	0.626	0.546	0.538	0.543	0.515
2.50	0.737	0.802	0.745	0.693	0.621	0.465	0.409	0.394	0.496
3.00	0.736	0.802	0.745	0.693	0.620	0.464	0.331	0.304	0.284
3.50	0.736	0.802	0.745	0.693	0.620	0.464	0.324	0.246	0.223
4.00	0.736	0.802	0.746	0.692	0.619	0.464	0.323	0.215	0.183
5.00	0.735	0.802	0.746	0.692	0.620	0.465	0.321	0.214	0.143
6.00	0.734	0.802	0.746	0.692	0.620	0.465	0.321	0.214	0.143
7.00	0.733	0.801	0.746	0.692	0.621	0.465	0.320	0.214	0.144
7.90	0.733	0.801	0.746	0.692	0.621	0.465	0.320	0.215	0.144

(b) Lower flap

NPR	Static pressure ratios at x_r/l_r of—						
	−0.308	−0.170	−0.032	0.037	0.079	0.120	0.162
2.00	0.907	0.864	0.711	0.659	0.592	0.546	0.479
2.50	0.907	0.863	0.709	0.657	0.589	0.543	0.476
3.00	0.907	0.863	0.707	0.657	0.588	0.543	0.476
3.50	0.907	0.863	0.706	0.656	0.588	0.543	0.475
4.00	0.908	0.862	0.705	0.656	0.588	0.542	0.475
5.00	0.908	0.862	0.704	0.656	0.587	0.541	0.474
6.00	0.908	0.861	0.703	0.655	0.586	0.541	0.474
7.00	0.909	0.861	0.702	0.655	0.586	0.541	0.473
7.90	0.909	0.860	0.701	0.654	0.585	0.540	0.473

Table 153. Static Pressure Ratios for Nozzle 94, $x_r/l_r = 0.42$, $\theta = 30°$, $\phi = 0°$, Medium Sidewall, $\delta_{v,p} = 20°$, and $\delta_{v,y} = 0°$

(a) Upper ramp

NPR	Static pressure ratios at x_r/l_r of—								
	−0.170	−0.032	0.106	0.175	0.244	0.382	0.520	0.659	0.797
2.00	0.738	0.803	0.746	0.697	0.628	0.549	0.538	0.544	0.515
2.50	0.737	0.802	0.744	0.694	0.621	0.465	0.414	0.420	0.454
3.00	0.736	0.802	0.746	0.693	0.621	0.465	0.333	0.310	0.308
3.50	0.736	0.802	0.745	0.693	0.619	0.465	0.326	0.250	0.234
4.00	0.735	0.802	0.746	0.693	0.620	0.465	0.325	0.218	0.190
5.00	0.735	0.802	0.746	0.693	0.621	0.466	0.323	0.217	0.148
6.00	0.734	0.802	0.746	0.693	0.621	0.466	0.323	0.217	0.148
7.00	0.733	0.801	0.746	0.692	0.622	0.466	0.322	0.217	0.148
7.40	0.733	0.801	0.746	0.692	0.622	0.466	0.322	0.217	0.149

(b) Lower flap

NPR	Static pressure ratios at x_r/l_r of—						
	−0.308	−0.170	−0.032	0.037	0.079	0.120	0.162
2.00	0.907	0.864	0.712	0.659	0.592	0.545	0.480
2.50	0.906	0.863	0.709	0.657	0.589	0.542	0.476
3.00	0.906	0.863	0.707	0.657	0.588	0.541	0.476
3.50	0.907	0.863	0.706	0.656	0.588	0.541	0.475
4.00	0.907	0.862	0.705	0.656	0.588	0.541	0.475
5.00	0.908	0.862	0.704	0.656	0.587	0.540	0.474
6.00	0.908	0.861	0.703	0.655	0.586	0.540	0.474
7.00	0.908	0.861	0.702	0.655	0.586	0.539	0.473
7.40	0.908	0.861	0.702	0.655	0.585	0.539	0.473

Table 154. Static Pressure Ratios for Nozzle 95, $x_r/l_r = 0.42$, $\theta = 30°$, $\phi = 0°$, Maximum Sidewall, $\delta_{v,p} = 20°$, and $\delta_{v,y} = 0°$

(a) Upper ramp

NPR	Static pressure ratios at x_r/l_r of—								
	−0.170	−0.032	0.106	0.175	0.244	0.382	0.520	0.659	0.797
2.00	0.739	0.804	0.749	0.698	0.631	0.550	0.539	0.543	0.515
2.50	0.738	0.803	0.746	0.694	0.622	0.466	0.413	0.420	0.452
3.00	0.737	0.803	0.746	0.694	0.622	0.465	0.332	0.310	0.309
3.50	0.737	0.803	0.746	0.694	0.620	0.465	0.326	0.249	0.234
4.00	0.737	0.803	0.746	0.693	0.621	0.465	0.324	0.217	0.190
5.00	0.736	0.802	0.747	0.693	0.621	0.465	0.323	0.217	0.148
6.00	0.735	0.802	0.746	0.693	0.621	0.465	0.322	0.217	0.148
7.00	0.734	0.802	0.746	0.693	0.622	0.465	0.322	0.217	0.148
7.39	0.733	0.802	0.746	0.692	0.622	0.465	0.322	0.217	0.148

(b) Lower flap

NPR	Static pressure ratios at x_r/l_r of—						
	−0.308	−0.170	−0.032	0.037	0.079	0.120	0.162
2.00	0.908	0.864	0.713	0.659	0.595	0.546	0.481
2.50	0.907	0.863	0.710	0.657	0.592	0.543	0.477
3.00	0.907	0.863	0.708	0.657	0.591	0.542	0.477
3.50	0.907	0.863	0.707	0.657	0.591	0.542	0.476
4.00	0.908	0.863	0.706	0.656	0.591	0.542	0.476
5.00	0.908	0.862	0.705	0.656	0.590	0.541	0.475
6.00	0.908	0.862	0.704	0.655	0.589	0.540	0.474
7.00	0.909	0.861	0.703	0.655	0.588	0.540	0.474
7.39	0.909	0.861	0.702	0.655	0.587	0.540	0.473

Table 155. Static Pressure Ratios for Nozzle 96, $x_r/l_r = 0.20$, $\theta = 30°$, $\phi = 0°$, Minimum Sidewall, $\delta_{v,p} = 20°$, and $\delta_{v,y} = 0°$

(a) Upper ramp

NPR	Static pressure ratios at x_r/l_r of—								
	−0.170	−0.032	0.106	0.175	0.244	0.382	0.520	0.659	0.797
2.00	0.730	0.794	0.749	0.690	0.621	0.546	0.544	0.505	0.537
2.50	0.729	0.793	0.749	0.688	0.616	0.475	0.417	0.479	0.386
3.00	0.729	0.793	0.748	0.688	0.615	0.475	0.341	0.271	0.296
3.50	0.728	0.793	0.749	0.688	0.614	0.475	0.337	0.213	0.241
4.00	0.728	0.793	0.750	0.687	0.614	0.476	0.336	0.175	0.213
5.00	0.727	0.792	0.750	0.687	0.614	0.476	0.335	0.139	0.212
6.00	0.726	0.792	0.750	0.687	0.614	0.477	0.335	0.139	0.213
7.00	0.725	0.792	0.750	0.687	0.614	0.477	0.335	0.139	0.213
8.00	0.725	0.791	0.750	0.687	0.615	0.478	0.335	0.139	0.213

(b) Lower flap

NPR	Static pressure ratios at x_r/l_r of—						
	−0.308	−0.170	−0.032	0.037	0.079	0.120	0.162
2.00	0.906	0.861	0.707	0.648	0.588	0.541	0.476
2.50	0.905	0.860	0.705	0.645	0.585	0.538	0.473
3.00	0.905	0.860	0.703	0.644	0.584	0.537	0.472
3.50	0.906	0.860	0.702	0.645	0.584	0.537	0.472
4.00	0.906	0.859	0.701	0.644	0.583	0.537	0.471
5.00	0.907	0.859	0.700	0.644	0.582	0.536	0.471
6.00	0.907	0.859	0.699	0.643	0.582	0.536	0.470
7.00	0.907	0.858	0.699	0.643	0.581	0.536	0.469
8.00	0.907	0.857	0.698	0.643	0.581	0.535	0.469

Table 156. Static Pressure Ratios for Nozzle 97, $x_r/l_r = 0.20$, $\theta = 30°$, $\phi = 0°$, Medium Sidewall, $\delta_{v,p} = 20°$, and $\delta_{v,y} = 0°$

(a) Upper ramp

NPR	Static pressure ratios at x_r/l_r of—								
	−0.170	−0.032	0.106	0.175	0.244	0.382	0.520	0.659	0.797
2.00	0.730	0.794	0.750	0.691	0.624	0.547	0.543	0.504	0.536
2.50	0.729	0.793	0.749	0.688	0.616	0.477	0.418	0.481	0.393
3.00	0.728	0.793	0.748	0.688	0.614	0.475	0.342	0.278	0.298
3.50	0.728	0.793	0.749	0.688	0.614	0.476	0.338	0.215	0.241
4.00	0.728	0.793	0.749	0.687	0.614	0.476	0.337	0.176	0.214
5.00	0.727	0.792	0.750	0.687	0.614	0.477	0.336	0.140	0.213
6.00	0.726	0.792	0.750	0.687	0.614	0.478	0.335	0.140	0.213
6.99	0.725	0.792	0.750	0.687	0.615	0.479	0.335	0.140	0.214
8.00	0.725	0.791	0.750	0.687	0.615	0.479	0.336	0.140	0.214

(b) Lower flap

NPR	Static pressure ratios at x_r/l_r of—						
	−0.308	−0.170	−0.032	0.037	0.079	0.120	0.162
2.00	0.905	0.861	0.707	0.649	0.586	0.540	0.476
2.50	0.905	0.860	0.705	0.647	0.584	0.538	0.473
3.00	0.905	0.860	0.703	0.646	0.583	0.537	0.472
3.50	0.906	0.860	0.702	0.646	0.583	0.536	0.472
4.00	0.906	0.859	0.701	0.645	0.582	0.536	0.471
5.00	0.906	0.859	0.700	0.645	0.582	0.536	0.471
6.00	0.907	0.858	0.699	0.644	0.581	0.536	0.470
6.99	0.907	0.858	0.699	0.643	0.580	0.535	0.469
8.00	0.907	0.857	0.698	0.642	0.580	0.535	0.469

Table 157. Static Pressure Ratios for Nozzle 98, $x_r/l_r = 0.20$, $\theta = 30°$, $\phi = 0°$, Maximum Sidewall, $\delta_{v,p} = 20°$, and $\delta_{v,y} = 0°$

(a) Upper ramp

NPR	Static pressure ratios at x_r/l_r of—								
	−0.170	−0.032	0.106	0.175	0.244	0.382	0.520	0.659	0.797
2.00	0.731	0.794	0.753	0.692	0.626	0.545	0.543	0.505	0.536
2.50	0.730	0.793	0.748	0.689	0.614	0.471	0.415	0.482	0.392
3.00	0.729	0.793	0.748	0.689	0.614	0.471	0.339	0.277	0.298
3.51	0.729	0.793	0.749	0.688	0.613	0.472	0.334	0.215	0.241
4.01	0.729	0.793	0.749	0.688	0.614	0.472	0.334	0.176	0.213
5.01	0.728	0.793	0.750	0.688	0.613	0.473	0.333	0.140	0.213
6.00	0.727	0.792	0.750	0.688	0.614	0.474	0.332	0.140	0.213
7.00	0.726	0.791	0.750	0.688	0.614	0.474	0.332	0.140	0.213
8.00	0.725	0.791	0.750	0.687	0.614	0.475	0.332	0.140	0.213

(b) Lower flap

NPR	Static pressure ratios at x_r/l_r of—						
	−0.308	−0.170	−0.032	0.037	0.079	0.120	0.162
2.00	0.906	0.861	0.707	0.654	0.589	0.541	0.473
2.50	0.905	0.860	0.703	0.652	0.586	0.538	0.470
3.00	0.906	0.860	0.702	0.651	0.586	0.537	0.470
3.51	0.906	0.860	0.701	0.651	0.585	0.537	0.469
4.01	0.907	0.860	0.701	0.651	0.585	0.537	0.469
5.01	0.907	0.859	0.699	0.650	0.584	0.536	0.468
6.00	0.907	0.859	0.698	0.649	0.584	0.535	0.468
7.00	0.907	0.858	0.697	0.648	0.583	0.535	0.467
8.00	0.907	0.857	0.696	0.648	0.583	0.534	0.466

Table 158. Static Pressure Ratios for Nozzle 99, $x_r/l_r = 0.02$, $\theta = 30°$, $\phi = 0°$, Minimum Sidewall, $\delta_{v,p} = 20°$, and $\delta_{v,y} = 0°$

(a) Upper ramp

NPR	Static pressure ratios at x_r/l_r of—								
	−0.170	−0.032	0.106	0.175	0.244	0.382	0.520	0.659	0.797
2.00	0.700	0.780	0.717	0.668	0.599	0.524	0.533	0.527	0.506
2.50	0.694	0.777	0.711	0.662	0.590	0.429	0.385	0.431	0.430
3.00	0.692	0.776	0.709	0.660	0.587	0.426	0.306	0.274	0.348
3.50	0.691	0.776	0.708	0.659	0.586	0.425	0.303	0.216	0.258
4.00	0.690	0.776	0.708	0.658	0.586	0.424	0.302	0.189	0.170
5.00	0.688	0.775	0.707	0.657	0.586	0.423	0.299	0.188	0.123
6.00	0.686	0.775	0.706	0.657	0.587	0.423	0.298	0.188	0.123
8.00	0.684	0.775	0.705	0.655	0.587	0.422	0.297	0.188	0.124

(b) Lower flap

NPR	Static pressure ratios at x_r/l_r of—						
	−0.308	−0.170	−0.032	0.037	0.079	0.120	0.162
2.00	0.901	0.856	0.710	0.626	0.564	0.499	0.472
2.50	0.899	0.854	0.705	0.621	0.557	0.489	0.464
3.00	0.898	0.854	0.703	0.619	0.555	0.486	0.461
3.50	0.898	0.854	0.702	0.618	0.555	0.485	0.460
4.00	0.899	0.854	0.702	0.618	0.555	0.484	0.459
5.00	0.899	0.853	0.701	0.617	0.554	0.483	0.458
6.00	0.899	0.853	0.700	0.617	0.554	0.482	0.457
8.00	0.899	0.852	0.699	0.616	0.553	0.480	0.455

Table 159. Static Pressure Ratios for Nozzle 100, $x_r/l_r = 0.02$, $\theta = 30°$, $\phi = 0°$, Medium Sidewall, $\delta_{v,p} = 20°$, and $\delta_{v,y} = 0°$

(a) Upper ramp

NPR	Static pressure ratios at x_r/l_r of—								
	−0.170	−0.032	0.106	0.175	0.244	0.382	0.520	0.659	0.797
2.01	0.700	0.780	0.713	0.667	0.595	0.523	0.532	0.523	0.504
2.50	0.694	0.777	0.711	0.662	0.591	0.430	0.385	0.431	0.428
3.01	0.692	0.776	0.708	0.660	0.586	0.426	0.307	0.273	0.334
3.50	0.690	0.776	0.708	0.659	0.586	0.425	0.303	0.215	0.205
4.00	0.689	0.775	0.707	0.658	0.586	0.424	0.302	0.189	0.159
5.00	0.687	0.775	0.707	0.657	0.586	0.423	0.300	0.189	0.123
6.00	0.686	0.775	0.706	0.656	0.586	0.422	0.299	0.188	0.123
8.00	0.684	0.774	0.705	0.655	0.587	0.421	0.297	0.188	0.124

(b) Lower flap

NPR	Static pressure ratios at x_r/l_r of—						
	−0.308	−0.170	−0.032	0.037	0.079	0.120	0.162
2.01	0.901	0.856	0.710	0.626	0.564	0.498	0.472
2.50	0.899	0.854	0.706	0.621	0.557	0.490	0.465
3.01	0.899	0.854	0.703	0.619	0.555	0.486	0.461
3.50	0.899	0.853	0.703	0.618	0.555	0.485	0.460
4.00	0.899	0.853	0.702	0.618	0.554	0.484	0.459
5.00	0.899	0.853	0.701	0.617	0.554	0.482	0.457
6.00	0.900	0.853	0.700	0.617	0.554	0.481	0.456
8.00	0.900	0.852	0.699	0.616	0.553	0.480	0.455

Table 160. Static Pressure Ratios for Nozzle 101, $x_r/l_r = 0.02$, $\theta = 30°$, $\phi = 0°$, Maximum Sidewall, $\delta_{v,p} = 20°$, and $\delta_{v,y} = 0°$

(a) Upper ramp

NPR	Static pressure ratios at x_r/l_r of—								
	−0.170	−0.032	0.106	0.175	0.244	0.382	0.520	0.659	0.797
2.00	0.701	0.781	0.715	0.668	0.597	0.524	0.533	0.524	0.504
2.50	0.695	0.777	0.711	0.662	0.590	0.430	0.384	0.428	0.431
3.00	0.693	0.777	0.710	0.660	0.588	0.427	0.307	0.274	0.346
3.50	0.691	0.776	0.707	0.659	0.587	0.425	0.303	0.215	0.209
4.00	0.690	0.776	0.708	0.659	0.587	0.425	0.302	0.189	0.159
5.00	0.688	0.776	0.707	0.658	0.586	0.423	0.300	0.189	0.123
6.00	0.687	0.775	0.706	0.657	0.586	0.423	0.299	0.188	0.123
8.00	0.684	0.775	0.705	0.656	0.587	0.422	0.298	0.188	0.124

(b) Lower flap

NPR	Static pressure ratios at x_r/l_r of—						
	−0.308	−0.170	−0.032	0.037	0.079	0.120	0.162
2.00	0.901	0.857	0.711	0.627	0.565	0.500	0.473
2.50	0.900	0.855	0.707	0.622	0.558	0.490	0.465
3.00	0.899	0.854	0.704	0.620	0.556	0.487	0.462
3.50	0.899	0.854	0.703	0.619	0.555	0.485	0.461
4.00	0.899	0.854	0.703	0.618	0.555	0.484	0.459
5.00	0.900	0.853	0.701	0.618	0.554	0.483	0.458
6.00	0.900	0.853	0.701	0.617	0.554	0.482	0.457
8.00	0.900	0.852	0.699	0.616	0.553	0.480	0.455

Table 161. Static Pressure Ratios for Nozzle 106, $x_r/l_r = 0.42$, $\theta = 30°$, $\phi = 0°$, Maximum Sidewall, $\delta_{v,p} = 20°$, and $\delta_{v,y} = -30°$

(a) Upper ramp

NPR	Static pressure ratios at x_r/l_r of—								
	−0.170	−0.032	0.106	0.175	0.244	0.382	0.520	0.659	0.797
2.00	0.739	0.805	0.749	0.699	0.634	0.566	0.553	0.550	0.523
2.50	0.737	0.802	0.746	0.693	0.622	0.467	0.469	0.473	0.424
3.00	0.736	0.802	0.745	0.693	0.620	0.465	0.333	0.401	0.374
3.40	0.735	0.802	0.746	0.693	0.620	0.465	0.326	0.274	0.348
3.50	0.735	0.802	0.745	0.693	0.619	0.465	0.326	0.253	0.339
4.00	0.735	0.802	0.745	0.693	0.620	0.465	0.325	0.218	0.284
5.00	0.734	0.802	0.746	0.692	0.620	0.466	0.323	0.218	0.175
6.00	0.733	0.801	0.746	0.692	0.620	0.466	0.322	0.218	0.172
6.90	0.733	0.801	0.745	0.692	0.621	0.466	0.322	0.218	0.172

(b) Lower flap

NPR	Static pressure ratios at x_r/l_r of—						
	−0.308	−0.170	−0.032	0.037	0.079	0.120	0.162
2.00	0.908	0.864	0.713	0.661	0.596	0.549	0.482
2.50	0.907	0.862	0.709	0.657	0.590	0.543	0.475
3.00	0.907	0.862	0.707	0.656	0.589	0.542	0.474
3.40	0.907	0.862	0.706	0.656	0.589	0.541	0.474
3.50	0.907	0.862	0.706	0.656	0.589	0.542	0.474
4.00	0.907	0.862	0.705	0.656	0.588	0.541	0.474
5.00	0.908	0.862	0.703	0.655	0.588	0.541	0.474
6.00	0.908	0.861	0.702	0.655	0.587	0.540	0.473
6.90	0.908	0.861	0.701	0.654	0.586	0.540	0.473

Table 162. Static Pressure Ratios for Nozzle 107, $x_r/l_r = 0.20$, $\theta = 30°$, $\phi = 0°$, Medium Sidewall, $\delta_{v,p} = 20°$, and $\delta_{v,y} = -30°$

(a) Upper ramp

NPR	Static pressure ratios at x_r/l_r of—								
	−0.170	−0.032	0.106	0.175	0.244	0.382	0.520	0.659	0.797
2.01	0.764	0.819	0.780	0.728	0.669	0.592	0.563	0.502	0.543
2.50	0.758	0.814	0.774	0.718	0.651	0.523	0.485	0.424	0.420
3.00	0.757	0.813	0.773	0.716	0.647	0.506	0.427	0.292	0.376
3.50	0.756	0.813	0.772	0.716	0.645	0.504	0.379	0.247	0.345
4.00	0.756	0.813	0.773	0.716	0.646	0.505	0.376	0.226	0.308
5.01	0.755	0.812	0.773	0.716	0.645	0.504	0.374	0.195	0.277
6.00	0.754	0.812	0.773	0.715	0.645	0.505	0.374	0:183	0.276
7.00	0.754	0.811	0.773	0.715	0.646	0.506	0.374	0.182	0.277
7.50	0.753	0.811	0.773	0.715	0.646	0.506	0.375	0.187	0.277

(b) Lower flap

NPR	Static pressure ratios at x_r/l_r of—						
	−0.308	−0.170	−0.032	0.037	0.079	0.120	0.162
2.01	0.917	0.877	0.741	0.688	0.633	0.590	0.527
2.50	0.915	0.875	0.734	0.680	0.623	0.579	0.513
3.00	0.915	0.874	0.731	0.677	0.621	0.576	0.510
3.50	0.915	0.874	0.730	0.676	0.620	0.576	0.509
4.00	0.915	0.873	0.729	0.677	0.620	0.575	0.508
5.01	0.916	0.873	0.728	0.678	0.619	0.575	0.507
6.00	0.916	0.872	0.728	0.677	0.619	0.574	0.506
7.00	0.916	0.872	0.727	0.676	0.618	0.574	0.506
7.50	0.916	0.871	0.727	0.676	0.618	0.574	0.505

Table 163. Static Pressure Ratios for Nozzle 108, $x_r/l_r = 0.20$, $\theta = 30°$, $\phi = 0°$, Maximum Sidewall, $\delta_{v,p} = 20°$, and $\delta_{v,y} = -30°$

(a) Upper ramp

NPR	Static pressure ratios at x_r/l_r of—								
	−0.170	−0.032	0.106	0.175	0.244	0.382	0.520	0.659	0.797
2.00	0.764	0.819	0.776	0.727	0.666	0.590	0.564	0.511	0.545
2.50	0.758	0.814	0.773	0.718	0.649	0.519	0.481	0.443	0.423
3.00	0.757	0.813	0.772	0.716	0.645	0.505	0.426	0.300	0.378
3.50	0.756	0.813	0.772	0.715	0.644	0.504	0.378	0.266	0.348
4.00	0.756	0.813	0.772	0.715	0.644	0.504	0.375	0.249	0.311
5.00	0.755	0.812	0.773	0.715	0.645	0.505	0.374	0.220	0.279
6.00	0.754	0.812	0.772	0.715	0.645	0.505	0.373	0.207	0.278
7.00	0.754	0.812	0.773	0.715	0.645	0.506	0.373	0.207	0.278
7.40	0.754	0.811	0.773	0.715	0.645	0.506	0.374	0.207	0.278

(b) Lower flap

NPR	Static pressure ratios at x_r/l_r of—						
	−0.308	−0.170	−0.032	0.037	0.079	0.120	0.162
2.00	0.917	0.877	0.741	0.685	0.631	0.589	0.525
2.50	0.915	0.874	0.734	0.677	0.622	0.579	0.513
3.00	0.914	0.873	0.731	0.675	0.621	0.576	0.510
3.50	0.915	0.873	0.730	0.674	0.620	0.576	0.509
4.00	0.915	0.873	0.730	0.674	0.620	0.575	0.509
5.00	0.916	0.873	0.729	0.673	0.619	0.575	0.507
6.00	0.916	0.872	0.728	0.671	0.618	0.574	0.506
7.00	0.916	0.872	0.727	0.670	0.619	0.574	0.506
7.40	0.916	0.871	0.727	0.670	0.618	0.574	0.506

Table 164. Static Pressure Ratios for Nozzle 109, $x_r/l_r = 0.02$, $\theta = 30°$, $\phi = 0°$, Minimum Sidewall, $\delta_{v,p} = 20°$, and $\delta_{v,y} = -30°$

(a) Upper ramp

NPR	Static pressure ratios at x_r/l_r of—								
	−0.170	−0.032	0.106	0.175	0.244	0.382	0.520	0.659	0.797
2.01	0.763	0.819	0.757	0.711	0.643	0.530	0.531	0.524	0.504
2.50	0.758	0.816	0.754	0.704	0.633	0.457	0.383	0.399	0.452
3.00	0.757	0.816	0.753	0.703	0.631	0.453	0.314	0.258	0.341
3.50	0.756	0.816	0.752	0.703	0.629	0.451	0.308	0.207	0.254
4.00	0.756	0.816	0.752	0.700	0.630	0.451	0.306	0.189	0.203
5.00	0.754	0.815	0.752	0.699	0.629	0.450	0.304	0.186	0.119
6.00	0.754	0.815	0.751	0.699	0.629	0.449	0.302	0.185	0.118
8.00	0.752	0.815	0.750	0.697	0.630	0.448	0.302	0.185	0.118

(b) Lower flap

NPR	Static pressure ratios at x_r/l_r of—						
	−0.308	−0.170	−0.032	0.037	0.079	0.120	0.162
2.01	0.921	0.885	0.762	0.683	0.628	0.570	0.523
2.50	0.920	0.884	0.758	0.678	0.622	0.563	0.514
3.00	0.919	0.883	0.757	0.677	0.621	0.561	0.513
3.50	0.920	0.883	0.756	0.676	0.621	0.560	0.512
4.00	0.920	0.883	0.756	0.676	0.620	0.560	0.511
5.00	0.920	0.883	0.755	0.675	0.620	0.558	0.510
6.00	0.920	0.883	0.754	0.674	0.620	0.557	0.509
8.00	0.920	0.881	0.753	0.673	0.619	0.556	0.507

Table 165. Static Pressure Ratios for Nozzle 110, $x_r/l_r = 0.02$, $\theta = 30°$, $\phi = 0°$, Medium Sidewall, $\delta_{v,p} = 20°$, and $\delta_{v,y} = -30°$

(a) Upper ramp

	Static pressure ratios at x_r/l_r of—								
NPR	−0.170	−0.032	0.106	0.175	0.244	0.382	0.520	0.659	0.797
2.00	0.781	0.832	0.775	0.732	0.671	0.567	0.537	0.524	0.507
2.50	0.776	0.828	0.770	0.723	0.657	0.508	0.438	0.384	0.446
3.00	0.774	0.828	0.769	0.721	0.654	0.490	0.404	0.290	0.317
3.50	0.774	0.828	0.769	0.720	0.653	0.487	0.376	0.255	0.253
4.00	0.773	0.828	0.768	0.720	0.653	0.486	0.369	0.239	0.206
5.00	0.772	0.828	0.768	0.719	0.653	0.485	0.366	0.227	0.136
6.00	0.771	0.828	0.768	0.718	0.654	0.485	0.365	0.227	0.129
7.60	0.770	0.827	0.768	0.718	0.655	0.484	0.364	0.227	0.129

(b) Lower flap

	Static pressure ratios at x_r/l_r of						
NPR	−0.308	−0.170	−0.032	0.037	0.079	0.120	0.162
2.00	0.926	0.893	0.778	0.705	0.653	0.600	0.552
2.50	0.925	0.891	0.773	0.699	0.645	0.590	0.541
3.00	0.924	0.891	0.772	0.697	0.644	0.588	0.538
3.50	0.924	0.891	0.771	0.696	0.643	0.587	0.537
4.00	0.925	0.891	0.771	0.696	0.643	0.586	0.536
5.00	0.925	0.890	0.770	0.695	0.643	0.586	0.535
6.00	0.926	0.890	0.770	0.695	0.643	0.585	0.534
7.60	0.925	0.889	0.769	0.693	0.642	0.584	0.533

Table 166. Static Pressure Ratios for Nozzle 111, $x_r/l_r = 0.02$, $\theta = 30°$, $\phi = 0°$, Maximum Sidewall, $\delta_{v,p} = 20°$, and $\delta_{v,y} = -30°$

(a) Upper ramp

NPR	Static pressure ratios at x_r/l_r of								
	−0.170	−0.032	0.106	0.175	0.244	0.382	0.520	0.659	0.797
2.00	0.780	0.832	0.775	0.732	0.672	0.574	0.548	0.525	0.509
2.50	0.775	0.828	0.769	0.722	0.656	0.509	0.458	0.399	0.430
3.00	0.773	0.827	0.769	0.720	0.652	0.490	0.415	0.342	0.326
3.50	0.773	0.827	0.768	0.720	0.652	0.487	0.381	0.321	0.270
4.00	0.772	0.827	0.768	0.719	0.652	0.485	0.371	0.304	0.225
5.00	0.771	0.827	0.768	0.718	0.653	0.485	0.367	0.284	0.170
6.00	0.770	0.827	0.768	0.718	0.653	0.484	0.366	0.282	0.162
7.21	0.769	0.827	0.767	0.717	0.654	0.484	0.365	0.284	0.161

(b) Lower flap

NPR	Static pressure ratios at x_r/l_r of						
	−0.308	−0.170	−0.032	0.037	0.079	0.120	0.162
2.00	0.926	0.893	0.778	0.705	0.653	0.600	0.552
2.50	0.924	0.891	0.773	0.698	0.645	0.590	0.540
3.00	0.924	0.890	0.771	0.696	0.643	0.588	0.538
3.50	0.924	0.890	0.771	0.696	0.643	0.587	0.537
4.00	0.925	0.890	0.770	0.695	0.643	0.586	0.536
5.00	0.925	0.890	0.770	0.695	0.643	0.585	0.534
6.00	0.925	0.890	0.770	0.694	0.642	0.585	0.534
7.21	0.925	0.889	0.769	0.693	0.642	0.584	0.533

Table 167. Static Pressure Ratios for Nozzle 122, $x_r/l_r = 0.20$, $\theta = 30°$, $\phi = 15°$, Medium Sidewall, $\delta_{v,p} = 0°$, and $\delta_{v,y} = -15°$

(a) Upper ramp

NPR	Static pressure ratios at x_r/l_r of—											
	−0.308	−0.170	−0.101	−0.032	0.037	0.106	0.175	0.244	0.382	0.520	0.659	0.797
2.00	0.856	0.645	0.583	0.526	0.489	0.458	0.423	0.550	0.558	0.556	0.536	0.503
2.51	0.856	0.643	0.578	0.524	0.486	0.456	0.419	0.376	0.341	0.527	0.470	0.366
3.00	0.856	0.643	0.580	0.524	0.487	0.457	0.417	0.376	0.274	0.347	0.417	0.452
3.50	0.856	0.643	0.580	0.524	0.486	0.457	0.416	0.376	0.274	0.248	0.343	0.305
4.00	0.856	0.642	0.580	0.523	0.487	0.457	0.415	0.376	0.274	0.249	0.201	0.266
5.00	0.855	0.641	0.580	0.523	0.486	0.457	0.413	0.376	0.273	0.270	0.199	0.159
6.00	0.855	0.640	0.579	0.522	0.486	0.456	0.413	0.376	0.273	0.273	0.199	0.158
7.00	0.854	0.640	0.579	0.522	0.486	0.457	0.412	0.376	0.273	0.275	0.199	0.158
8.01	0.854	0.639	0.579	0.522	0.487	0.457	0.412	0.377	0.273	0.274	0.199	0.158

(b) Lower flap

NPR	Static pressure ratios at x_r/l_r of—						
	−0.308	−0.170	−0.032	0.037	0.079	0.120	0.162
2.00	0.894	0.832	0.616	0.479	0.395	0.422	0.465
2.51	0.893	0.832	0.616	0.478	0.395	0.336	0.259
3.00	0.894	0.832	0.616	0.478	0.394	0.320	0.258
3.50	0.894	0.832	0.616	0.478	0.394	0.305	0.258
4.00	0.895	0.832	0.616	0.478	0.394	0.297	0.258
5.00	0.895	0.832	0.616	0.477	0.393	0.289	0.257
6.00	0.895	0.832	0.616	0.477	0.393	0.286	0.257
7.00	0.896	0.832	0.616	0.477	0.393	0.284	0.256
8.01	0.896	0.831	0.615	0.477	0.393	0.283	0.257

Table 168. Static Pressure Ratios for Nozzle 123, $x_r/l_r = 0.20$, $\theta = 30°$, $\phi = 15°$, Maximum Sidewall, $\delta_{v,p} = 0°$, and $\delta_{v,y} = -15°$

(a) Upper ramp

NPR	Static pressure ratios at x_r/l_r of—											
	−0.308	−0.170	−0.101	−0.032	0.037	0.106	0.175	0.244	0.382	0.520	0.659	0.797
2.00	0.856	0.644	0.580	0.525	0.488	0.456	0.423	0.553	0.560	0.568	0.544	0.513
2.50	0.856	0.643	0.578	0.524	0.486	0.455	0.419	0.376	0.356	0.526	0.475	0.397
3.00	0.856	0.643	0.579	0.523	0.486	0.456	0.417	0.376	0.274	0.346	0.418	0.469
3.50	0.855	0.642	0.579	0.523	0.486	0.456	0.415	0.375	0.274	0.221	0.346	0.303
4.00	0.855	0.642	0.579	0.523	0.486	0.456	0.414	0.375	0.274	0.220	0.202	0.269
5.00	0.855	0.641	0.579	0.522	0.485	0.456	0.413	0.375	0.274	0.220	0.200	0.160
6.00	0.854	0.640	0.579	0.521	0.485	0.456	0.412	0.375	0.274	0.220	0.200	0.159
7.00	0.854	0.639	0.578	0.521	0.486	0.456	0.411	0.375	0.273	0.219	0.199	0.159
8.00	0.853	0.638	0.578	0.521	0.486	0.456	0.411	0.376	0.273	0.219	0.200	0.160

(b) Lower flap

NPR	Static pressure ratios at x_r/l_r of—						
	−0.308	−0.170	−0.032	0.037	0.079	0.120	0.162
2.00	0.894	0.831	0.616	0.479	0.395	0.424	0.464
2.50	0.893	0.831	0.616	0.478	0.394	0.338	0.259
3.00	0.893	0.832	0.616	0.478	0.394	0.320	0.259
3.50	0.894	0.832	0.615	0.478	0.393	0.304	0.259
4.00	0.894	0.832	0.615	0.477	0.393	0.296	0.258
5.00	0.895	0.832	0.615	0.477	0.393	0.289	0.257
6.00	0.895	0.832	0.615	0.477	0.393	0.285	0.257
7.00	0.895	0.831	0.615	0.477	0.393	0.284	0.256
8.00	0.895	0.831	0.615	0.477	0.393	0.283	0.256

Table 169. Static Pressure Ratios for Nozzle 124, $x_r/l_r = 0.20$, $\theta = 30°$, $\phi = 15°$, Medium Sidewall, $\delta_{v,p} = 0°$, and $\delta_{v,y} = -30°$

(a) Upper ramp

NPR	Static pressure ratios at x_r/l_r of—											
	−0.308	−0.170	−0.101	−0.032	0.037	0.106	0.175	0.244	0.382	0.520	0.659	0.797
2.00	0.838	0.644	0.574	0.526	0.490	0.462	0.501	0.584	0.580	0.573	0.546	0.531
2.50	0.837	0.642	0.569	0.523	0.484	0.455	0.426	0.403	0.522	0.528	0.432	0.428
3.00	0.837	0.642	0.569	0.522	0.484	0.454	0.422	0.399	0.329	0.466	0.409	0.390
3.50	0.837	0.641	0.569	0.522	0.484	0.454	0.420	0.398	0.327	0.393	0.363	0.281
4.00	0.837	0.641	0.569	0.522	0.483	0.454	0.419	0.398	0.326	0.329	0.339	0.252
5.00	0.837	0.640	0.569	0.521	0.483	0.454	0.417	0.398	0.325	0.323	0.290	0.222
6.00	0.837	0.640	0.568	0.520	0.483	0.454	0.416	0.398	0.325	0.323	0.282	0.202
7.00	0.836	0.639	0.568	0.520	0.482	0.453	0.415	0.399	0.325	0.323	0.282	0.199
8.00	0.836	0.639	0.568	0.519	0.483	0.453	0.415	0.399	0.325	0.323	0.282	0.199

(b) Lower flap

NPR	Static pressure ratios at x_r/l_r of —						
	−0.308	−0.170	−0.032	0.037	0.079	0.120	0.162
2.00	0.895	0.833	0.615	0.480	0.398	0.316	0.481
2.50	0.895	0.833	0.613	0.478	0.396	0.312	0.258
3.00	0.895	0.833	0.613	0.478	0.395	0.311	0.256
3.50	0.895	0.833	0.613	0.477	0.395	0.311	0.256
4.00	0.896	0.833	0.613	0.477	0.395	0.311	0.255
5.00	0.896	0.833	0.613	0.476	0.395	0.310	0.255
6.00	0.896	0.833	0.612	0.476	0.395	0.310	0.255
7.00	0.897	0.832	0.612	0.476	0.395	0.309	0.254
8.00	0.897	0.832	0.612	0.475	0.395	0.309	0.254

Table 170. Static Pressure Ratios for Nozzle 125, $x_r/l_r = 0.20$, $\theta = 30°$, $\phi = 15°$, Maximum Sidewall, $\delta_{v,p} = 0°$, and $\delta_{v,y} = -30°$

(a) Upper ramp

NPR	Static pressure ratios at x_r/l_r of—											
	−0.308	−0.170	−0.101	−0.032	0.037	0.106	0.175	0.244	0.382	0.520	0.659	0.797
2.00	0.838	0.645	0.575	0.527	0.490	0.463	0.503	0.587	0.595	0.602	0.583	0.555
2.50	0.838	0.644	0.573	0.525	0.488	0.457	0.426	0.401	0.533	0.549	0.513	0.478
3.00	0.838	0.643	0.570	0.524	0.484	0.455	0.422	0.396	0.327	0.481	0.483	0.467
3.50	0.838	0.642	0.570	0.523	0.484	0.455	0.420	0.395	0.324	0.399	0.414	0.393
4.00	0.838	0.642	0.570	0.523	0.484	0.455	0.419	0.395	0.323	0.330	0.374	0.366
5.00	0.837	0.642	0.570	0.522	0.483	0.455	0.417	0.395	0.323	0.323	0.303	0.320
6.00	0.837	0.641	0.569	0.522	0.483	0.455	0.417	0.395	0.322	0.323	0.289	0.284
7.00	0.837	0.640	0.569	0.521	0.483	0.455	0.416	0.395	0.322	0.323	0.289	0.270
8.00	0.836	0.640	0.569	0.521	0.483	0.455	0.415	0.396	0.322	0.323	0.289	0.269

(b) Lower flap

NPR	Static pressure ratios at x_r/l_r of						
	−0.308	−0.170	−0.032	0.037	0.079	0.120	0.162
2.00	0.895	0.833	0.614	0.480	0.398	0.315	0.480
2.50	0.895	0.833	0.614	0.478	0.396	0.312	0.258
3.00	0.895	0.833	0.613	0.478	0.396	0.311	0.257
3.50	0.895	0.833	0.612	0.477	0.395	0.311	0.256
4.00	0.896	0.833	0.613	0.477	0.395	0.310	0.256
5.00	0.896	0.833	0.613	0.476	0.395	0.310	0.255
6.00	0.896	0.832	0.612	0.476	0.395	0.310	0.255
7.00	0.896	0.832	0.612	0.476	0.395	0.310	0.255
8.00	0.897	0.832	0.612	0.475	0.395	0.309	0.254

Table 171. Static Pressure Ratios for Nozzle 126, $x_r/l_r = 0.20$, $\theta = 30°$, $\phi = 30°$, Medium Sidewall, $\delta_{v,p} = 0°$, and $\delta_{v,y} = -15°$

(a) Upper ramp

NPR	Static pressure ratios at x_r/l_r of—											
	−0.308	−0.170	−0.101	−0.032	0.037	0.106	0.175	0.244	0.382	0.520	0.659	0.797
2.00	0.854	0.650	0.562	0.534	0.490	0.450	0.427	0.547	0.557	0.550	0.533	0.527
2.51	0.853	0.649	0.559	0.534	0.489	0.450	0.424	0.372	0.297	0.518	0.477	0.404
3.00	0.853	0.649	0.559	0.534	0.490	0.450	0.422	0.372	0.273	0.317	0.398	0.468
3.50	0.852	0.648	0.558	0.533	0.489	0.448	0.420	0.371	0.272	0.221	0.333	0.312
4.00	0.852	0.648	0.557	0.533	0.488	0.448	0.419	0.370	0.272	0.221	0.195	0.274
5.00	0.852	0.647	0.556	0.533	0.487	0.447	0.417	0.370	0.272	0.219	0.196	0.166
6.00	0.851	0.647	0.555	0.532	0.488	0.447	0.417	0.370	0.272	0.219	0.195	0.166
6.99	0.851	0.646	0.554	0.532	0.488	0.447	0.416	0.370	0.271	0.219	0.195	0.166
8.00	0.850	0.645	0.554	0.531	0.488	0.446	0.416	0.370	0.272	0.218	0.195	0.166

(b) Lower flap

NPR	Static pressure ratios at x_r/l_r of—						
	−0.308	−0.170	−0.032	0.037	0.079	0.120	0.162
2.00	0.894	0.832	0.621	0.486	0.394	0.315	0.481
2.51	0.894	0.832	0.621	0.486	0.394	0.308	0.258
3.00	0.894	0.832	0.621	0.485	0.393	0.308	0.256
3.50	0.894	0.832	0.621	0.485	0.393	0.307	0.255
4.00	0.894	0.832	0.621	0.485	0.392	0.307	0.255
5.00	0.895	0.832	0.621	0.485	0.392	0.306	0.254
6.00	0.895	0.832	0.621	0.485	0.392	0.306	0.254
6.99	0.895	0.831	0.621	0.485	0.392	0.305	0.254
8.00	0.896	0.831	0.621	0.485	0.392	0.305	0.254

Table 172. Static Pressure Ratios for Nozzle 127, $x_r/l_r = 0.20$, $\theta = 30°$, $\phi = 30°$, Maximum Sidewall, $\delta_{v,p} = 0°$, and $\delta_{v,y} = -15°$

(a) Upper ramp

NPR	Static pressure ratios at x_r/l_r of—											
	−0.308	−0.170	−0.101	−0.032	0.037	0.106	0.175	0.244	0.382	0.520	0.659	0.797
2.00	0.854	0.651	0.564	0.535	0.494	0.452	0.427	0.547	0.558	0.552	0.539	0.531
2.50	0.854	0.650	0.561	0.535	0.492	0.450	0.424	0.372	0.316	0.523	0.479	0.421
3.00	0.853	0.649	0.559	0.534	0.490	0.449	0.421	0.371	0.273	0.317	0.399	0.475
3.50	0.853	0.649	0.558	0.534	0.489	0.449	0.420	0.371	0.272	0.220	0.335	0.312
4.00	0.853	0.649	0.557	0.534	0.489	0.449	0.419	0.370	0.272	0.219	0.196	0.274
5.00	0.852	0.648	0.556	0.533	0.488	0.448	0.418	0.370	0.272	0.218	0.195	0.166
6.00	0.851	0.647	0.555	0.533	0.488	0.447	0.417	0.370	0.272	0.218	0.195	0.166
7.00	0.851	0.646	0.554	0.532	0.488	0.447	0.416	0.370	0.272	0.218	0.195	0.167
7.99	0.850	0.645	0.553	0.532	0.488	0.446	0.416	0.370	0.272	0.218	0.195	0.167

(b) Lower flap

NPR	Static pressure ratios at x_r/l_r of—						
	−0.308	−0.170	−0.032	0.037	0.079	0.120	0.162
2.00	0.894	0.832	0.622	0.486	0.395	0.315	0.481
2.50	0.894	0.832	0.622	0.486	0.394	0.309	0.258
3.00	0.894	0.832	0.621	0.486	0.393	0.308	0.256
3.50	0.894	0.832	0.621	0.486	0.393	0.307	0.255
4.00	0.894	0.832	0.621	0.486	0.393	0.307	0.255
5.00	0.895	0.832	0.621	0.485	0.392	0.306	0.254
6.00	0.895	0.832	0.621	0.485	0.392	0.306	0.254
7.00	0.895	0.831	0.621	0.486	0.392	0.305	0.254
7.99	0.896	0.831	0.621	0.485	0.392	0.305	0.254

Table 173. Static Pressure Ratios for Nozzle 128, $x_r/l_r = 0.20$, $\theta = 30°$, $\phi = 30°$, Medium Sidewall, $\delta_{v,p} = 0°$, and $\delta_{v,y} = -30°$

(a) Upper ramp

NPR	Static pressure ratios at x_r/l_r of—											
	−0.308	−0.170	−0.101	−0.032	0.037	0.106	0.175	0.244	0.382	0.520	0.659	0.797
2.00	0.832	0.649	0.585	0.531	0.497	0.467	0.486	0.580	0.573	0.568	0.543	0.518
2.50	0.832	0.648	0.583	0.529	0.494	0.461	0.441	0.411	0.500	0.527	0.445	0.404
3.00	0.831	0.648	0.581	0.528	0.491	0.459	0.438	0.408	0.329	0.449	0.393	0.370
3.50	0.830	0.648	0.581	0.527	0.491	0.459	0.436	0.407	0.327	0.327	0.360	0.262
4.00	0.829	0.647	0.581	0.527	0.490	0.458	0.435	0.407	0.327	0.314	0.331	0.245
5.01	0.829	0.647	0.581	0.526	0.489	0.458	0.434	0.407	0.326	0.312	0.271	0.217
6.00	0.828	0.646	0.581	0.525	0.489	0.457	0.433	0.407	0.325	0.312	0.269	0.197
7.00	0.827	0.646	0.581	0.524	0.489	0.457	0.433	0.407	0.325	0.312	0.269	0.197
8.00	0.826	0.645	0.580	0.524	0.489	0.456	0.432	0.407	0.325	0.312	0.269	0.197

(b) Lower flap

NPR	Static pressure ratios at x_r/l_r of—						
	−0.308	−0.170	−0.032	0.037	0.079	0.120	0.162
2.00	0.894	0.833	0.619	0.478	0.405	0.329	0.463
2.50	0.894	0.833	0.618	0.476	0.404	0.312	0.256
3.00	0.893	0.833	0.616	0.475	0.404	0.311	0.251
3.50	0.893	0.833	0.616	0.474	0.403	0.311	0.251
4.00	0.894	0.833	0.616	0.474	0.403	0.310	0.250
5.01	0.894	0.833	0.615	0.472	0.403	0.310	0.249
6.00	0.895	0.832	0.615	0.472	0.403	0.309	0.249
7.00	0.895	0.832	0.614	0.471	0.403	0.309	0.249
8.00	0.895	0.831	0.614	0.470	0.403	0.309	0.248

Table 174. Static Pressure Ratios for Nozzle 129, $x_r/l_r = 0.20$, $\theta = 30°$, $\phi = 30°$, Maximum Sidewall, $\delta_{v,p} = 0°$, and $\delta_{v,y} = -30°$

(a) Upper ramp

NPR	Static pressure ratios at x_r/l_r of—											
	−0.308	−0.170	−0.101	−0.032	0.037	0.106	0.175	0.244	0.382	0.520	0.659	0.797
2.00	0.832	0.649	0.585	0.531	0.496	0.467	0.489	0.581	0.584	0.589	0.569	0.537
2.50	0.831	0.648	0.582	0.528	0.491	0.460	0.440	0.409	0.507	0.546	0.486	0.442
3.00	0.831	0.648	0.582	0.528	0.491	0.459	0.437	0.407	0.329	0.453	0.437	0.447
3.50	0.830	0.648	0.581	0.527	0.490	0.458	0.435	0.406	0.327	0.329	0.382	0.342
4.00	0.829	0.647	0.581	0.527	0.489	0.458	0.434	0.406	0.326	0.314	0.341	0.317
5.00	0.828	0.647	0.581	0.525	0.489	0.457	0.433	0.406	0.325	0.312	0.272	0.277
6.00	0.828	0.646	0.581	0.525	0.489	0.456	0.432	0.406	0.325	0.312	0.270	0.245
7.00	0.827	0.646	0.580	0.524	0.489	0.456	0.432	0.406	0.325	0.312	0.270	0.239
8.01	0.826	0.645	0.580	0.523	0.488	0.456	0.431	0.406	0.324	0.312	0.270	0.239

(b) Lower flap

NPR	Static pressure ratios at x_r/l_r of—						
	−0.308	−0.170	−0.032	0.037	0.079	0.120	0.162
2.00	0.893	0.833	0.619	0.479	0.405	0.329	0.459
2.50	0.893	0.833	0.618	0.477	0.404	0.312	0.256
3.00	0.893	0.833	0.617	0.475	0.404	0.311	0.251
3.50	0.893	0.833	0.616	0.474	0.403	0.311	0.251
4.00	0.894	0.833	0.616	0.474	0.403	0.310	0.250
5.00	0.894	0.833	0.615	0.473	0.403	0.310	0.249
6.00	0.894	0.832	0.615	0.472	0.403	0.309	0.249
7.00	0.895	0.832	0.614	0.471	0.403	0.309	0.248
8.01	0.894	0.831	0.614	0.470	0.403	0.308	0.248

Table 175. Static Pressure Ratios for Nozzle 130, $x_r/l_r = 0.20$, $\theta = 30°$, $\phi = 15°$, Medium Sidewall, $\delta_{v,p} = -20°$, and $\delta_{v,y} = -15°$

(a) Upper ramp

NPR	Static pressure ratios at x_r/l_r of—											
	−0.308	−0.170	−0.101	−0.032	0.037	0.106	0.175	0.244	0.382	0.520	0.659	0.797
2.00	0.834	0.642	0.577	0.478	0.248	0.369	0.382	0.401	0.454	0.492	0.514	0.519
2.50	0.834	0.642	0.575	0.478	0.244	0.186	0.306	0.325	0.344	0.377	0.423	0.441
3.00	0.834	0.641	0.574	0.478	0.245	0.187	0.189	0.172	0.258	0.276	0.393	0.397
3.50	0.834	0.642	0.575	0.478	0.243	0.186	0.187	0.172	0.150	0.238	0.269	0.350
4.00	0.833	0.642	0.575	0.478	0.243	0.186	0.186	0.171	0.136	0.225	0.235	0.273
5.00	0.833	0.641	0.575	0.478	0.242	0.186	0.184	0.171	0.136	0.119	0.097	0.196
6.00	0.833	0.640	0.574	0.478	0.242	0.185	0.183	0.171	0.135	0.118	0.096	0.112
7.00	0.832	0.639	0.574	0.477	0.241	0.184	0.182	0.170	0.135	0.118	0.096	0.112
8.00	0.832	0.639	0.573	0.477	0.241	0.184	0.181	0.170	0.135	0.118	0.096	0.112

(b) Lower flap

NPR	Static pressure ratios at x_r/l_r of—						
	−0.308	−0.170	−0.032	0.037	0.079	0.120	0.162
2.00	0.895	0.833	0.617	0.476	0.389	0.417	0.462
2.50	0.895	0.833	0.617	0.476	0.389	0.327	0.310
3.00	0.894	0.833	0.616	0.475	0.388	0.312	0.243
3.50	0.895	0.833	0.616	0.475	0.388	0.298	0.243
4.00	0.896	0.833	0.616	0.475	0.388	0.291	0.242
5.00	0.896	0.833	0.616	0.475	0.388	0.284	0.242
6.00	0.896	0.833	0.616	0.475	0.388	0.280	0.242
7.00	0.896	0.832	0.616	0.475	0.388	0.279	0.241
8.00	0.896	0.832	0.616	0.474	0.388	0.278	0.241

Table 176. Static Pressure Ratios for Nozzle 131, $x_r/l_r = 0.20$, $\theta = 30°$, $\phi = 15°$, Maximum Sidewall, $\delta_{v,p} = -20°$, and $\delta_{v,y} = -15°$

(a) Upper ramp

NPR	Static pressure ratios at x_r/l_r of—											
	−0.308	−0.170	−0.101	−0.032	0.037	0.106	0.175	0.244	0.382	0.520	0.659	0.797
2.00	0.834	0.642	0.577	0.479	0.250	0.371	0.385	0.396	0.448	0.495	0.520	0.522
2.50	0.834	0.643	0.575	0.479	0.246	0.186	0.328	0.336	0.355	0.381	0.427	0.459
3.00	0.833	0.642	0.574	0.478	0.245	0.187	0.188	0.172	0.282	0.305	0.351	0.391
3.50	0.833	0.642	0.575	0.478	0.244	0.186	0.187	0.172	0.234	0.252	0.280	0.343
4.00	0.833	0.641	0.574	0.478	0.243	0.186	0.186	0.171	0.137	0.189	0.217	0.261
5.00	0.833	0.640	0.574	0.478	0.242	0.185	0.184	0.171	0.136	0.118	0.097	0.193
6.00	0.832	0.640	0.574	0.477	0.241	0.185	0.182	0.170	0.136	0.118	0.096	0.112
7.00	0.832	0.639	0.573	0.477	0.241	0.184	0.181	0.170	0.136	0.117	0.096	0.112
8.00	0.831	0.638	0.573	0.476	0.240	0.184	0.181	0.170	0.136	0.117	0.096	0.112

(b) Lower flap

NPR	Static pressure ratios at x_r/l_r of—						
	−0.308	−0.170	−0.032	0.037	0.079	0.120	0.162
2.00	0.894	0.833	0.617	0.476	0.389	0.417	0.462
2.50	0.894	0.833	0.617	0.476	0.389	0.329	0.303
3.00	0.894	0.833	0.616	0.475	0.389	0.312	0.24?
3.50	0.895	0.833	0.616	0.475	0.388	0.298	0.24
4.00	0.895	0.833	0.616	0.475	0.388	0.290	0.2?3
5.00	0.896	0.833	0.616	0.475	0.388	0.282	0.242
6.00	0.896	0.833	0.616	0.475	0.388	0.279	0.242
7.00	0.896	0.832	0.616	0.475	0.388	0.277	0.241
8.00	0.896	0.832	0.616	0.475	0.388	0.275	0.241

Table 177. Static Pressure Ratios for Nozzle 132, $x_r/l_r = 0.20$, $\theta = 30°$, $\phi = 15°$, Medium Sidewall, $\delta_{v,p} = -20°$, and $\delta_{v,y} = -30°$

(a) Upper ramp

NPR	Static pressure ratios at x_r/l_r of—											
	−0.308	−0.170	−0.101	−0.032	0.037	0.106	0.175	0.244	0.382	0.520	0.659	0.797
2.00	0.855	0.647	0.573	0.483	0.298	0.402	0.418	0.437	0.460	0.485	0.519	0.529
2.50	0.855	0.647	0.572	0.482	0.233	0.187	0.259	0.329	0.375	0.448	0.478	0.451
3.00	0.855	0.646	0.571	0.482	0.230	0.187	0.188	0.172	0.304	0.389	0.413	0.390
3.50	0.854	0.646	0.571	0.482	0.230	0.187	0.186	0.172	0.236	0.325	0.383	0.421
4.00	0.854	0.646	0.570	0.482	0.228	0.187	0.185	0.171	0.186	0.233	0.286	0.439
5.00	0.853	0.645	0.570	0.482	0.227	0.186	0.183	0.171	0.192	0.199	0.150	0.168
6.00	0.853	0.645	0.571	0.482	0.226	0.185	0.182	0.170	0.193	0.198	0.148	0.156
7.00	0.852	0.644	0.570	0.482	0.226	0.184	0.181	0.170	0.192	0.198	0.148	0.152
8.00	0.852	0.644	0.570	0.482	0.225	0.184	0.180	0.170	0.190	0.198	0.148	0.152

(b) Lower flap

NPR	Static pressure ratios at x_r/l_r of—						
	−0.308	−0.170	−0.032	0.037	0.079	0.120	0.162
2.00	0.892	0.832	0.612	0.474	0.389	0.350	0.479
2.50	0.892	0.832	0.611	0.473	0.389	0.300	0.298
3.00	0.892	0.832	0.611	0.473	0.388	0.299	0.240
3.50	0.893	0.832	0.611	0.472	0.388	0.299	0.240
4.00	0.893	0.832	0.611	0.472	0.387	0.299	0.240
5.00	0.893	0.832	0.611	0.471	0.387	0.299	0.239
6.00	0.894	0.832	0.611	0.471	0.387	0.298	0.239
7.00	0.894	0.832	0.611	0.471	0.388	0.298	0.239
8.00	0.894	0.831	0.611	0.470	0.388	0.298	0.239

Table 178. Static Pressure Ratios for Nozzle 133, $x_r/l_r = 0.20$, $\theta = 30°$, $\phi = 15°$, Maximum Sidewall, $\delta_{v,p} = -20°$, and $\delta_{v,y} = -30°$

(a) Upper ramp

NPR	Static pressure ratios at x_r/l_r of—											
	−0.308	−0.170	−0.101	−0.032	0.037	0.106	0.175	0.244	0.382	0.520	0.659	0.797
2.00	0.855	0.647	0.575	0.485	0.304	0.406	0.422	0.437	0.460	0.496	0.561	0.571
2.50	0.855	0.647	0.573	0.484	0.233	0.187	0.315	0.344	0.376	0.454	0.552	0.496
3.00	0.854	0.647	0.572	0.483	0.232	0.188	0.188	0.173	0.311	0.418	0.542	0.475
3.50	0.854	0.647	0.571	0.483	0.229	0.187	0.186	0.173	0.252	0.370	0.457	0.484
4.00	0.854	0.646	0.572	0.483	0.229	0.187	0.185	0.172	0.162	0.254	0.364	0.503
4.99	0.853	0.646	0.571	0.483	0.228	0.186	0.183	0.171	0.171	0.198	0.167	0.258
6.00	0.853	0.645	0.571	0.482	0.226	0.185	0.182	0.171	0.170	0.197	0.161	0.230
7.00	0.852	0.644	0.571	0.482	0.226	0.184	0.181	0.171	0.167	0.196	0.160	0.220
8.00	0.852	0.644	0.570	0.482	0.225	0.184	0.180	0.170	0.172	0.197	0.160	0.215

(b) Lower flap

NPR	Static pressure ratios at x_r/l_r of—						
	−0.308	−0.170	−0.032	0.037	0.079	0.120	0.162
2.00	0.892	0.832	0.611	0.473	0.389	0.353	0.479
2.50	0.892	0.832	0.611	0.473	0.388	0.300	0.304
3.00	0.892	0.832	0.611	0.472	0.388	0.299	0.240
3.50	0.892	0.832	0.610	0.472	0.388	0.299	0.240
4.00	0.893	0.832	0.610	0.472	0.387	0.298	0.239
4.99	0.893	0.832	0.610	0.471	0.387	0.298	0.239
6.00	0.894	0.832	0.610	0.471	0.388	0.298	0.239
7.00	0.894	0.832	0.610	0.471	0.388	0.298	0.239
8.00	0.894	0.831	0.610	0.470	0.388	0.298	0.239

Table 179. Static Pressure Ratios for Nozzle 130, $x_r/l_r = 0.20$, $\theta = 30°$, $\phi = 30°$, Medium Sidewall, $\delta_{v,p} = -20°$, and $\delta_{v,y} = -15°$

(a) Upper ramp

NPR	Static pressure ratios at x_r/l_r of—											
	−0.308	−0.170	−0.101	−0.032	0.037	0.106	0.175	0.244	0.382	0.520	0.659	0.797
2.01	0.836	0.654	0.568	0.447	0.234	0.341	0.362	0.377	0.445	0.500	0.527	0.521
2.50	0.835	0.654	0.567	0.445	0.230	0.193	0.191	0.315	0.327	0.342	0.397	0.444
3.00	0.834	0.654	0.566	0.444	0.231	0.195	0.189	0.168	0.269	0.280	0.294	0.353
3.50	0.834	0.653	0.565	0.443	0.230	0.194	0.187	0.167	0.139	0.240	0.261	0.310
4.00	0.833	0.653	0.565	0.442	0.229	0.194	0.186	0.167	0.138	0.212	0.226	0.257
5.01	0.832	0.653	0.564	0.441	0.228	0.193	0.184	0.165	0.138	0.115	0.094	0.165
6.00	0.832	0.652	0.564	0.440	0.227	0.193	0.183	0.165	0.137	0.115	0.094	0.095
7.00	0.831	0.652	0.564	0.439	0.226	0.192	0.182	0.164	0.137	0.115	0.094	0.093
7.99	0.830	0.651	0.563	0.438	0.226	0.192	0.181	0.164	0.137	0.114	0.094	0.093

(b) Lower flap

NPR	Static pressure ratios at x_r/l_r of—						
	−0.308	−0.170	−0.032	0.037	0.079	0.120	0.162
2.01	0.893	0.831	0.618	0.482	0.387	0.361	0.477
2.50	0.893	0.831	0.618	0.481	0.386	0.296	0.318
3.00	0.893	0.831	0.618	0.481	0.386	0.295	0.239
3.50	0.893	0.831	0.617	0.481	0.386	0.294	0.239
4.00	0.894	0.831	0.617	0.481	0.386	0.294	0.238
5.01	0.895	0.831	0.617	0.481	0.385	0.294	0.238
6.00	0.895	0.831	0.617	0.481	0.385	0.293	0.238
7.00	0.895	0.831	0.617	0.481	0.385	0.293	0.238
7.99	0.895	0.830	0.618	0.481	0.385	0.293	0.237

Table 180. Static Pressure Ratios for Nozzle 135, $x_r/l_r = 0.20$, $\theta = 30°$, $\phi = 30°$, Maximum Sidewall, $\delta_{v,p} = -20°$, and $\delta_{v,y} = -15°$

(a) Upper ramp

NPR	Static pressure ratios at x_r/l_r of—											
	−0.308	−0.170	−0.101	−0.032	0.037	0.106	0.175	0.244	0.382	0.520	0.659	0.797
2.00	0.836	0.654	0.567	0.450	0.232	0.331	0.360	0.375	0.439	0.498	0.532	0.528
2.50	0.835	0.655	0.570	0.449	0.233	0.196	0.191	0.309	0.329	0.342	0.414	0.469
3.00	0.834	0.654	0.567	0.447	0.229	0.195	0.189	0.168	0.264	0.275	0.297	0.382
3.50	0.834	0.654	0.566	0.447	0.228	0.194	0.188	0.167	0.138	0.246	0.259	0.286
4.00	0.833	0.654	0.566	0.445	0.228	0.194	0.186	0.167	0.138	0.116	0.195	0.219
5.00	0.832	0.653	0.566	0.444	0.226	0.194	0.185	0.166	0.138	0.115	0.094	0.164
6.00	0.832	0.653	0.565	0.443	0.226	0.193	0.183	0.165	0.137	0.115	0.094	0.099
7.00	0.831	0.652	0.564	0.442	0.225	0.193	0.182	0.164	0.137	0.115	0.094	0.094
8.00	0.830	0.652	0.564	0.441	0.225	0.192	0.182	0.164	0.137	0.115	0.094	0.094

(b) Lower flap

NPR	Static pressure ratios at x_r/l_r of—						
	−0.308	−0.170	−0.032	0.037	0.079	0.120	0.162
2.00	0.893	0.831	0.618	0.480	0.386	0.368	0.477
2.50	0.894	0.831	0.618	0.480	0.386	0.297	0.317
3.00	0.893	0.831	0.618	0.480	0.386	0.296	0.239
3.50	0.894	0.832	0.618	0.480	0.385	0.296	0.239
4.00	0.894	0.832	0.618	0.480	0.385	0.295	0.239
5.00	0.895	0.831	0.618	0.480	0.385	0.295	0.238
6.00	0.895	0.831	0.618	0.480	0.385	0.294	0.238
7.00	0.895	0.831	0.618	0.480	0.385	0.294	0.238
8.00	0.895	0.830	0.618	0.480	0.385	0.294	0.238

Table 181. Static Pressure Ratios for Nozzle 136, $x_r/l_r = 0.20$, $\theta = 30°$, $\phi = 30°$, Medium Sidewall, $\delta_{v,p} = -20°$, and $\delta_{v,y} = -30°$

(a) Upper ramp

NPR	Static pressure ratios at x_r/l_r of—											
	−0.308	−0.170	−0.101	−0.032	0.037	0.106	0.175	0.244	0.382	0.520	0.659	0.797
2.00	0.855	0.629	0.576	0.474	0.240	0.375	0.393	0.415	0.447	0.477	0.513	0.528
2.51	0.855	0.626	0.574	0.473	0.234	0.178	0.295	0.316	0.340	0.382	0.448	0.456
3.00	0.854	0.625	0.574	0.472	0.232	0.178	0.190	0.177	0.268	0.311	0.447	0.382
3.50	0.854	0.623	0.573	0.472	0.231	0.177	0.188	0.176	0.248	0.262	0.333	0.409
4.00	0.854	0.622	0.573	0.472	0.230	0.176	0.187	0.176	0.133	0.249	0.263	0.340
5.00	0.854	0.620	0.572	0.471	0.229	0.176	0.185	0.176	0.132	0.173	0.148	0.166
6.00	0.853	0.619	0.572	0.471	0.228	0.175	0.184	0.175	0.132	0.173	0.148	0.164
7.00	0.853	0.617	0.571	0.471	0.227	0.174	0.183	0.175	0.132	0.173	0.148	0.164
8.00	0.852	0.616	0.571	0.470	0.226	0.174	0.182	0.175	0.131	0.172	0.148	0.165

(b) Lower flap

NPR	Static pressure ratios at x_r/l_r of—						
	−0.308	−0.170	−0.032	0.037	0.079	0.120	0.162
2.00	0.892	0.832	0.614	0.469	0.395	0.376	0.474
2.51	0.893	0.831	0.613	0.467	0.395	0.298	0.317
3.00	0.892	0.832	0.612	0.467	0.395	0.298	0.233
3.50	0.893	0.832	0.612	0.466	0.395	0.298	0.233
4.00	0.893	0.832	0.612	0.465	0.395	0.297	0.232
5.00	0.894	0.831	0.611	0.465	0.395	0.297	0.232
6.00	0.894	0.831	0.611	0.464	0.395	0.296	0.231
7.00	0.894	0.831	0.612	0.464	0.395	0.296	0.231
8.00	0.894	0.830	0.612	0.464	0.395	0.296	0.231

C-3

Table 182. Static Pressure Ratios for Nozzle 137, $x_r/l_r = 0.20$, $\theta = 30°$, $\phi = 30°$, Maximum Sidewall, $\delta_{v,p} = -20°$, and $\delta_{v,y} = -30°$

(a) Upper ramp

NPR	Static pressure ratios at x_r/l_r of—											
	−0.308	−0.170	−0.101	−0.032	0.037	0.106	0.175	0.244	0.382	0.520	0.659	0.797
2.00	0.855	0.629	0.575	0.474	0.240	0.374	0.394	0.419	0.454	0.492	0.539	0.556
2.50	0.855	0.627	0.575	0.473	0.234	0.177	0.212	0.317	0.329	0.423	0.539	0.478
3.00	0.854	0.625	0.574	0.473	0.233	0.178	0.190	0.177	0.265	0.314	0.571	0.461
3.50	0.854	0.623	0.573	0.472	0.231	0.177	0.188	0.177	0.134	0.250	0.370	0.508
4.00	0.854	0.622	0.572	0.472	0.230	0.176	0.187	0.176	0.133	0.239	0.257	0.359
5.00	0.854	0.620	0.572	0.472	0.229	0.176	0.185	0.176	0.133	0.176	0.150	0.176
6.00	0.853	0.618	0.571	0.471	0.227	0.175	0.184	0.175	0.132	0.176	0.149	0.170
7.00	0.853	0.617	0.571	0.471	0.227	0.174	0.183	0.175	0.132	0.176	0.149	0.170
7.99	0.852	0.616	0.570	0.471	0.226	0.174	0.182	0.175	0.132	0.176	0.149	0.170

(b) Lower flap

NPR	Static pressure ratios at x_r/l_r of—						
	−0.308	−0.170	−0.032	0.037	0.079	0.120	0.162
2.00	0.893	0.831	0.615	0.470	0.394	0.373	0.474
2.50	0.893	0.831	0.615	0.469	0.394	0.298	0.321
3.00	0.893	0.831	0.614	0.468	0.394	0.298	0.233
3.50	0.893	0.831	0.614	0.468	0.394	0.297	0.233
4.00	0.893	0.831	0.613	0.467	0.394	0.297	0.232
5.00	0.894	0.831	0.613	0.466	0.394	0.297	0.232
6.00	0.894	0.831	0.613	0.466	0.394	0.297	0.231
7.00	0.894	0.831	0.612	0.465	0.395	0.296	0.231
7.99	0.894	0.830	0.612	0.465	0.395	0.296	0.231

Table 183. Static Pressure Ratios for Nozzle 138, $x_r/l_r = 0.20$, $\theta = 30°$, $\phi = 15°$, Medium Sidewall, $\delta_{v,p} = 20°$, and $\delta_{v,y} = -15°$

(a) Upper ramp

NPR	Static pressure ratios at x_r/l_r of—								
	−0.170	−0.032	0.106	0.175	0.244	0.382	0.520	0.659	0.797
2.00	0.746	0.807	0.758	0.703	0.643	0.554	0.540	0.540	0.513
2.50	0.743	0.804	0.754	0.697	0.631	0.478	0.433	0.402	0.445
3.00	0.743	0.804	0.754	0.696	0.630	0.476	0.338	0.330	0.296
3.50	0.742	0.804	0.754	0.696	0.630	0.477	0.335	0.253	0.253
4.01	0.742	0.804	0.754	0.696	0.629	0.476	0.334	0.224	0.206
5.00	0.741	0.804	0.755	0.696	0.630	0.476	0.333	0.223	0.155
6.01	0.741	0.804	0.755	0.696	0.630	0.477	0.332	0.223	0.155
7.00	0.740	0.803	0.755	0.696	0.631	0.477	0.332	0.223	0.156
7.76	0.740	0.803	0.754	0.696	0.631	0.477	0.331	0.224	0.156

(b) Lower flap

NPR	Static pressure ratios at x_r/l_r of—						
	−0.308	−0.170	−0.032	0.037	0.079	0.120	0.162
2.00	0.912	0.873	0.744	0.652	0.602	0.554	0.502
2.50	0.911	0.872	0.741	0.653	0.595	0.546	0.493
3.00	0.911	0.871	0.740	0.651	0.593	0.545	0.491
3.50	0.911	0.872	0.739	0.651	0.593	0.544	0.490
4.01	0.912	0.871	0.739	0.653	0.592	0.543	0.489
5.00	0.912	0.871	0.738	0.652	0.591	0.542	0.487
6.01	0.912	0.871	0.738	0.651	0.589	0.542	0.486
7.00	0.912	0.870	0.738	0.650	0.588	0.541	0.484
7.76	0.912	0.869	0.737	0.650	0.587	0.540	0.483

Table 184. Static Pressure Ratios for Nozzle 139, $x_r/l_r = 0.20$, $\theta = 30°$, $\phi = 15°$, Maximum Sidewall, $\delta_{v,p} = 20°$, and $\delta_{v,y} = -15°$

(a) Upper ramp

NPR	Static pressure ratios at x_r/l_r of—								
	−0.170	−0.032	0.106	0.175	0.244	0.382	0.520	0.659	0.797
2.00	0.746	0.807	0.757	0.703	0.643	0.554	0.542	0.539	0.513
2.50	0.743	0.804	0.754	0.697	0.630	0.478	0.433	0.402	0.449
3.00	0.742	0.804	0.754	0.696	0.629	0.477	0.338	0.331	0.301
3.50	0.742	0.804	0.754	0.696	0.629	0.477	0.336	0.254	0.254
4.00	0.742	0.804	0.754	0.696	0.629	0.477	0.334	0.224	0.208
5.01	0.741	0.804	0.754	0.696	0.630	0.477	0.333	0.224	0.156
6.01	0.740	0.804	0.755	0.696	0.630	0.477	0.332	0.224	0.156
7.01	0.740	0.803	0.754	0.696	0.630	0.477	0.332	0.224	0.156
7.62	0.739	0.803	0.755	0.696	0.631	0.477	0.332	0.224	0.156

(b) Lower flap

NPR	Static pressure ratios at x_r/l_r of—						
	−0.308	−0.170	−0.032	0.037	0.079	0.120	0.162
2.00	0.912	0.873	0.744	0.659	0.602	0.553	0.502
2.50	0.911	0.872	0.740	0.655	0.595	0.546	0.493
3.00	0.911	0.871	0.739	0.654	0.593	0.545	0.491
3.50	0.911	0.871	0.739	0.653	0.592	0.544	0.489
4.00	0.911	0.871	0.738	0.653	0.592	0.543	0.489
5.01	0.912	0.871	0.738	0.652	0.590	0.542	0.487
6.01	0.912	0.870	0.738	0.651	0.589	0.541	0.485
7.01	0.912	0.870	0.737	0.650	0.588	0.540	0.484
7.62	0.912	0.869	0.737	0.650	0.587	0.540	0.483

Table 185. Static Pressure Ratios for Nozzle 140, $x_r/l_r = 0.20$, $\theta = 30°$, $\phi = 15°$, Medium Sidewall, $\delta_{v,p} = 20°$, and $\delta_{v,y} = -30°$

(a) Upper ramp

NPR	Static pressure ratios at x_r/l_r of—								
	−0.170	−0.032	0.106	0.175	0.244	0.382	0.520	0.659	0.797
2.00	0.778	0.827	0.782	0.734	0.669	0.588	0.558	0.542	0.514
2.50	0.774	0.823	0.778	0.725	0.652	0.525	0.473	0.387	0.461
3.01	0.772	0.822	0.776	0.723	0.647	0.508	0.430	0.334	0.288
3.51	0.771	0.822	0.777	0.722	0.647	0.508	0.392	0.310	0.222
4.00	0.771	0.822	0.776	0.722	0.645	0.507	0.387	0.285	0.199
5.00	0.770	0.821	0.776	0.722	0.646	0.507	0.385	0.267	0.172
6.00	0.769	0.821	0.776	0.722	0.646	0.508	0.385	0.267	0.165
7.01	0.769	0.821	0.776	0.721	0.646	0.509	0.385	0.267	0.165
7.90	0.768	0.821	0.776	0.721	0.646	0.509	0.385	0.268	0.165

(b) Lower flap

NPR	Static pressure ratios at x_r/l_r of—						
	−0.308	−0.170	−0.032	0.037	0.079	0.120	0.162
2.00	0.921	0.886	0.770	0.696	0.646	0.598	0.536
2.50	0.920	0.884	0.766	0.691	0.637	0.588	0.524
3.01	0.919	0.883	0.764	0.691	0.635	0.585	0.521
3.51	0.920	0.883	0.764	0.690	0.634	0.585	0.520
4.00	0.920	0.883	0.763	0.691	0.634	0.584	0.519
5.00	0.921	0.883	0.763	0.692	0.634	0.583	0.518
6.00	0.921	0.882	0.763	0.693	0.634	0.583	0.517
7.01	0.921	0.882	0.763	0.692	0.633	0.583	0.517
7.90	0.921	0.881	0.763	0.692	0.633	0.582	0.516

Table 186. Static Pressure Ratios for Nozzle 141, $x_r/l_r = 0.20$, $\theta = 30°$, $\phi = 15°$, Maximum Sidewall, $\delta_{v,p} = 20°$, and $\delta_{v,y} = -30°$

(a) Upper ramp

NPR	Static pressure ratios at x_r/l_r of—								
	−0.170	−0.032	0.106	0.175	0.244	0.382	0.520	0.659	0.797
2.00	0.778	0.826	0.782	0.734	0.667	0.591	0.567	0.546	0.517
2.50	0.773	0.822	0.777	0.724	0.651	0.526	0.484	0.418	0.448
3.00	0.771	0.821	0.776	0.722	0.647	0.509	0.437	0.370	0.304
3.50	0.770	0.821	0.775	0.722	0.645	0.507	0.393	0.344	0.252
4.01	0.770	0.821	0.775	0.721	0.645	0.507	0.387	0.318	0.232
5.00	0.769	0.821	0.775	0.721	0.645	0.507	0.384	0.291	0.209
6.00	0.768	0.820	0.775	0.721	0.645	0.507	0.384	0.289	0.199
7.01	0.768	0.820	0.775	0.720	0.645	0.508	0.384	0.289	0.199
7.63	0.767	0.820	0.775	0.720	0.645	0.508	0.384	0.290	0.199

(b) Lower flap

NPR	Static pressure ratios at x_r/l_r of—						
	−0.308	−0.170	−0.032	0.037	0.079	0.120	0.162
2.00	0.921	0.886	0.770	0.702	0.645	0.598	0.537
2.50	0.920	0.883	0.765	0.695	0.636	0.588	0.523
3.00	0.919	0.882	0.763	0.693	0.634	0.585	0.520
3.50	0.919	0.883	0.763	0.693	0.633	0.584	0.519
4.01	0.920	0.882	0.763	0.692	0.633	0.583	0.518
5.00	0.920	0.882	0.762	0.692	0.633	0.583	0.517
6.00	0.921	0.882	0.762	0.692	0.632	0.582	0.516
7.01	0.921	0.881	0.762	0.691	0.632	0.581	0.516
7.63	0.921	0.881	0.762	0.691	0.632	0.581	0.515

Table 187. Static Pressure Ratios for Nozzle 142, $x_r/l_r = 0.20$, $\theta = 30°$, $\phi = 30°$, Medium Sidewall, $\delta_{v,p} = 20°$, and $\delta_{v,y} = -15°$

(a) Upper ramp

NPR	Static pressure ratios at x_r/l_r of—								
	−0.170	−0.032	0.106	0.175	0.244	0.382	0.520	0.659	0.797
2.00	0.754	0.807	0.760	0.709	0.642	0.566	0.550	0.546	0.518
2.50	0.751	0.804	0.758	0.704	0.631	0.486	0.440	0.408	0.459
3.00	0.751	0.804	0.758	0.704	0.630	0.485	0.348	0.329	0.299
3.50	0.750	0.804	0.759	0.704	0.629	0.485	0.343	0.254	0.252
4.00	0.750	0.804	0.760	0.704	0.629	0.485	0.342	0.223	0.209
5.01	0.749	0.804	0.760	0.704	0.630	0.486	0.340	0.222	0.155
6.00	0.749	0.804	0.760	0.704	0.631	0.487	0.340	0.222	0.155
7.00	0.748	0.803	0.760	0.704	0.631	0.487	0.340	0.222	0.156
7.79	0.747	0.803	0.760	0.704	0.631	0.488	0.339	0.223	0.156

(b) Lower flap

NPR	Static pressure ratios at x_r/l_r of—						
	−0.308	−0.170	−0.032	0.037	0.079	0.120	0.162
2.00	0.911	0.872	0.740	0.664	0.606	0.544	0.497
2.50	0.911	0.871	0.737	0.661	0.601	0.537	0.490
3.00	0.911	0.870	0.736	0.660	0.600	0.536	0.489
3.50	0.911	0.870	0.735	0.660	0.599	0.534	0.488
4.00	0.912	0.870	0.735	0.659	0.599	0.533	0.487
5.01	0.912	0.870	0.735	0.659	0.598	0.531	0.486
6.00	0.912	0.869	0.734	0.658	0.597	0.530	0.485
7.00	0.912	0.869	0.734	0.658	0.597	0.528	0.484
7.79	0.913	0.868	0.733	0.657	0.596	0.528	0.483

Table 188. Static Pressure Ratios for Nozzle 143, $x_r/l_r = 0.20$, $\theta = 30°$, $\phi = 30°$, Maximum Sidewall, $\delta_{v,p} = 20°$, and $\delta_{v,y} = -15°$

(a) Upper ramp

NPR	Static pressure ratios at x_r/l_r of—								
	−0.170	−0.032	0.106	0.175	0.244	0.382	0.520	0.659	0.797
2.00	0.754	0.807	0.760	0.709	0.642	0.565	0.551	0.546	0.518
2.50	0.751	0.804	0.758	0.704	0.630	0.485	0.439	0.408	0.455
3.00	0.751	0.804	0.759	0.704	0.631	0.485	0.347	0.328	0.302
3.51	0.750	0.804	0.759	0.704	0.629	0.485	0.342	0.253	0.253
4.00	0.750	0.804	0.760	0.704	0.630	0.485	0.341	0.223	0.211
5.00	0.749	0.804	0.760	0.704	0.630	0.486	0.340	0.222	0.155
6.00	0.749	0.804	0.760	0.704	0.630	0.486	0.339	0.222	0.155
7.00	0.748	0.803	0.760	0.704	0.631	0.487	0.339	0.222	0.156
7.70	0.748	0.803	0.760	0.704	0.631	0.487	0.339	0.222	0.156

(b) Lower flap

NPR	Static pressure ratios at x_r/l_r of—						
	−0.308	−0.170	−0.032	0.037	0.079	0.120	0.162
2.00	0.911	0.872	0.740	0.665	0.606	0.544	0.497
2.50	0.911	0.871	0.737	0.661	0.600	0.537	0.490
3.00	0.911	0.870	0.736	0.660	0.600	0.536	0.488
3.51	0.911	0.870	0.736	0.660	0.599	0.534	0.488
4.00	0.911	0.870	0.736	0.659	0.599	0.533	0.487
5.00	0.912	0.870	0.735	0.659	0.598	0.531	0.486
6.00	0.912	0.870	0.734	0.658	0.597	0.530	0.485
7.00	0.912	0.869	0.734	0.658	0.597	0.529	0.484
7.70	0.912	0.869	0.734	0.657	0.596	0.528	0.483

Table 189. Static Pressure Ratios for Nozzle 144, $x_r/l_r = 0.20$, $\theta = 30°$, $\phi = 30°$, Medium Sidewall, $\delta_{v,p} = 20°$, and $\delta_{v,y} = -30°$

(a) Upper ramp

NPR	Static pressure ratios at x_r/l_r of—								
	−0.170	−0.032	0.106	0.175	0.244	0.382	0.520	0.659	0.797
2.00	0.788	0.830	0.783	0.738	0.678	0.586	0.550	0.539	0.514
2.50	0.784	0.827	0.778	0.730	0.663	0.525	0.457	0.380	0.463
3.00	0.783	0.826	0.778	0.729	0.661	0.511	0.417	0.320	0.290
3.50	0.782	0.826	0.779	0.728	0.661	0.509	0.381	0.298	0.212
4.00	0.782	0.826	0.779	0.728	0.660	0.508	0.375	0.275	0.191
5.00	0.781	0.826	0.779	0.728	0.660	0.508	0.372	0.256	0.167
6.00	0.781	0.825	0.780	0.728	0.661	0.509	0.371	0.256	0.160
7.00	0.780	0.825	0.780	0.728	0.662	0.510	0.371	0.256	0.160
7.99	0.780	0.825	0.780	0.728	0.662	0.510	0.371	0.256	0.160

(b) Lower flap

NPR	Static pressure ratios at x_r/l_r of—						
	−0.308	−0.170	−0.032	0.037	0.079	0.120	0.162
2.00	0.922	0.886	0.772	0.707	0.656	0.595	0.557
2.50	0.920	0.885	0.767	0.701	0.648	0.585	0.545
3.00	0.920	0.884	0.765	0.700	0.646	0.583	0.542
3.50	0.921	0.884	0.765	0.699	0.646	0.581	0.541
4.00	0.921	0.884	0.764	0.699	0.646	0.581	0.540
5.00	0.922	0.883	0.762	0.698	0.646	0.580	0.540
6.00	0.922	0.883	0.761	0.698	0.645	0.578	0.539
7.00	0.922	0.882	0.761	0.698	0.645	0.577	0.538
7.99	0.922	0.881	0.761	0.697	0.645	0.576	0.537

Table 190. Static Pressure Ratios for Nozzle 145, $x_r/l_r = 0.20$, $\theta = 30°$, $\phi = 30°$, Maximum Sidewall, $\delta_{v,p} = 20°$, and $\delta_{v,y} = -30°$

(a) Upper ramp

NPR	Static pressure ratios at x_r/l_r of—								
	−0.170	−0.032	0.106	0.175	0.244	0.382	0.520	0.659	0.797
2.00	0.787	0.830	0.785	0.739	0.681	0.592	0.556	0.541	0.516
2.50	0.783	0.826	0.778	0.730	0.663	0.527	0.465	0.403	0.458
3.00	0.782	0.826	0.778	0.729	0.661	0.512	0.423	0.347	0.303
3.50	0.782	0.825	0.779	0.728	0.661	0.510	0.387	0.323	0.245
4.00	0.781	0.825	0.779	0.728	0.660	0.509	0.380	0.299	0.216
5.01	0.781	0.825	0.779	0.728	0.661	0.509	0.376	0.278	0.194
6.00	0.780	0.825	0.779	0.728	0.661	0.510	0.375	0.277	0.186
7.00	0.780	0.825	0.779	0.728	0.661	0.510	0.375	0.277	0.185
7.85	0.779	0.825	0.780	0.727	0.662	0.511	0.375	0.277	0.185

(b) Lower flap

NPR	Static pressure ratios at x_r/l_r of—						
	−0.308	−0.170	−0.032	0.037	0.079	0.120	0.162
2.00	0.922	0.886	0.773	0.707	0.656	0.597	0.557
2.50	0.920	0.884	0.767	0.701	0.648	0.586	0.545
3.00	0.920	0.884	0.765	0.699	0.646	0.583	0.542
3.50	0.921	0.883	0.764	0.699	0.646	0.581	0.541
4.00	0.921	0.883	0.764	0.698	0.645	0.580	0.540
5.01	0.921	0.883	0.763	0.698	0.645	0.579	0.539
6.00	0.921	0.882	0.762	0.698	0.645	0.578	0.538
7.00	0.922	0.882	0.762	0.697	0.645	0.577	0.538
7.85	0.922	0.881	0.761	0.697	0.644	0.576	0.537

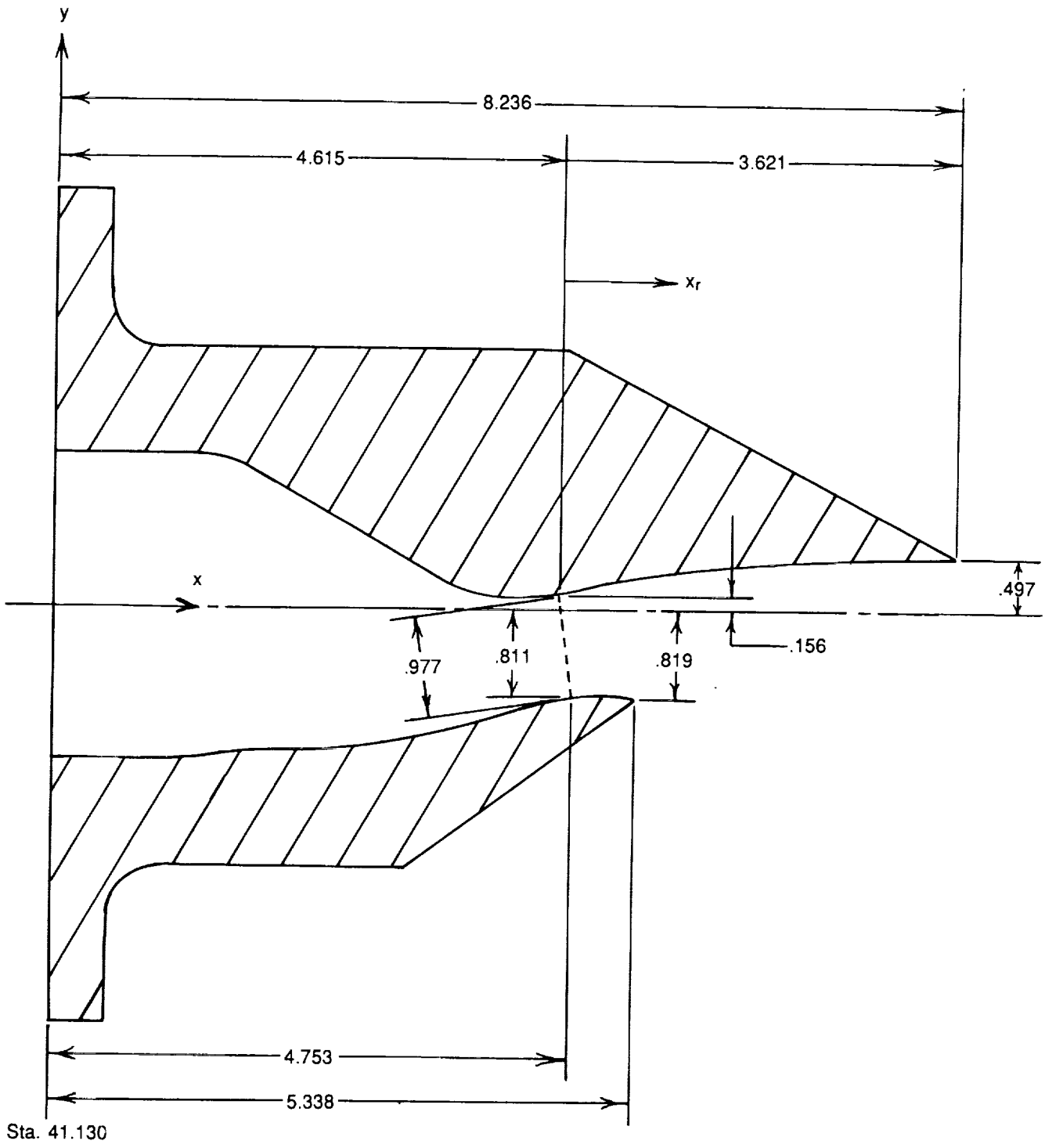

(a) Baseline unvectored nozzle.

Figure 1. Sketches defining nozzle geometric parameters.

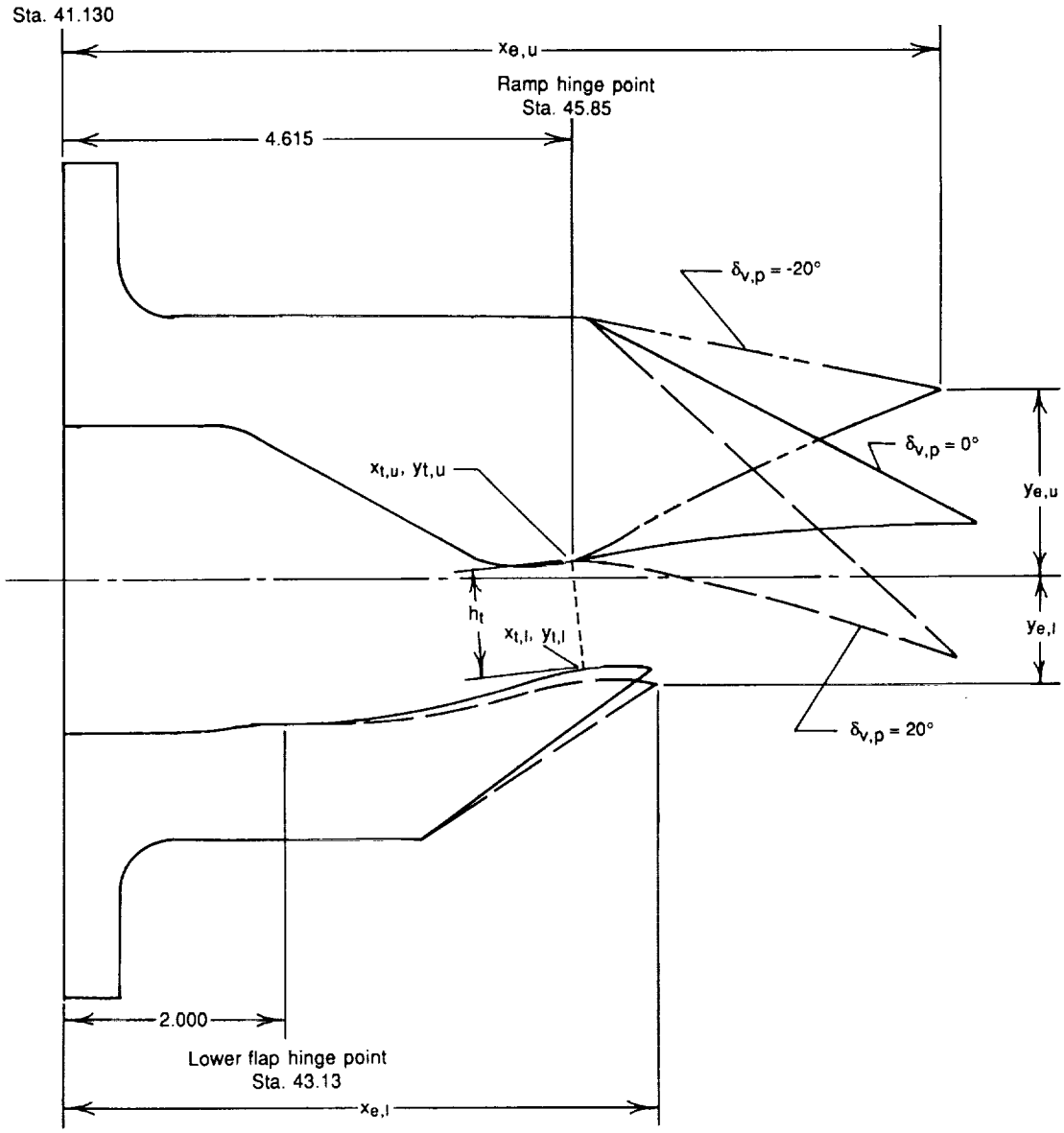

$\delta_{v,p}$, deg	$x_{t,u}$, in.	$y_{t,u}$, in.	$x_{t,l}$, in.	$y_{t,l}$, in.	h_t, in.	$(A_e/A_t)_i$	$(NPR)_{des}$
-20	4.664	0.155	4.753	-0.811	0.971	1.34	4.94
0	4.615	0.156	4.753	-0.811	0.977	1.12	3.23
20	5.457	0.011	5.283	-0.954	0.980	1.00	1.89

$\delta_{v,p}$, deg	$x_{e,u}$, in.	$y_{e,u}$, in.	$x_{e,l}$, in.	$y_{e,l}$, in.
-20	7.950	1.714	5.338	-0.819
0	8.236	0.497	5.338	-0.819
20	8.088	-0.744	5.366	-0.970

(b) Pitch-vectored nozzles.

Figure 1. Continued.

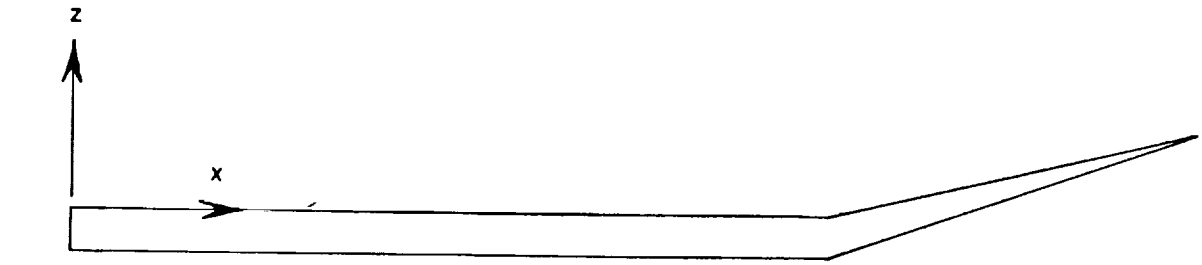

Top view

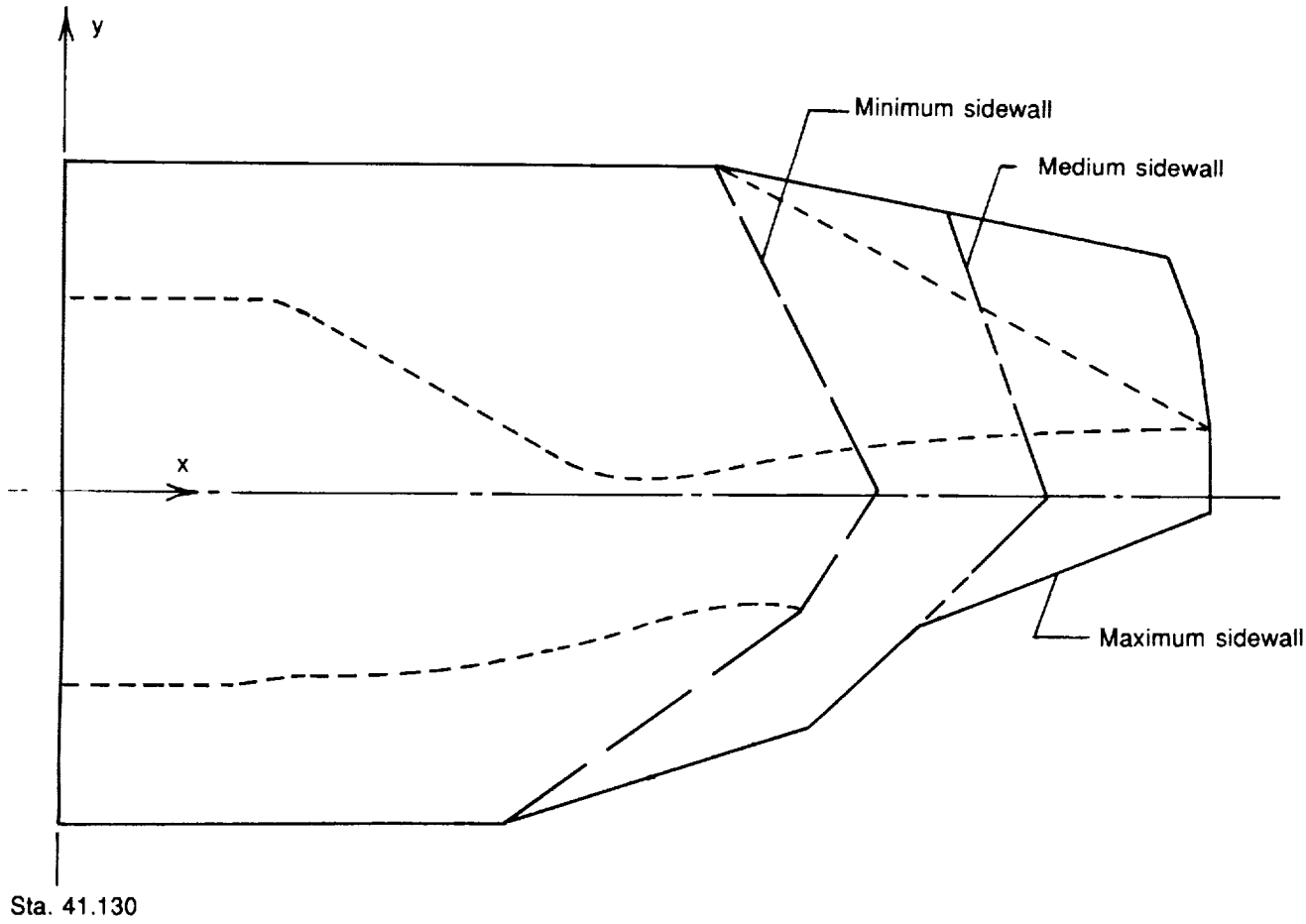

Side view

(c) Nozzle sidewalls.

Figure 1. Continued.

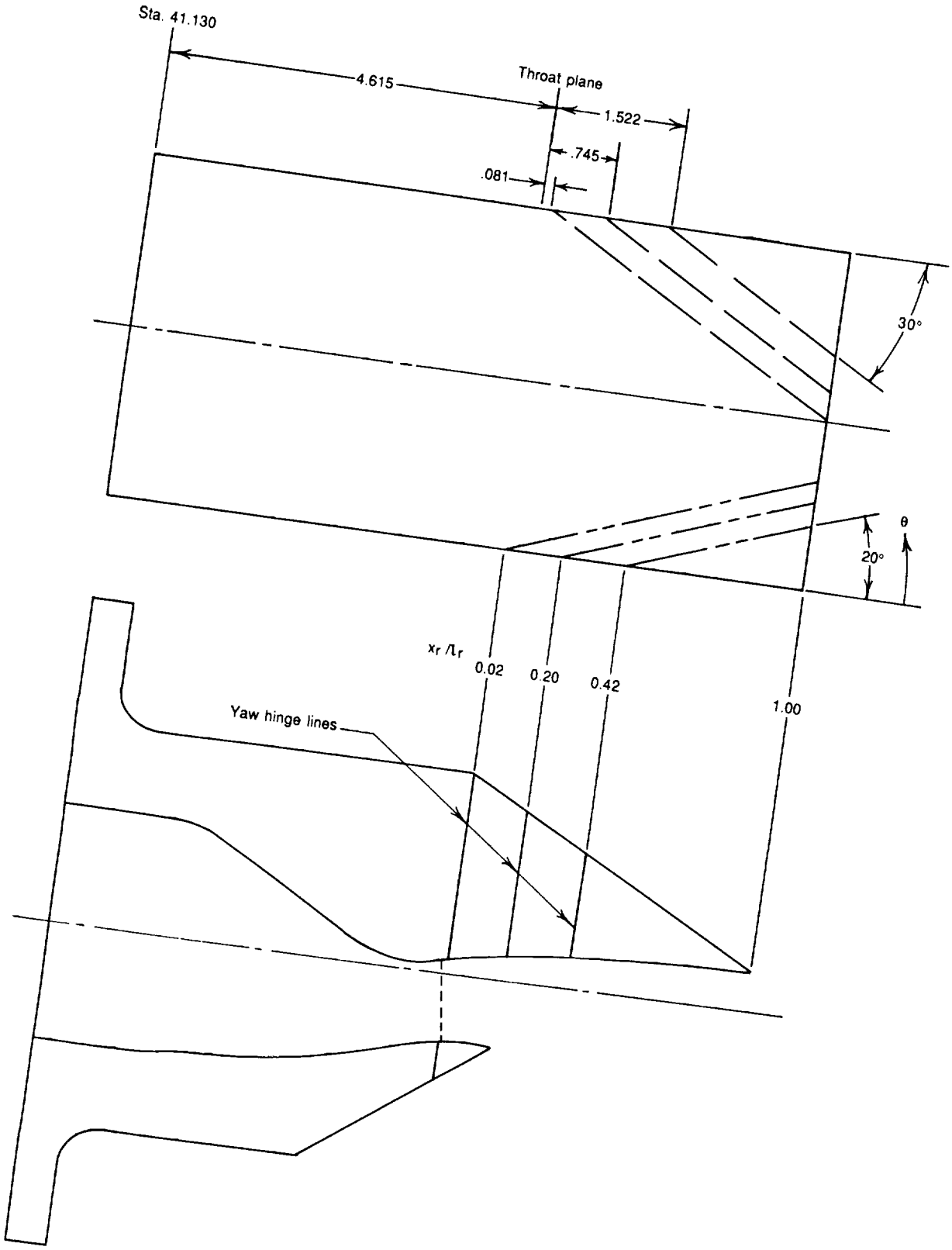

(d) Ramp cutoff angle and yaw hinge line locations.

Figure 1. Continued.

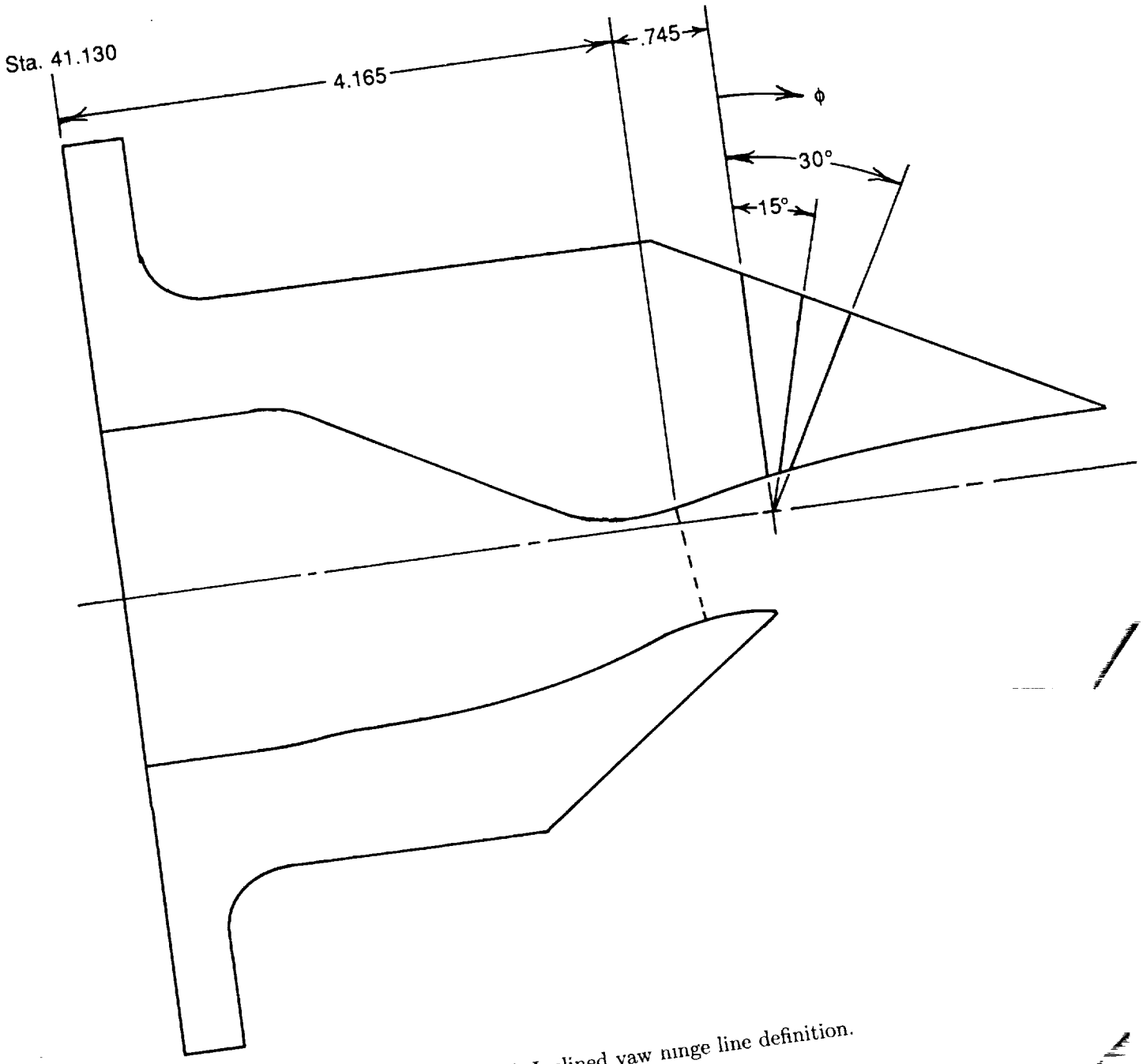

(e) Inclined yaw hinge line definition.

Figure 1. Continued.

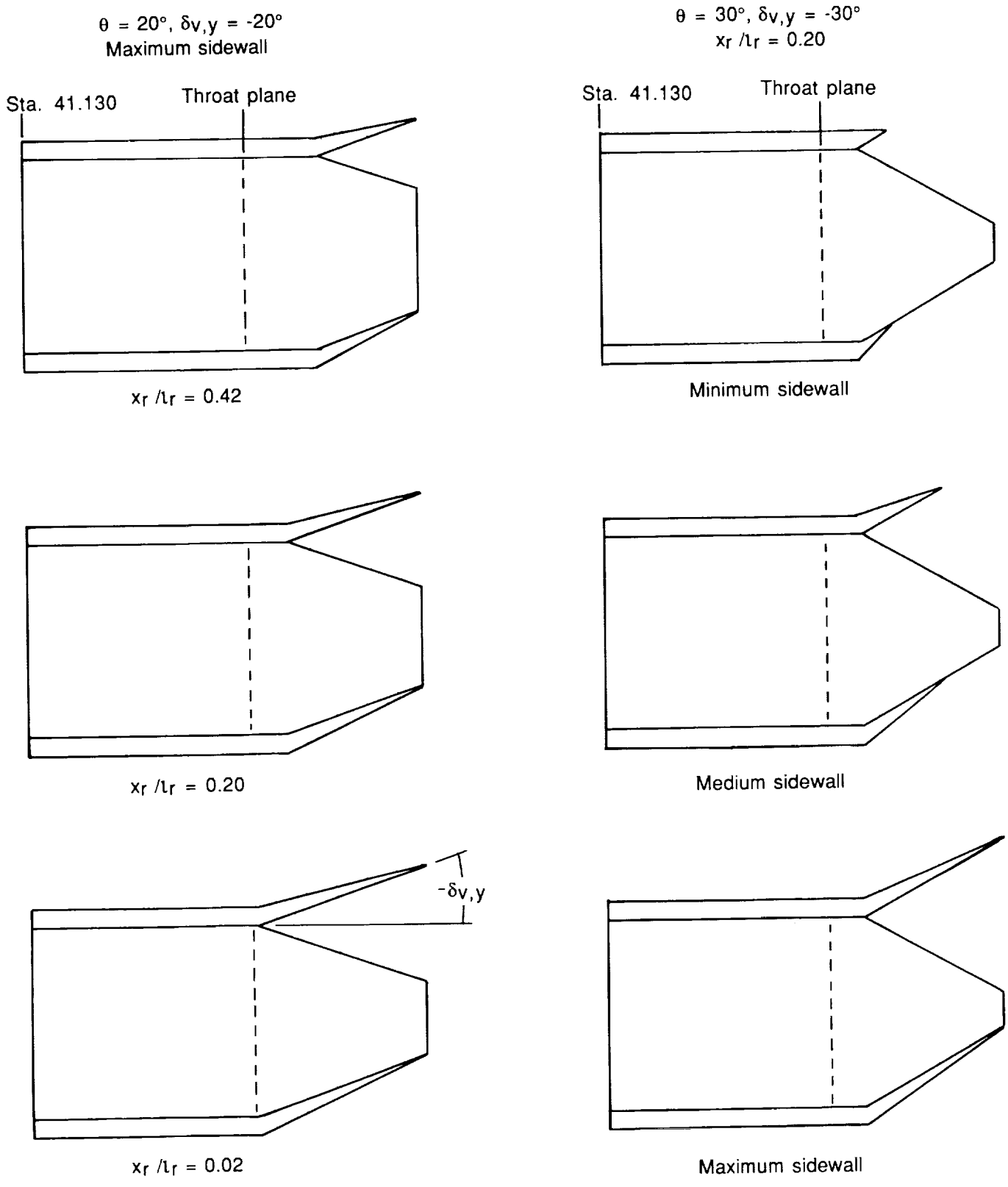

(f) Typical yaw vector configurations. $\phi = 0°$.

Figure 1. Concluded.

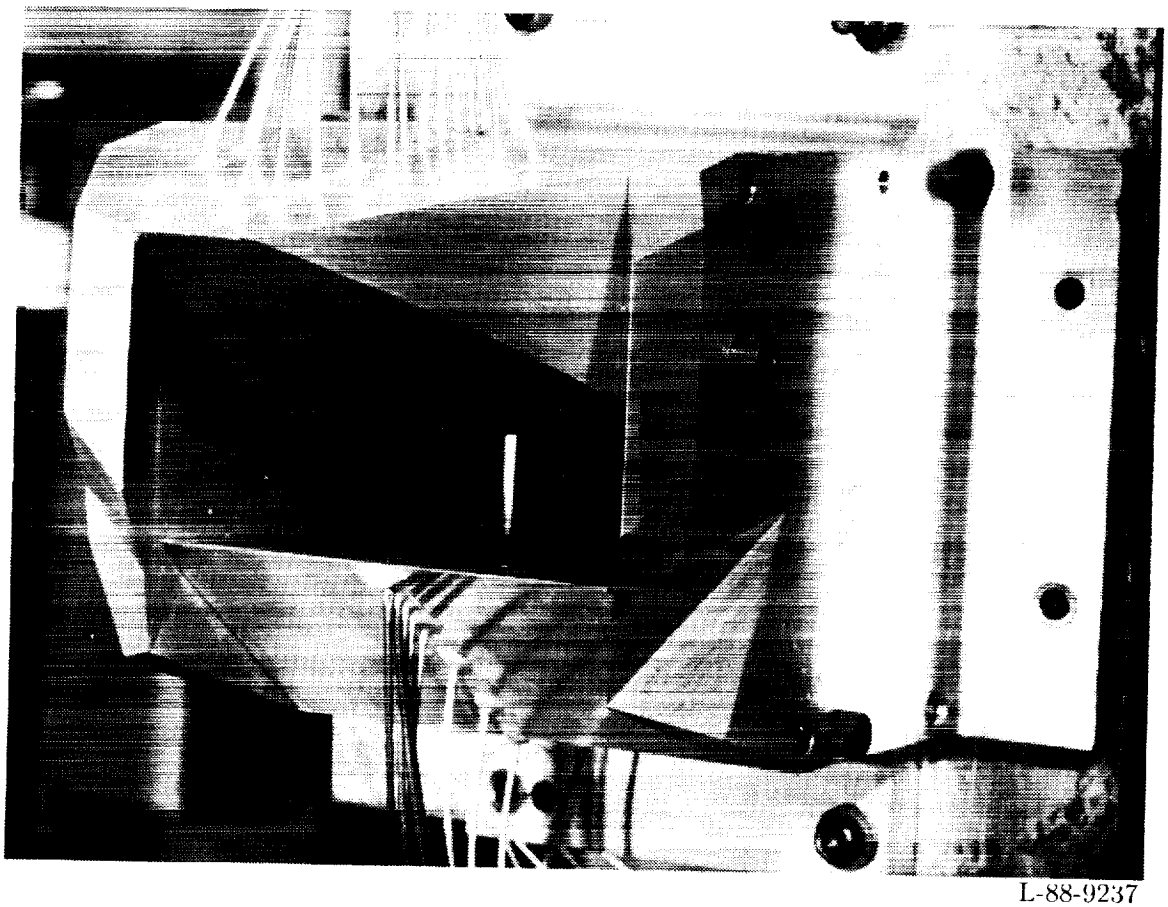

L-88-9237

Figure 2. Photograph of SERN. View is from the rear.

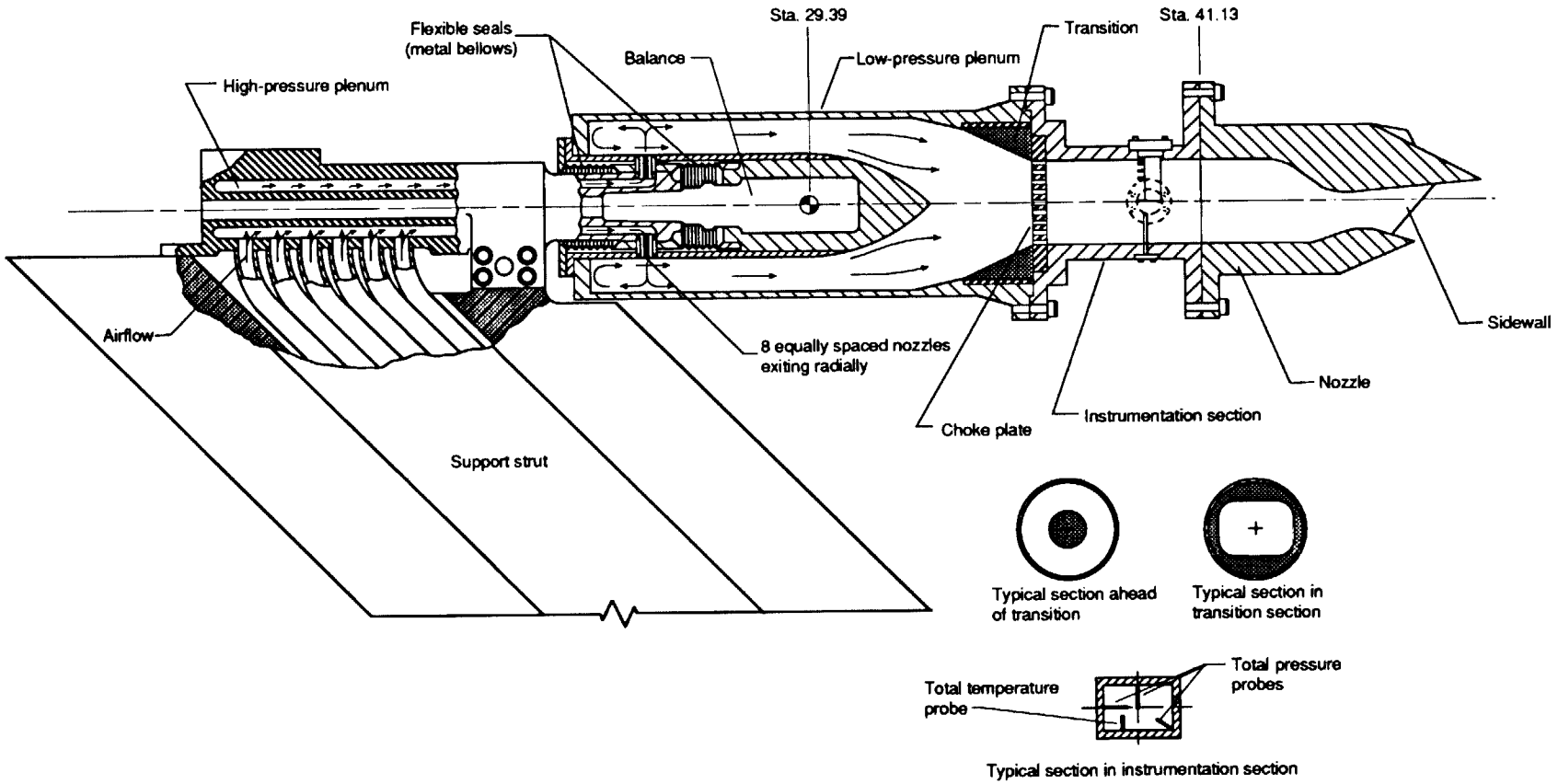

Figure 3. Sketch of single-engine propulsion simulation system with SERN installed.

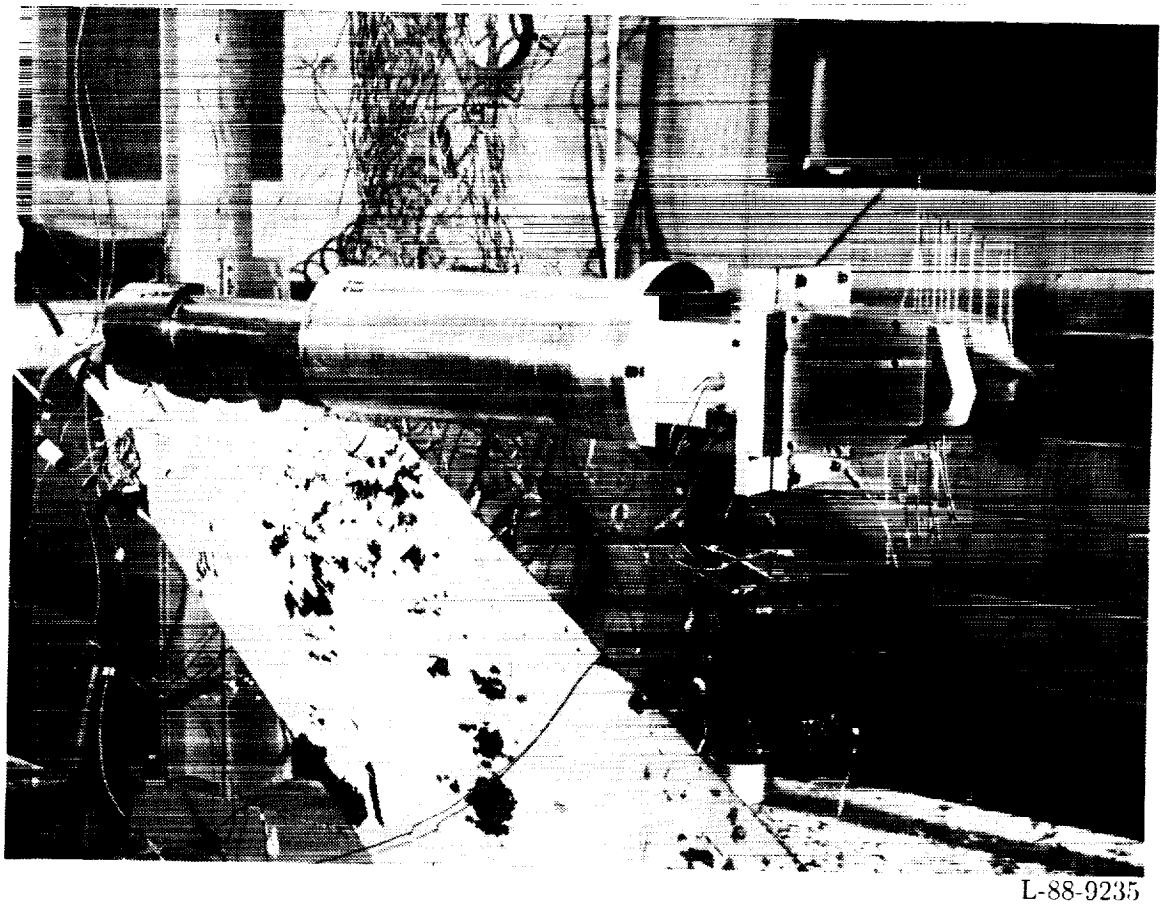

L-88-9235

Figure 4. SERN mounted on single-engine propulsion simulation system.

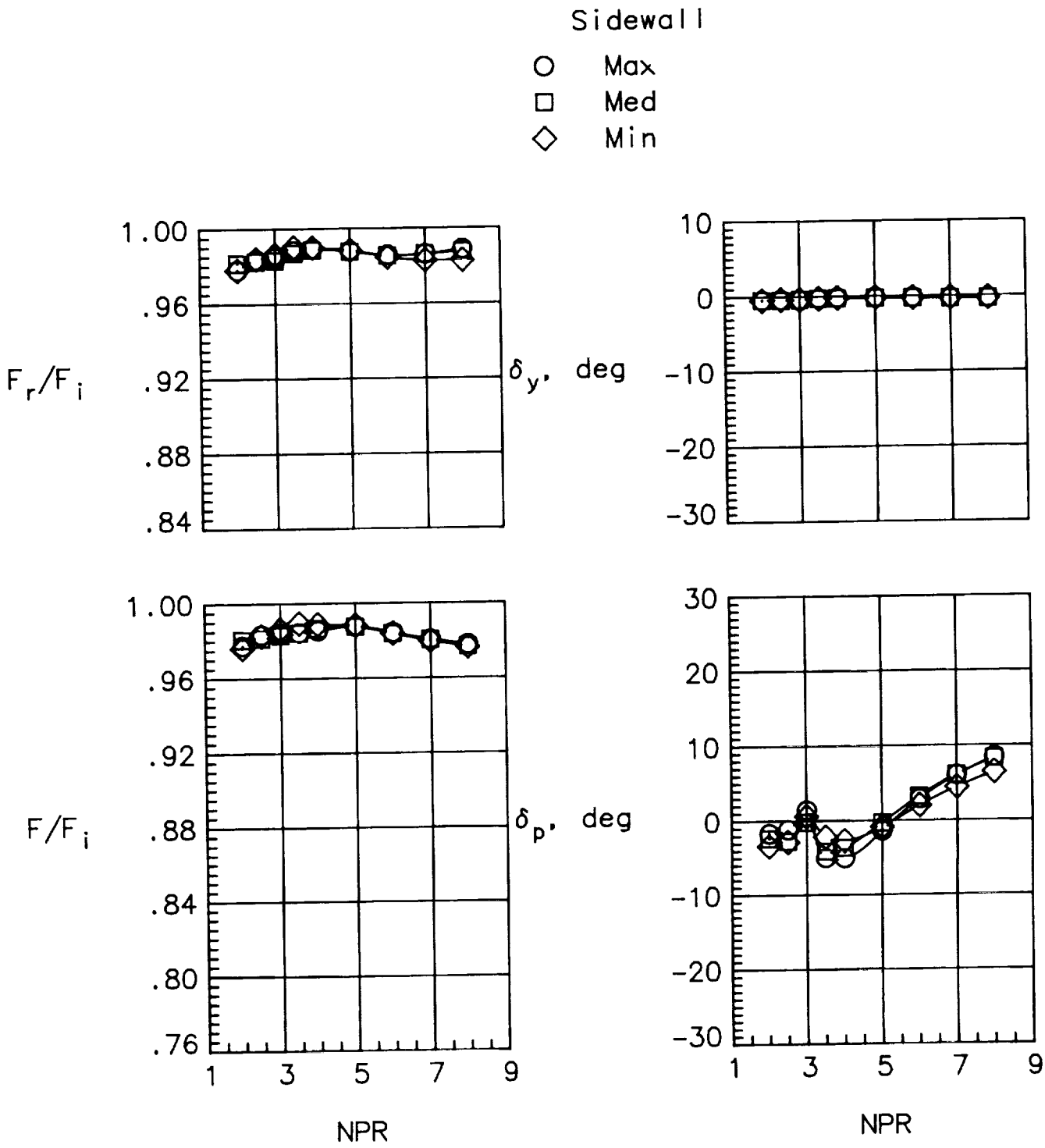

Figure 5. Effect of sidewall containment on nozzle performance. $x_r/l_r = 1.00$; $\theta = 0°$; $\phi = 0°$; $\delta_{v,p} = 0°$; $\delta_{v,y} = 0°$.

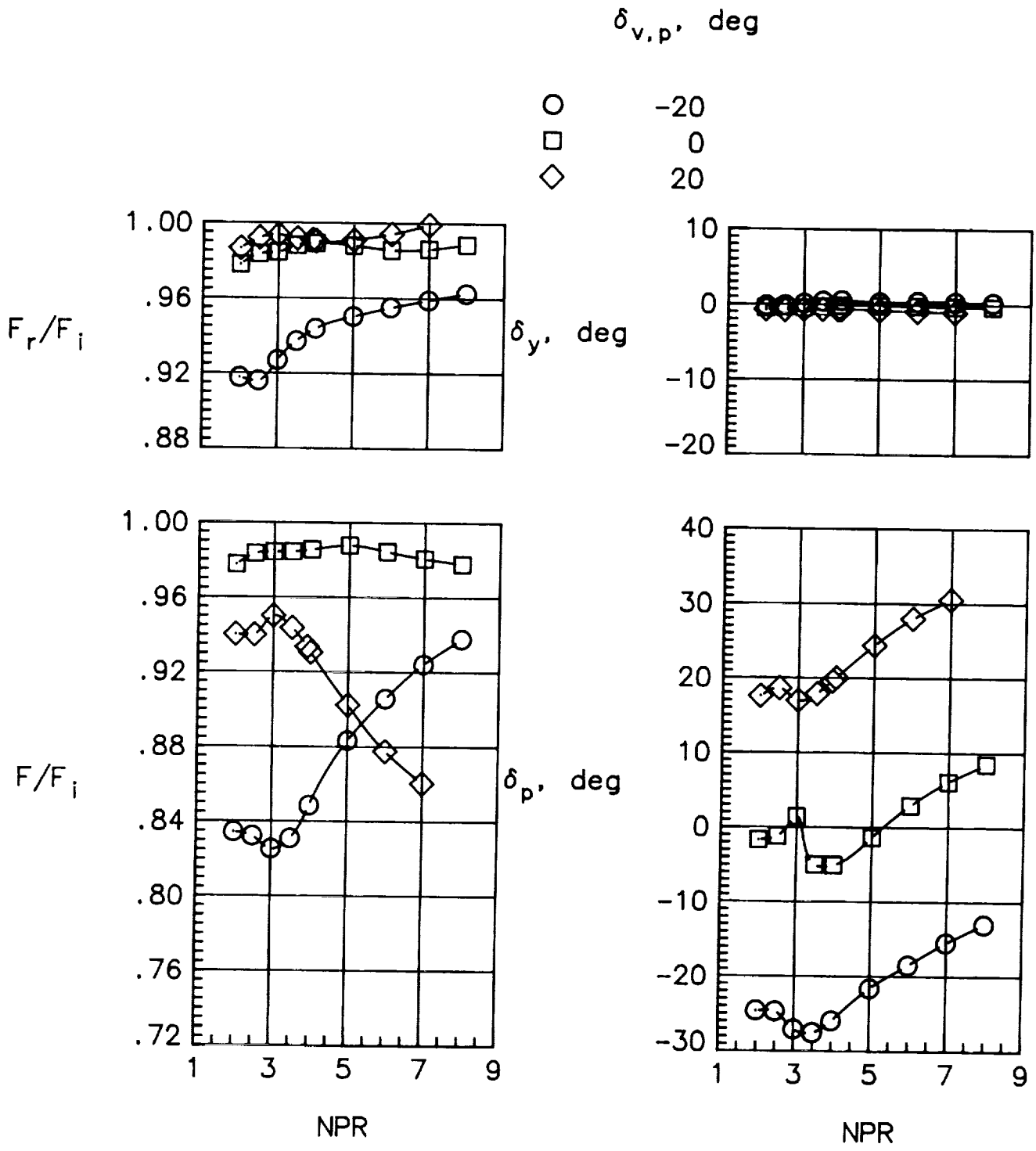

Figure 6. Effect of pitch vectoring on nozzle internal performance. Max sidewall; $x_r/l_r = 1.00$; $\theta = 0°$; $\phi = 0°$; $\delta_{v,y} = 0°$.

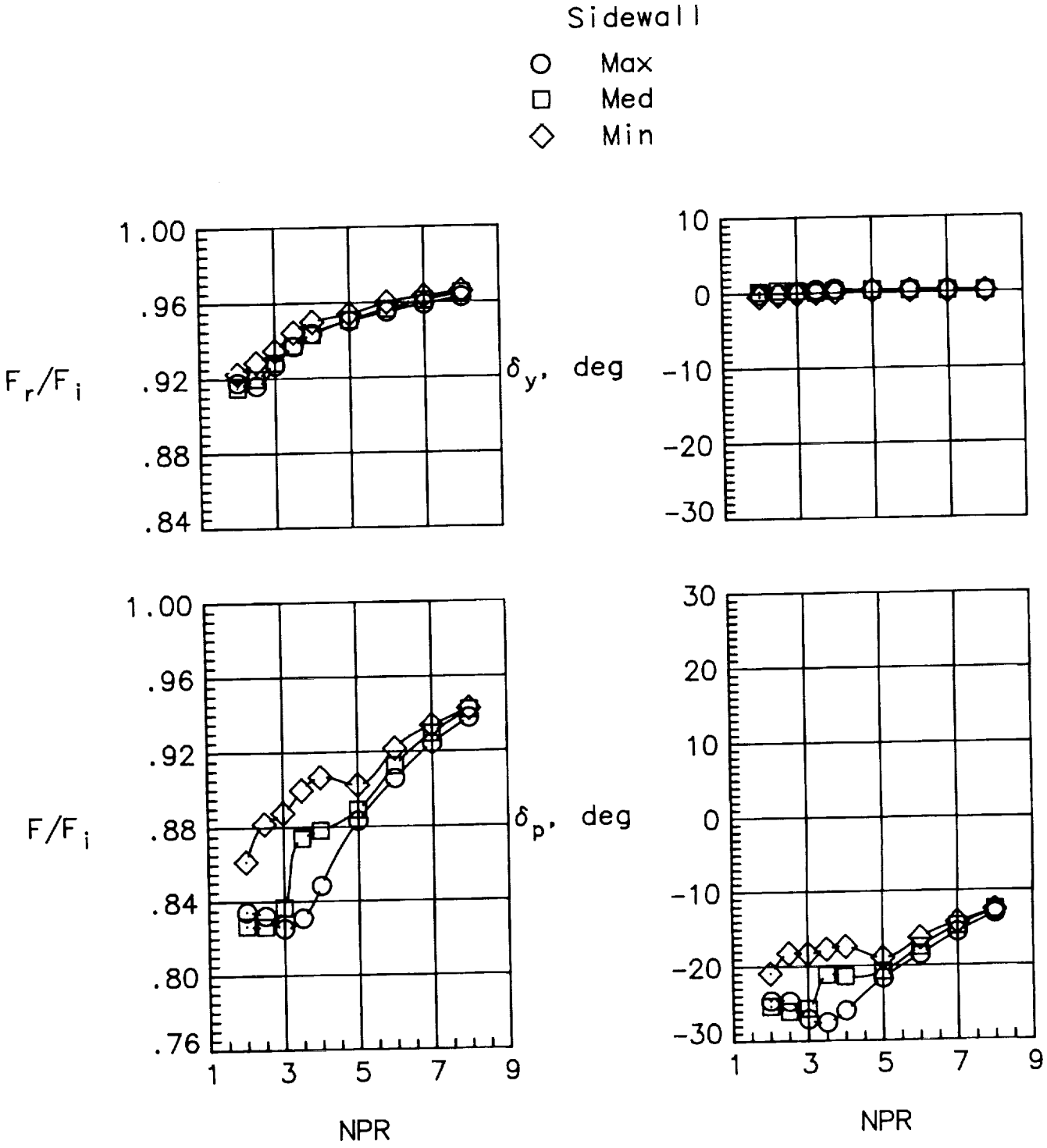

(a) $\delta_{v,p} = -20°$.

Figure 7. Effect of sidewall containment on nozzle internal performance at various geometric pitch vector angles. $x_r/l_r = 1.00$; $\theta = 0°$; $\phi = 0°$; $\delta_{v,y} = 0°$.

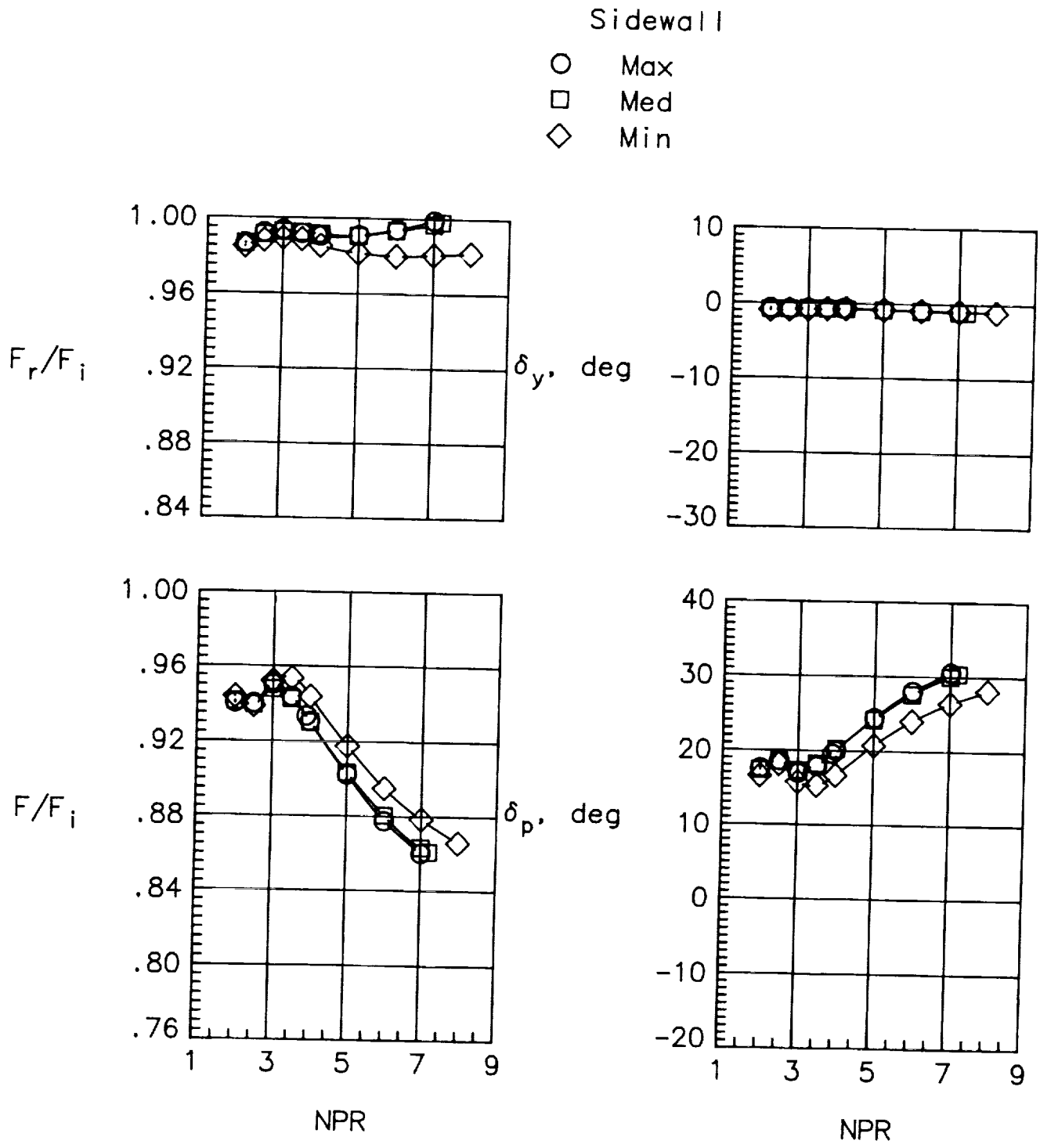

(b) $\delta_{r,p} = 20°$.

Figure 7. Concluded.

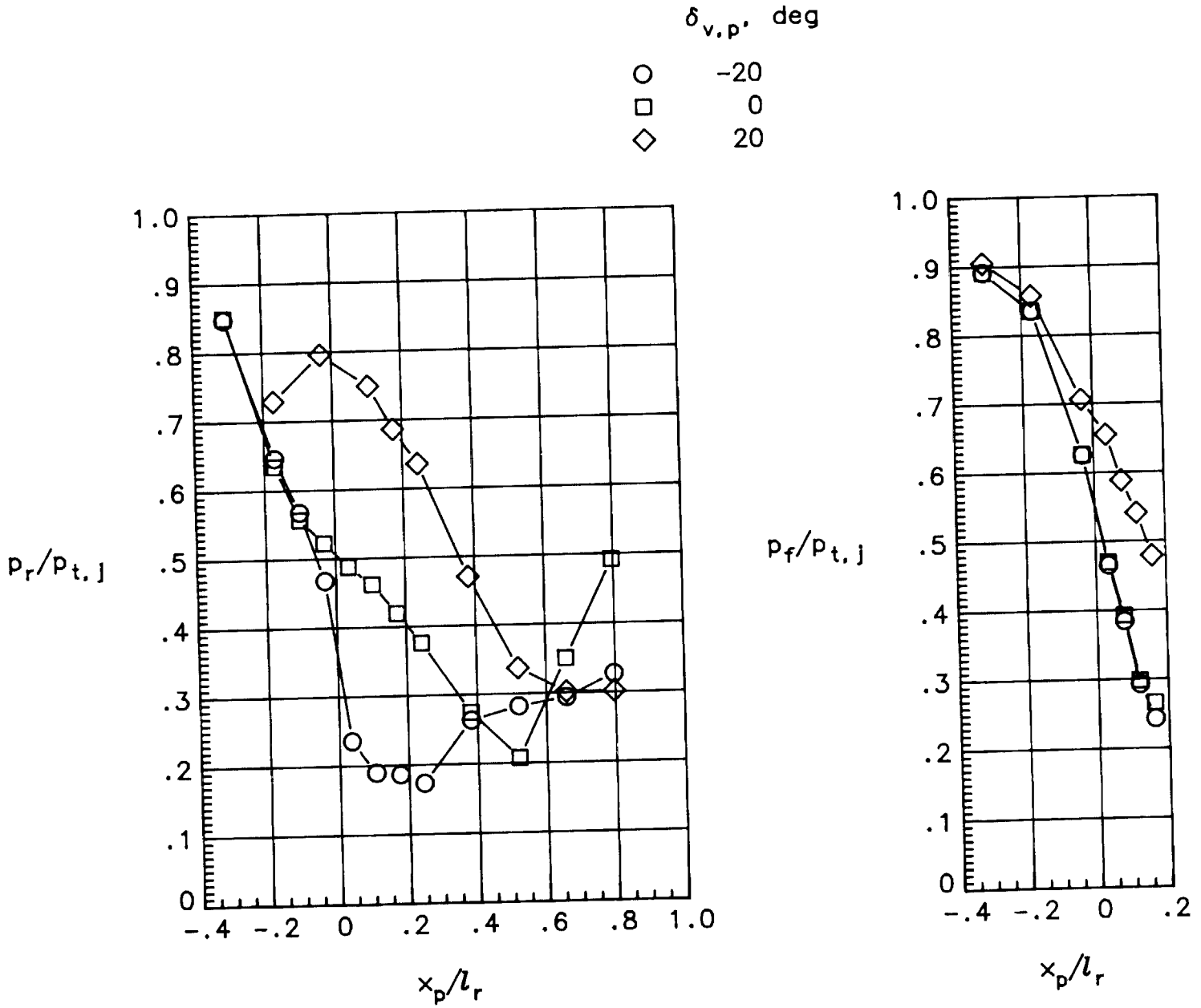

Figure 8. Effect of pitch vectoring on internal pressures. Max sidewall; $x_r/l_r = 1.00$; $\theta = 0°$; $\phi = 0°$; $\delta_{v,y} = 0°$; NPR = 3.0.

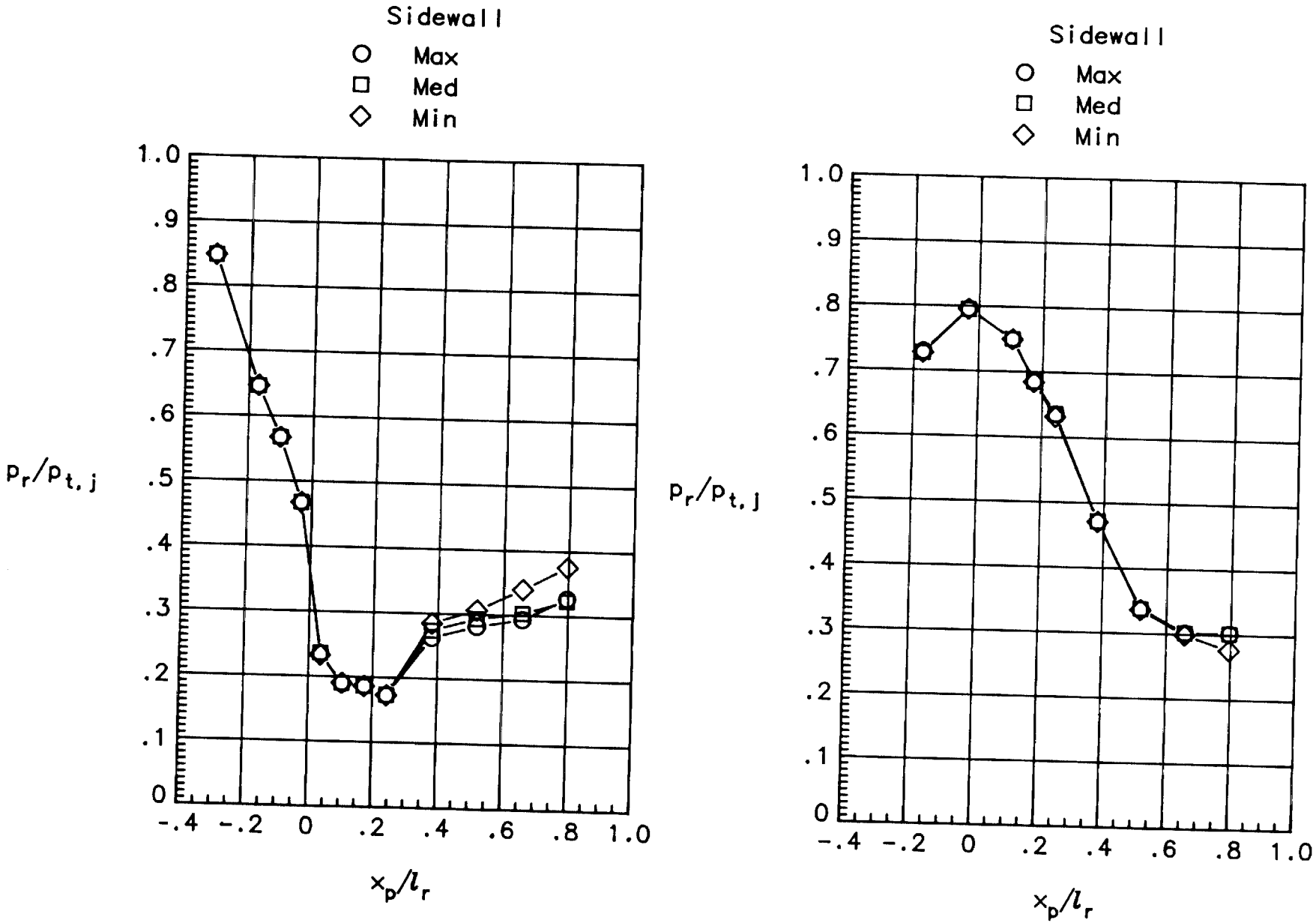

(a) $\delta_{v,p} = -20°$.

(b) $\delta_{v,p} = 20°$.

Figure 9. Effect of sidewall containment on nozzle internal pressures at various geometric pitch vector angles. NPR = 3.0; $x_r/l_r = 1.00$; $\theta = 0°$; $\phi = 0°$; $\delta_{v,y} = 0°$.

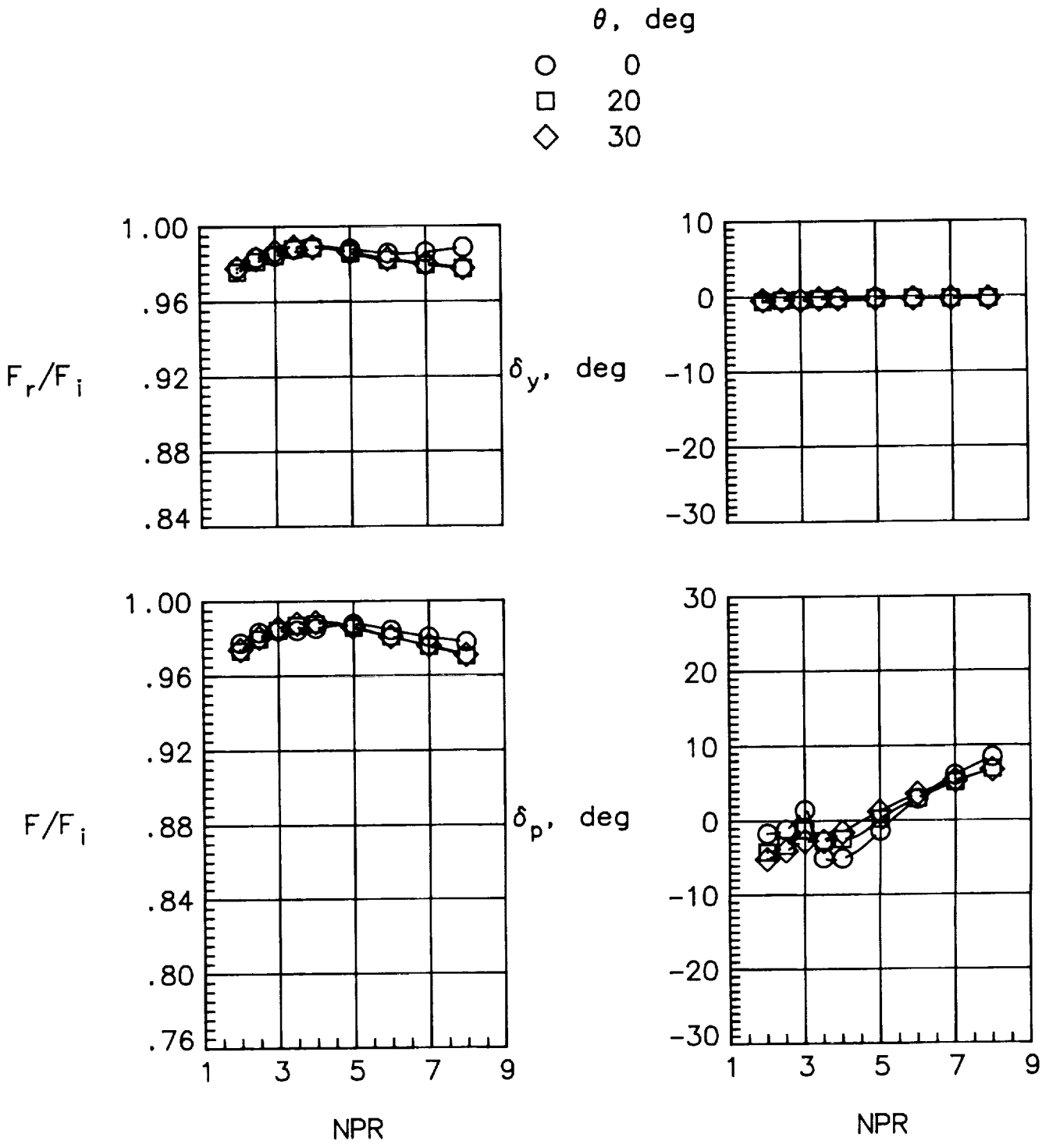

(a) $\delta_{v,p} = 0°$.

Figure 10. Effect of flap cutout angle on nozzle internal performance at various geometric pitch vector angles. Max sidewall; $x_r/l_r = 0.20$; $\phi = 0°$; $\delta_{v,y} = 0°$.

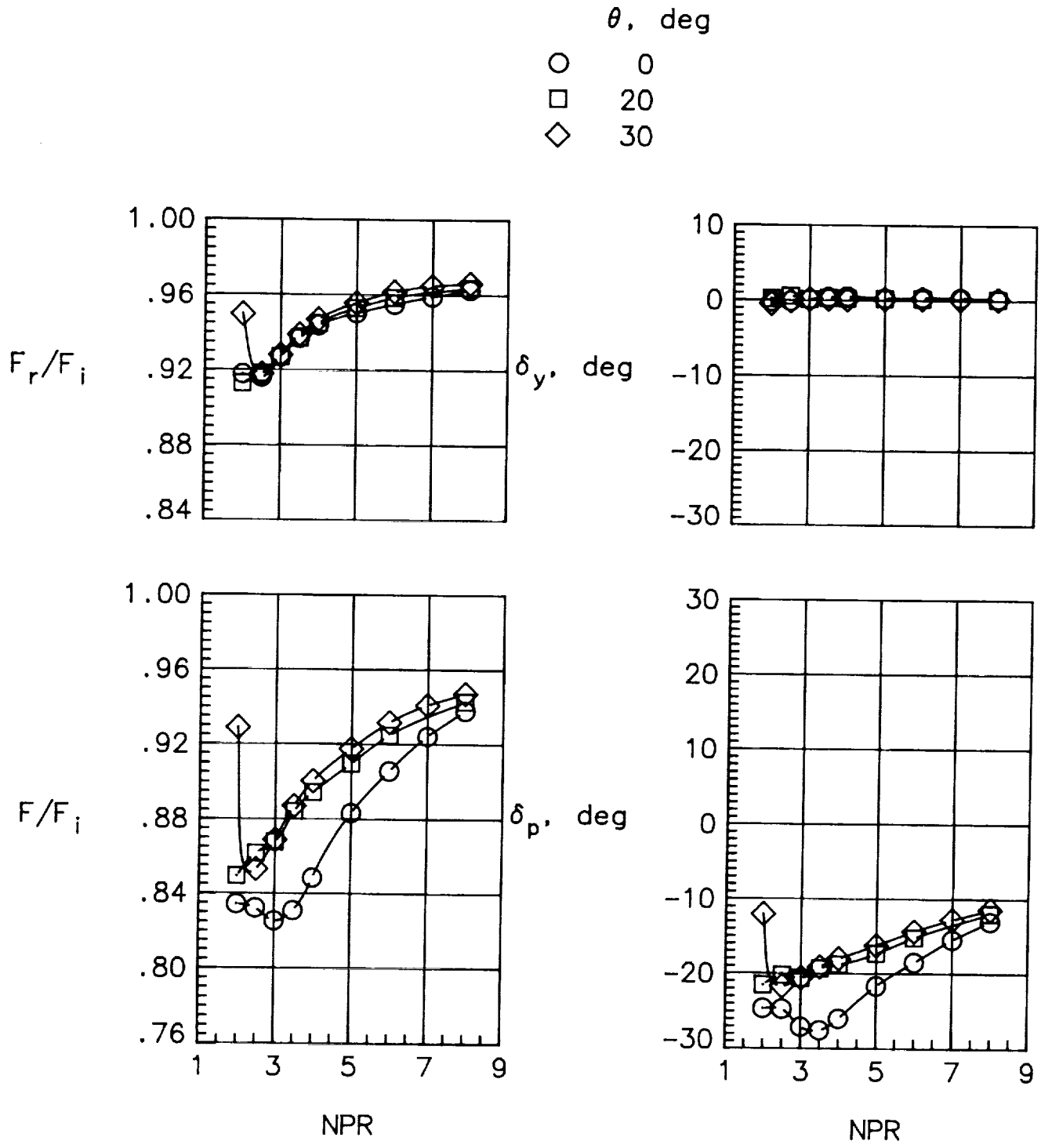

(b) $\delta_{v,p} = -20°$.

Figure 10. Continued.

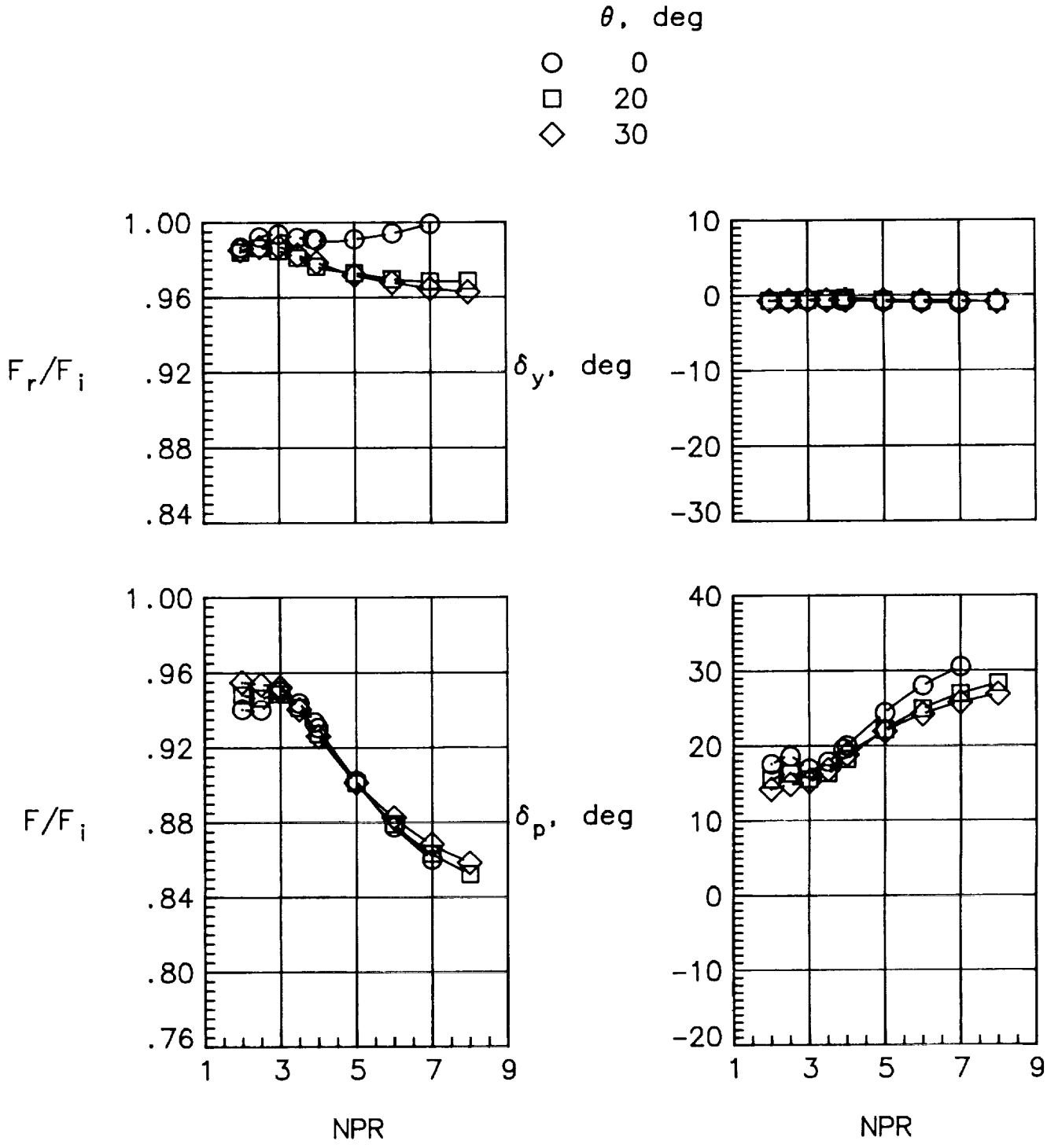

(c) $\delta_{v,p} = 20°$.

Figure 10. Concluded.

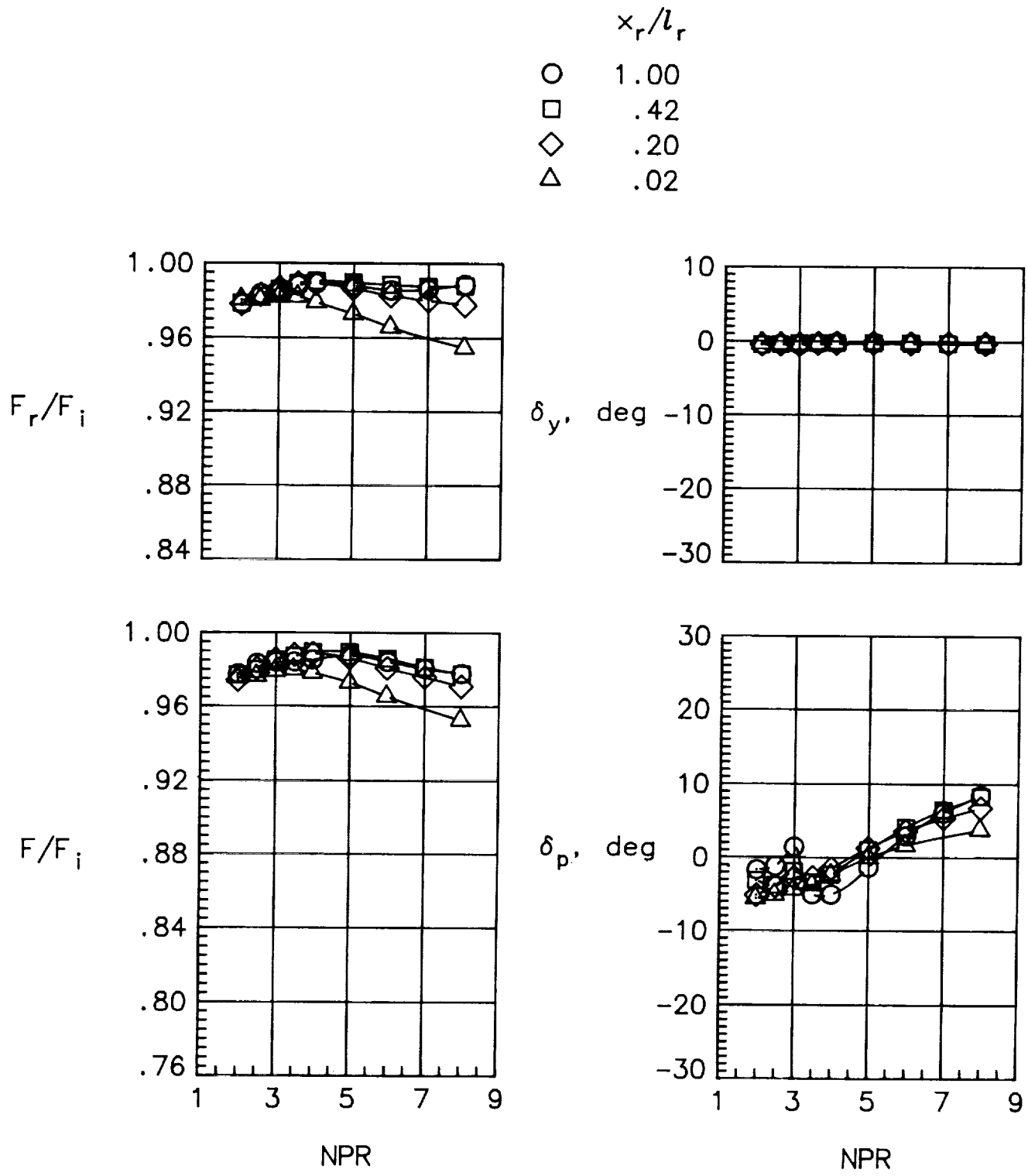

(a) $\delta_{v,p} = 0°$.

Figure 11. Effect of yaw hinge line location on nozzle internal performance at various geometric pitch vector angles. Max sidewall; $\theta = 30°$; $\phi = 0°$; $\delta_{v,y} = 0°$; NPR = 3.0.

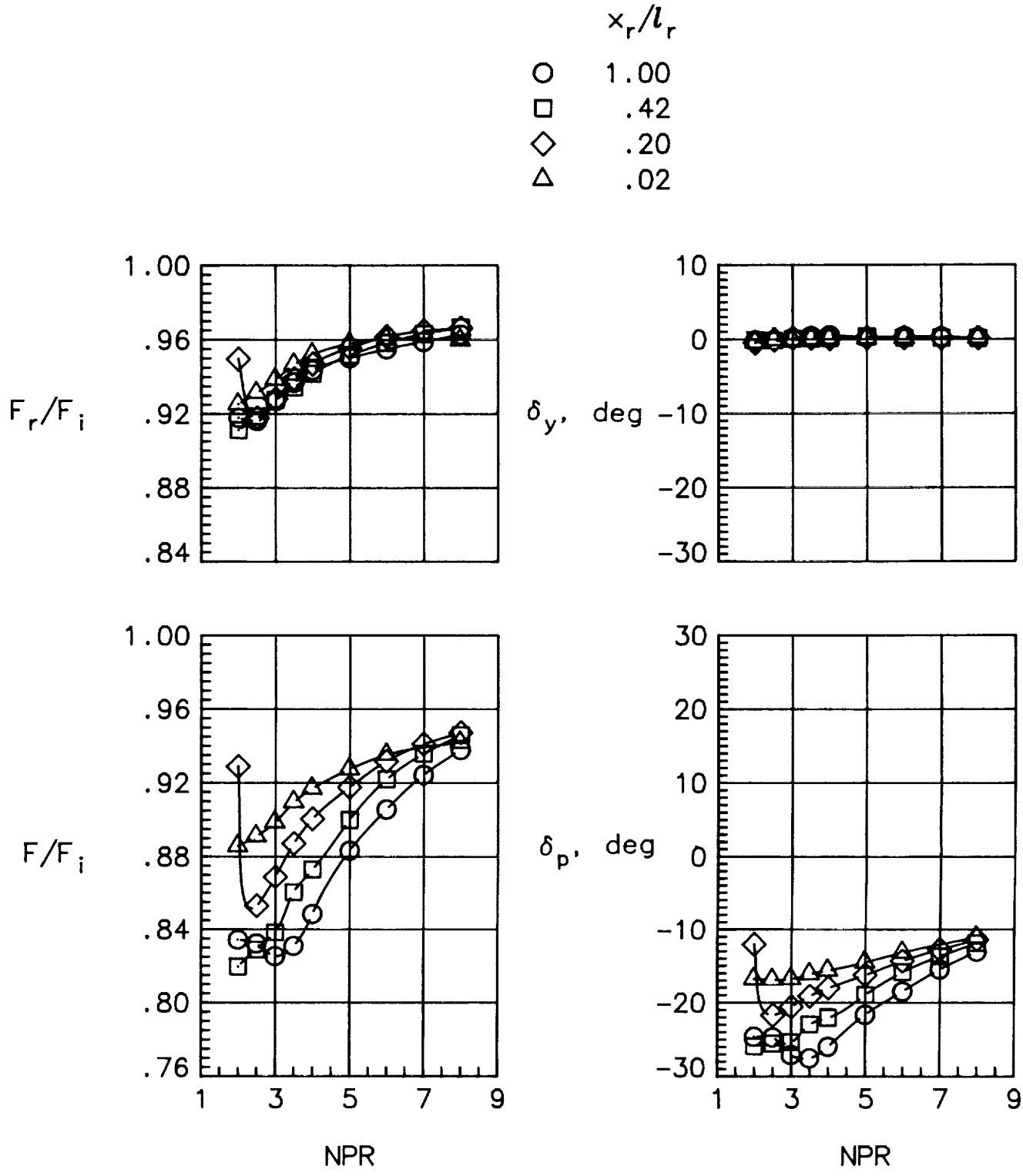

(b) $\delta_{v,p} = -20°$.

Figure 11. Continued.

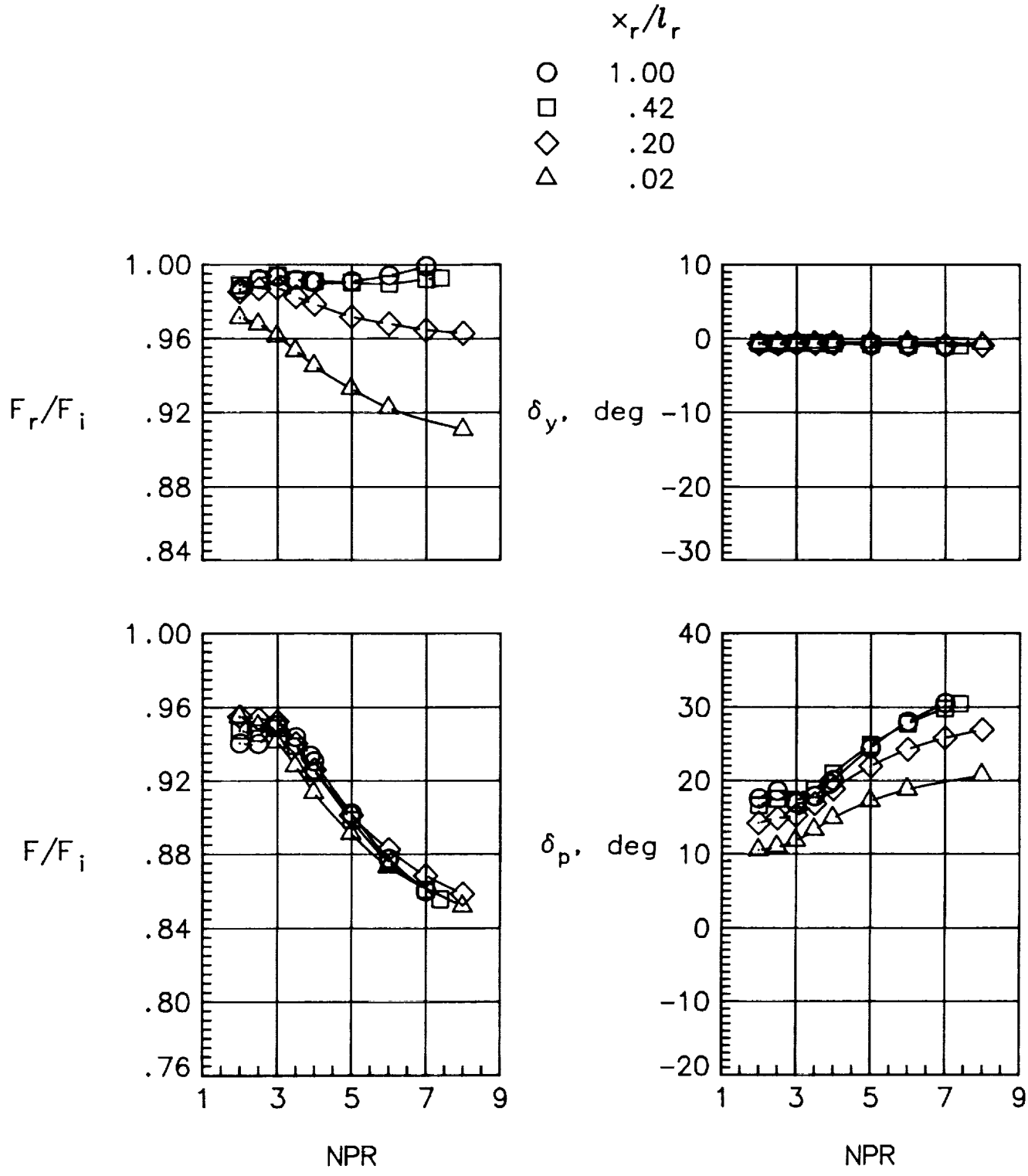

(c) $\delta_{v,p} = 20°$.

Figure 11. Concluded.

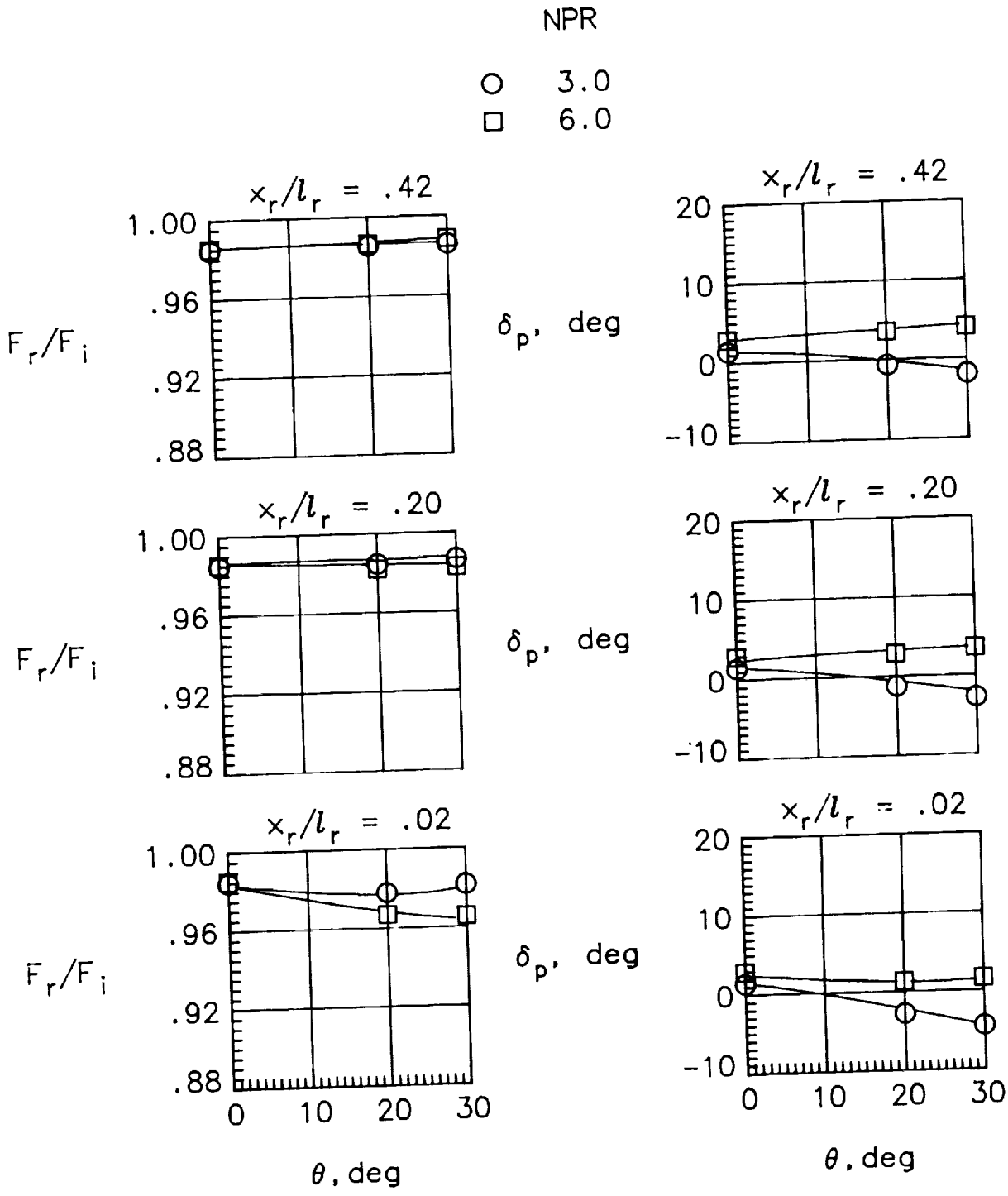

(a) Max sidewall.

Figure 12. Summary of effects of flap cutout angle on nozzle internal performance with various sidewall containments for $\phi = 0°$, $\delta_{v,p} = 0°$, and $\delta_{v,y} = 0°$.

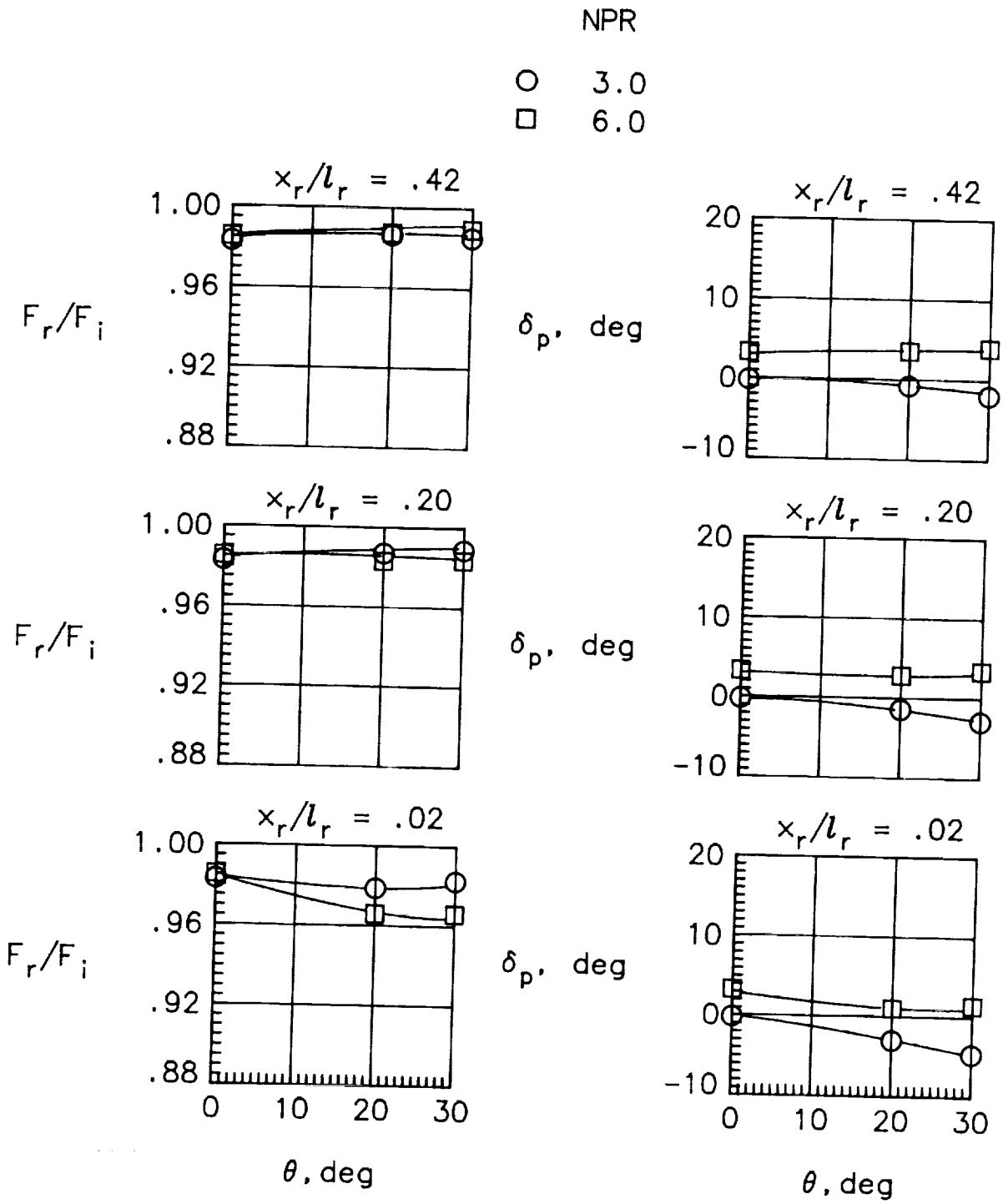

(b) Med sidewall.

Figure 12. Continued.

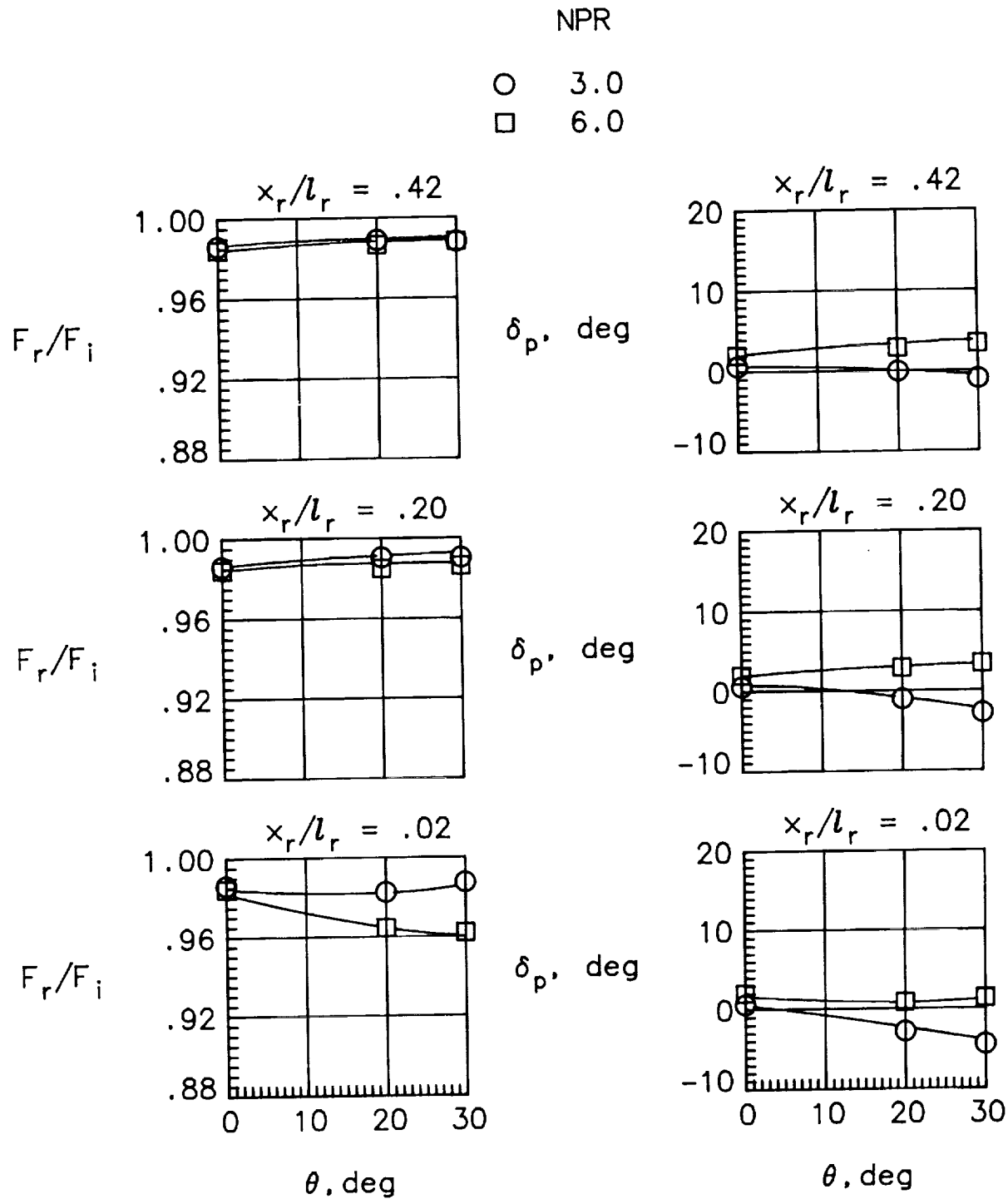

(c) Min sidewall.

Figure 12. Concluded.

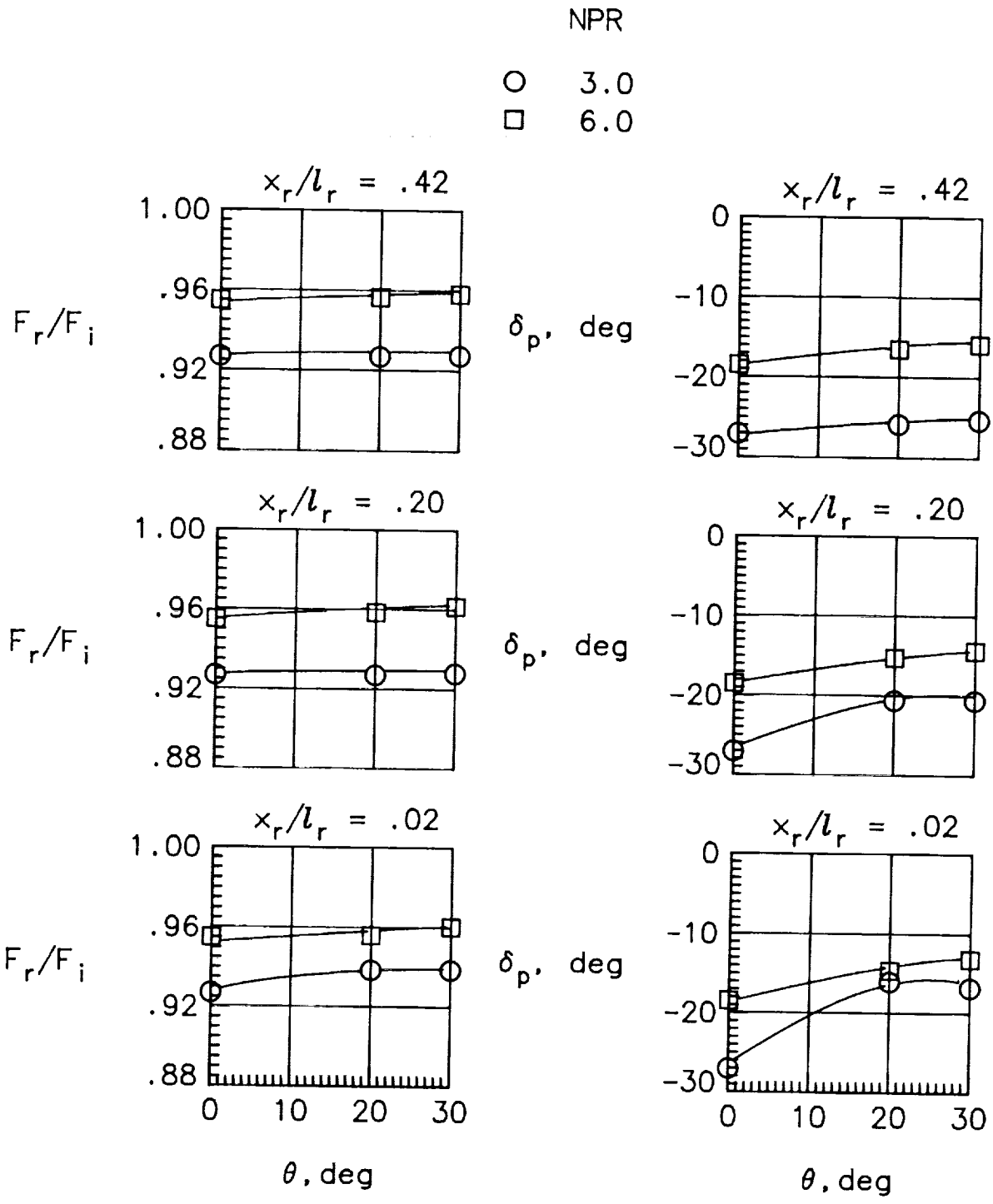

(a) Max sidewall.

Figure 13. Summary of effects of flap cutout angle on nozzle internal performance with various sidewall containments for $\phi = 0°$, $\delta_{v,p} = -20°$, and $\delta_{v,y} = 0°$.

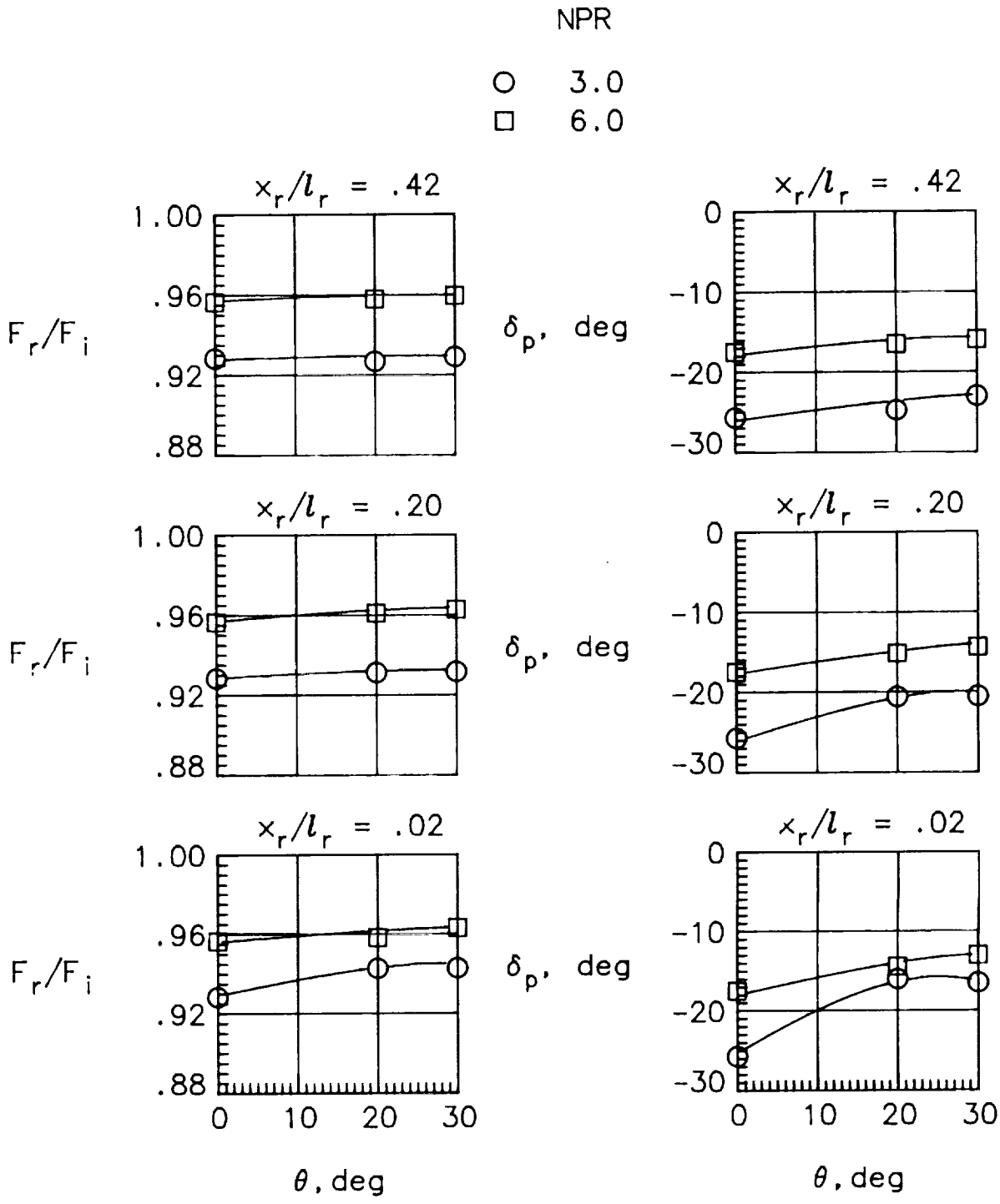

(b) Med sidewall.

Figure 13. Continued.

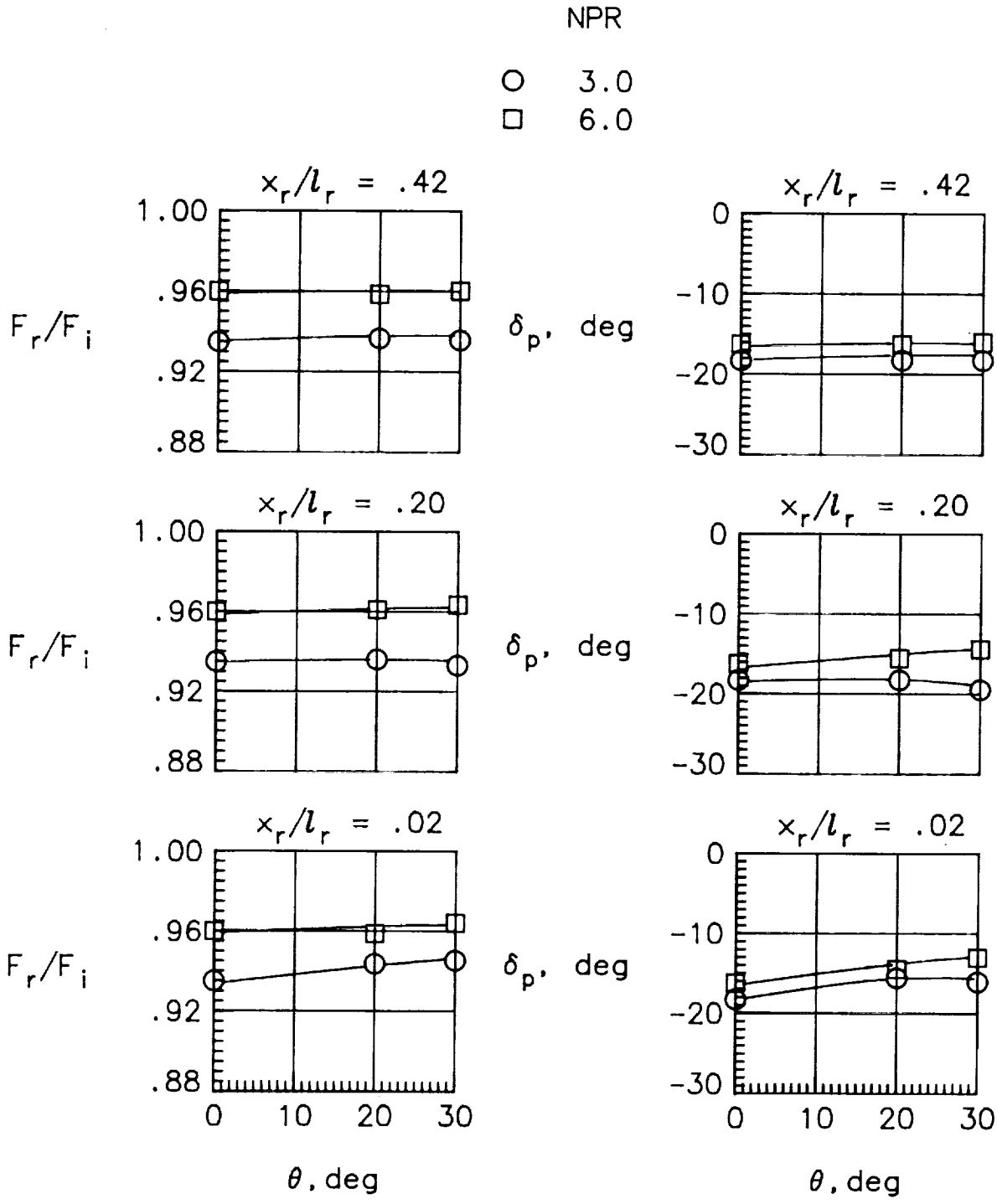

(c) Min sidewall.

Figure 13. Concluded.

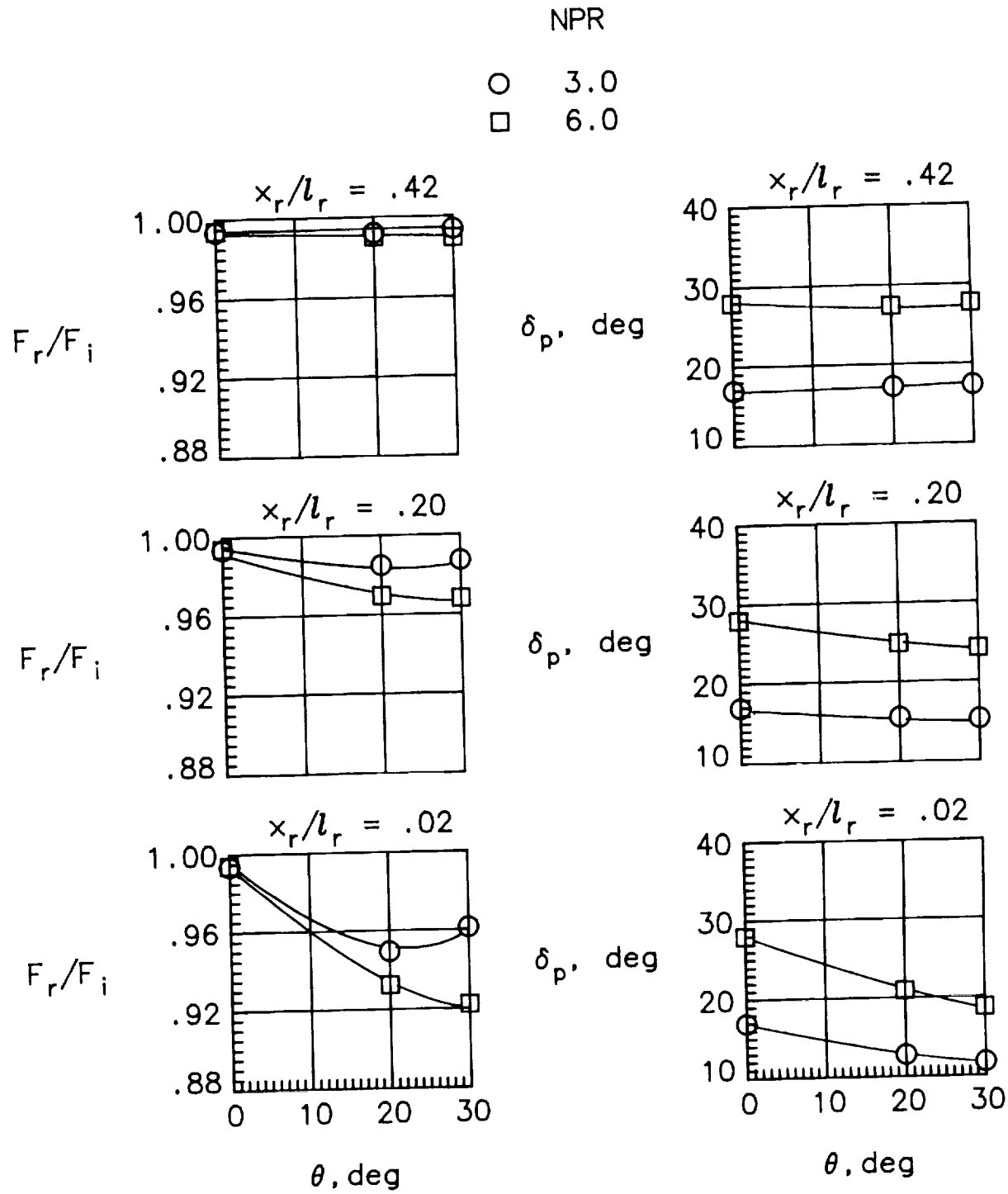

(a) Max sidewall.

Figure 14. Summary of effects of flap cutout angle on nozzle internal performance with various sidewall containments for $\phi = 0°$, $\delta_{v,p} = 20°$, and $\delta_{v,y} = 0°$.

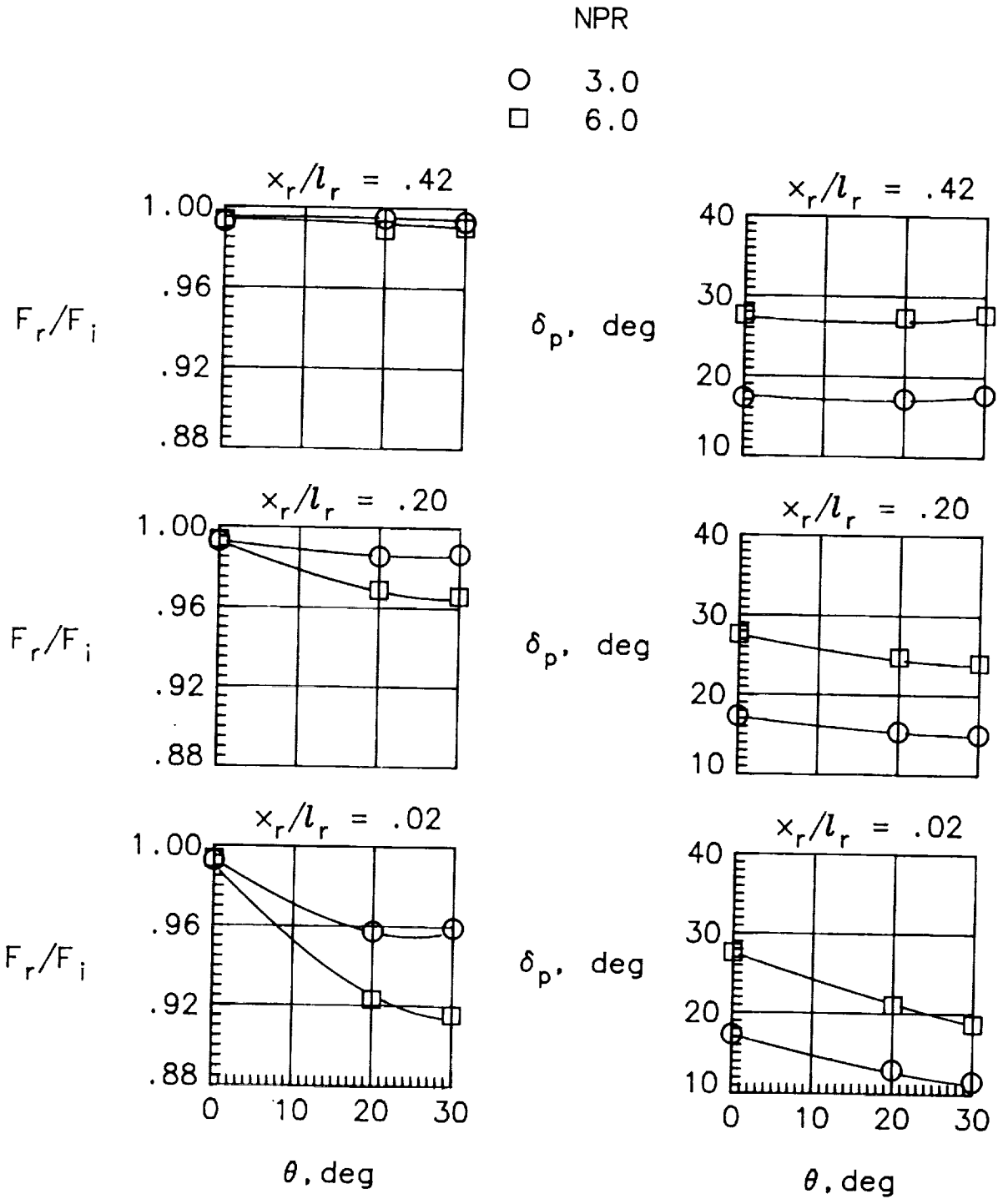

(b) Med sidewall.

Figure 14. Continued.

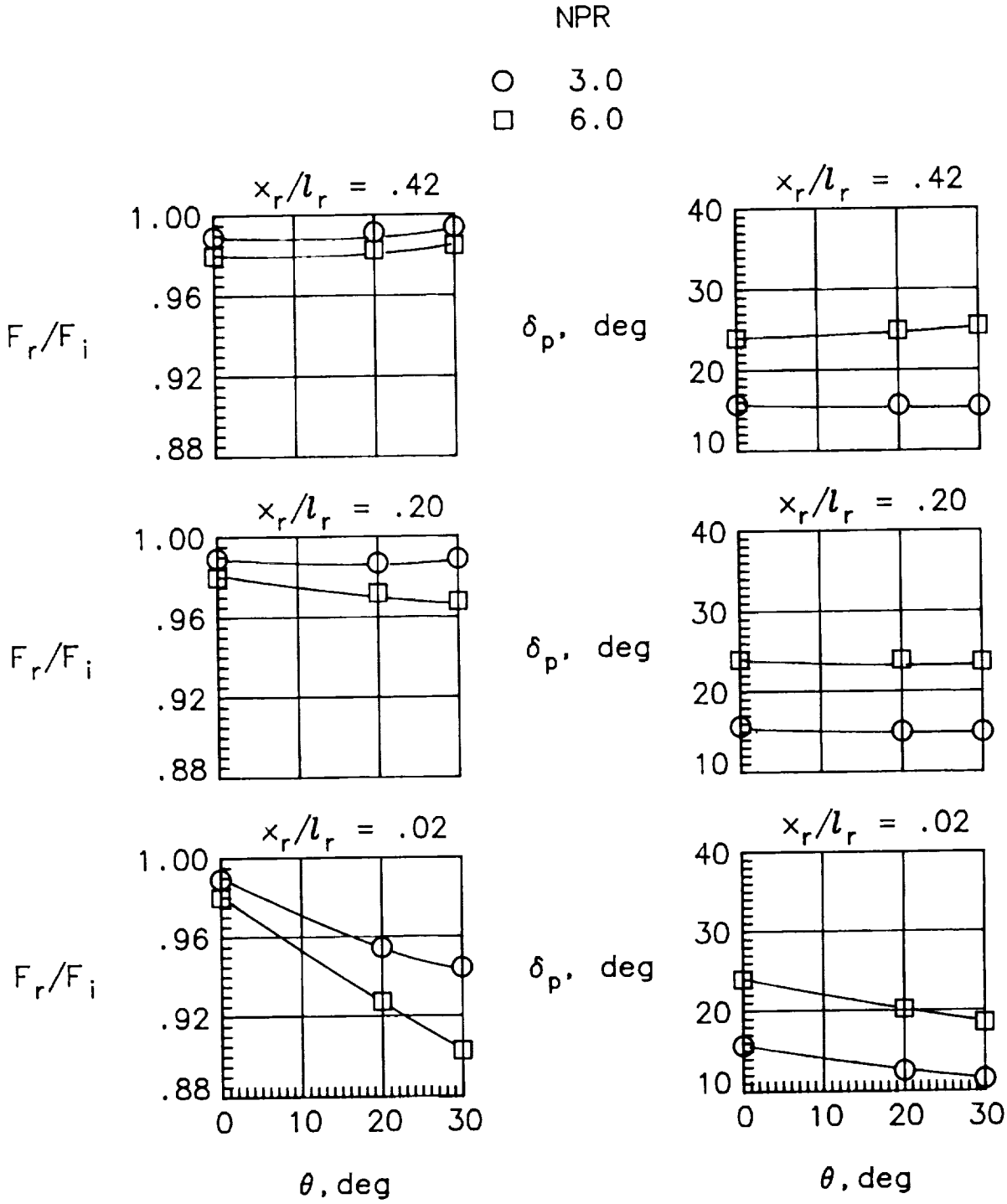

(c) Min sidewall.

Figure 14. Concluded.

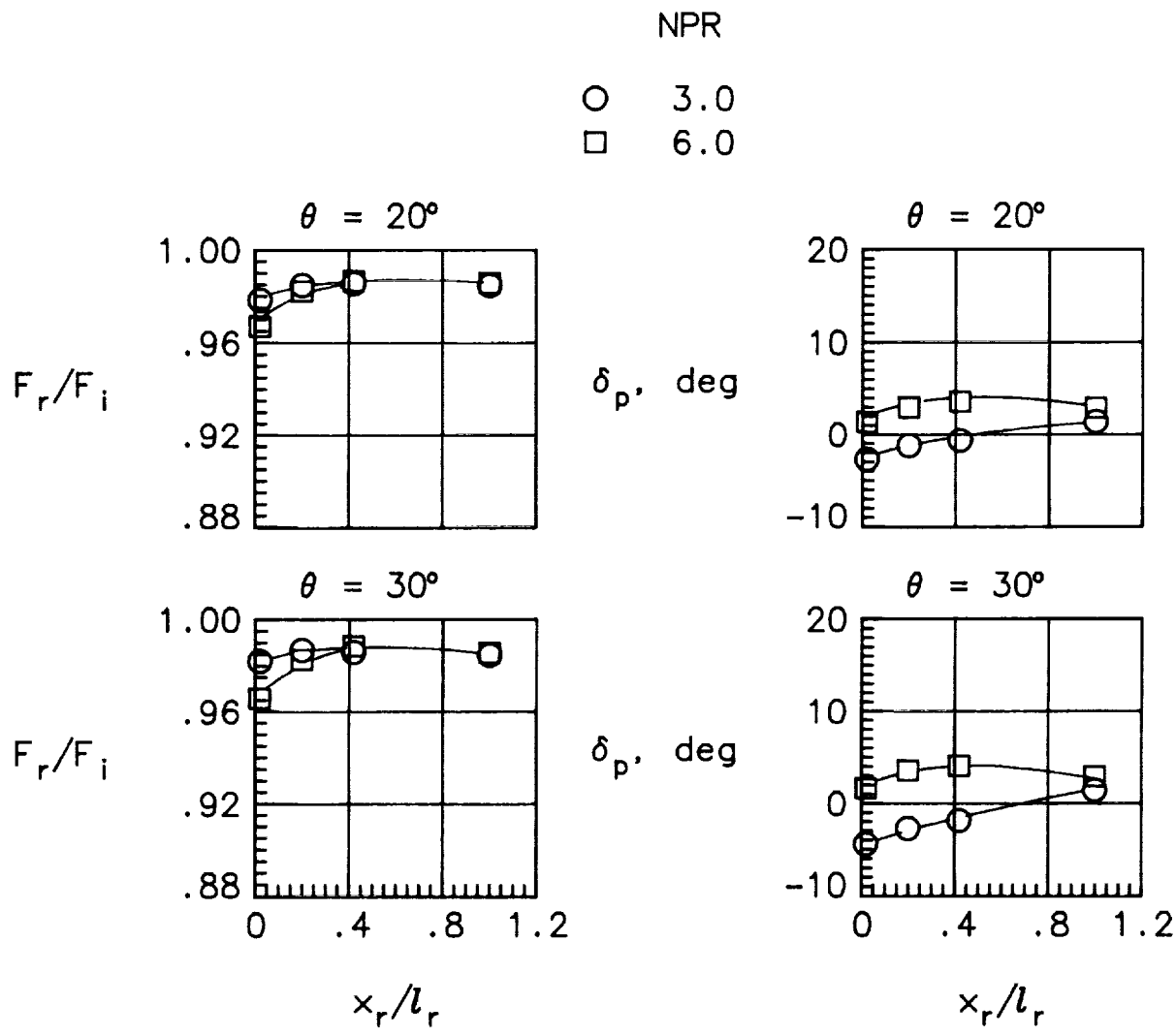

(a) Max sidewall.

Figure 15. Summary of effects of hinge line location on nozzle internal performance with various sidewall containments for $\phi = 0°$, $\delta_{v,p} = 0°$, and $\delta_{v,y} = 0°$.

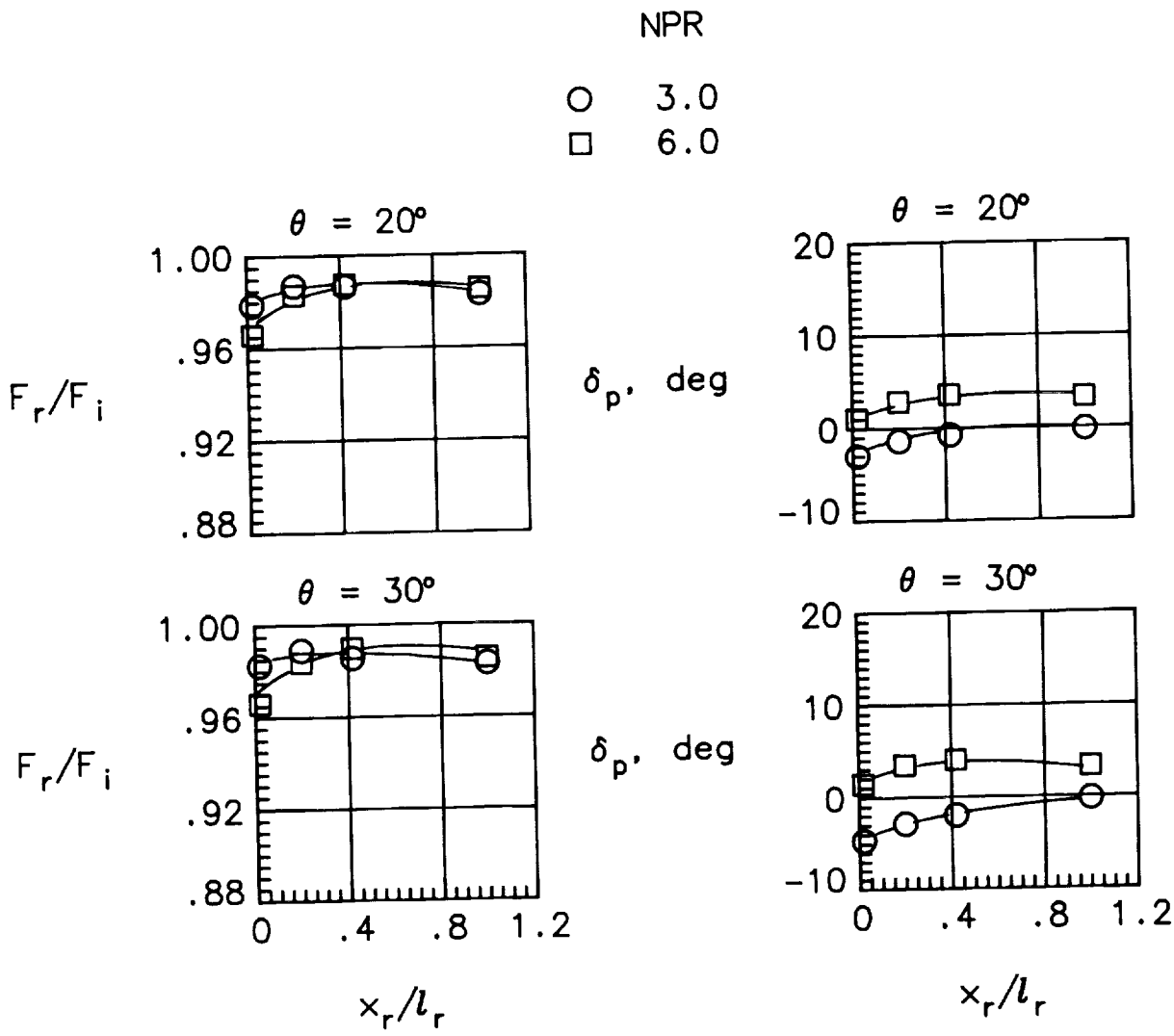

(b) Med sidewall.

Figure 15. Continued.

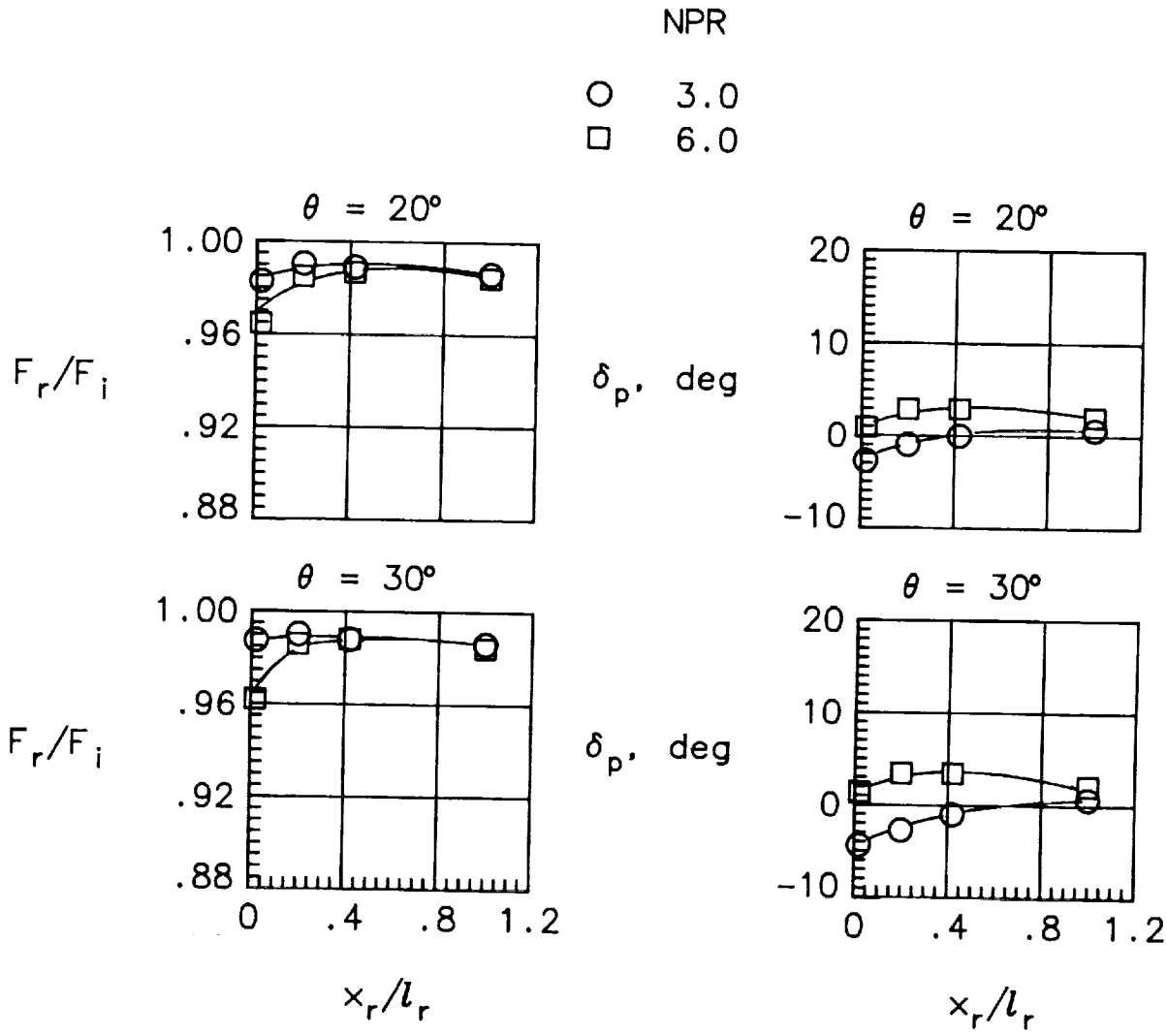

(c) Min sidewall.

Figure 15. Concluded.

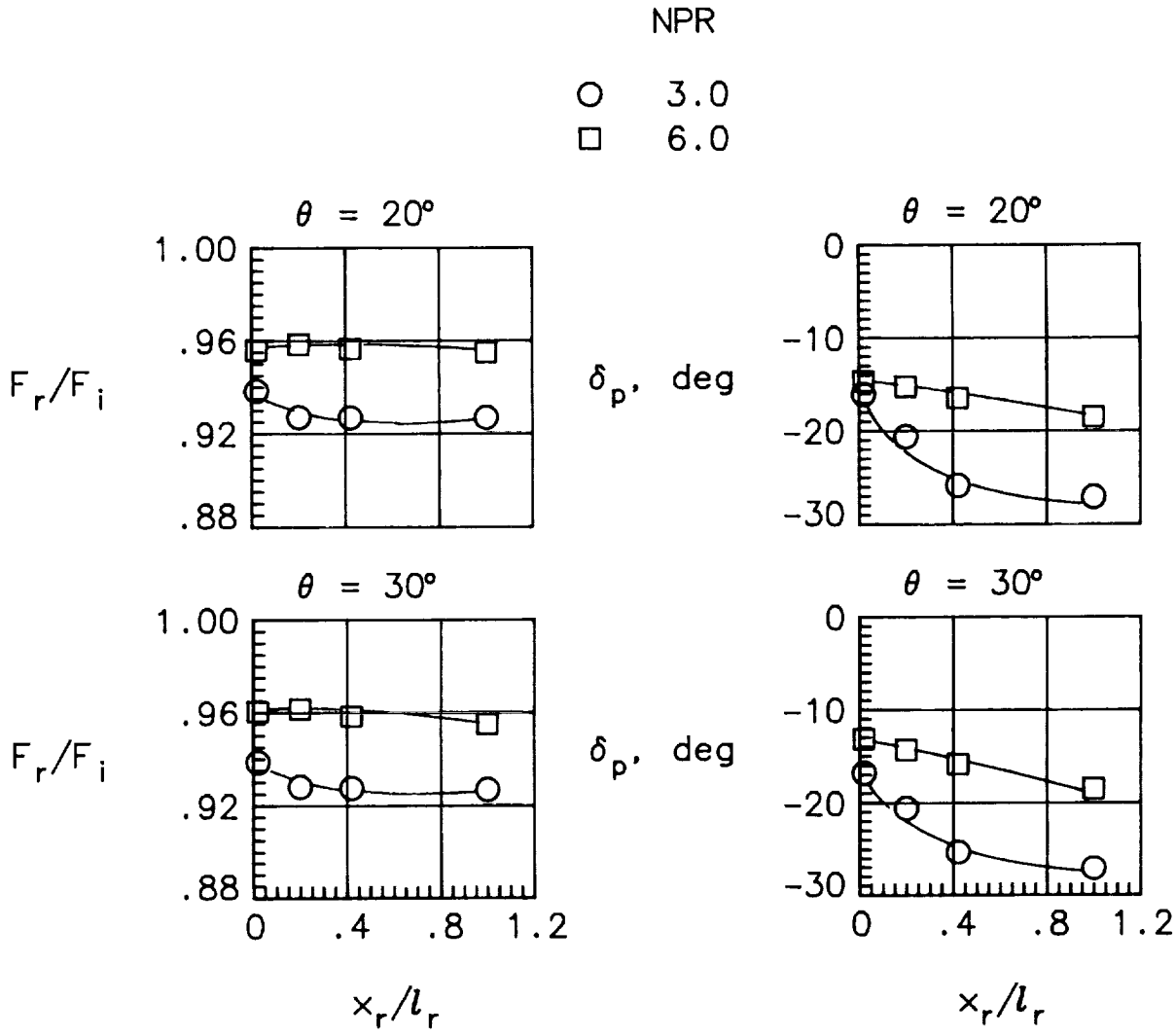

(a) Max sidewall.

Figure 16. Summary of effects of hinge line location on nozzle internal performance with various sidewall containments for $\phi = 0°$, $\delta_{v,p} = -20°$, and $\delta_{v,y} = 0°$.

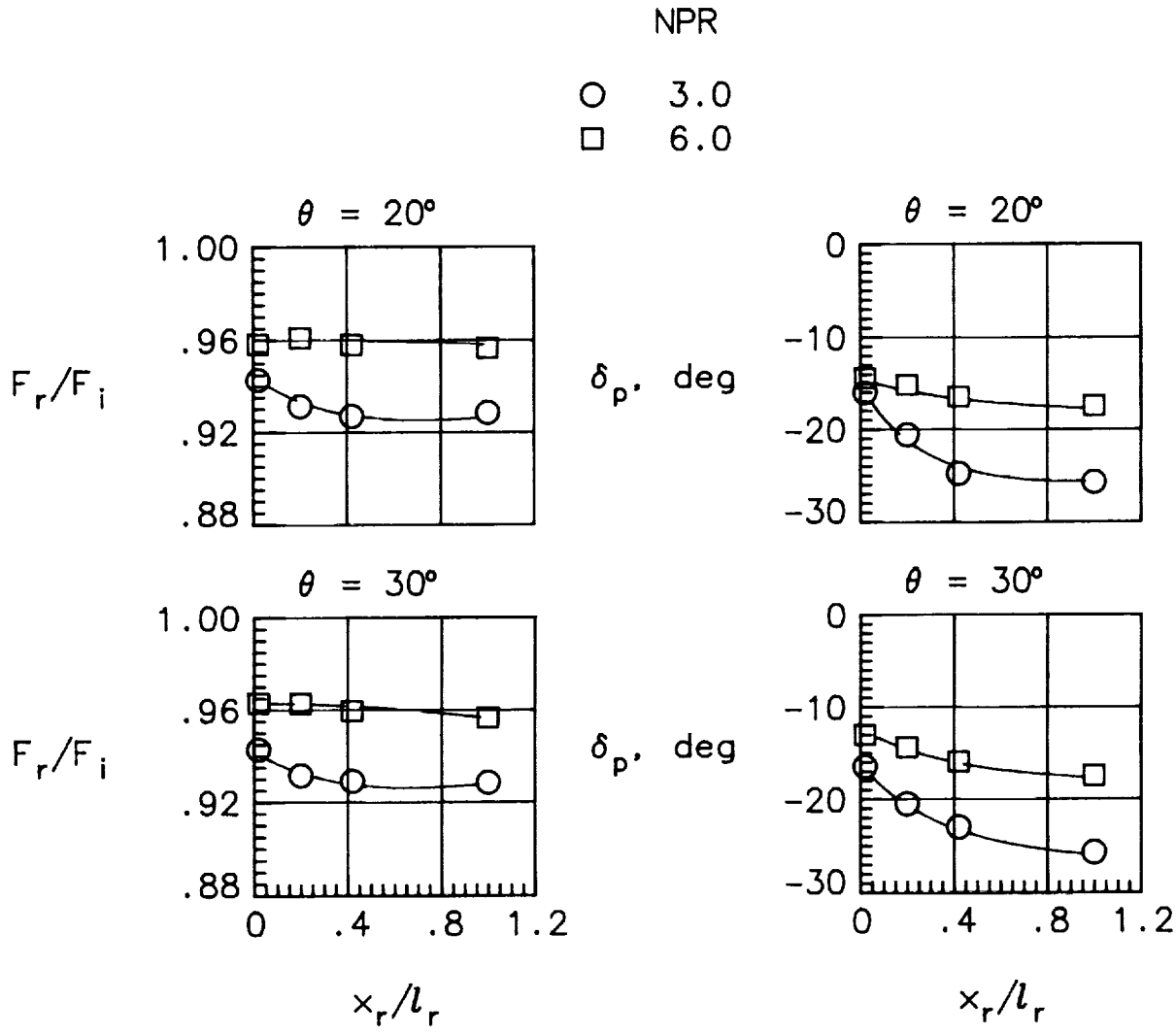

(b) Med sidewall.

Figure 16. Continued.

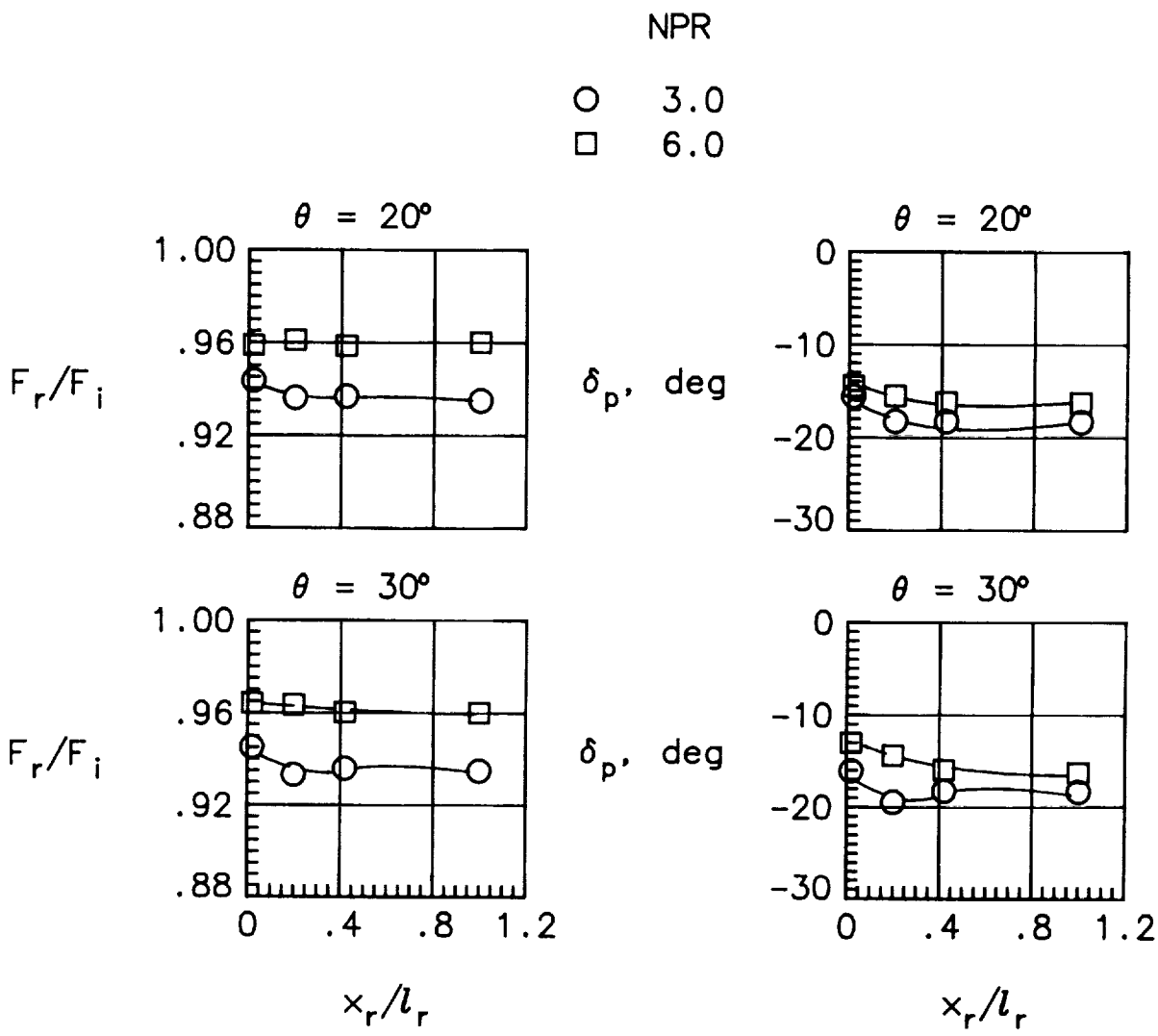

(c) Min sidewall.

Figure 16. Concluded.

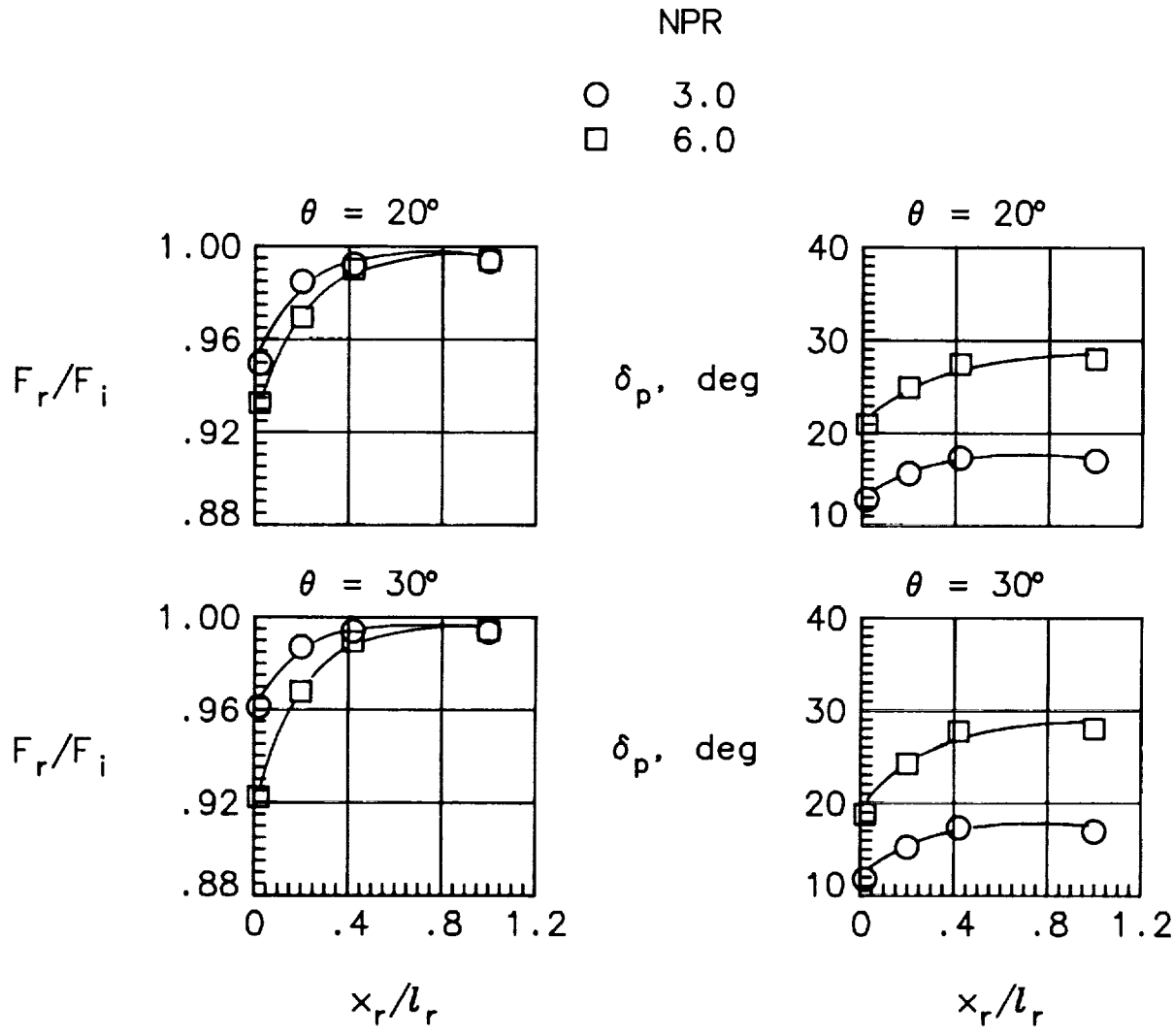

(a) Max sidewall.

Figure 17. Summary of effects of hinge line location on nozzle internal performance with various sidewall containments for $\phi = 0°$, $\delta_{v,p} = 20°$, and $\delta_{v,y} = 0°$.

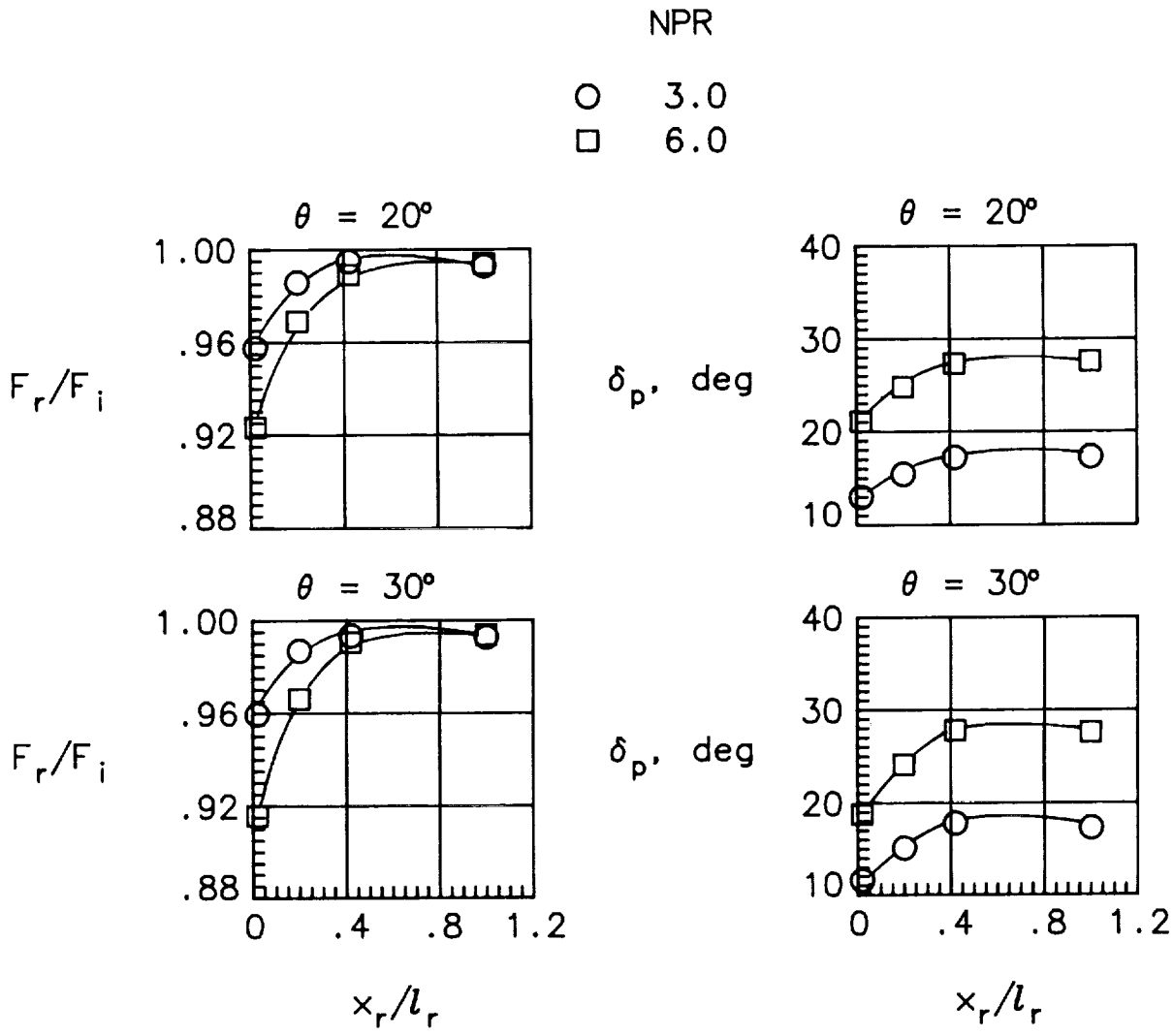

(b) Med sidewall.

Figure 17. Continued.

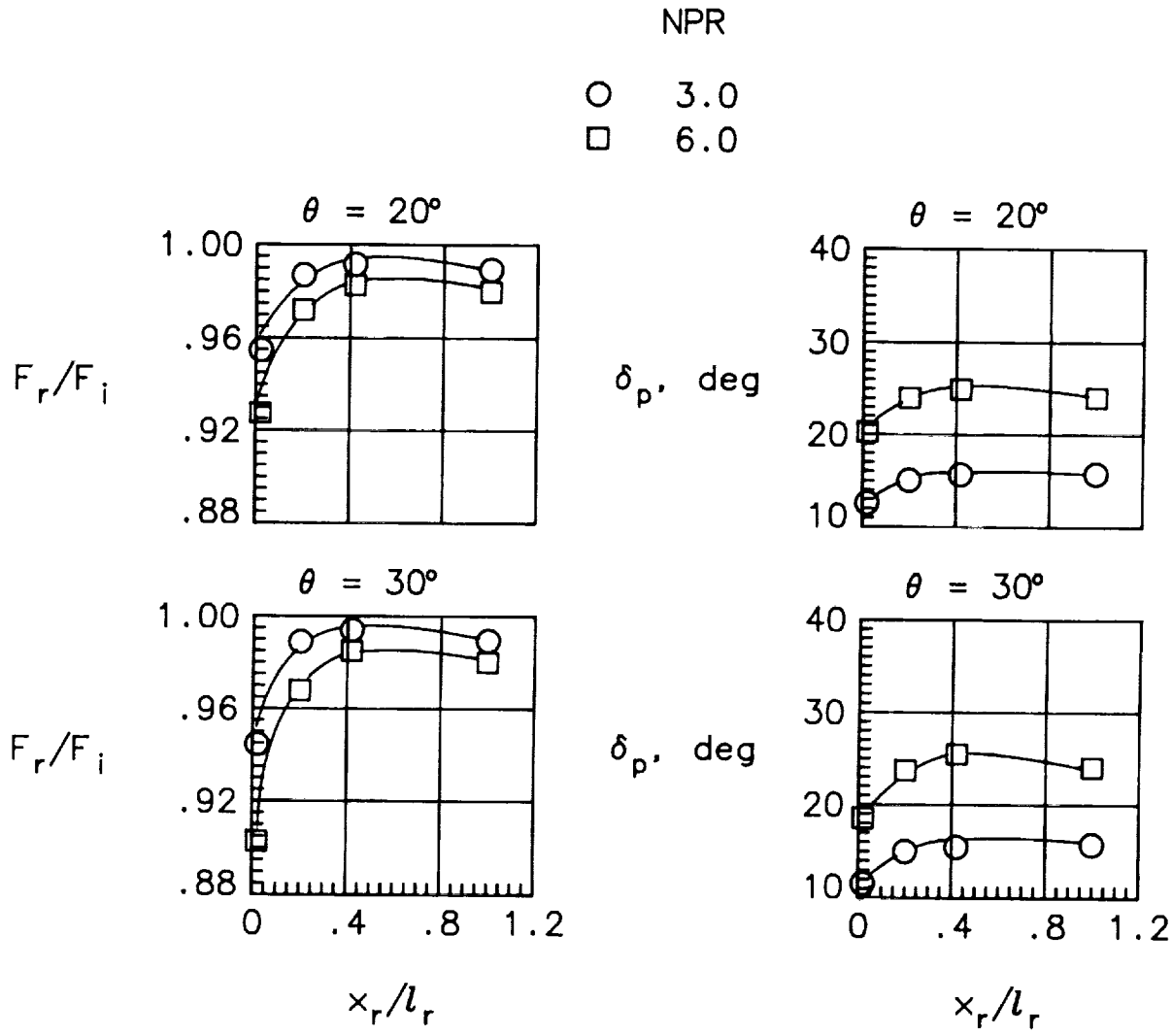

(c) Min sidewall.

Figure 17. Concluded.

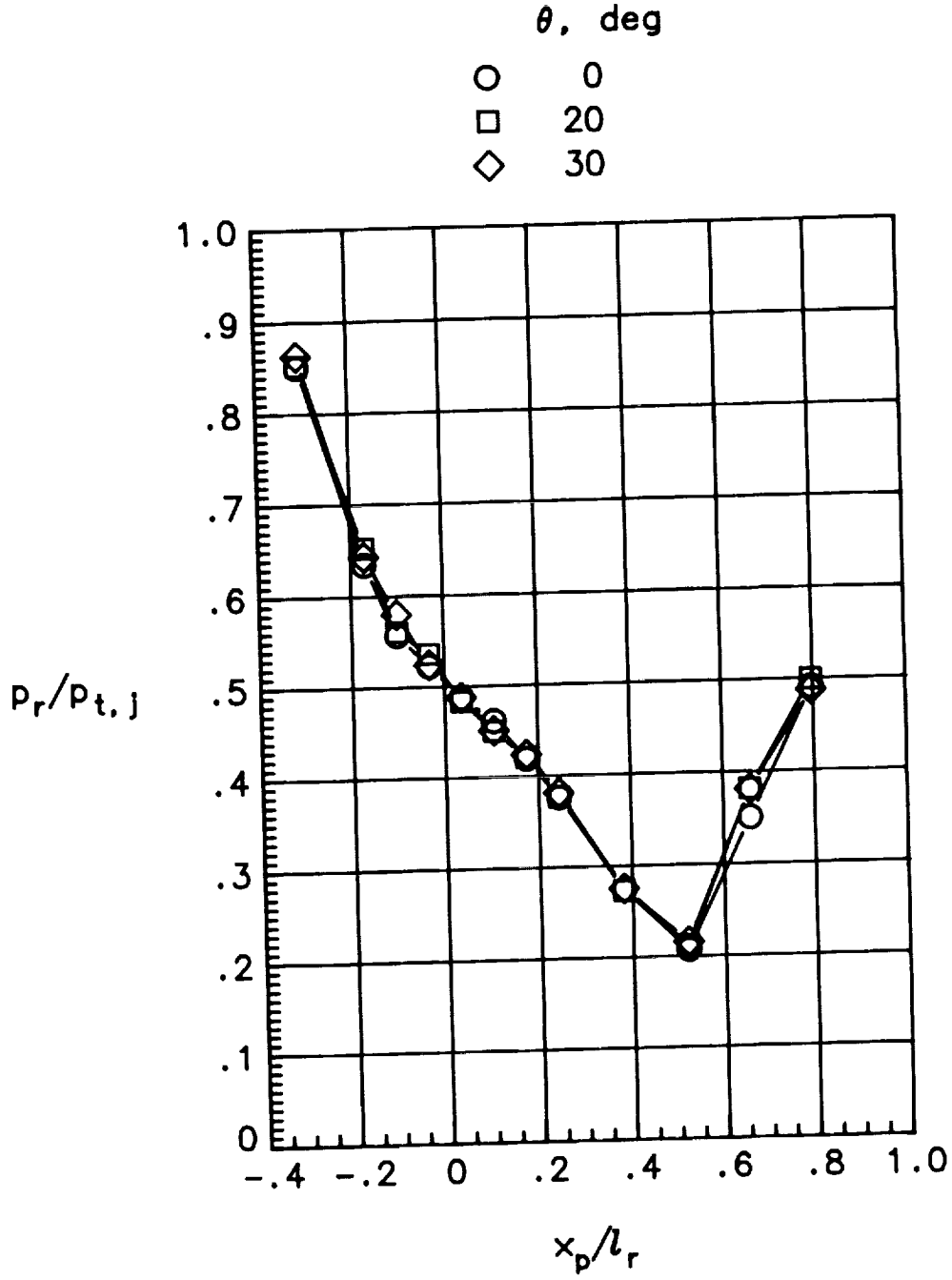

(a) $\delta_{r,p} = 0°$.

Figure 18. Effect of cutout angle on internal pressures at various geometric pitch vector angles. Max sidewall: $x_r/l_r = 0.20$; $\phi = 0°$; $\delta_{r,y} = 0°$; NPR = 3.0.

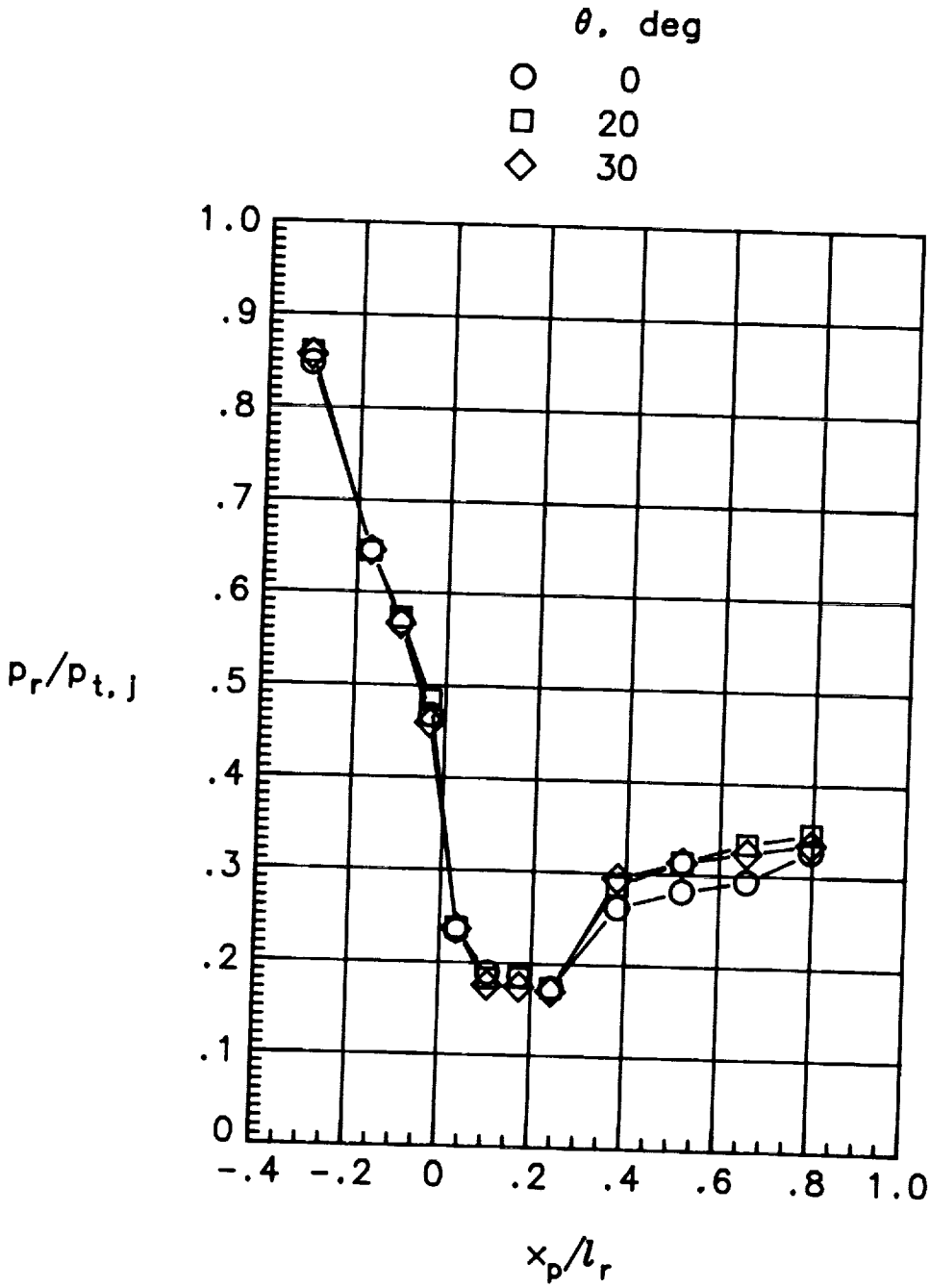

(b) $\delta_{v,p} = -20°$.

Figure 18. Continued.

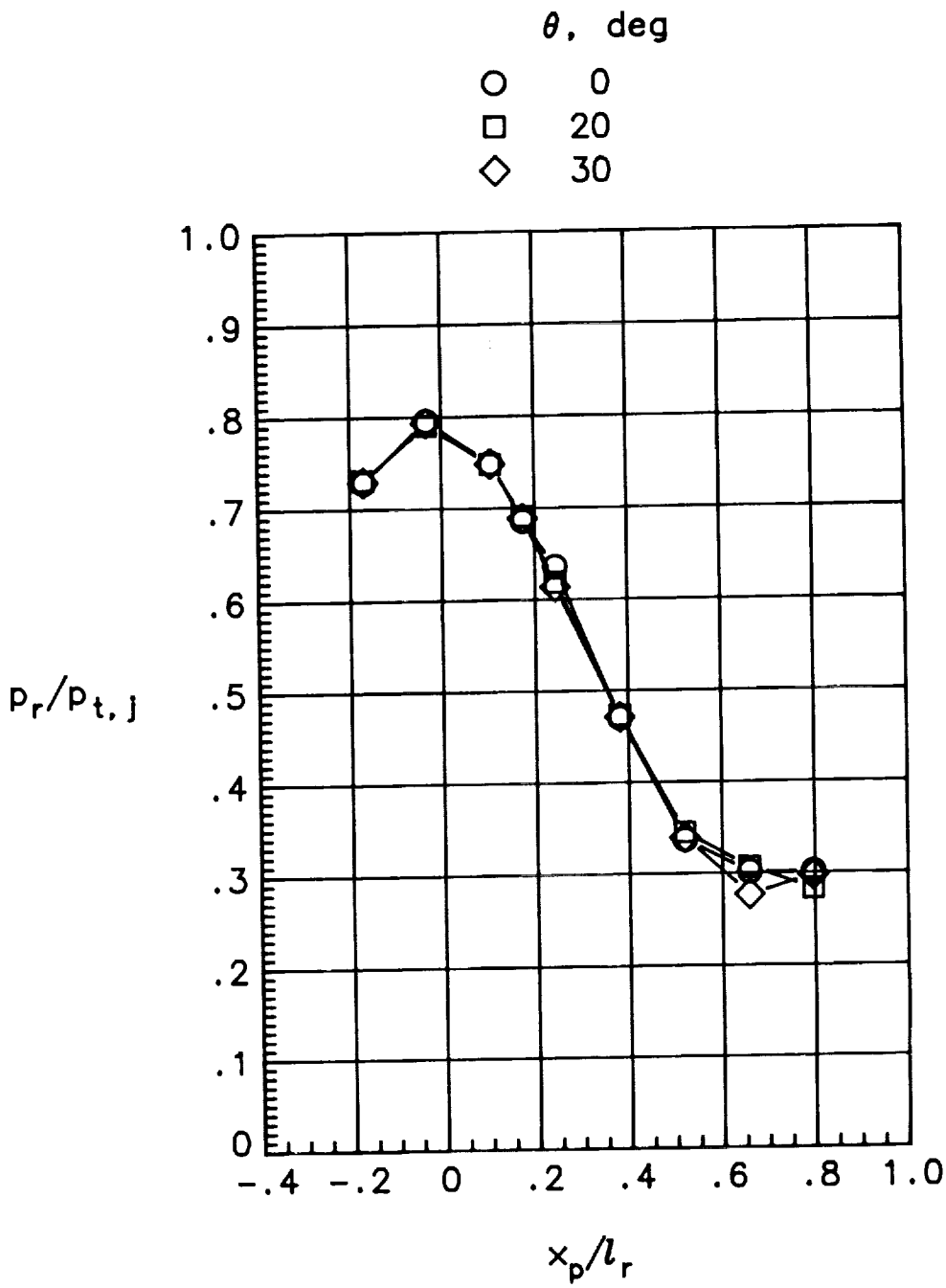

(c) $\delta_{v,p} = 20°$.

Figure 18. Concluded.

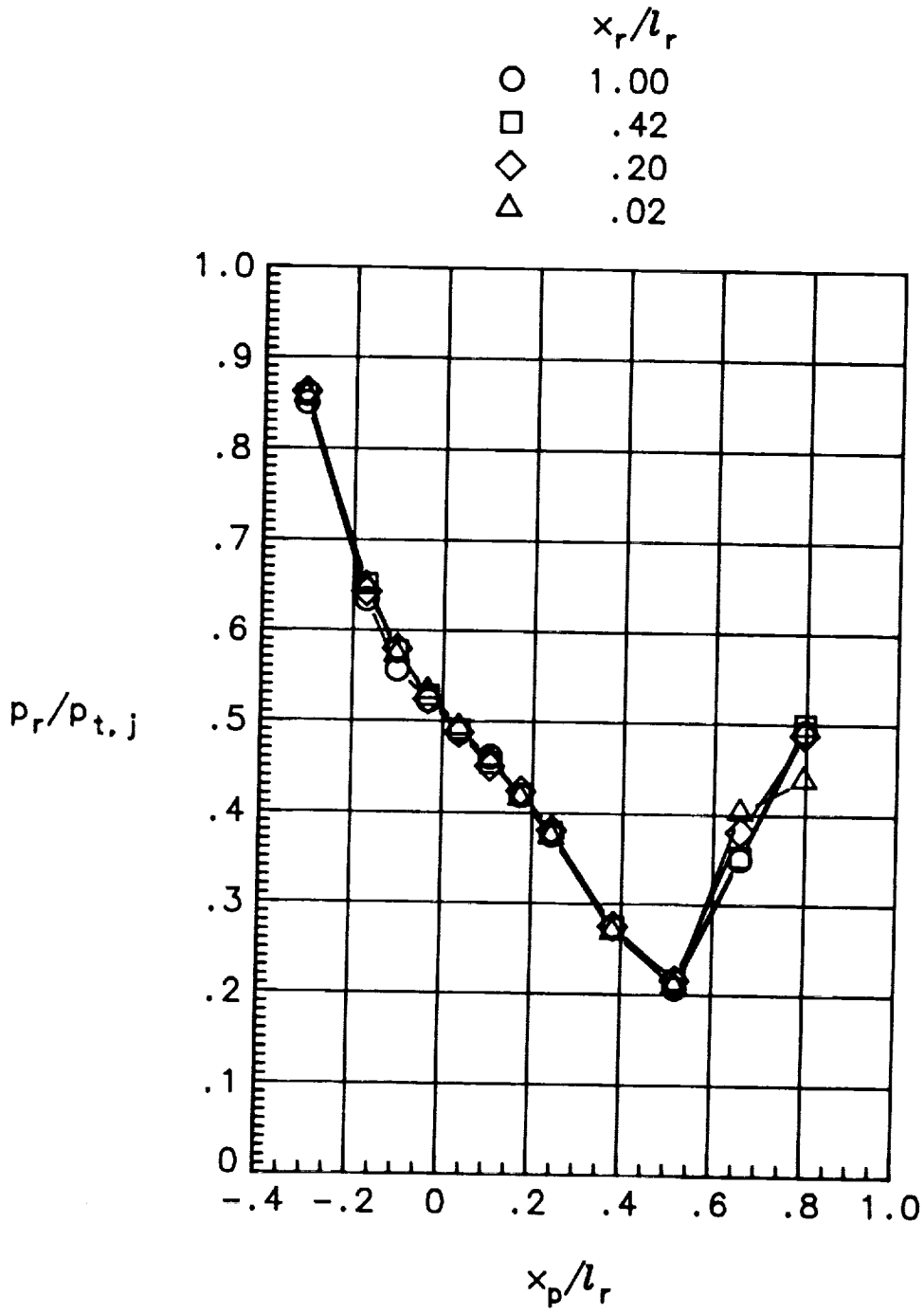

(a) $\delta_{r,p} = 0°$.

Figure 19. Effect of hinge line location on internal pressures at various geometric pitch vector angles. Max sidewall: $\theta = 30°$; $\phi = 0°$; $\delta_{r,y} = 0°$; NPR = 3.0.

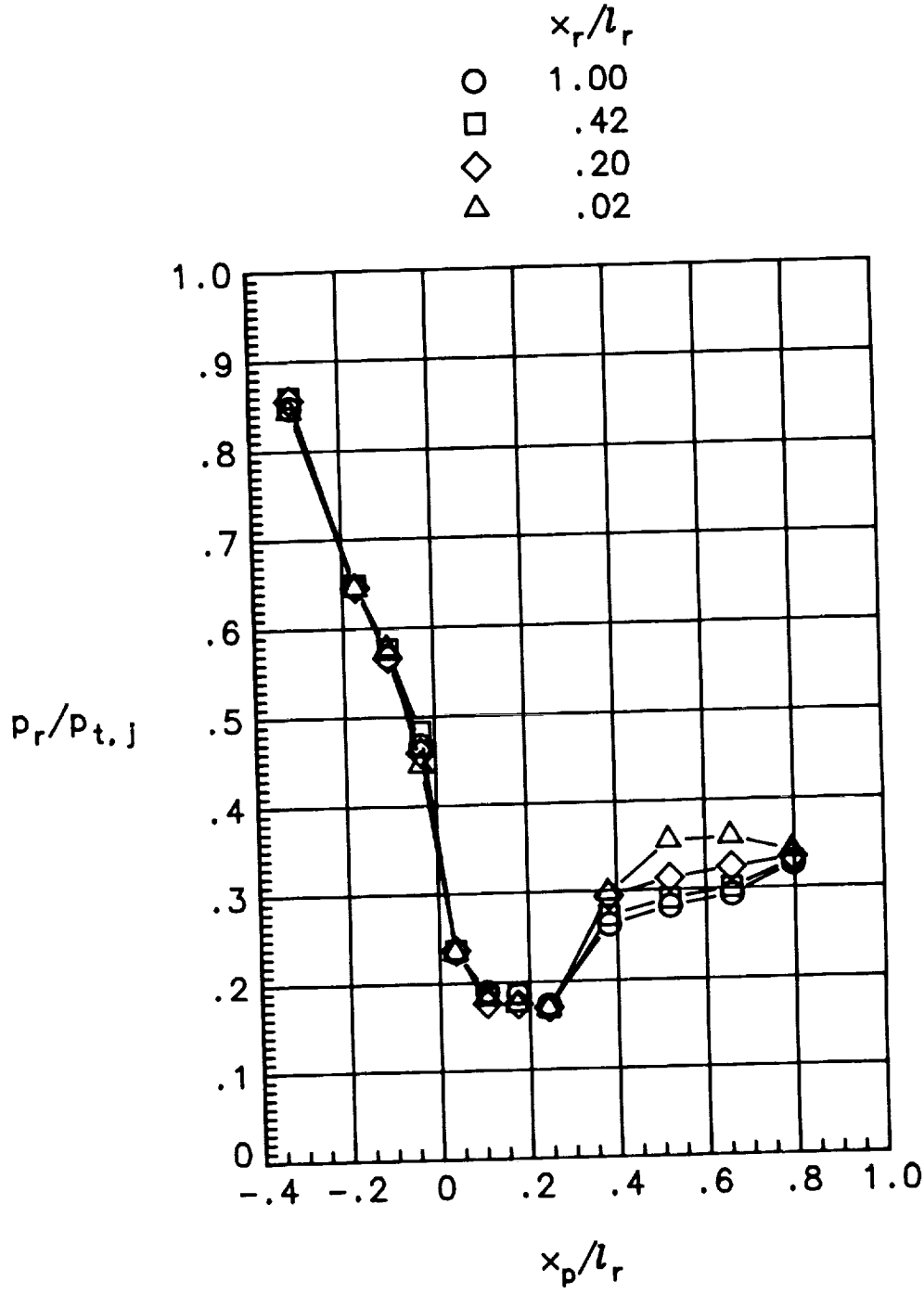

(b) $\delta_{e,p} = -20°$.

Figure 19. Continued.

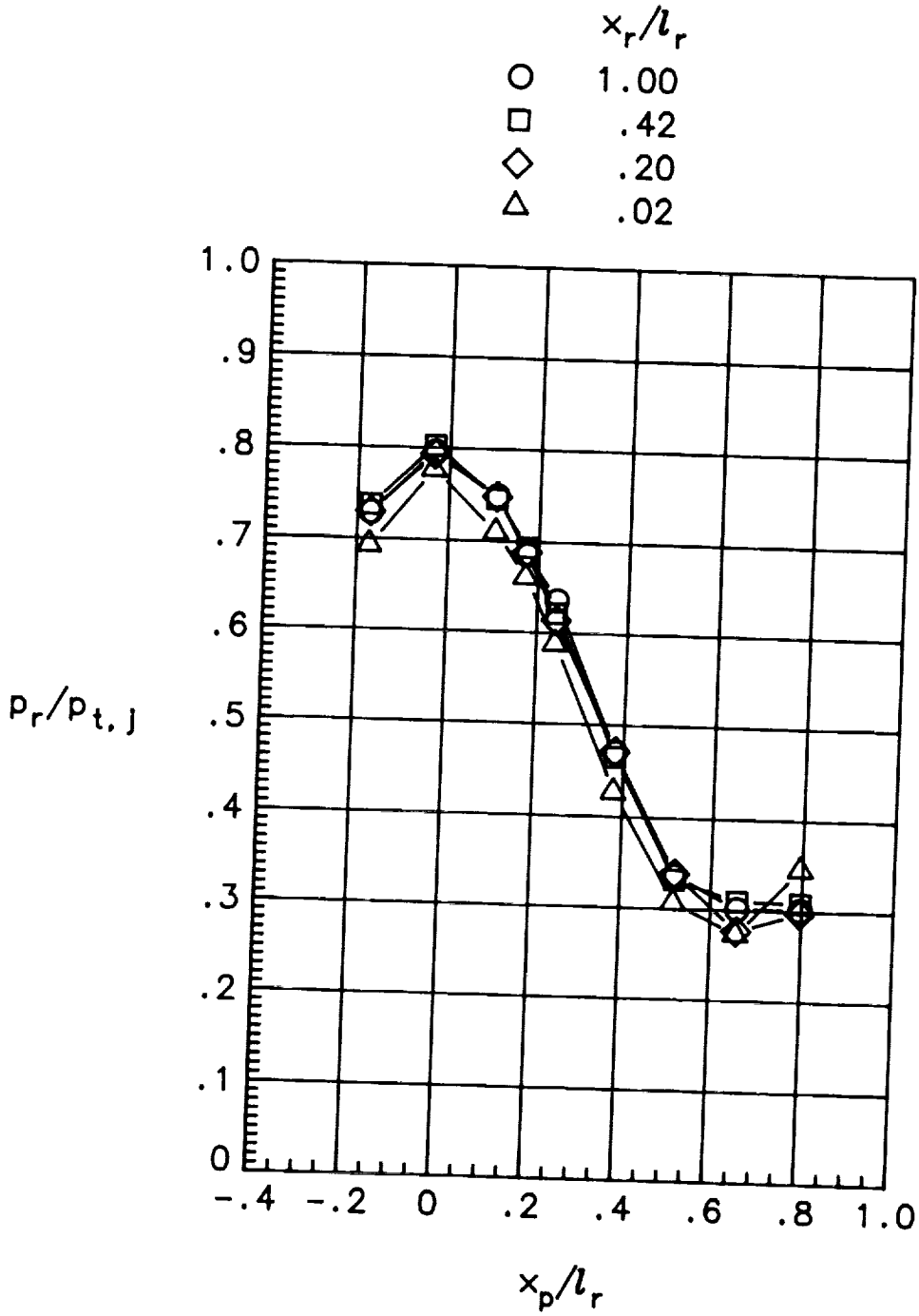

(c) $\delta_{r,p} = 20°$.

Figure 19. Concluded.

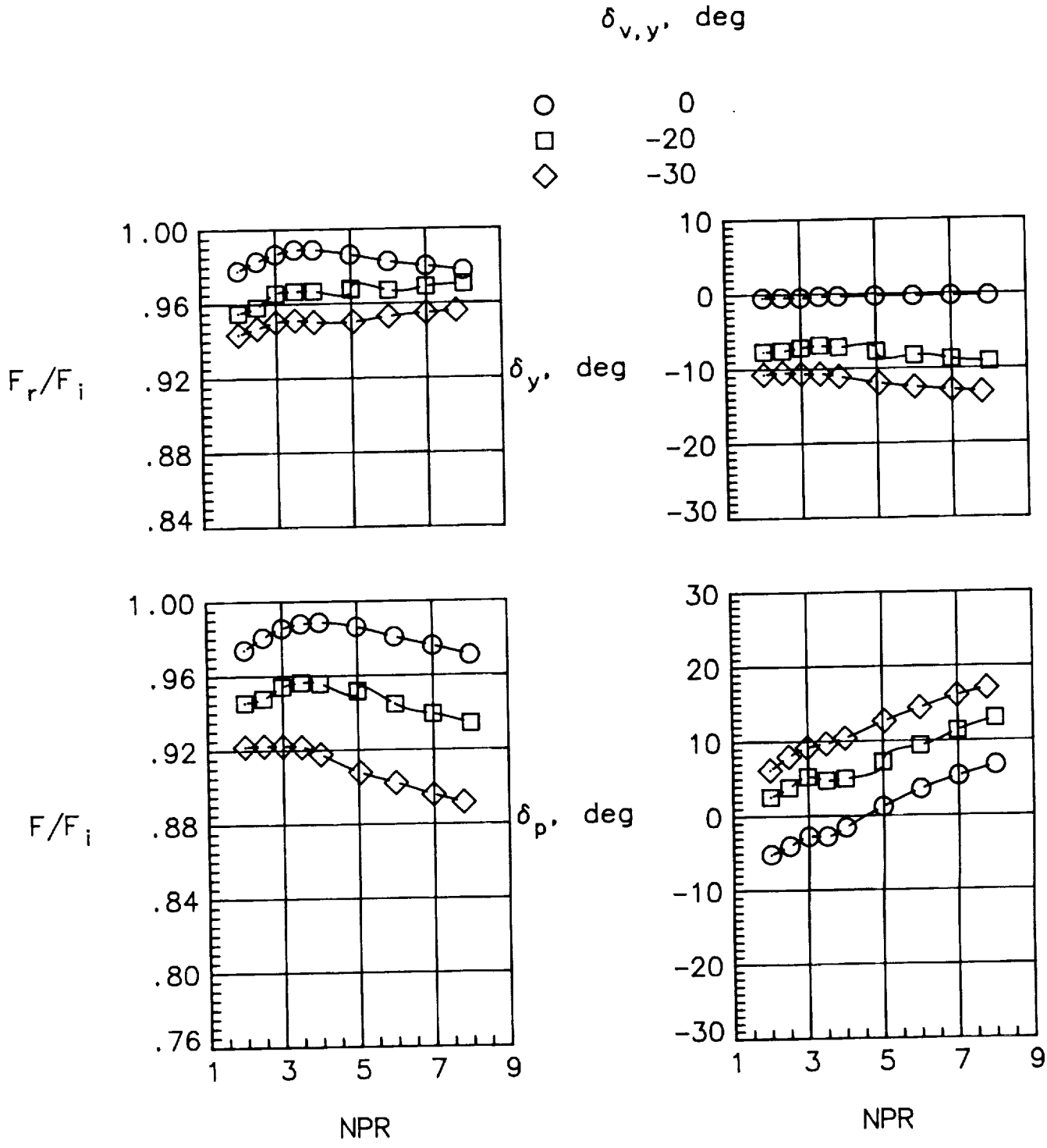

(a) $\delta_{v,p} = 0°$.

Figure 20. Effect of yaw vectoring on nozzle performance at various geometric pitch vector angles. Max sidewall; $x_r/l_r = 0.20$; $\theta = 30°$; $\phi = 0°$.

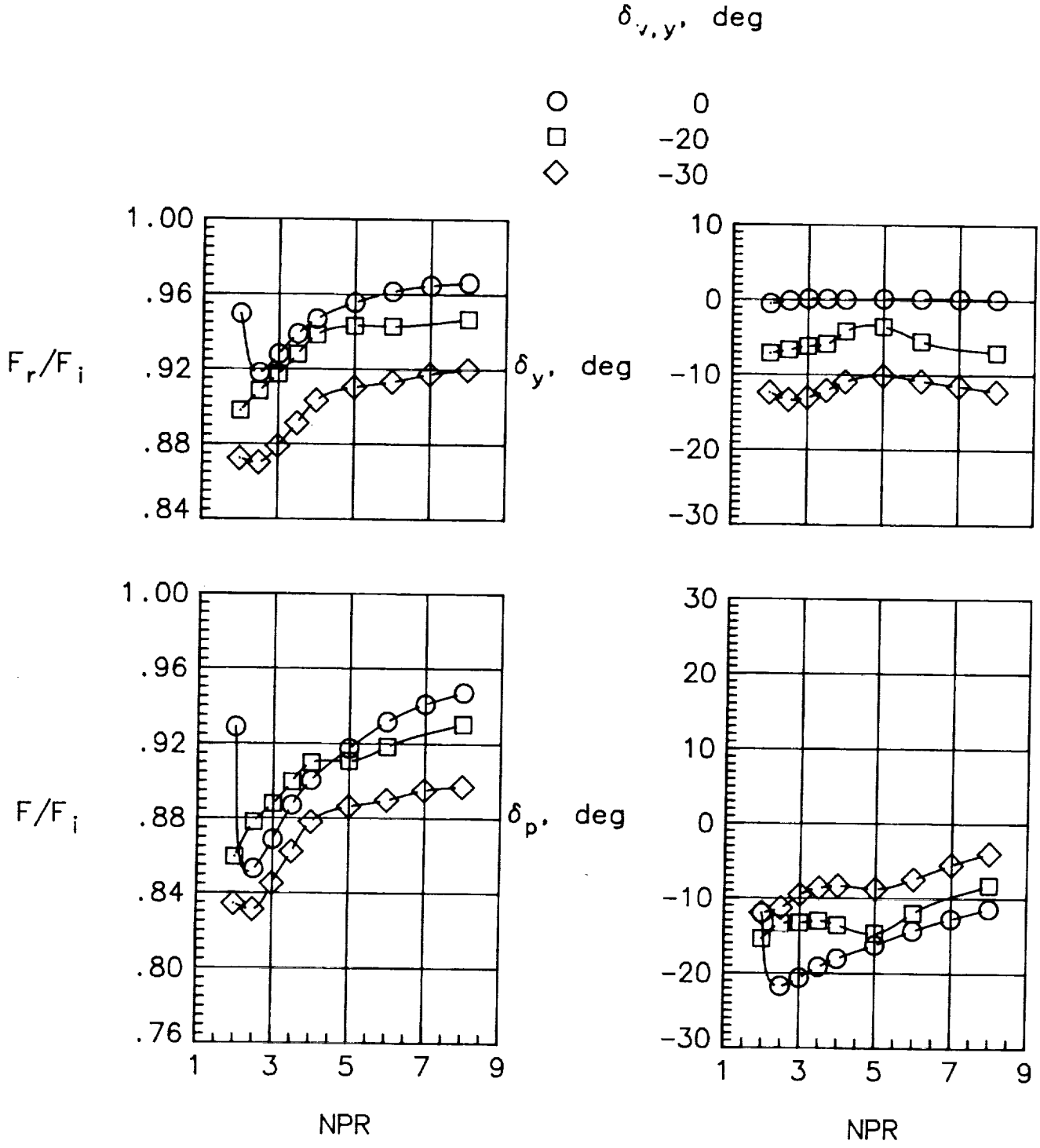

(b) $\delta_{v,p} = -20°$.

Figure 20. Continued.

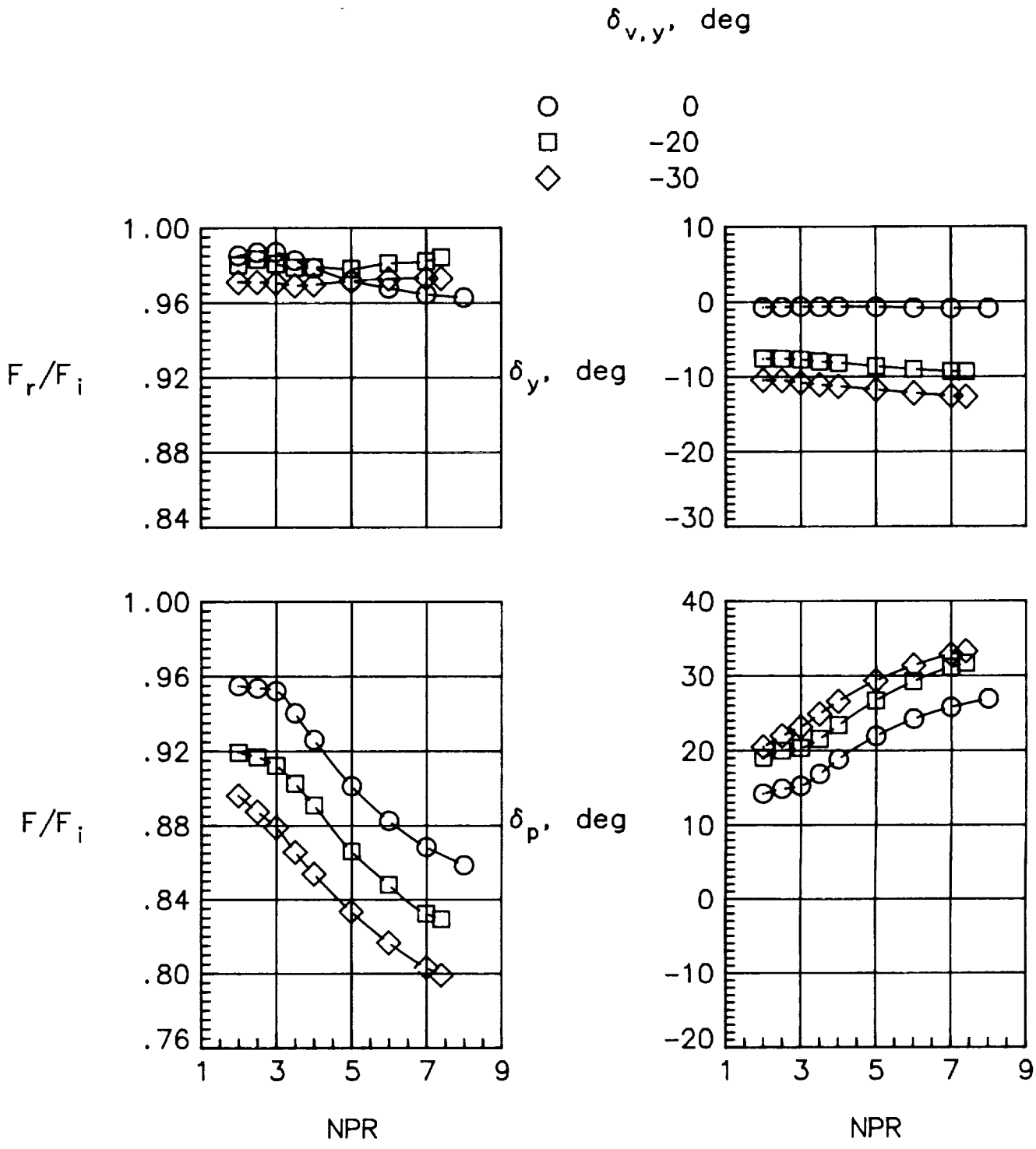

(c) $\delta_{v,p} = 20°$.

Figure 20. Concluded.

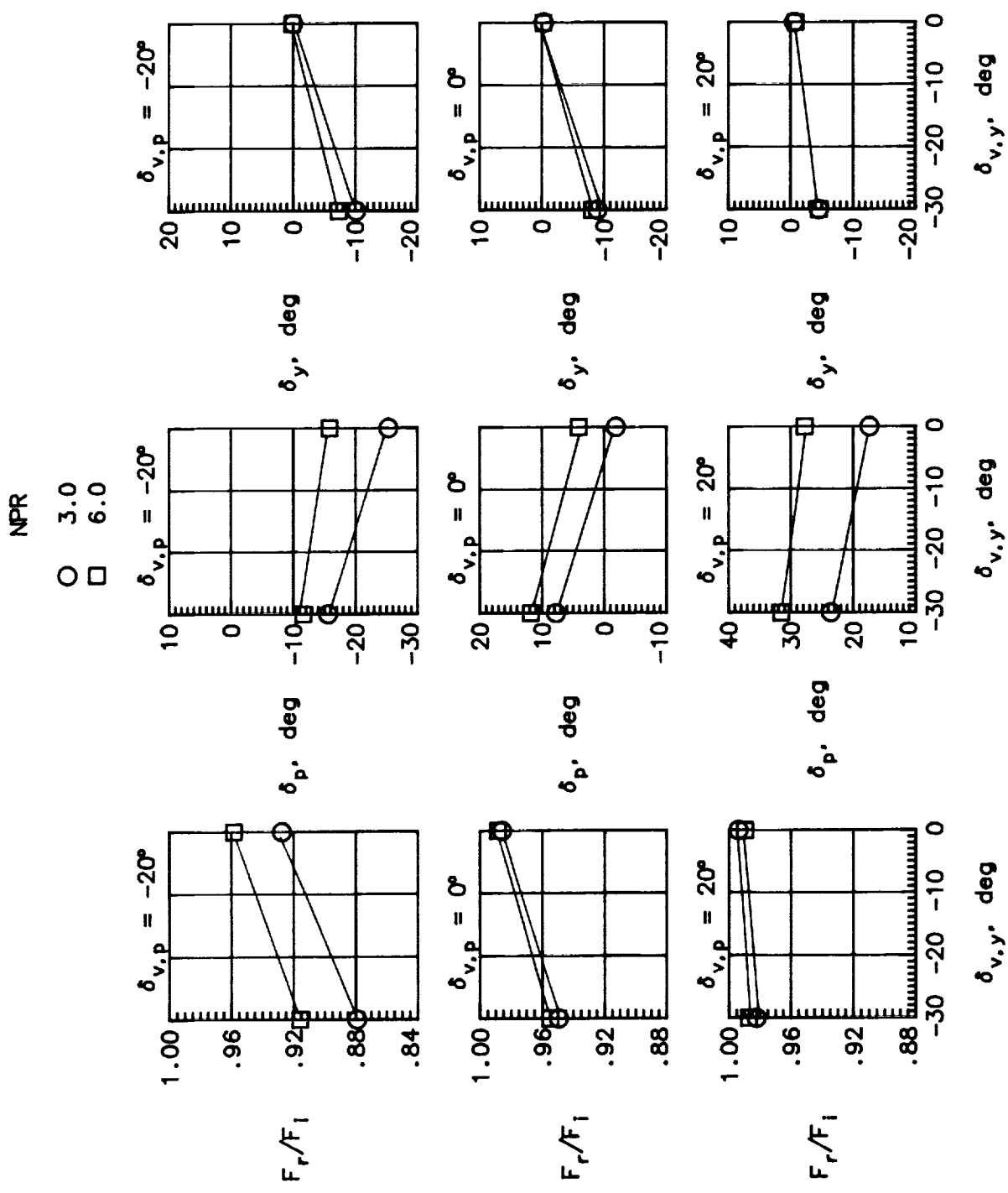

Figure 21. Summary of effects of yaw vectoring on nozzle performance with max sidewall, $x_r/l_r = 0.42$, $\theta = 30°$, and $\phi = 0°$.

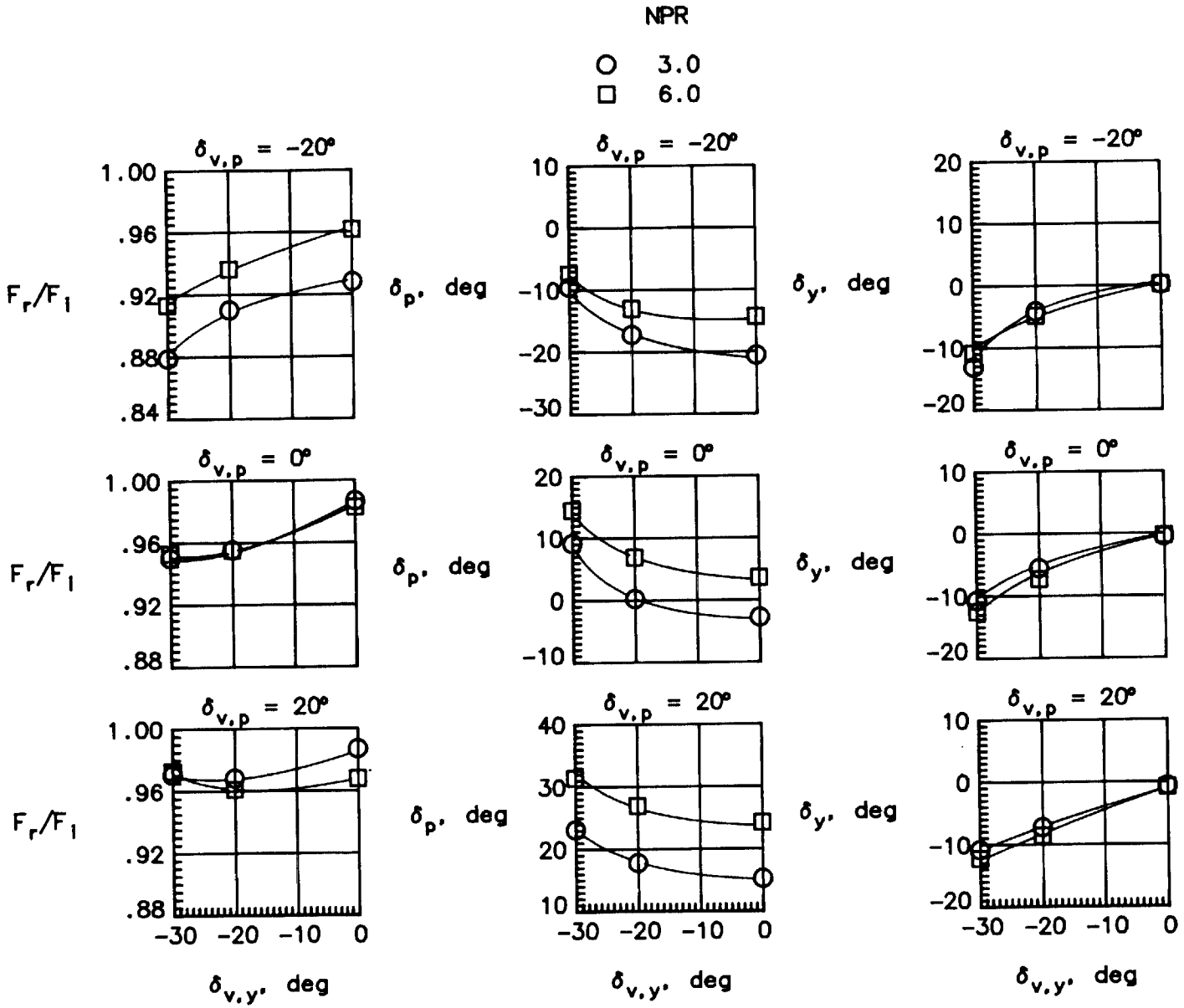

(a) Max sidewall.

Figure 22. Summary of effects of yaw vectoring on nozzle performance with various sidewall containments, $x_r/l_r = 0.20$, $\theta = 30°$, and $\phi = 0°$.

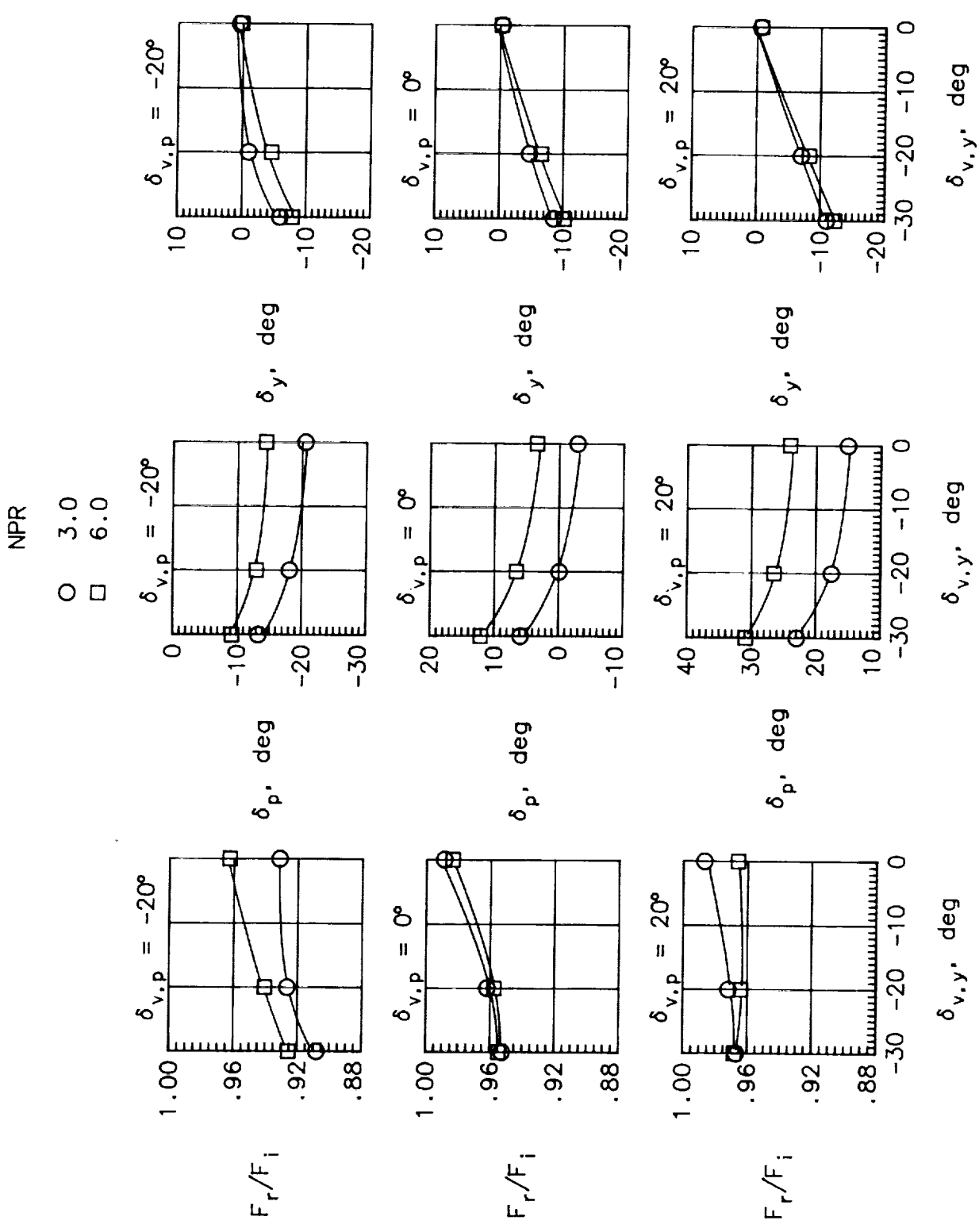

(b) Med sidewall.

Figure 22. Concluded.

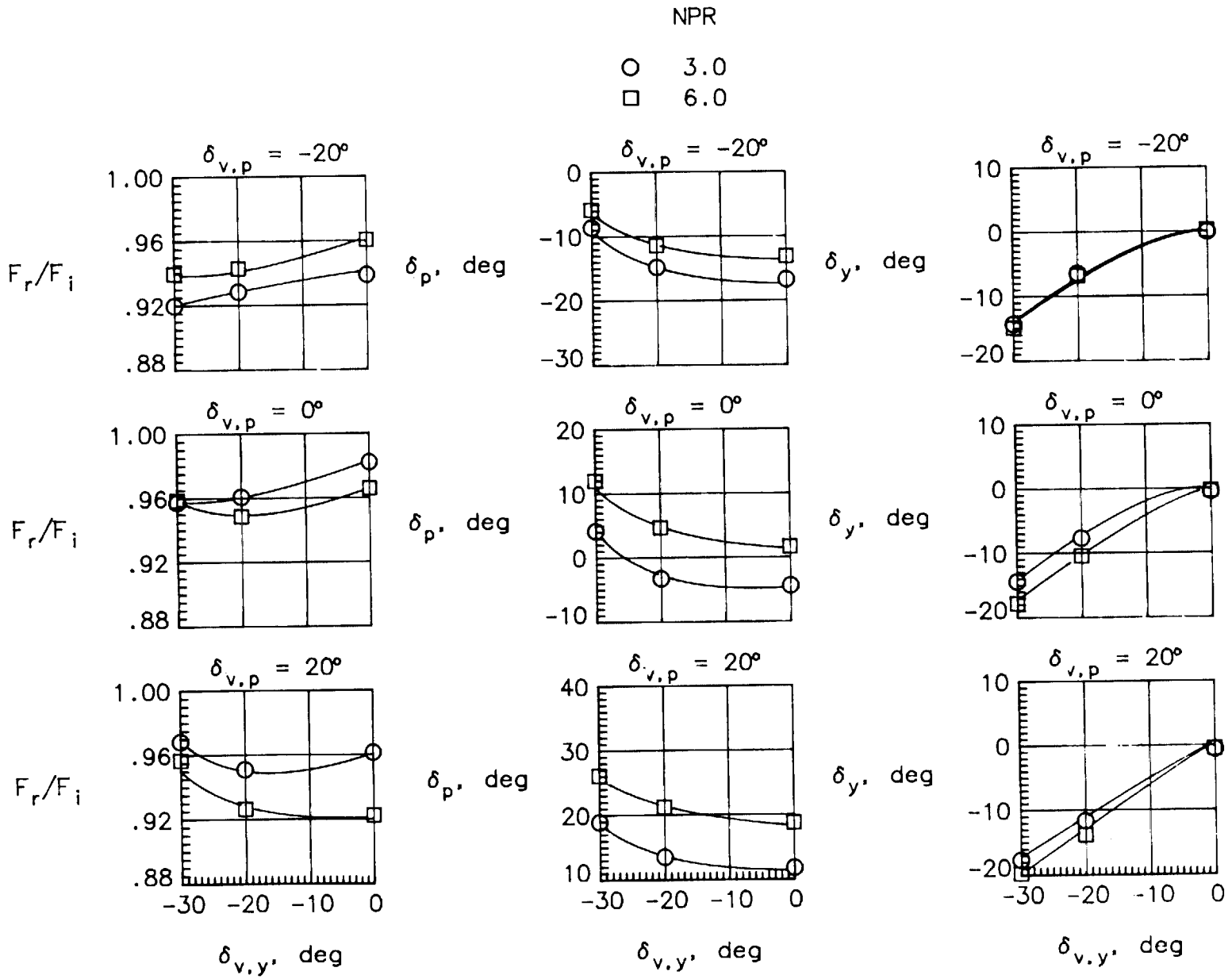

(a) Max sidewall.

Figure 23. Summary of effects of yaw vectoring on nozzle performance with various sidewall containments, $x_r/l_r = 0.02$, $\theta = 30°$, and $\phi = 0°$.

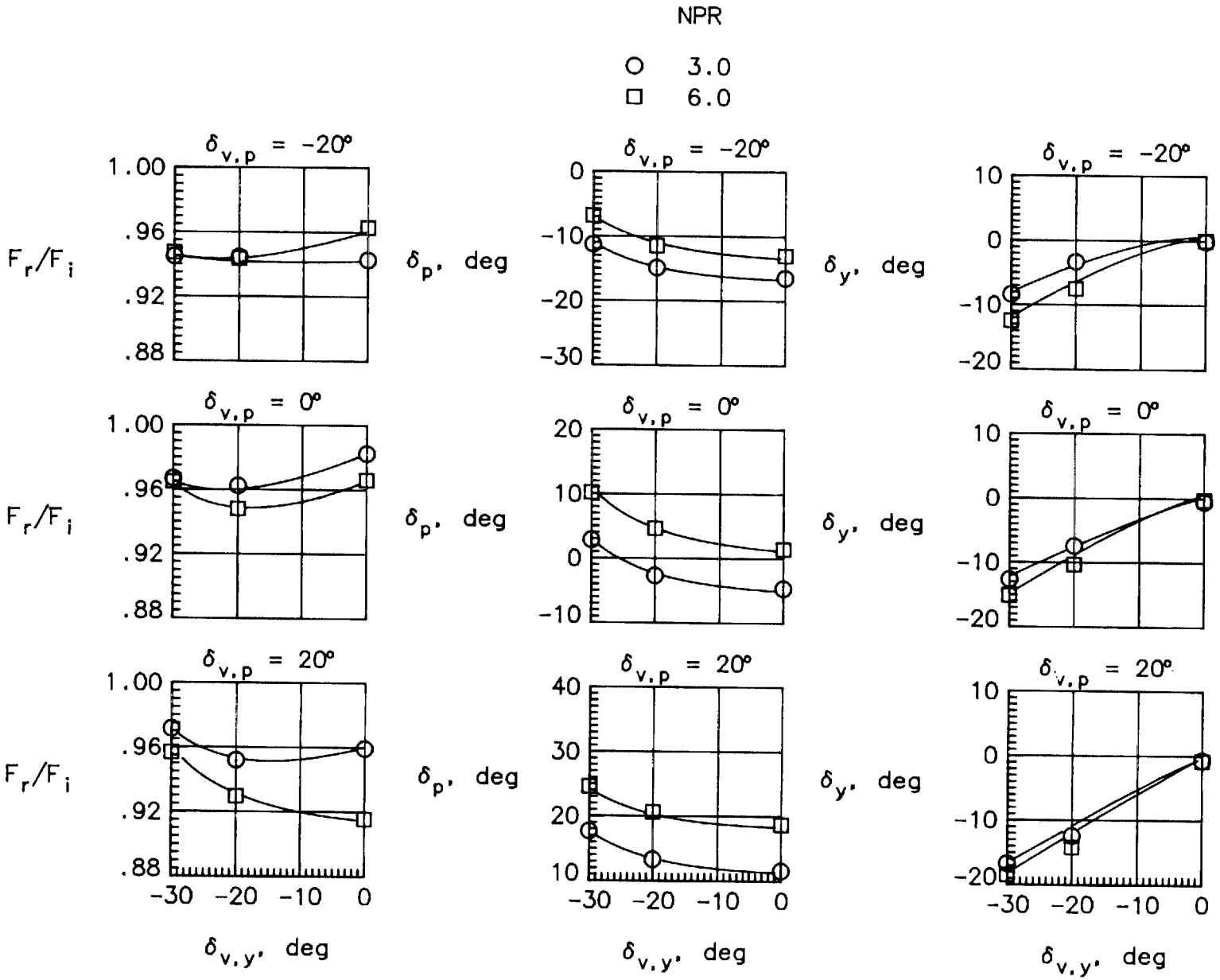

(b) Med sidewall.

Figure 23. Continued.

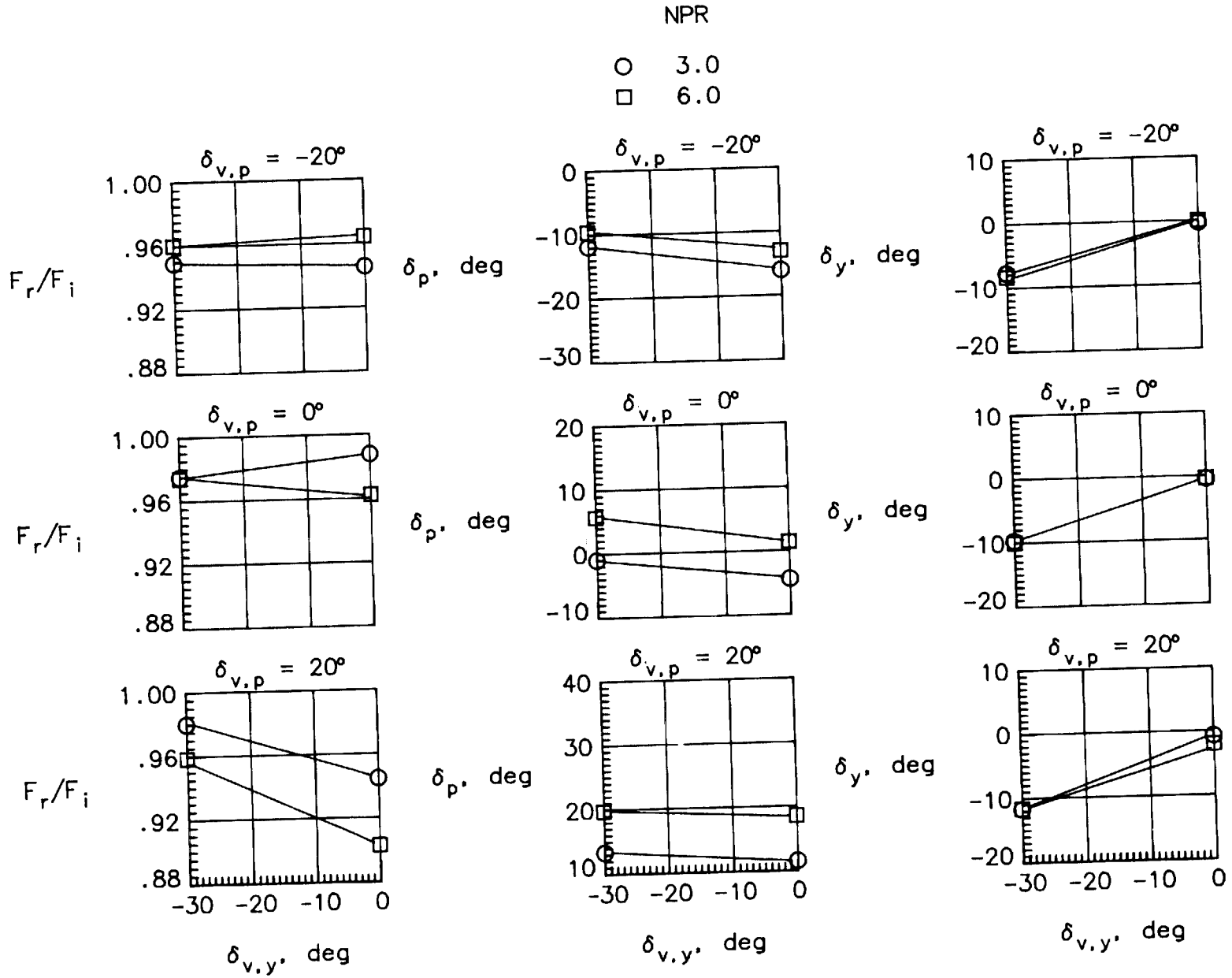

(c) Min sidewall.

Figure 23. Concluded.

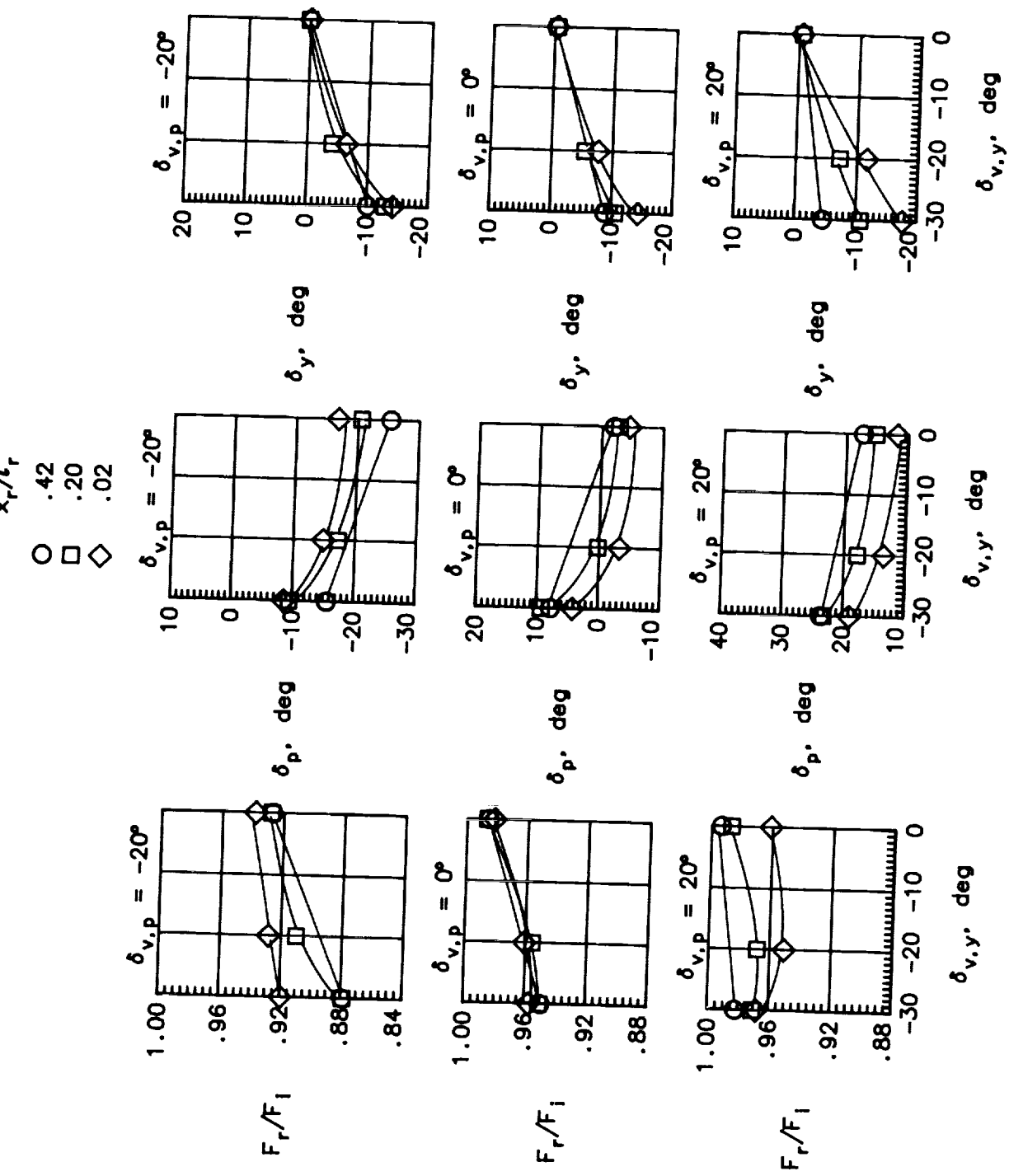

(a) NPR = 3.0.

Figure 24. Summary of yaw vectoring effects on nozzle performance at various values of NPR. max sidewall. $\theta = 30°$, and $\phi = 0°$.

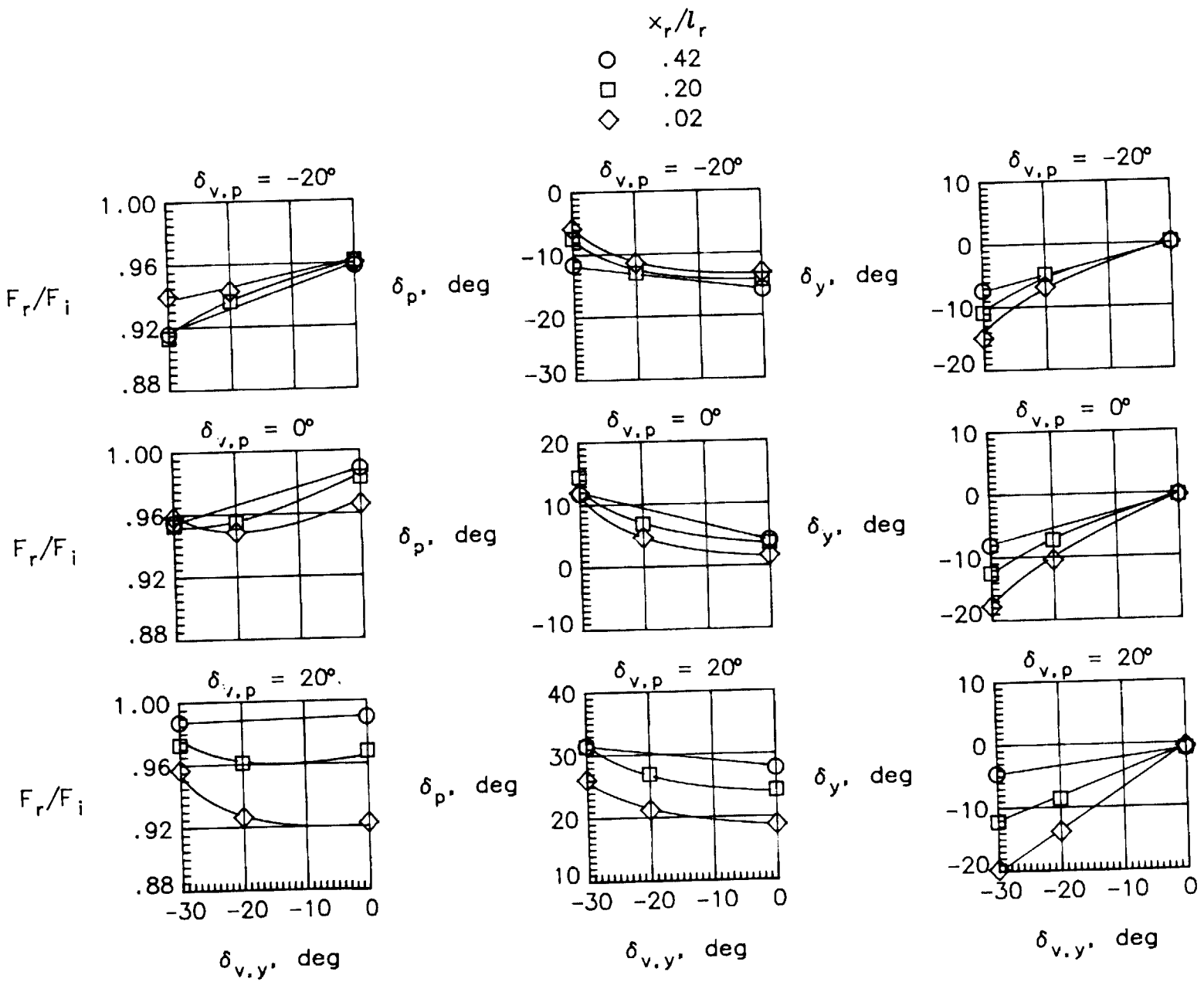

(b) NPR = 6.0.

Figure 24. Concluded.

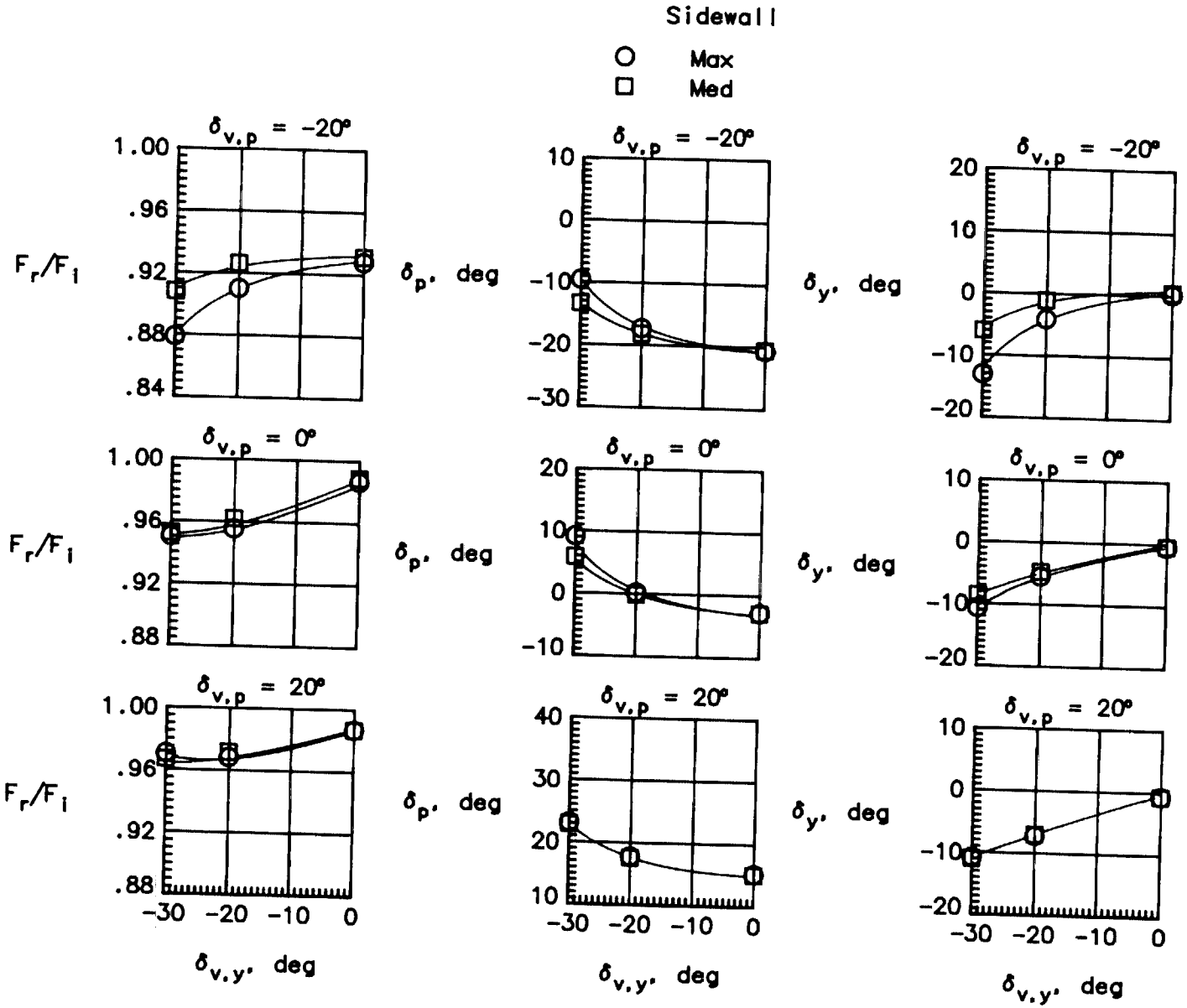

(a) NPR = 3.0.

Figure 25. Summary of yaw vectoring effects on nozzle performance at various values of NPR, $x_r/l_r = 0.20$, $\theta = 30°$, and $\phi = 0°$.

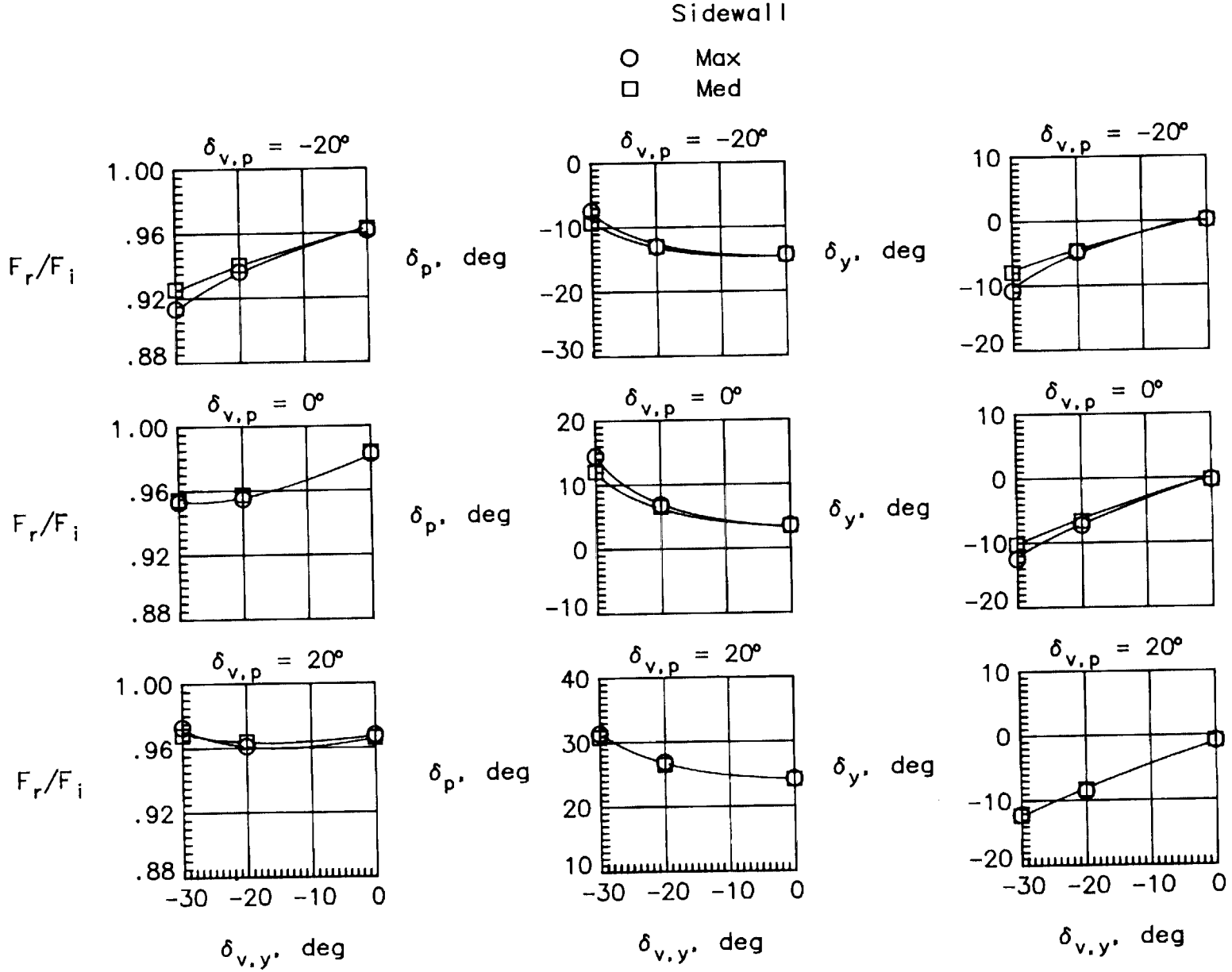

(b) NPR = 6.0.

Figure 25. Concluded.

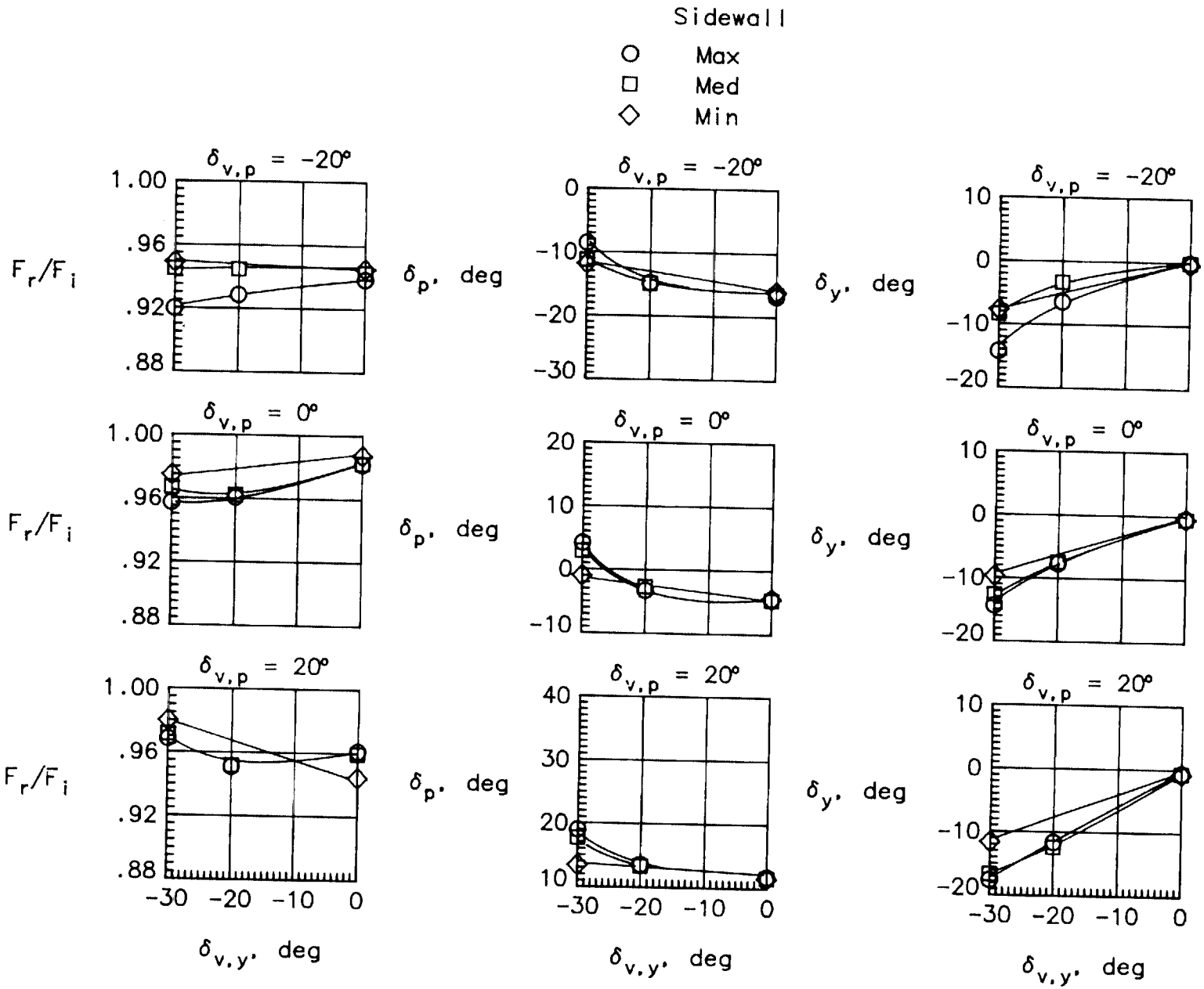

(a) NPR = 3.0.

Figure 26. Summary of yaw vectoring effects on nozzle performance at various values of NPR, $x_r/l_r = 0.02$, $\theta = 30°$, and $\phi = 0°$.

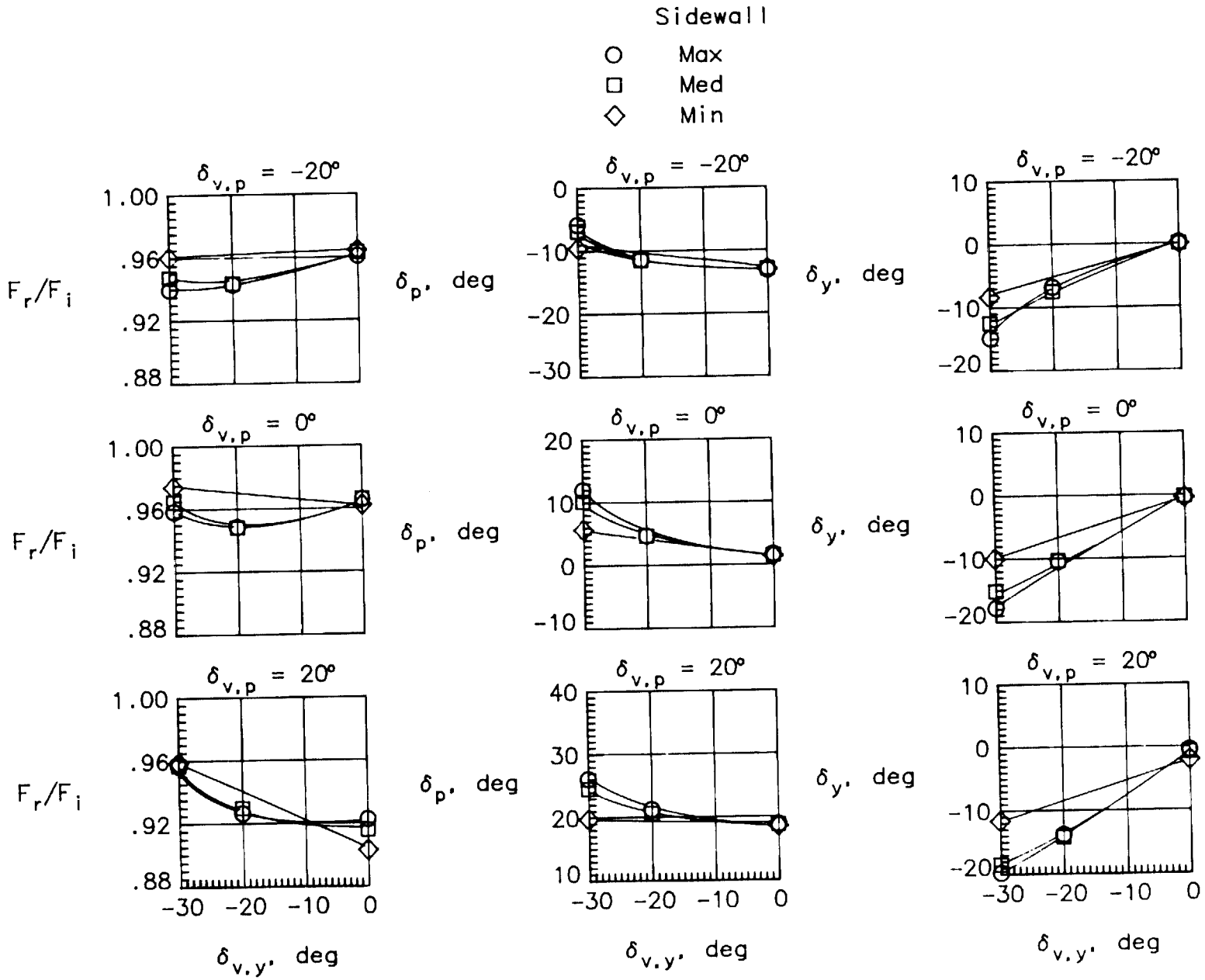

(b) NPR = 6.0.

Figure 26. Concluded.

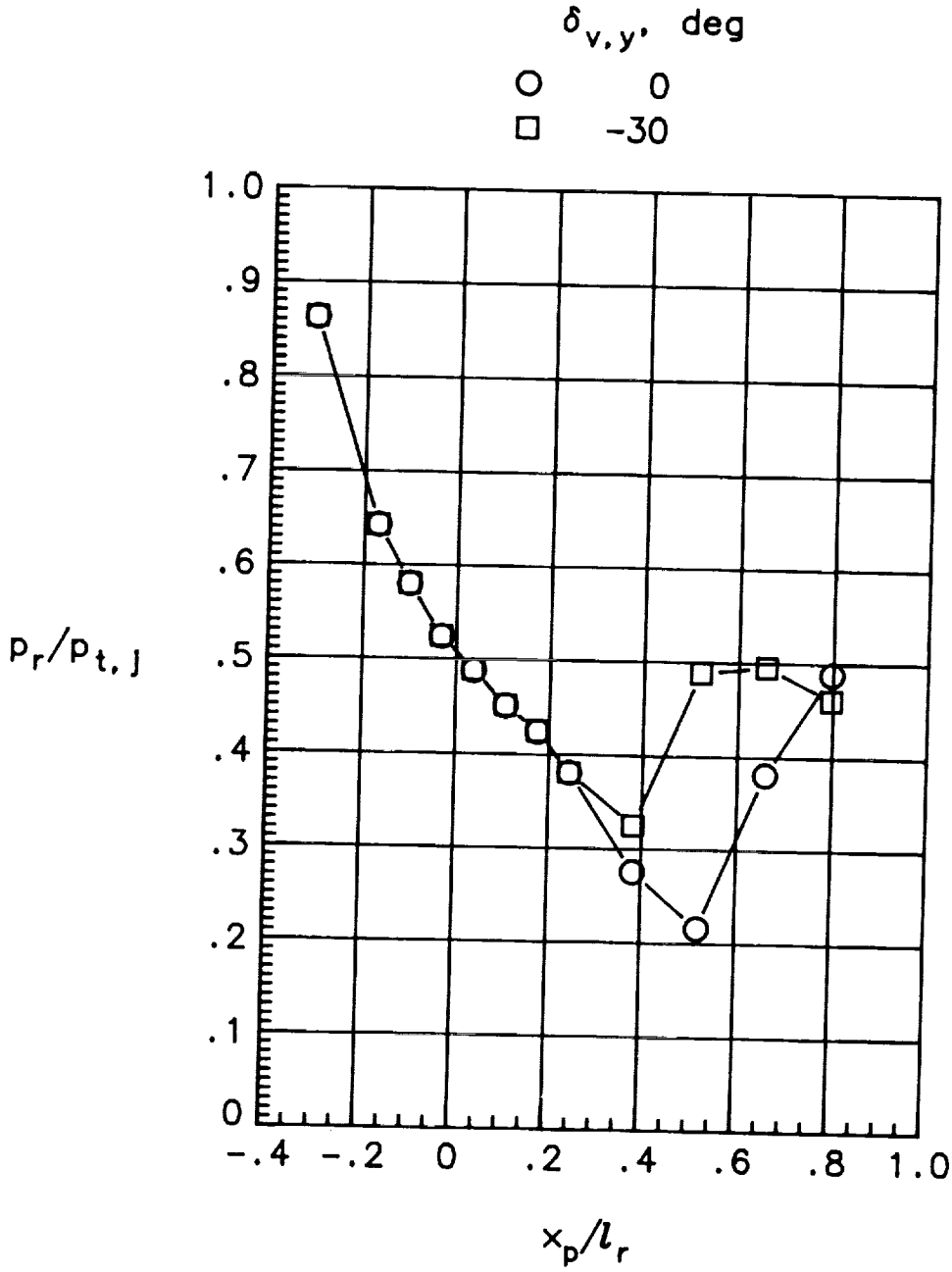

(a) $\delta_{v,p} = 0°$.

Figure 27. Effect of yaw vectoring on internal pressures at various geometric pitch vector angles. NPR = 3.0; max sidewall; $x_r/l_r = 0.20$; $\theta = 30°$; $\phi = 0°$.

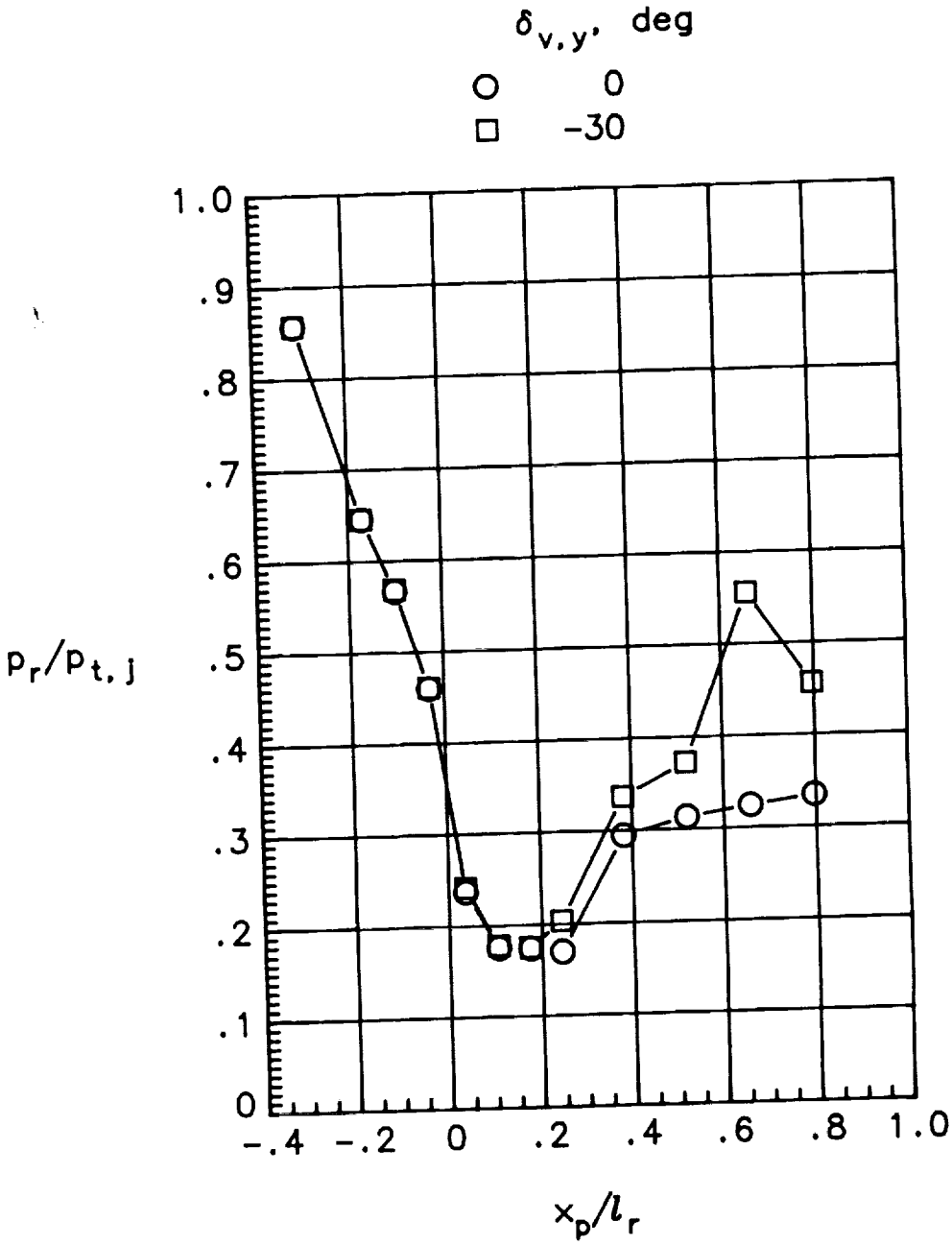

(b) $\delta_{v,p} = -20°$.

Figure 27. Continued.

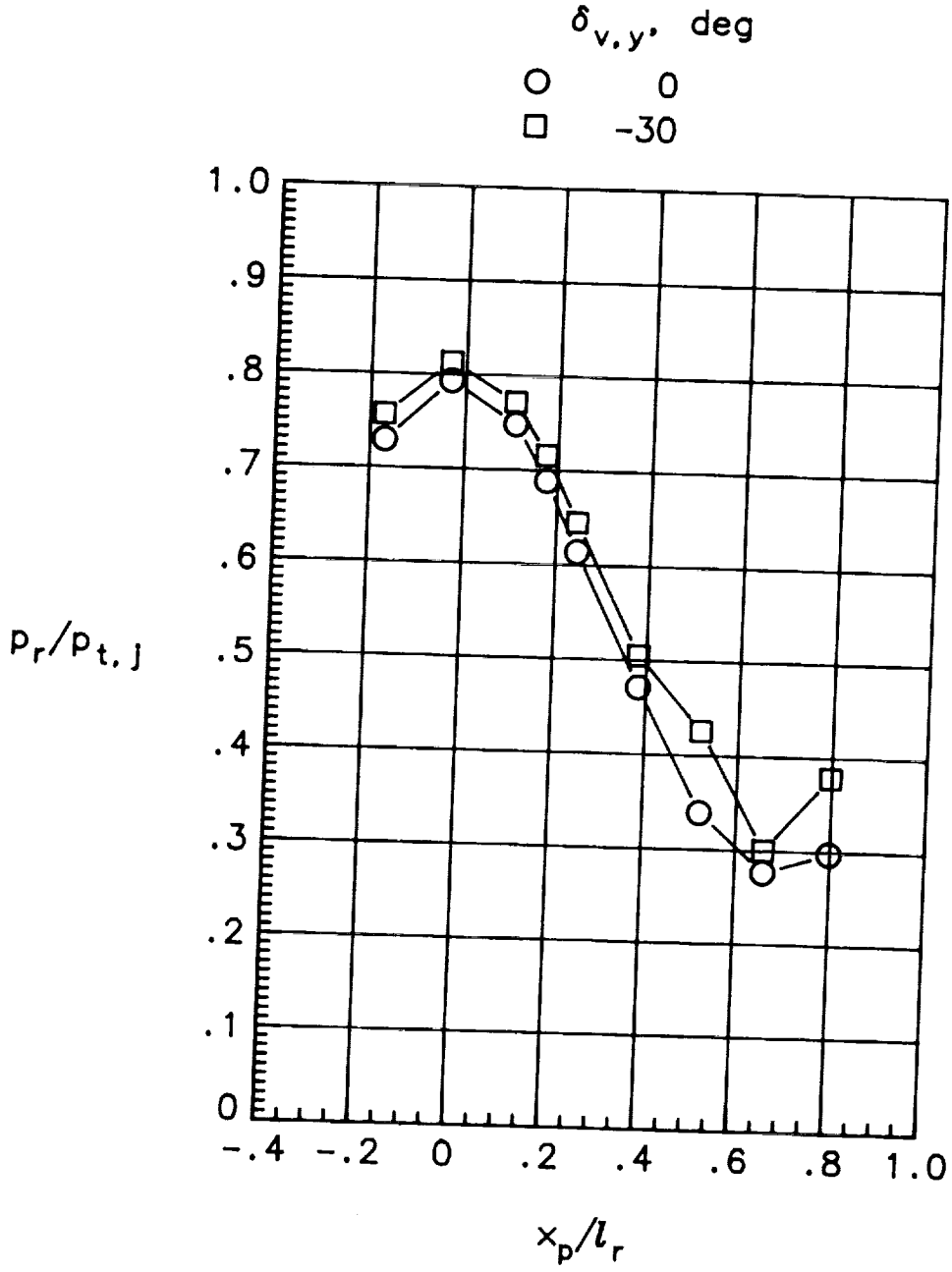

(c) $\delta_{v,p} = 20°$.

Figure 27. Concluded.

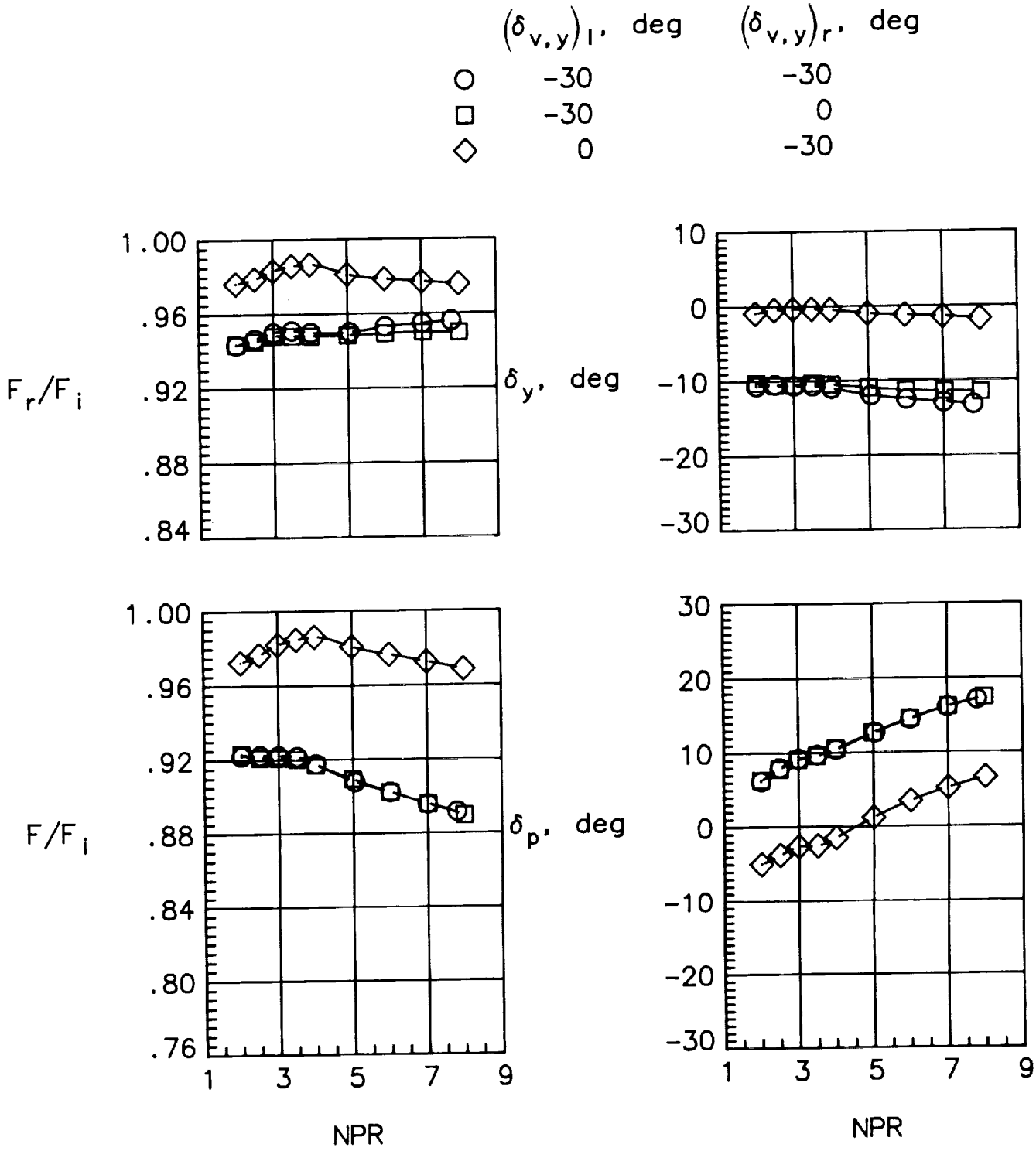

(a) $\delta_{v,p} = 0°$.

Figure 28. Effect of single yaw vectoring on nozzle performance at various geometric pitch vector angles. Max sidewall; $x_r/l_r = 0.20$; $\theta = 30°$; $\phi = 0°$.

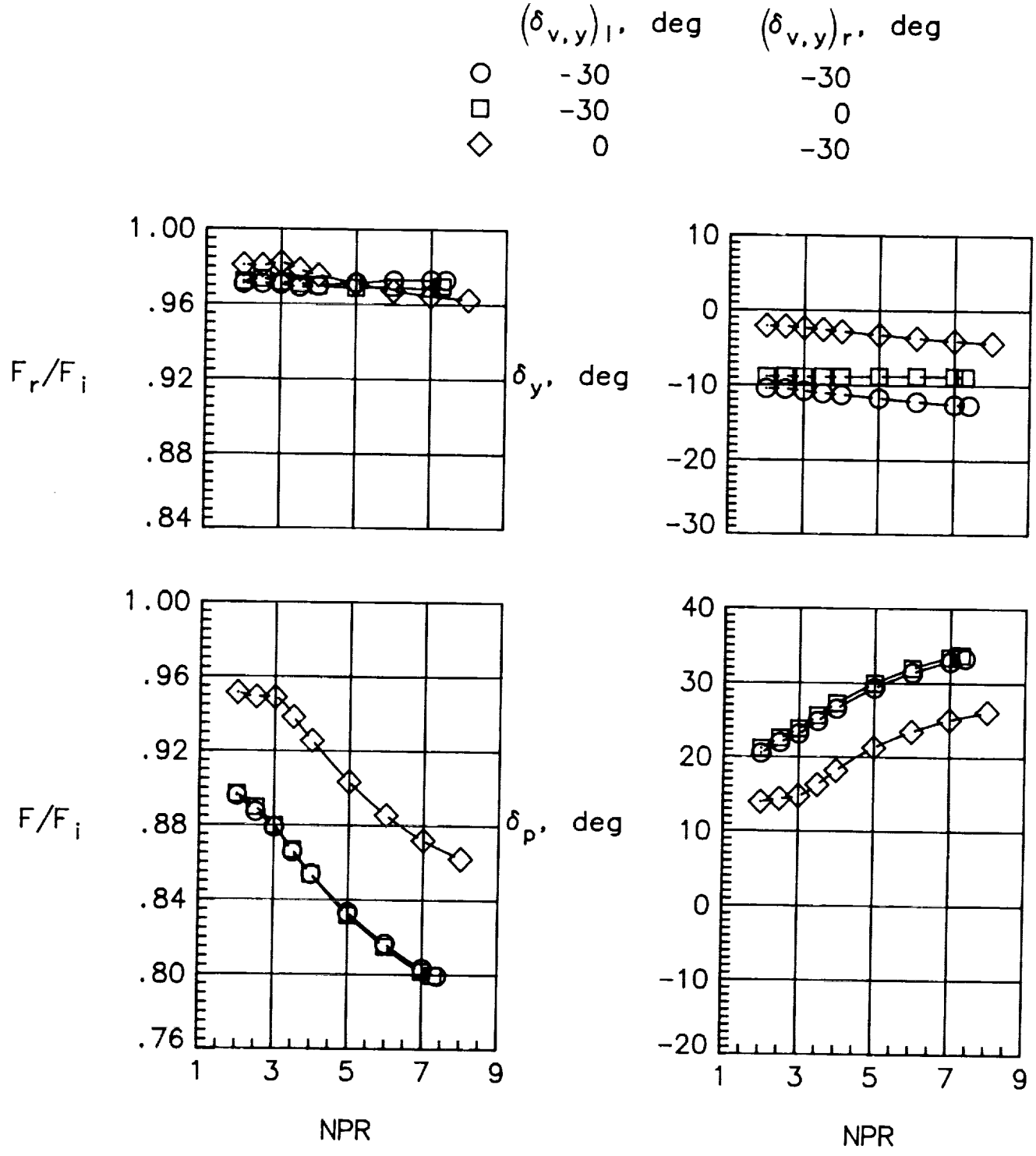

(b) $\delta_{v,p} = 20°$.

Figure 28. Concluded.

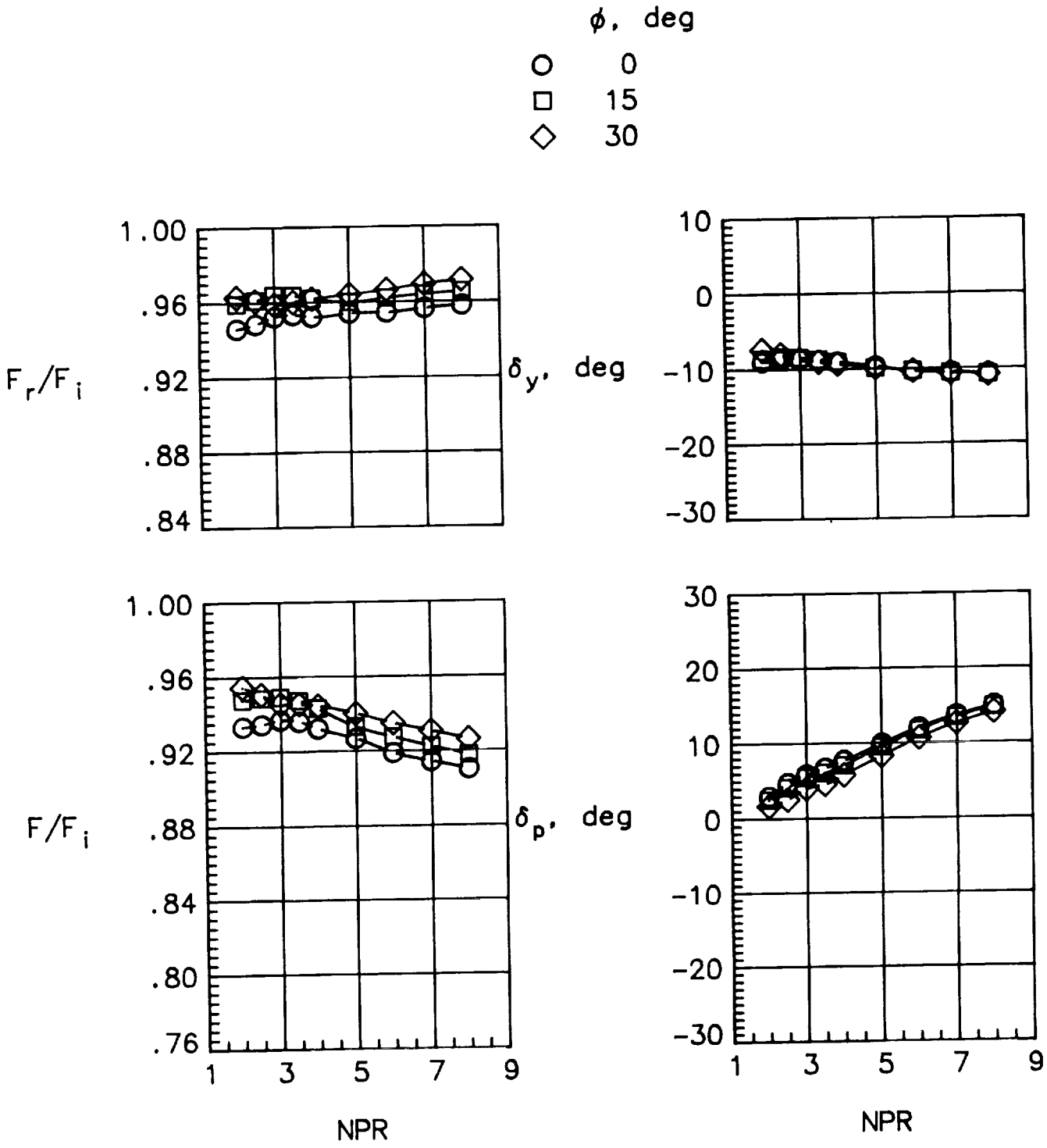

(a) $\delta_{v,p} = 0°$.

Figure 29. Effect of hinge line inclination on nozzle performance at various geometric pitch vector angles. Max sidewall; $x_r/l_r = 0.20$; $\theta = 30°$; and $\delta_{v,y} = -30°$.

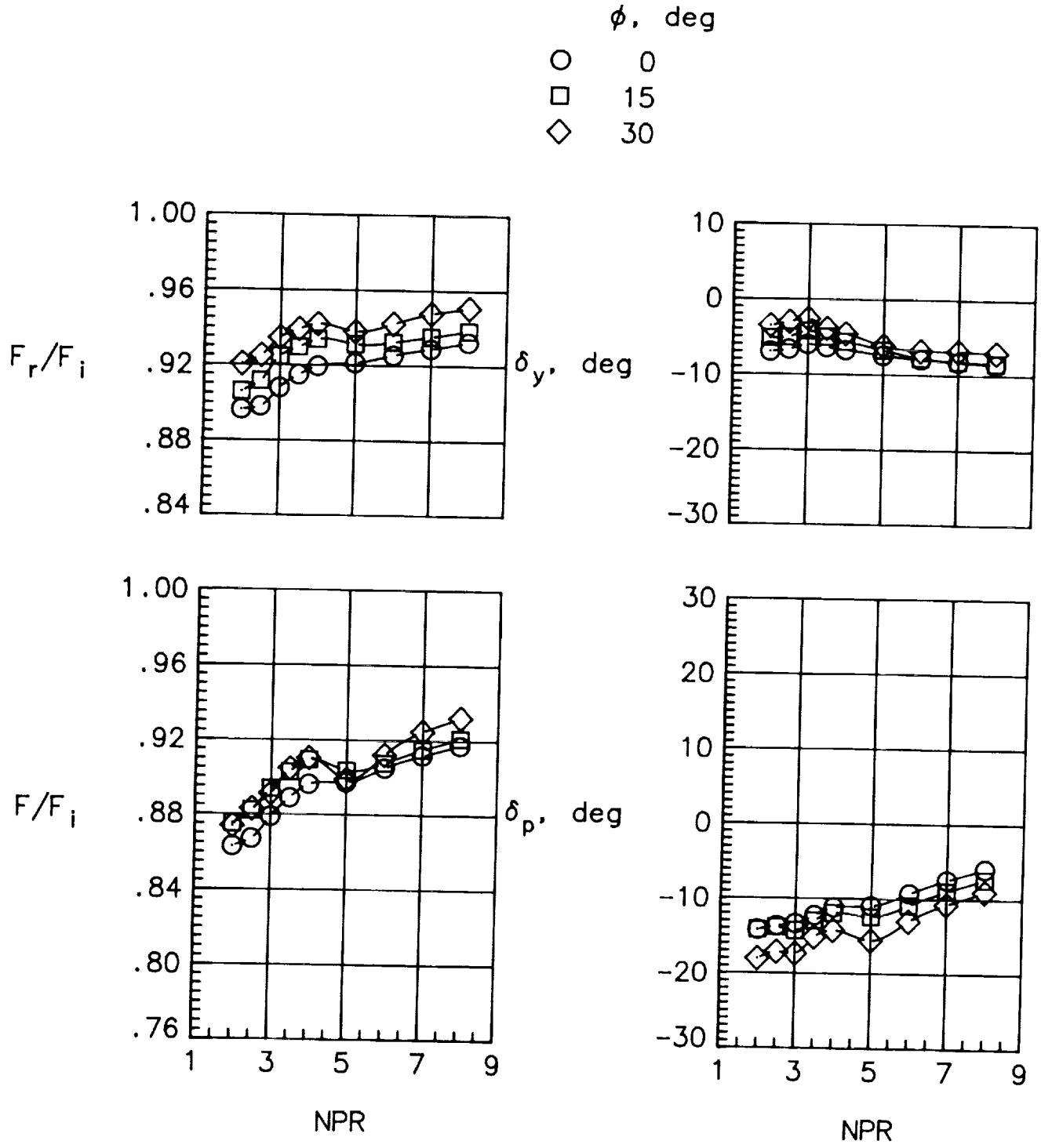

(b) $\delta_{c,p} = -20°$.

Figure 29. Continued.

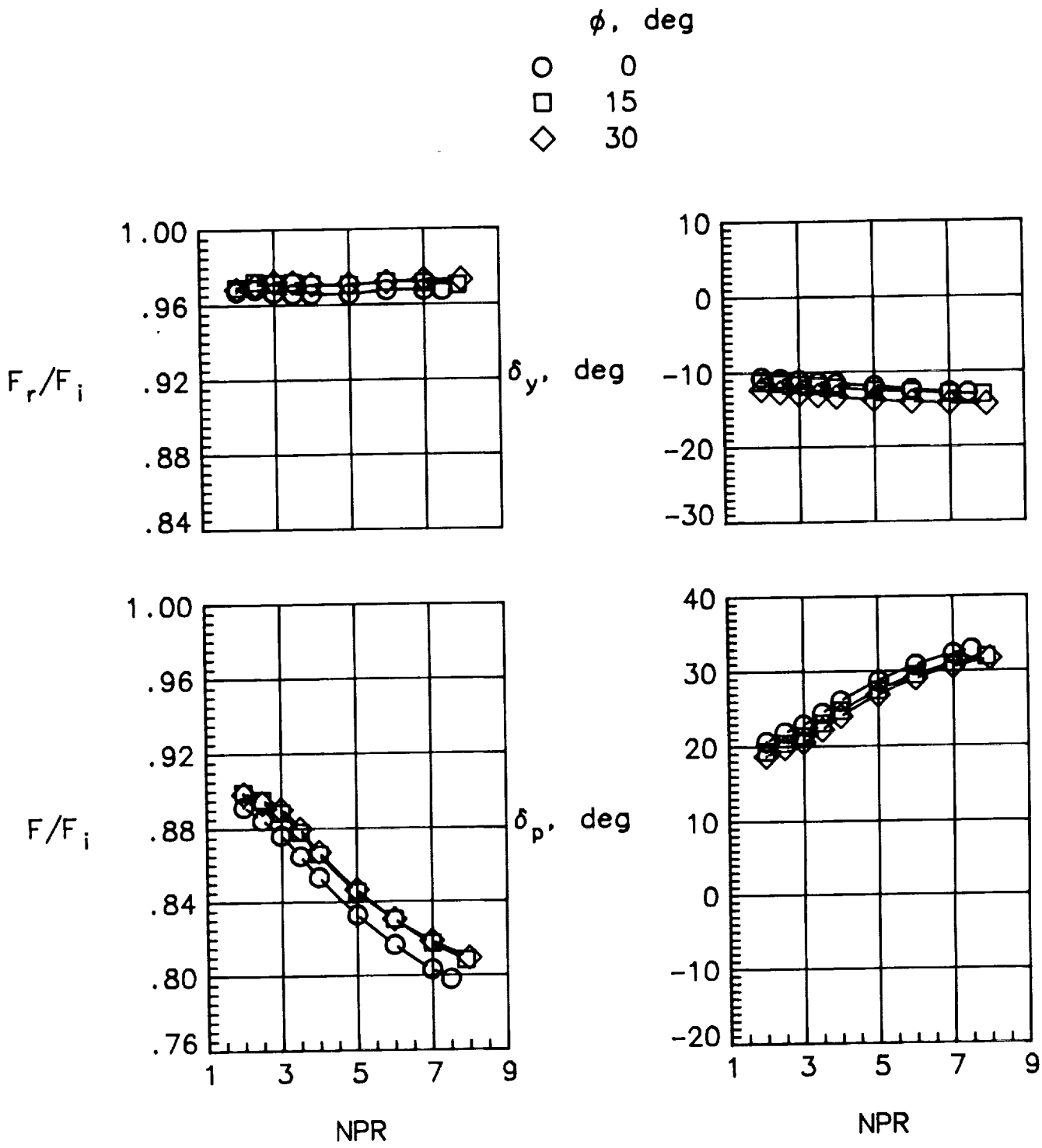

(c) $\delta_{v,p} = 20°$.

Figure 29. Concluded.

*U.S. GOVERNMENT PRINTING OFFICE: 1993-728-150-60057

REPORT DOCUMENTATION PAGE

Form Approved
OMB No. 0704-0188

1. AGENCY USE ONLY *(Leave blank)*	2. REPORT DATE	3. REPORT TYPE AND DATES COVERED
	July 1993	Technical Memorandum

4. TITLE AND SUBTITLE
Static Internal Performance of a Single Expansion Ramp Nozzle With Multiaxis Thrust Vectoring Capability

5. FUNDING NUMBERS
WU 505-62-30-01

6. AUTHOR(S)
Francis J. Capone and Alberto W. Schirmer

7. PERFORMING ORGANIZATION NAME(S) AND ADDRESS(ES)
NASA Langley Research Center
Hampton, VA 23681-0001

8. PERFORMING ORGANIZATION REPORT NUMBER
L-17163

9. SPONSORING/MONITORING AGENCY NAME(S) AND ADDRESS(ES)
National Aeronautics and Space Administration
Washington, DC 20546-0001

10. SPONSORING/MONITORING AGENCY REPORT NUMBER
NASA TM-4450

11. SUPPLEMENTARY NOTES
Capone: Langley Research Center, Hampton, VA; Schirmer: The George Washington University, Joint Institute for Advancement of Flight Sciences, Langley Research Center, Hampton, VA.

12a. DISTRIBUTION/AVAILABILITY STATEMENT
Unclassified–Unlimited

Subject Category 02

12b. DISTRIBUTION CODE

13. ABSTRACT *(Maximum 200 words)*
An investigation has been conducted at static conditions in order to determine the internal performance characteristics of a multiaxis thrust vectoring single expansion ramp nozzle. Yaw vectoring was achieved by deflecting yaw flaps in the nozzle sidewall into the nozzle exhaust flow. In order to eliminate any physical interference between the variable angle yaw flap deflected into the exhaust flow and the nozzle upper ramp and lower flap which were deflected for pitch vectoring, the downstream corners of both the nozzle ramp and lower flap were cut off to allow for up to 30° of yaw vectoring. The effects of nozzle upper ramp and lower flap cutout, yaw flap hinge line location and hinge inclination angle, sidewall containment, geometric pitch vector angle, and geometric yaw vector angle were studied. This investigation was conducted in the static-test facility of the Langley 16-Foot Transonic Tunnel at nozzle pressure ratios up to 8.0.

14. SUBJECT TERMS
Single expansion ramp nozzle; Multiaxis thrust vectoring; Internal performance

15. NUMBER OF PAGES
270

16. PRICE CODE
A12

17. SECURITY CLASSIFICATION OF REPORT	18. SECURITY CLASSIFICATION OF THIS PAGE	19. SECURITY CLASSIFICATION OF ABSTRACT	20. LIMITATION OF ABSTRACT
Unclassified	Unclassified		

NSN 7540-01-280-5500

Standard Form 298(Rev. 2-89)
Prescribed by ANSI Std Z39-18
298-102

NASA-Langley, 1993